UNIVERSITY OF SOUTHAMPTON

THE INFLUENCE OF EPIDERMAL GROWTH FACTOR RECEPTOR LIGANDS ON CD44 AND ERM PROTEINS IN BRONCHIAL EPITHELIAL CELLS

Caroline Jane Bell

A PhD thesis submitted for the Degree of Doctor of Philosophy.

Division of Infection, Inflammation and Repair
School of Medicine
Faculty of Medicine, Health and Biological sciences
University of Southampton

August 2002

UNIVERSITY OF SOUTHAMPTON

ABSTRACT

FACULTY OF MEDICINE, HEALTH AND BIOLOGICAL SCIENCES
DIVISION OF INFECTION, INFLAMMATION AND REPAIR

Doctor of Philosophy

THE INFLUENCE OF EPIDERMAL GROWTH FACTOR RECEPTOR LIGANDS ON CD44 AND ERM PROTEINS IN BRONCHIAL EPITHELIAL CELLS

By Caroline Jane Bell

The bronchial epithelium of asthmatic airways exhibits structural modifications including loss of columnar cells, which compromises the barrier function of the airway epithelium. Greater understanding of the regulators and molecules involved in epithelial repair might provide new targets for therapeutic intervention. Epidermal growth factor (EGF) and its receptor (EGFR) have pleiotropic effects on cells and likely orchestrate, at least in part, repair processes through changes in cell motility, adhesion and proliferation. More specifically, EGF enhances repair of scrape wounded bronchial epithelial cells in an *in vitro* system. Bronchial biopsies from asthmatics show increased staining for the EGFR and the cell adhesion molecule, CD44 on basal cells within areas of epithelial damage implicating a role for these proteins in damage/repair processes. Initial experiments examined the hypothesis that increased EGFR signalling could cause an upregulation of CD44 and regulate cell adhesion. In the bronchial epithelial cell lines, NCI-H292 and 16HBE 14o-, measurement of CD44 expression by flow cytometry and Western blotting showed that EGF and HB-EGF had no influence on the expression of surface or total CD44 levels, respectively. This observation suggests that, in this system, EGF through its divergent signalling pathways, may regulate other processes required for epithelial repair such as migration. ERM proteins (ezrin, radixin and moesin), can link the actin cytoskeleton with the plasma membrane via cell adhesion molecules such as CD44 and can be activated by EGF. A role for ERM proteins in cell adhesion, migration and cellular morphology has been shown in other systems, therefore changes in their regulation by EGF might be important during bronchial epithelial repair processes and was examined here.

Ezrin and moesin were detected in bronchial epithelial cell cultures where under basal conditions they had a cytoplasmic distribution as well as at plasma membrane regions co-localised with CD44. Following treatment with 1nM EGF (15 minutes), enhanced cytoskeletal association along with redistribution of ezrin and moesin to membrane projections resembling lamellipodia and microvilli-like structures was observed and cells appeared to adopt a more migratory phenotype. This EGF stimulated redistribution of ezrin and moesin did not appear to be as a result of activation by phosphorylation on tyrosine residues as determined by immunoprecipitation using anti-phosphotyrosine antibodies followed by Western blotting.

Previously published data showing enhanced repair with EGF were confirmed here in primary bronchial epithelial cells as well as the 16HBE 14o- cell line. As EGF stimulated enhanced migration might act in part by modulation of ERM proteins the distribution of ERM proteins and CD44 during repair was observed using double immunofluorescent staining. However at the earlier time points (0-3 hours) cells did not appear to be migrating and ERM proteins were not seen in lamellipodia structures as observed previously. Instead, CD44 and ERM proteins were co-localised in microvilli-like extensions might reflect enhanced adhesion processes following damage. A study of the later phase of repair might confirm an involvement of ERM proteins in migratory processes during repair. In addition to the effects of EGF, the mast cell stabiliser, sodium cromoglycate was shown here to enhance repair of damaged 16HBE 14o- cell monolayers ($P<0.03$ and <0.02 at 3 and 9 hours respectively) and this was shown to act through an EGFR dependent mechanism as 1μM tyrphostin AG1478 blocked this effect and EGF receptors phosphorylated on tyrosine residues were detected in anti-phosphotyrosine immunoprecipitates of 16HBE 14o- cells treated with sodium cromoglycate.

In conclusion these data have shown that, ezrin and moesin are associated with the actin cytoskeleton and co-localised with CD44 and can be modulated by EGF in bronchial epithelial cells. However a role for ERM proteins during repair could not be established. EGF stimulated enhancement of bronchial epithelial repair could be attributed to, in part, by the modulation of ERM proteins allowing modifications to cell shape, motility and spreading enabling restitution of the damaged bronchial epithelium in asthma.

CONTENTS

LIST OF FIGURES

Chapter 4

Chapter 5

Chapter 6

LIST OF TABLES

Chapter 1

Chapter 2

DECLARATION

The work contained within this thesis, except where specifically specified is entirely the work of the author. Work contained within this thesis is reproduced in part in the following publications.

ABSTRACTS

Bell CJ, Davies DE, Lackie PM, Holgate ST. CD44 expression and ERM proteins; interactions with epidermal growth factors in bronchial epithelial cell lines. Abstract. Respiratory Medicine, 1998, 92:A.

CJ Bell, PM Lackie, DE Davies and ST Holgate. Epidermal growth factor (EGF) stimulates altered distribution of ezrin and moesin in bronchial epithelial cells. Abstract. American Journal of Respiratory and Critical Care Medicine. Vol 163, No 5, Abstract Issue.

ACKNOWLEDGEMENTS

I would like to thank my supervisors Dr. Peter Lackie and Dr. Donna Davies, for their endless advice, encouragement and support during my laboratory research and the construction of this thesis. I would also like to thank other members of the Brooke Laboratory at Southampton for their help and in particular Sarah Puddicombe, Will Howat, S-H Leir and Audrey Richter, for their technical advice. I am also grateful to the Medical Research Council, UK who supported this work. Finally I would like to thank my parents and friends for all their patience and support.

ABBREVIATIONS

ADAM	A Disintegrin And Metalloproteinase
aFGF	acidic Fibroblast Growth Factor
APS (or AMPS)	Ammonium persulphate
Asn	Asparagine
BAL	Bronchoalveolar Lavage
BCA	Bicinchoninic acid
BEBM	Bronchial Epithelial Basal Medium
BEGM	Bronchial Epithelial Growth Medium
bFGF	basic Fibroblast Growth Factor
BSA	Bovine Serum Albumin
CD44v3	CD44 proteins containing variant exon 3
dH_20	distilled water
DABCO	1,4-Diazabicyclo-[2.2.2] Octane
DAG	Diacylglycerol
DMSO	Dimethylsulphoxide
EBP	ERM-binding phosphoprotein
ECL	Enhanced Chemiluminescence
EDTA	Ethylenediaminetetraacetic acid
EGF	Epidermal Growth Factor
EGFR	Epidermal Growth Factor Receptor
EGTA	Ethylene Glycol-bis(β-aminoethyl Ether) N, N, N', N',-Tetraacetic acid
ERM	Ezrin Radixin Moesin
F-actin	Fibrous actin
FACS	Fluorescence Activated Cell Sorter
FAK	Focal Adhesion Kinase
FBS	Foetal Bovine Serum
FGF	Fibroblast Growth Factor
FGFR	Fibroblast Growth Factor Receptor
FITC	Fluorescein Isothiocyanate
G-actin	Globular actin
GAG	Glycosaminoglycan

Glu	Glutamate
GM-CSF	Granulocyte-macrophage colony-stimulating factor
GPCR	G-Protein Coupled Receptor
HA	Hyaluronic Acid
HB-EGF	Heparin-Binding Epidermal Growth Factor
HBSS	Hank's Balanced Salt Solution
HEPES	N-[2-Hydroxyethyl]piperazine-N'-[2-ethanesulphonic acid]
HGF/SF	Hepatocyte Growth Factor/Scatter Factor
HRP	Horseradish Peroxidase
HSPG	Heparan Sulphate Proteoglycan
ICAM	Intercellular Cell Adhesion Molecule
Ig	Immunoglobulin
IL	Interleukin
iNOS	inducible Nitric Oxide Synthase
IP3	Inositol-trisphosphate
KGF	Keratinocyte Growth Factor
M	Molar
MEM	Minimum Essential Medium
MES	2-[N-morpholino] ethanesulfonic acid
MMP	Matrix Metalloproteinase
nm	nanometre
Nonidet P40 (NP40)	Ethyl phenyl-polyethylene glycol
OD	Optical Density
PBS	Phosphate Buffered Saline
PI3-kinase	Phosphatidylinositol 3-kinase
PIP2	Phosphatidylinositol-bisphosphate
PKC	Protein Kinase C
PLC	Phospholipase C
PMSF	Phenylmethylsulphonyl fluoride
PY	Phosphotyrosine
SDS	Sodium Dodecyl Sulphate
SDS-PAGE	Sodium Dodecyl Sulphate-Polyacrylamide Gel Electrophoresis
SD	Standard Deviation
SH2	*Src*-homology 2

TEMED	N,N,N',N'-Tetramethylethylenediamine
TGF	Transforming Growth Factor
Thr	Threonine
Tris	Tris(hydroxymethyl)aminomethane
TRITC	Tetramethyl Rhodamine Isothiocyanate
Triton X-100	Octyl phenoxy polyethoxyethanol
Tween-20	Polyoxyethylene Sorbitan monolaurate
Tyr	Tyrosine
v	volume
w	weight

1 CHAPTER ONE

INTRODUCTION

1.1 Overview

Asthma is a chronic, respiratory disease with a complex aetiology involving inflammation, tissue damage, restitution and remodelling processes. The bronchial epithelium of asthmatics exhibits loss of columnar cells and likely undergoes frequent damage/repair cycles during exacerbations of the disease, leading to altered or remodelled airways. Bronchial epithelial repair is a complex process involving modifications to cell adhesion, motility, morphology and proliferation by the co-ordinated control of cytoskeletal proteins, cell adhesion molecules, growth factors and extracellular matrix proteins. The detailed role of these proteins in bronchial epithelial repair is not yet fully understood, however elucidation of the control and functions could enable greater understanding of repair and the potential for novel therapeutic interventions.

1.2 Asthma and the bronchial epithelium

Asthma is a chronic disease of the airways characterised by clinical symptoms of wheeze, cough and breathlessness. Physiologically, the disease comprises abnormal bronchial smooth muscle contraction in response to non-specific stimuli which is termed bronchial hyper-responsiveness and is accompanied by variable airflow obstruction. In addition to the atypical broncho-constriction of asthmatic airways it is well established that an inflammatory component involving lymphocytes, eosinophils, mast cells and macrophages contributes to the pathology of the disease. These inflammatory cells are increased in the airways of asthmatic subjects (airway wall and fluids) and through the release of an array of proinflammatory mediators including IL-3, IL-4, IL-5, IL-6, IL-9, IL-13 and GM-CSF (reviewed in (154)) contribute to the abnormal pathophysiological features of asthma. In addition to the inflammation, these features include oedema, epithelial damage and permanent modifications of the airway wall termed remodelling (reviewed in (20)). This remodelling is characterised by thickening of the airway wall as a result of sub-epithelial fibrosis and smooth muscle

hyperplasia along with increased collagen (types III and V) deposition, goblet cell hyperplasia (109), increased sub-mucosal glands and increased vascularity (162).

1.2.1 The structure and function of the bronchial epithelium

1.2.1.1 Structure

The bronchial epithelium has a stratified structure with ciliated and goblet columnar epithelial cells attached to a basal epithelial cell layer, which is in turn bound to the basement membrane and the submucosa (see figure 1.1) (151). In the bronchi, the majority of the columnar cells are of the ciliated type and their motile cilia function to remove mucus, irritants, bacteria, viruses and other foreign particulates up and out of the respiratory tract by the mucociliary escalator. Goblet cells are a type of secretory cell which secrete mucins into the airways and make up a small proportion (15-25%) of the population of columnar cells of the bronchial epithelium. The sub-basement membrane layers are made up of lamina propria, muscularis mucosa and submucosa (145).

The integrity of the epithelium is essential for its barrier function and adjacent cells are held together and bound to the underlying extracellular matrix by cell adhesion molecules and junctional complexes to form a continuous, cohesive, impermeable epithelium (reviewed in (102)). Several junctional adhesion structures exist in the bronchial epithelium and the desmosomes, hemidesmosomes and adherens junctions contribute most to adhesion. The desmosomes (macula adherens) are button-like symmetrical points of contact whose structure can include proteins from the following three families, desmosomal cadherins (desmogleins, desmocollins), the armadillo protein family (plakoglobin, plakophilins 1-3) and the plakins (desmoplakin, plectin). These protein structures bind and connect the keratin-intermediate filaments from two adjacent cells and as junctions are responsible for the attachment of columnar cells to each other and to the basal cells (reviewed in (47)). Hemidesmosomes are asymmetric points of contact between the basal cells and the underlying basement membrane. The adherens junctions (intermediate junctions, zonula adherens-ZA) comprise a belt of adherens junctions around individual columnar cells. Adherens junctions are specialised regions made up of cadherins which function as cell adhesion molecules to

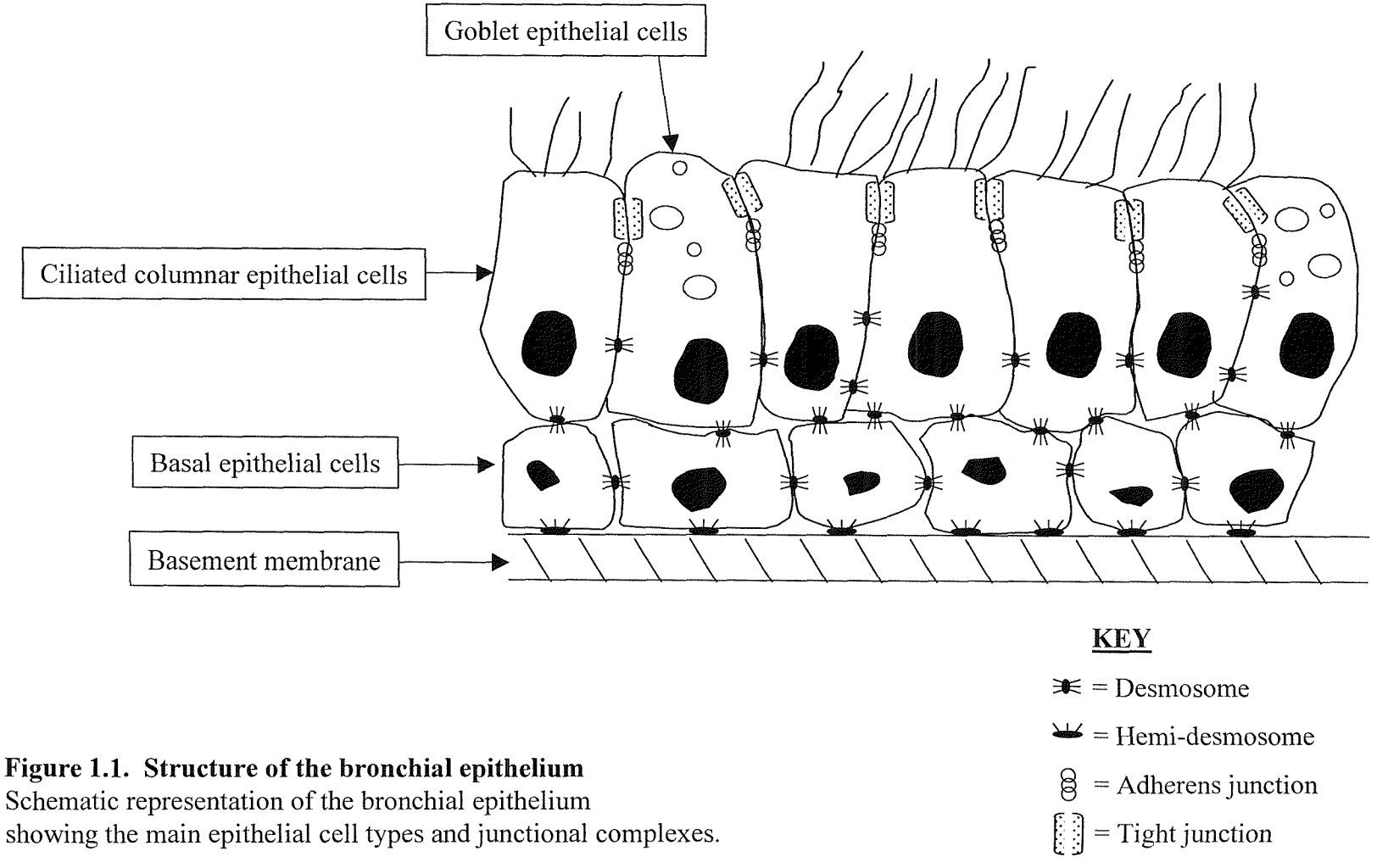

Figure 1.1. Structure of the bronchial epithelium
Schematic representation of the bronchial epithelium showing the main epithelial cell types and junctional complexes.

connect the actin filaments from one cell to the next via crosslinking proteins including catenins and vinculin (reviewed in (104)). Finally, tight junctions (zonula occludens-ZO), comprise transmembrane proteins, occludin and claudins, which link the cytoplasmic, ZO-1 proteins in the cytoplasm of neighbouring cells which in turn can interact with actin. These junctions divide the cell into apical and basolateral regions and serve as permeability barriers (reviewed in (100), (135)).

The structure provided by junctional complexes made up of the tight junctions, adherens junctions and desmosomes is important for the function of the epithelium in the respiratory tract where it exists to provide a barrier between the external and internal environments.

1.2.1.2 Function of the bronchial epithelium

Bronchial epithelial cells provide a barrier function as they form a continuous physical barrier against potentially harmful environmental agents such as allergens, pollutants and infectious agents including bacteria and viruses. In addition specific functions are provided by goblet cells which produce mucus that traps foreign inhaled particles and ciliated epithelial cells are able to exclude irritants and mucus from the airway by means of the mucociliary escalator.

1.2.2 The bronchial epithelium in asthma

1.2.2.1 Phenotype

In asthma damage to the bronchial epithelium characterised by epithelial cell shedding is frequently seen (see figure 1.2A). Bronchial biopsies from asthmatics consistently show damaged areas (75) where there appears to be selective loss of columnar cells (103) to leave an exposed basal cell layer. Furthermore clusters of columnar epithelial cells (known as Creola bodies), but not basal cells, are found in the sputum (103) and bronchial alveolar lavage fluid (BAL) (12) of asthmatic patients suggesting areas of damage seen in biopsies are not artefactual damage as a result of the biopsy procedure.

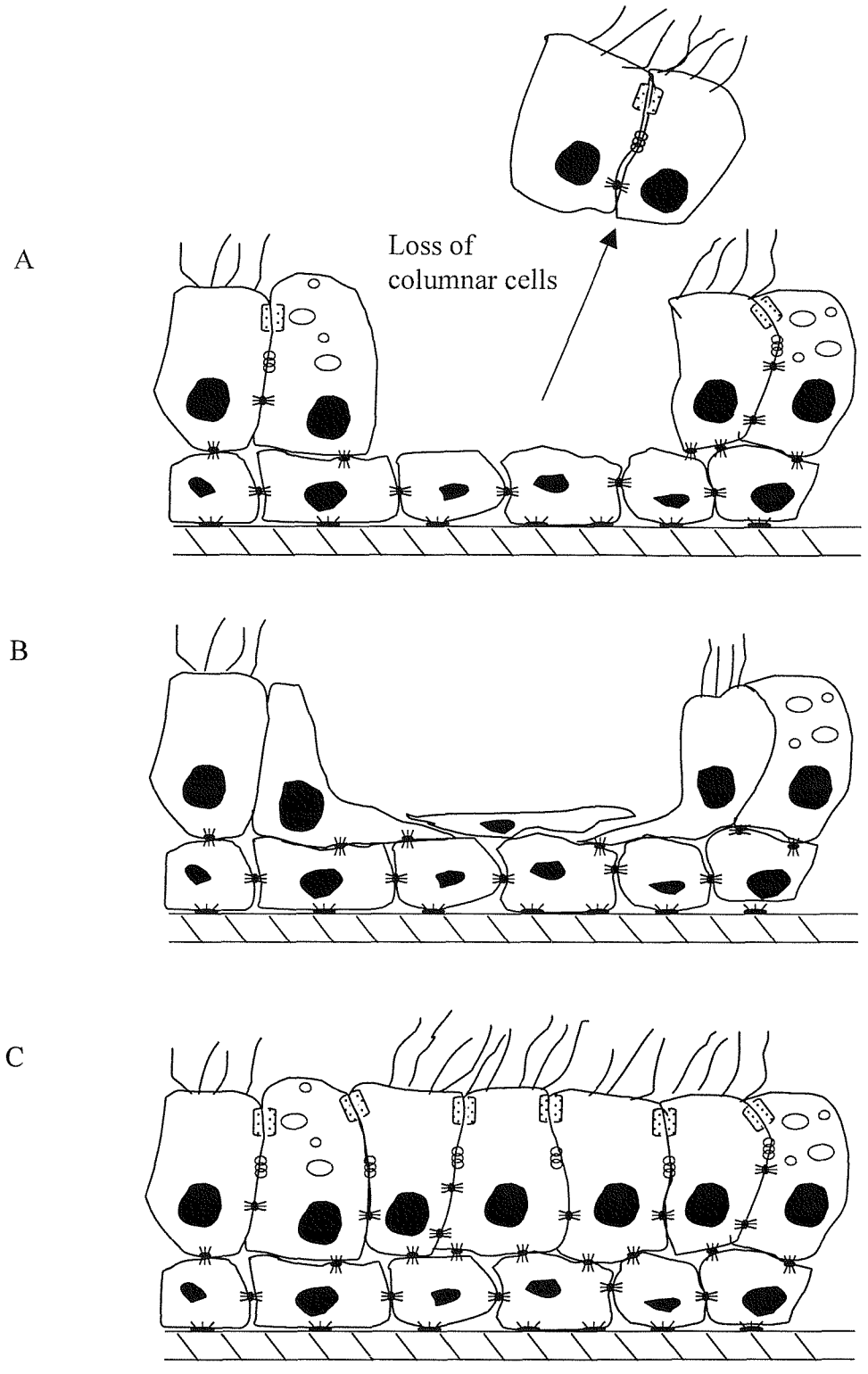

Figure 1.2. The bronchial epithelium in asthma.
Shows schematically the damage/repair phenotype of asthmatic bronchial epithelium. Picture A represents the damage seen where columnar cells are shed to leave a basal cell layer. The surrounding columnar cells differentiate and spread to cover the wound (B) and these cells or the basal cells then proliferate and differentiate to form an intact epithelium (C).

As well as the presence of damage to the asthmatic epithelium, other alterations have also been observed. The cell adhesion molecule, CD44, is increased in asthmatic and damaged epithelium in bronchial biopsies (73) and ICAM-1 (intercellular adhesion molecule-1) expression is higher on asthmatics epithelial cells than those from normal subjects (152). Growth factor receptors and their ligands have also been studied; the epidermal growth factor receptor (EGFR) is increased in the bronchial epithelium of mild and severe asthmatics (115), (5). The growth factors, epidermal growth factor (EGF) (5) and transforming growth factor-beta (TGF-β) (153) also have increased expression in the bronchial epithelium of asthmatics.

1.2.2.2 Consequences of damage to the bronchial epithelium

Loss of columnar cells from the bronchial epithelium has several consequences. The loss of the physical barrier allows entry of potentially harmful environmental agents, such as allergens, bacteria and viruses into the underlying mucosa. In addition, the increased inflammatory mediators present in the airway are also able to impact on the underlying cells of the airway wall. In clinical terms, there is also a correlation between epithelial damage and airway hyperresponsiveness (12), (66) and this might be as a result of increased exposure of nerves and increased permeability of the sub-mucosa to broncho-constricting mediators.

1.2.2.3 Epithelial repair

Bronchial epithelial repair is likely to comprise several stages or mechanisms but as yet these processes have not been fully characterised. *In vivo* studies have described how columnar cells surrounding the area of damage de-differentiate and spread to cover the area. These cells then proliferate and differentiate into ciliated and goblet columnar cells to reform a stratified bronchial epithelium (see figure 1.2 B and C) (38). This process likely involves complex changes in cell morphology, migration, adhesion, proliferation and phenotype which probably require the involvement and regulation of cell adhesion molecules, growth factors and cytoskeletal proteins. These will be discussed in turn below.

1.3 Cell adhesion molecules

As well as the cell-cell and cell-substrate adhesion provided by junctional complexes, non-junctional cell adhesion molecules such as integrins, ICAM-1 (intercellular adhesion molecule-1) and CD44 are also present within the bronchial epithelium and involved in both intercellular and cell-extracellular matrix adhesion (123).

1.3.1 CD44

CD44 is a cell surface glycoprotein that is expressed on many cell types and has many isoforms; the standard or haematopoietic form (CD44s or CD44H) is expressed as a protein of 80-95 kDa and has been detected on most cell types and has been characterised on haematopoietic cells, fibroblasts, keratinocytes and epithelial cells. The diversity of this protein arises as a result of alternative splicing of variant exons and post-translational glycosylation to generate variant isoforms which have been detected on many cell types but are largely restricted to cells of epithelial origin and these forms are expressed in a range of molecular weights from 110-300 kDa (90).

During the process of the characterisation of CD44, the molecules H-CAM, $GP90^{Hermes}$, Pgp-1, ECMR III, lymphocyte homing receptor and Hermes antigen were assumed to be distinct molecules. Subsequently these multi-functional molecules were discovered to consist of the same standard CD44 protein and hence in the literature CD44 may be referred to as one of these synonyms.

1.3.1.1 CD44 gene structure

CD44 is encoded by a single gene (figure 1.3), located on the short arm of chromosome 11, and comprises 20 exons (126). Expression of the diverse isoforms of CD44 is enabled by post-transcriptional alternative splicing of 12 of these exons termed variant (v) exons. Further variation arises as a result of post-translational glycosylation at selected sites on the CD44 molecule. At two regions of the CD44 mRNA molecule exons can be alternatively spliced during mRNA processing. The first of these variable regions is in the membrane proximal extracellular domain between amino acids 202 and 203 where 10 exons may be alternatively spliced. The standard form contains none

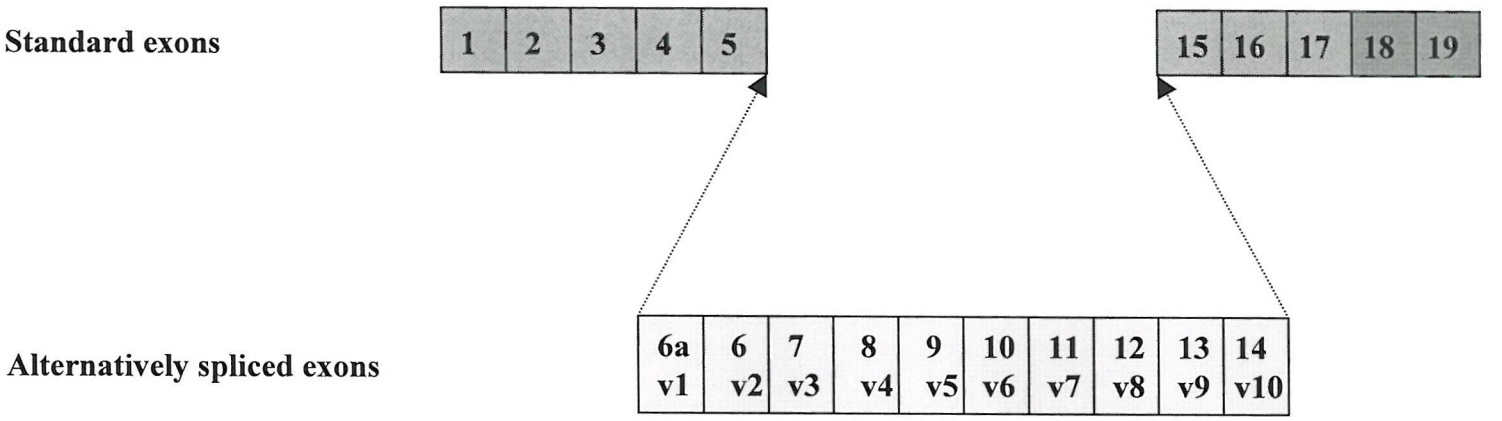

Figure 1.3. Schematic diagram of CD44 gene organisation.
Exons 1-5 and 15-19 ( ) are standard exons expressed in all CD44 proteins and exons 6a-14 (or v1-v10) ( ) are alternatively spliced exons which when expressed give rise to variant CD44 isoforms. Exons 18 and 19 ( ) of the cytoplasmic tail can also be alternatively spliced. Exon 6a or v1 is not expressed in humans.

of these exons and is almost ubiquitously expressed. Other forms contain various combinations of the 10 alternatively spliced exons for example CD44E is the epithelial form which is predominantly expressed on cells of epithelial origin and contains the additional variant exons v8, v9 and v10. The cytoplasmic tail or domain is also subject to variation and is described as either long or short depending upon which of exons 18 or 19, respectively, is spliced out (19).

1.3.1.2 CD44 protein structure

The core of the standard CD44 protein comprises 341 amino acids and can be sub-divided into 3 domains, a 248 amino acid extracellular domain, a 21 amino acid transmembrane domain and a 72 amino acid cytoplasmic tail (134). As described above (section 1.3.1.1) alternative splicing inserts additional amino acid sequences into the membrane proximal extracellular domain.

In addition to alternative splicing of variant exons, post-translational modifications give rise to further diversity of the protein. The addition of glycosaminoglycans (GAG), such as heparan sulphate, heparin, chondroitin sulphate, dermatan sulphate and keratan sulphate, as well as N- and O-linked glycans by glycosylation generates CD44 molecules of a much higher molecular mass than that expected by deduction based on the amino acid sequence of CD44 (25).

GAG modification of CD44 has only been demonstrated on CD44 proteins containing the alternatively spliced exon v3 (CD44v3) which encodes a serine-glycine-serine-glycine consensus motif for GAG addition (63). Modification of CD44 with GAG enables binding of CD44 to heparin binding growth factors. For example the CD44v3 isoform modified with heparan sulphate (also termed a heparan sulphate proteoglycan - HSPG) has been found to interact with heparin binding epidermal growth factor (HB-EGF) and basic fibroblast growth factor (bFGF) (14).

1.3.1.3 Function

The heterogeneous structure of the CD44 molecule probably provides for a wider range of functions than would otherwise be expected of a single molecule. Originally CD44

was termed the lymphocyte homing receptor but it is now thought to be involved in a much wider range of functions which include extracellular matrix binding, ligand binding, cell migration and cell adhesion (83).

CD44 has been studied to determine its ligand binding sites which enable it to carry out its array of functions. The extracellular domain has binding sites for the extracellular matrix components, hyaluronic acid (HA) (7), fibronectin, laminin (64), (65) and collagen types I and VI (157) enabling it to function as a cell-substrate adhesion molecule. Binding sites have also been characterised on the cytoplasmic domain of CD44 for the cytoskeletal binding proteins ankyrin (87) and the ERM family (ezrin, radixin, moesin) protein, ezrin (79) which might be involved in cell migration and morphology.

1.3.1.4 CD44 in asthma and bronchial epithelial repair

Changes in the expression of CD44 isoforms in the airway epithelium of asthmatics have been documented. The epithelial cells of asthmatic bronchial biopsies show increased expression of CD44 proteins when compared to non-asthmatic subjects, as shown by a two-fold increase in expression on the basal cell membranes of asthmatics. In areas of damaged epithelium, changes in the pattern of expression are also seen with higher CD44 expression in areas of damage in both normal and asthmatic epithelium. This suggests a role for CD44 after damage has taken place rather than during the inflammatory process characteristic of asthma (73). In addition, in an *in vitro* study of bronchial epithelial repair CD44 expression was increased at the wound edge 12-48 hours following damage further implying a role for this cell adhesion molecule in epithelial repair (80).

1.4 Growth factors

Growth factors are extracellular signalling molecules that bind to cell surface receptors on a variety of cell types to stimulate cell proliferation. In addition growth factors are able to influence cell migration, survival, differentiation and function.

1.4.1 Epidermal Growth Factor

Epidermal growth factor (EGF) has multiple effects on epithelial, mesenchymal and stromal cells and regulates proliferation, apoptosis, cell motility, differentiation and dedifferentiation. It exerts these effects through its binding and activation of some members of the EGF receptor family, which have intrinsic tyrosine kinase activity.

EGF belongs to a family of ligands that includes heparin-binding EGF (HB-EGF), transforming growth factor-alpha (TGFα), amphiregulin (AR), betacellulin (BTC) and epiregulin. These ligands characteristically bind to the EGF receptor (EGFR), the prototype member of the c-erbB family and activate one or more of the members of the EGFR family by dimerisation. The EGF receptor family is made up of 4 members, EGFR (c-erbB1/HER1 (Human Epidermal growth factor Receptor), c-erbB2/HER2/ p185/neu, c-erbB3/HER3 and c-erbB4/HER4 (reviewed in (158)). Table 1.1 summarises the receptor specificity of the ligands for individual members of the EGF receptor family. In bronchial epithelial cell cultures the EGFR, c-erbB2 and c-erbB3 but not c-erbB4 are expressed (116).

The EGFR is tyrosine kinase linked which upon binding of ligand undergoes dimerisation to form a homodimer (with the same type of receptor) or a heterodimer with a different member of the EGF receptor family (see table 1.1). The receptors then cross-phosphorylate each other on tyrosine residues and these phosphorylated tyrosines act as docking sites for intracellular signalling molecules which are in turn phosphorylated on tyrosine and trigger downstream signalling pathways (158).

Ligands for the EGFR are synthesised as membrane-bound pre-cursor molecules then proteolytically cleaved by metalloproteinases to allow for activity at receptors (35). For example, HB-EGF is expressed on the cell surface as a membrane bound form where it can act as a juxtacrine growth factor. This transmembrane precursor molecule is proteolytically cleaved to release soluble, mature HB-EGF which can act as a paracrine or autocrine growth factor. In an *in vitro* assay matrix metalloproteinase-3 (MMP-3 or stromelysin-1) was able to cleave membrane bound HB-EGF at a specific juxtamembrane site (Glu151 and Asn 152) (137) and ADAM10 (a disintegrin and

Table 1.1. EGF receptor subtypes, their ligands and heterodimers formed.

EGF receptor family member	Ligands	Heterodimers formed	Other information
EGFR1 (c-erbB1)	EGF, TGF-α, HB-EGF, amphiregulin	c-erbB2 c-erbB3 c-erbB4	
c-erbB2	-	c-erbB3 c-erbB4	No known ligand
c-erbB3	Heregulin	c-erbB4	
c-erbB4	HB-EGF Betacellulin Neuregulin	c-erbB1 c-erbB2 c-erbB3	Lacks intrinsic tyrosine kinase activity. Not expressed by bronchial epithelial cells.

metalloproteinase) has also been implicated in membrane-bound growth factor processing (82).

1.4.2 Heparin-binding Epidermal Growth Factor

Heparin-binding epidermal growth factor (HB-EGF) was initially identified as a heparin-binding protein, which had mitogenic properties and was present in the conditioned medium of macrophage-like cells (54). Further characterisation of the structure of HB-EGF revealed an EGF-like domain and a hydrophilic region which might constitute a heparin-binding domain (55). The heparin-binding region was subsequently found to be a 21 amino acid sequence within this hydrophilic region (146). In addition to the EGFR, HB-EGF binds to and activates the c-erbB4 another member of the EGF receptor family (see section 1.4.1).

HB-EGF is able to bind to cell surface heparan sulphate proteoglycans (HSPGs), such as CD44v3 (see section 1.3.1.2), through its heparin-binding domain (14). Binding of this growth factor to the cell surface may have important implications as, unlike other EGF family growth factors, binding of the EGF-like domain of HB-EGF to the EGFR is not sufficient for optimal activity; and tyrosine phosphorylation of the EGF receptor by HB-EGF is enhanced in the presence of heparin (9) and optimal stimulation of smooth muscle cell migration by HB-EGF is dependent upon the interaction of HB-EGF with cell surface HSPG (53).

Other growth factors have also been shown to bind HSPGs. Fibroblast growth factors (FGF) α and β are also known to bind to HSPG and this appears to stabilise the interaction of FGF with its receptor (FGFR) (24), protect the growth factor from degradation and also establish a cell surface bound reservoir of FGF. Hepatocyte growth factor/scatter factor (HGF/SF) binds the heparan sulphate chains of CD44v3 and this interaction increases tyrosine phosphorylation of the HGF/SF receptor *c-met* above that seen in the absence of heparan sulphate (150).

Similarly, HB-EGF binding to a HSPG such as heparan sulphate modified CD44v3 may serve several functions, the HSPG may modulate growth factor function and provide a mechanism for growth factor recruitment at the cell surface to establish a

growth factor pool and gradient within a tissue or prevent degradation of the growth factor.

1.4.3 Growth factors in asthma and bronchial epithelial repair

Several lines of evidence suggest that the EGFR and its ligands could play a role in asthma. Bronchial biopsies obtained from asthmatic subjects show intense EGFR staining on basal cells within areas of epithelial damage (115) but a role for the receptor has not been identified. The enhanced staining in areas of damage suggest a role for the EGFR in the damage or repair of the bronchial epithelium. Additionally another study showed enhanced EGF immunoreactivity in submucosal cells of asthmatics and in areas of damaged epithelium (153). In skin wounds, HB-EGF, is found in the fluid bathing the wound (93), (99) and in scrape wounded intestinal epithelial cell cultures HB-EGF gene expression is increased (37), further indication of an involvement of the EGFR and its ligands in wounding and repair. EGF and HB-EGF have been shown to enhance migration of numerous cell types including keratinocytes (61), fibroblasts (159), endothelium (78), mesothelial (39), smooth muscle cell (53), corneal epithelium (167), intestinal epithelium (141) and lung epithelial cells (71), (84), (118). *In vivo* studies have confirmed a role for EGF in epithelial repair following smoke damage to sheep trachea (11) and after allergen challenge in guinea pig trachea (38). On a more cellular level EGF, stimulates changes in cell morphology (13) and the actin cytoskeleton (112) functions likely to be involved in repair.

Other growth factors have been implicated in repair of the epithelium. Keratinocyte growth factor (KGF/FGF7) stimulates epithelial cells to proliferate, migrate and differentiate and its expression is also markedly increased after injury to mouse skin (161). Transforming growth factor-beta (TGFβ) immunoreactivity is increased in the epithelium and submucosa of asthmatic bronchial biopsies when compared to normal subjects (153) as well as in the bronchoalveolar lavage (BAL) fluid of asthmatics (120). TGFβ1 treatment of tracheal epithelial cells stimulated cell spreading which was accompanied by reduced cell-cell and cell-substrate adhesion, actin reorganisation and increased migration suggesting that TGFβ1, by stimulating migration, may be important in epithelial repair (17), (60).

1.5 The actin cytoskeleton

The actin cytoskeleton along with microtubules and intermediate filaments provides a dynamic structural framework within cells. Formation of actin filaments, or fibrous (F) actin, involves elongation at the (+) end of the polar filament with unbound globular (G) actin, to form long rod-like structures and disassembly of these structures involves removal of actin at the (-) end of the filament. Filaments go onto form parallel bundles, stress fibres or mesh-like structures and in epithelial cells support adherens junctions and are found in lamellipodia, microvilli and microspike projections of the plasma membrane (2).

1.5.1 Involvement of actin in cell morphology, migration and repair

Actin filament re-organisation probably implements changes in cell morphology and motility essential for the initial step in bronchial epithelial repair which is proposed to be migration of columnar cells surrounding the wound to cover the basal cell layer. It has been shown by the use of inhibitors of elongation of actin microfilaments (e.g. cytochalasin) that actin microfilaments are necessary for migratory movement of cells (164).

The involvement of actin filaments in wound healing is well documented. Actin filaments are arranged in cable-like structures at the leading edge of circular wounds in corneal epithelial (34) and embryonic skin wounds (95), implicating a contractile 'purse string' mechanism of cell movement at the leading edge to co-ordinate repair of circular wounds. Alternatively, in adult wounds and other *in vitro* wound systems (78) the formation of flat extensions of the plasma membrane, termed lamellipodia, is seen at the leading edge of cells to allow directional migration of cells. Actin filament polymerisation along with recruitment of actin-binding proteins drives the formation of these structures preceding the onset of migration (reviewed in (133)).

1.5.2 Regulation of actin

The modulation of actin microfilaments in orchestrating cell motility, proliferation and differentiation is not fully understood. However, it is has been shown that actin has

several binding sites for actin-associated proteins of which at least 25 have been identified. These binding sites include sites for other microfilaments, G-actin, microtubules and myosin. It has been observed that bundles of microfilaments terminate at the plasma membrane but don't themselves bind to proteins of the membrane. There are several proteins that form an intermediate linkage between actin filaments and transmembrane proteins (such as CD44, ICAM) and these include α-actinin, vinculin, talin and ERM proteins. These linker proteins are able to influence assembly, disassembly, form and function of actin. Intracellular signals may also impinge on these actin-binding proteins and act as regulators.

1.6 ERM proteins

The ERM protein family comprises three homologous proteins - ezrin, radixin and moesin and are proposed to act as membrane-cytoskeletal linker proteins. These proteins are part of a larger family of proteins, the band 4.1 superfamily that includes the erythrocyte membrane-cytoskeleton linker protein band 4.1, merlin (schwannomin) and talin (6). ERM proteins have a molecular mass of around 70kDa (ezrin 69.4kDa, radixin 68.5kDa and moesin 67.8kDa) and human ERM proteins share 75-80% homology with each other. Their protein structure is made up of three domains, a membrane-protein binding amino-terminal globular domain, an α-helical structure and an actin-binding carboxy-terminal domain (figure 1.4).

ERM proteins are expressed in fibroblasts, epithelial cells and other cells where they are predominantly found in actin-rich membrane/cell surface structures such as microvilli (22) and cell-cell adhesion sites (138).

As discussed in section 1.5 modulation of the actin cytoskeleton is not fully understood. Signal transduction events that regulate actin cytoskeleton dynamics might in part act through membrane-cytoskeletal linker proteins such as ERM proteins to modulate cell morphology, migration and adhesion. These diverse functions suggests that ERM proteins are highly regulated and so far they have been shown to be phosphorylated on tyrosine or threonine by growth factor receptors, Rho, protein kinase C and following treatment with sodium cromoglycate (an anti-allergic drug).

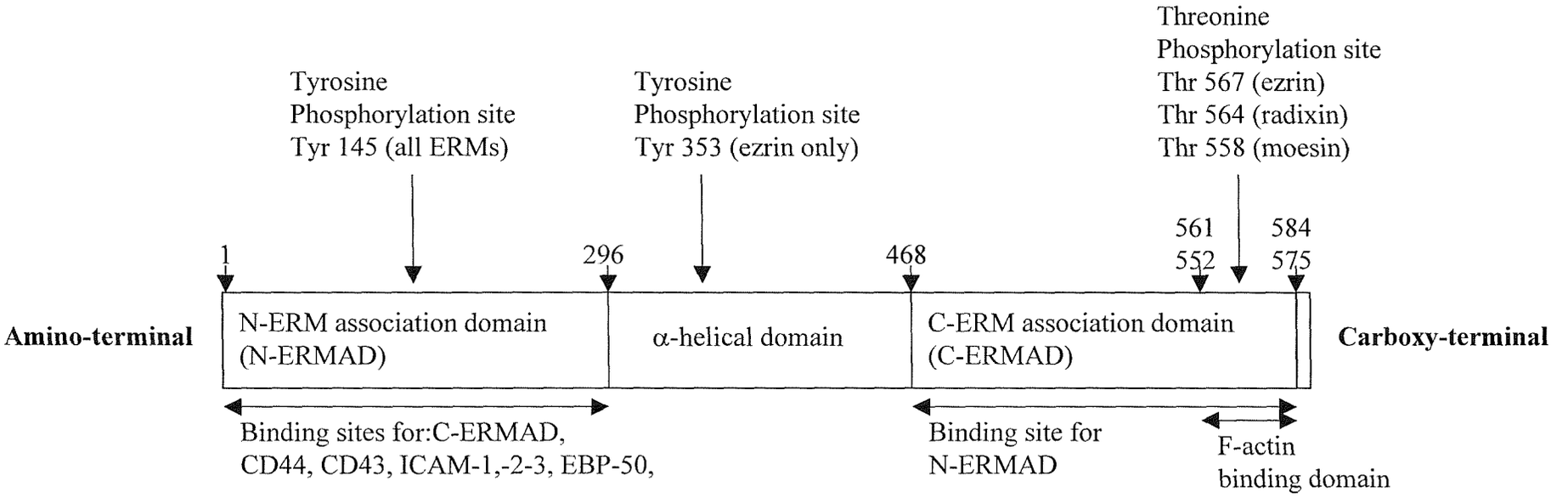

Figure 1.4. ERM protein structure.
Figure indicates functional binding domains and known threonine (Thr) and tyrosine (Tyr) phosphorylation sites. Ezrin and moesin share 74% sequence homology with identical sequences found predominantly in the N-ERM and C-ERM association domains. Ezrin and moesin comprise 577 and 586 amino acids respectively.

1.6.1 ERM binding proteins

ERM proteins are concentrated in actin-containing cell surface structures such as microvilli (22), suggesting they might interact with the proteins within these structures. This lead to the proposition that ERM proteins serve as membrane-cytoskeletal linker proteins by Gould *et al*, (45), who demonstrated that ezrin is found in an insoluble form in the A431, human vulval epidermoid carcinoma, cell line as if it was associated with the cytoskeleton. Studies looking at the co-localisation of ezrin in monkey kidney cells, confirmed its localisation beneath the plasma membrane and in actin containing cell surface structures and also showed that the protein is present in the detergent-insoluble fraction, further evidence that it interacts with the detergent-insoluble actin cytoskeleton (3). Additionally this group used truncated amino- and carboxy- terminal domains of ezrin to show that the amino- terminal domain is able to interact with the membrane and the carboxy- terminal domain with the cytoskeleton.

Once it had been established that one of the members of the ERM protein family, ezrin, had the ability to bind plasma membrane proteins and the actin cytoskeleton the search for plasma membrane binding partners of ERM proteins began. In baby hamster kidney cells immunoprecipitation with anti-CD44 monoclonal antibodies showed that all members of the ERM protein family are able to interact with the cell adhesion molecule CD44, additionally CD44 was co-localised with ERM proteins in these cells by immunofluorescence microscopy (148). This observation was confirmed in the mouse enamel organ where ezrin and radixin were co-localised with CD44 in microvilli (105), in active T lymphocytes where CD44 and moesin are co-immunoprecipitated (163) and in sections of cutaneous melanocytic tumours showing co-localisation of moesin and CD44 expression (62). ERM proteins have also been shown to interact with other transmembrane cell adhesion molecules such as CD43 (163), ICAM-1 (52), (127), ICAM-2 (52), (163), ICAM-3 (4), (127) and syndecan-2 (46).

The specific interaction of CD43, CD44 and ICAM-2 with the amino-terminal domain of ERM proteins has been examined in greater detail (163). In summary, it was shown that a positively charged (basic) 20-30 amino acid cluster in the cytoplasmic domain of these cell adhesion molecules is essential for binding to ERM proteins; addition of this domain to E-cadherin, a cell adhesion molecule that does not normally bind ERM

proteins, enabled co-localisation of this chimeric protein with ERM proteins at microvilli whereas a control chimeric protein without the positively charged domain had a diffuse cell surface distribution. This implies that it is the charged amino acid cluster rather than the specific cell adhesion molecule that is essential for ERM protein binding. Legg and Isacke, (79), went on to examine the putative ezrin binding site in CD44 and found that two clusters of basic amino acids in the membrane proximal region of the cytoplasmic domain of CD44 are required for binding.

In addition to the ability of the amino-terminal domain of ERM proteins to interact with the plasma membrane via a direct interaction with cell adhesion molecules, their amino-terminal domain has been shown to bind ERM-binding phosphoprotein 50 (EBP50) (119). EBP50 is a 50kD protein that is widely distributed in tissues, including the lung, and is particularly enriched in those containing polarised epithelia. Its protein structure contains two PDZ (PSD-95/DlgA/ZO-1-like) domains and these domains appear to mediate associations with the plasma membrane and be involved in the formation of multiprotein complexes beneath the plasma membrane. Therefore EBP50 could be a type of adapter protein linking ERM proteins to proteins other than cell adhesion molecules within the plasma membrane. For example in the lung EBP50 is localised to the apical surface of a human airway epithelial cell line (Calu-3) and associates with the cystic fibrosis transmembrane conductance regulator (CFTR) in *in vitro* binding assays (130).

The carboxy-terminal domain of ezrin has been shown to interact with the actin cytoskeleton (3). The actin-binding site on ezrin was subsequently localised to the end 34 amino acids of the carboxy-terminal of ezrin which has been demonstrated to be conserved in other members of the ERM protein family (149).

Taken together the membrane binding and actin binding data strongly suggest that ERM proteins act as membrane-cytoskeletal linkers.

As well as ERM proteins being bound and serving as membrane-cytoskeletal linkers these proteins are also found in an inactive, non-phosphorylated, soluble and unbound form in the cytoplasm where they are found as monomers, dimers (e.g. ezrin-ezrin) or heterodimers (e.g. ezrin-moesin) (22), (23). This self-association is enabled by head-

to-tail joining of distinct amino- and carboxy- terminal domains termed N- and C-ERMAD (ERM-association domain) (figure 1.4) and is likely to be regulated by unmasking and masking of these binding sites (42).

1.6.2 Activation and regulation of ERM proteins

As previously described, ERM proteins are found in cells in several forms, in an inactivated state (as momomers or dimers in head to tail association) where they are found in the cytoplasm or in an activated form where they are bound to actin and/or plasma membrane proteins.

The signals which regulate and activate ERM proteins have not been fully elucidated but it seems that regulatory signals could be divided into two types; firstly those that reduce the affinity of ERM proteins for each other i.e. break up the head-to-tail (amino- to carboxy- terminal domain) binding to allow ERM proteins to be free and unmask their binding sites and secondly those that then go on to activate ERM proteins to bind actin or plasma membrane proteins.

So far the involvement of tyrosine and threonine phosphorylation of ERM proteins has been described by the growth factors EGF and HGF/SF, as potential mechanisms of activation or regulation of ERM proteins.

1.6.2.1 Tyrosine phosphorylation

ERM protein activation was first described by Gould *et al,* (45), who showed that p81, a 81kDa protein which was phosphorylated on tyrosine residues after EGF treatment of A431 cells was homologous to ezrin. Following EGF treatment of A431 cells, ezrin was phosphorylated on tyrosine and threonine residues. The involvement of the EGF receptor tyrosine kinase was confirmed when it was shown that EGF treatment of A431 cells induced formation of microvilli, then membrane ruffles followed by rounding up of cells. These distinct morphological changes were accompanied by redistribution of ezrin into microvilli and membrane ruffle structures and its phosphorylation on tyrosine residues (23). In these cells, EGF has since been shown to stimulate the formation of ezrin oligomers which was coincident with the time course of microvilli assembly

suggesting that ezrin oligomerisation is an important step in the development of these structures (16). More recently, EGF has been shown to induce parallel changes in ovarian epithelial carcinoma cells, with an enhancement in tyrosine phosphorylation of ezrin along with the translocation of this protein to newly developed membrane ruffles and protrusions (29).

The potential tyrosine phosphorylation sites in all three members of the ERM protein family have been investigated (highlighted in figure 1.4). Tyr145 is common to ezrin, radixin and moesin and lies in the amino-terminal region of homology and is phosphorylated *in vitro* by the EGF receptor. An additional site, Tyr353, is also phosphorylated *in vitro* by EGF, but is found within the α-helical domain of ezrin only, and not radixin or moesin (72).

As well as the EGF receptor tyrosine kinase, other growth factors that act via tyrosine kinase receptors have been shown to activate ERM proteins. The hepatocyte growth factor/scatter factor (HGF/SF) receptor *c-met* has intrinsic tyrosine kinase activity and its activation leads to cell migration (scattering) and changes in cell morphology. Treatment of a colon epithelial cell line, HT115, with HGF/SF caused redistribution of ezrin to membrane ruffles and its phosphorylation on tyrosine residues (68). In a polarised kidney derived epithelial cell line (LLC-PK1) HGF/SF treatment stimulates tyrosine phosphorylation of ezrin and causes an enrichment of ezrin in the cytoskeletal fraction of these cells suggesting HGF/SF causes increased activation and binding of ezrin (33).

1.6.2.2 Threonine phosphorylation

ERM proteins are also phosphorylated on threonine residues by Rho (96), RhoA (129) and protein kinase C (PKC) -α (106) and -θ (114). The threonine phosphorylation site/s were examined and a single site was found to be located within the putative actin binding domain which is conserved in all ERM proteins and is Thr567 in ezrin, Thr564 in radixin and Thr558 of moesin (96).

The head-to-tail association of ERM proteins is thought to be important in regulating their activity and it is the carboxy-terminal end domain that is responsible for this

association. Threonine phosphorylation of ERM proteins has been shown in several systems to reduce the head-to-tail association of ERM proteins presumably to allow their interaction with actin and the plasma membrane. Matsui *et al,* (96), showed that phosphorylation of Thr564 of the recombinant carboxy-terminal half of radixin by Rho-kinase inhibited its binding to the amino-terminal half of radixin. However this did not affect its binding to actin filaments *in vitro* and it was speculated that Rho-kinase-dependent phosphorylation of ERM proteins does not activate (open) ERM proteins but stabilises the activated (opened) conformation. Similarly PKC-θ stimulated threonine phosphorylation of full length inactive ezrin and moesin inhibits the carboxy-terminal ERM-association domain (C-ERMAD) to expose the actin and EBP50 binding sites resulting in increased association with the actin cytoskeleton (132).

Treatment of moesin with protein phosphatase 2C *in vitro* has been shown to dephosphorylate Thr558 and prevent binding of moesin to filamentous actin (58) confirming the role of threonine phosphorylation in the regulation of moesin-actin binding.

1.6.2.3 Involvement of Rho

As members of the Rho-family GTPases are involved in actin cytoskeletal organisation, especially actin-plasma membrane association they might act in part through ERM proteins to do this. Expression of dominant active Rho-kinase in COS7 cells stimulated threonine phosphorylation of moesin, formation of apical microvilli-like structures and its recruitment into these structures, however when dominant-negative Rho-kinase was expressed in these cells these affects were not seen. Furthermore mutation of Thr558 to alanine in moesin prevented formation of microvilli-like structures even in the presence of dominant active Rho-kinase suggesting Rho-kinase threonine phosphorylation of moesin is essential for microvilli formation in these cells (110). Phosphorylation on Thr558 of moesin by RhoA has also been shown in neuronal cells (67), where ERM proteins are proposed to have a role in the development of neurones and their polarisation (111).

Other members of the Rho-family may also be important; RhoA activity in NIH3T3 cells stimulates the formation of apical membrane/actin protrusions and concentration

of ERM proteins in these structures as well as threonine phosphorylation of ERM proteins (129). Similarly, transfection of NIH3T3 or HeLa cells with constitutively active RhoA stimulated threonine phosphorylation of ERM proteins and induction of microvilli development (97).

Rho has been shown to regulate the association of ERM proteins with plasma membranes (121) and (122) and more specifically active Rho has been shown to be required for the formation of a CD44/ERM complex *in vitro* (56).

1.6.3 Function of ERM proteins

As it has been demonstrated that ERM proteins are able to crosslink actin filaments with the cytoplasmic domains of cell adhesion proteins, the function of these proteins is likely to relate to this binding. Hence, ERM protein research has concentrated on the role of these proteins as actin cytoskeleton and plasma membrane linkers in modulating cell morphology, motility and cell-cell and cell-substrate adhesion.

1.6.3.1 Cell morphology and differentiation

ERM proteins were initially shown to be present in the microvilli of intestinal epithelial brush border cells (22) and their presence in other plasma membrane cell surface structures such as microspikes (94), lamellipodia (76), filopodia and membrane ruffles (23) has since been shown. Functional analysis of ERM proteins has confirmed their role in the formation of these structures and overexpression of the carboxy-terminal domain of ezrin in insect cells caused cell spreading followed by formation of microspikes and lamellipodia (94) whereas suppression of ERM proteins using antisense oligonucleotides lead to the disappearance of microvilli-membrane structures in thymoma and mouse epithelial cells (138). As well as epithelial cells, ERM proteins are also crucial for differentiation and polarisation of fibroblasts (129) and neuronal cells (111).

In lung epithelial cells their distribution and function have not been widely studied. Staining of polarised bronchial epithelial cell cultures shows ezrin is localised to the apical membrane domain (101), (136). The apical distribution of ezrin in normal

undamaged tissue and polarised cell cultures has lead to suggestions of functions in cilia formation (77) and in anchoring the apically expressed CFTR (cystic fibrosis transmembrane conductance regulator) to the cytoskeleton (130).

1.6.3.2 Cell motility

During epithelial repair, cellular migration and motility are essential processes for regeneration and likely involve changes in cell adhesion and the actin cytoskeleton through as yet undetermined mechanisms. ERM proteins might act in part as regulators of these processes. Hepatocyte growth factor/scatter factor (HGF/SF) induces scattering and migration of epithelial cell monolayers and it has been shown that HGF/SF stimulated epithelial repair of a wounded subconfluent monolayer of LLC-PK1 kidney epithelial cells is enhanced in cells overproducing ezrin suggesting its involvement in HGF/SF mediated cell motility (33). In wounded carcinoma cells, ezrin is concentrated in plasma membrane protrusions at the wound edge and PKCα regulated migration is dependent upon ezrin phosphorylation on threonine residues (106).

1.6.3.3 Cell adhesion

ERM proteins are localised to sites of cell-cell and cell-substrate adhesion indicating their involvement in these structures. In mouse epithelial cells expression of anti-sense oligonucleotides complementary to ERM protein sequences resulted in loss of cell-cell and cell-substrate adhesion along with loss of microvilli surface structures (138). Conversely overexpression of either full length, carboxy-terminal or the amino-terminal domain of ezrin enhanced cell-cell adhesion of insect cells (94). These data demonstrated the role of ERM proteins in cell-cell and cell-substrate adhesion.

1.6.3.4 Apoptosis

Studies looking at tubulogenesis of a kidney derived cell line indicated that ezrin plays a role in cell survival. Ezrin interacts with p85, the regulatory subunit of PI3-kinase, to activate protein kinase Akt, which protects cells from apoptosis. In the kidney cell line LLC-PK1, overproduction of a mutant ezrin (tyrosine 353 to phenylalanine) prevented

activation of Akt and the cells underwent apoptosis when they were assayed for tubulogenesis (43).

1.6.3.5 Mast cells

The anti-allergic drug sodium cromoglycate (see section 1.7) inhibits mast cell secretion by an unknown mechanism but is assumed to involve stabilisation of the plasma membrane to inhibit release of mediators. When mast cells are treated with sodium cromoglycate *in vitro* there is phosphorylation of a 78kDa protein (143), (160) which was later characterised as moesin (31) and shown to be phosphorylated on threonine residues. Phosphorylation of moesin by this mechanism caused enhanced binding of moesin to actin and its association with actin at the plasma membrane and around secretory granules (144). This was speculated to stabilise the actin cytoskeleton to provide a rigid structure under the plasma membrane and prevent exocytosis of secretory granules by mast cells.

1.7 Sodium cromoglycate

Sodium Cromoglycate (chemical name: 1,3-bis-(2-carboxychromone-5-yloxy)-2-hydropropane) is also referred to as cromone, cromolyn sodium, disodium cromoglycate or sodium cromolyn (reviewed in (36), (128)). Sodium cromoglycate and another structurally related compound, nedocromil sodium are used in the treatment of asthma and allergic diseases. Pharmacologically they are able to inhibit histamine secretion by mast cells and reduce bronchial hyper-responsiveness, possibly through a reduction in pro-inflammatory mediators present in the airway (98), however they do not exhibit any broncodilator activity. There is also evidence that sodium cromoglycate enhances dermal wound repair (unpublished observations, Alan Edwards) an effect which might translate into the airway epithelium.

1.8 Aims

Epithelial repair is likely to involve the regulation of cell adhesion, morphology, motility and proliferation and Epidermal growth factor (EGF) and its receptor (EGFR) have pleiotropic effects on cells and likely orchestrate, at least in part, repair processes through changes in cell motility, adhesion and proliferation. Therefore its role in these processes will be examined here.

The regulation of cell adhesion molecule expression could be important during repair, and the initial aim of this study was to examine the expression of the cell adhesion molecule CD44 and to determine whether its expression was regulated by the EGFR ligands, EGF and HB-EGF, in human bronchial epithelial cells.

The EGF receptor tyrosine kinase has also been shown to elicit changes in cell morphology and to influence ERM protein activation and localisation. ERM proteins could regulate repair processes through the regulation of actin-filament-plasma membrane interactions. The ERM proteins, ezrin and moesin were investigated to determine the role of EGF and HB-EGF in the regulation of these proteins in bronchial epithelial cells. Here, the influence of EGF on the distribution and binding of ERM proteins in human bronchial epithelial cells was studied with a view to understanding the role that these cytoskeletal linker proteins might have in bronchial epithelial repair.

I therefore hypothesise that ERM proteins are involved in transduction of EGF-stimulated bronchial epithelial repair through their phosphorylation and activation leading to modulation of cell shape and motility.

2 CHAPTER TWO

MATERIALS AND METHODS

2.1 MATERIALS

Reagents were obtained from Sigma, Poole, Dorset, UK, unless otherwise stated.

2.1.1 General reagents

Mowiol mountant was obtained from Harlow Chemical Company, Harlow, Essex, UK and 1,4-Diazabicyclo-[2.2.2] Octane (DABCO) was obtained from Sigma, Poole, Dorset, UK. MicroBCA protein assay kit was purchased from Pierce and Warringer (UK) Ltd, Chester, UK. Hank's Balanced Salt Solution (HBSS) with $Ca^{2+}$and Mg^{2+} was obtained from GibcoBRL, Life Technologies, Paisley, UK. Mayer's Haematoxylin was obtained from Sigma. Crystal mount was purchased from Biomedia Biogenesis, Poole, UK.

2.1.2 Cell culture cell lines and reagents

NCI-H292 and A431 cells were obtained from the American Type Culture Collection and 16HBE 14o- cells were a gift from Dr. D. C. Gruenert (49). Minimum Essential Medium (MEM), RPMI-1640, Dulbecco's Modified Eagle Medium (DMEM), FBS (heat inactivated), L-glutamine (200mM/100x), penicillin-streptomycin solution (5000 IU/ml penicillin-5000µg/ml streptomycin), 100mM sodium pyruvate, 100x non-essential amino acid solution (MEM), 10x trypsin-EDTA solution, HBSS without Ca^{2+}, Mg^{2+} and L15 medium without sodium bicarbonate were all obtained from GibcoBRL, Life Technologies, Paisley, UK. UltraCulture serum free medium was obtained from BioWhittaker UK Ltd, Wokingham, Berkshire, UK. Bronchial epithelial growth medium (BEGM) and bullet kit supplements were obtained from Clonetics, BioWhittaker UK Ltd, Wokingham, Berkshire, UK. Collagen type I solution was obtained from Sigma, Poole, Dorset, UK. Trypan blue was obtained from Flow Laboratories, UK. Nunclon Surface cell culture flasks, petridishes, 96-well culture

plates and Lab-Tek II RS glass 8-well chamber slides were all obtained from GibcoBRL, Life Technologies, Paisley, UK.

2.1.3 Recombinant Growth Factors

Recombinant human Epidermal Growth Factor was obtained from GibcoBRL, Life Technologies, Paisley, UK. Recombinant human Heparin binding Epidermal Growth Factor was purchased from R&D Systems, Oxford, UK. Tyrphostin AG1478 was obtained from Biomol Research Labs (Affiniti Research Products Ltd, Exeter, UK). Sodium cromoglycate was purchased from Sigma, Poole, Dorset, UK.

2.1.4 Immunological reagents

For immunocytochemistry, anti-CD44 standard (clone 25-32) was purified from hybridoma supernatant and supplied by Dr S-H Leir. The 25-32 CD44s hybridoma was grown in Dulbecco's Modified Eagle Medium (DMEM) containing 10% FBS in a miniPERM bioreactor (Heraeus Instruments GmbH, Germany) at high cell density. Half of the culture medium was replaced every 2 days. Culture supernatants were collected and antibodies purified by protein A affinity column with MAPS II buffer system (BioRad Labs Hemel Hempstead, Herts, UK) to enhance the affinity of protein to protein A. The antibody against CD44v3 was purchased from R&D Systems, Abingdon, Oxon, UK. Mouse monoclonal ezrin and moesin antibodies used for immunocytochemistry were obtained from Transduction Laboratories (distributed by Becton and Dickinson, Cowley, Oxford, UK). Goat polyclonal ezrin and moesin antibodies used for double immunocytochemical staining were Santa Cruz Biotechnology products (distributed by Autogen Bioclear, Devizes, Wiltshire, UK).

Secondary anti-mouse -FITC and -TRITC conjugated antibodies were obtained from Dako Ltd (High Wycombe, Bucks, UK). The cross-absorbed FITC-conjugated anti-goat antibody used for double staining was a Jackson ImmunoResearch Laboratories Inc., product (distributed by Stratech Scientific Ltd., Luton, Bedfordshire). For negative controls Mouse IgG_1 and mouse IgG_{2B} were both purchased from Dako Ltd and goat serum was from Sigma, Poole, Dorset, UK.

For Western blotting anti-CD44, clone Hermes-3 was a gift from Dr. S. Jalkanen (64). Anti-CD44v3 was obtained from Chemicon International Ltd, Harrow, UK. Anti-phosphotyrosine-biotin, PY20-agarose and mouse monoclonal antibodies against ezrin and moesin were all Transduction Laboratories products. Anti-ezrin and moesin goat polyclonal antibodies were from Santa Cruz biotechnology. Anti-actin was obtained from Sigma Poole, Dorset, UK. Anti-EGFR (sheep 529) was raised using affinity purified EGFR's from A431 squamous carcinoma cells. The antibody was an IgG fraction prepared by ammonium sulphate precipitation and DEAE cellulose ion exchange chromatography and was supplied by Dr A. Richter.

Secondary rabbit anti-mouse, rabbit anti-goat, rabbit anti-sheep and swine anti-rabbit horseradish peroxidase (HRP) antibodies were all obtained from Dako Ltd (High Wycombe, Bucks, UK). Streptavidin-biotinylated HRP complex was obtained from Amersham Pharmacia Biotech, Little Chalfont, Bucks, UK.

2.1.5 SDS-PAGE and Western blotting Reagents

Acrylamide/bis-acrylamide was purchased from National Diagnostics (Hull, UK). Kaleidoscope Prestained standards gel markers were obtained from BioRad Labs (Hemel Hempstead, Herts, UK). Hybond-C nitrocellulose membrane, ECL Plus and Hyperfilm ECL were purchased from Amersham Pharmacia Biotech. Skimmed milk powder was from Marvel. Tween-20 and Nonidet P40 (NP40) detergents are NSB products and were obtained from Amersham Pharmacia Biotech (Little Chalfont, Bucks, UK).

2.2 METHODS

2.2.1 Cell Culture

2.2.1.1 Cell lines and Primary cells

NCI-H292 is a lung epithelial carcinoma cell line, 16HBE 14o- is an SV-40 large T antigen transformed human bronchial epithelial cell line and A431 is a vulval epidermoid carcinoma cell line. Primary bronchial epithelial cell cultures (passage 2-3) established from bronchial brushings were gifts from Dr J. Lordan, Dr S. Puddicombe and Dr A. Richter; the purity of these cells was checked by staining samples for epithelial cell markers, cytokeratins 13 and 18.

Primary bronchial epithelial cells were also grown up from bronchial explants from surgically resected lung. Following surgical resection tissue was stored in L15 medium without sodium bicarbonate until dissection. To dissect, the tissue was examined under a light microscope to orientate the epithelium and once established the epithelium was removed from the basement membrane using a fine scalpel. The epithelium was then cut up into small squares (1-2mm^2) before positioning 1 or 2 squares of tissue with the epithelium facing downwards in each well of a 6-well culture plate. Tissue pieces were then left to dry to allow adherence of the tissue to the plastic before carefully pipetting a drop of medium onto each piece of tissue, to cover. After 1-2 hours 1ml of medium was added to each well. Explants were fed every 2-3 days until wells were around 50% confluent when tissue pieces were transferred to new plates and cells were trypsinised for experiments.

2.2.1.2 General cell maintenance

All cell culture work was carried out in a Microflow Class II Biological safety cabinet (MDH Ltd) and cells maintained in Heraeus incubators (Heraeus Instruments GmbH, Germany) at 37°C, 5% (v/v) $C0_2$ in a humidified atmosphere.

Cells were routinely cultured in 80cm^3 culture flasks. NCI-H292 cells were cultured in RPMI-1640 medium containing 10% (v/v) FBS, 2mM L-glutamine, 50UI/ml penicillin and 50μg/ml streptomycin. 16HBE 14o- cells were cultured in MEM (Minimum

Essential Medium with Earle's Salts, 25mM HEPES) containing 10% (v/v) FBS, 2mM L-glutamine, 50UI/ml penicillin and 50µg/ml streptomycin. A431 cells were cultured in DMEM (Dulbecco's Modified Eagle Medium) containing 10% (v/v) FBS, 2mM L-glutamine, 50UI/ml penicillin and 50µg/ml streptomycin, 1mM sodium pyruvate and 1x non-essential amino acids (MEM). For cell lines growth medium was replaced every 2-3 days with 10mls fresh medium per medium flask until confluency was reached which took 3-4 days for NCI-H292 and 5-7 days for 16HBE 14o- and A431 cells when split at a ratio of 1:4-1:10, cells:medium.

Primary cell cultures were grown in bronchial epithelial growth medium (BEGM) prepared by the addition of Bullet kit supplements to BEBM to give final concentrations of 52µg/ml bovine pituitary extract, 0.5µg/ml hydrocortisone, 0.5ng/ml human EGF, 0.5µg/ml epinephrine, 10µg/ml transferrin, 5µg/ml insulin, 0.1ng/ml retinoic acid, 6.5ng/ml triiodothyronine, 50ng/ml amphotericin-B and 50µg/ml gentamicin in BEBM. Growth medium was replaced every 2 days until cells reached 90% confluency when cells were split in a ratio of 1:4, cells:medium.

2.2.1.3 Trypsinisation of cell monolayers

Upon confluence cell monolayers were detached from their flask to yield a single cell suspension using the following trypsinisation protocol. Following removal of growth medium the cell monolayer was washed twice with 5ml HBSS (without Ca^{2+}, Mg^{2+}) to remove residual FBS which inhibits trypsin. 1ml of 10x Trypsin-EDTA was diluted with 9ml of HBSS (without Ca^{2+}, Mg^{2+}) and a small volume (1-2mls) of this 1x trypsin-EDTA solution was added to the flask to just cover the cells. This was incubated for 5-10 minutes in the incubator until the cells had rounded up. The flask was then tapped gently on the workbench to aid the detachment of cells. Once a single cell suspension was established trypsin was inhibited by adding 10mls of cell medium containing 10% FBS. This suspension was transferred to a 20ml Universal tube and centrifuged for 5mins, at 600xg to obtain a cell pellet. The supernatant was then discarded and the cell pellet resuspended in appropriate medium containing 10% FBS or BEGM for primary cells. Viable cells were then counted using the trypan blue exclusion method (see

2.2.1.4 below) and plated for experiments and an aliquot of cell suspension used to inoculate a flask ($80cm^3$) of medium in a ratio of 1:4-1:10 (v/v) cells:medium.

2.2.1.4 Trypan blue counting of cells in suspension

Trypan blue solution was used to assess the viability of cells by their ability to exclude the blue dye. Briefly, a 200µl aliquot of the cell suspension was centrifuged at 600xg for 2 minutes. The cell pellet was resuspended in 200µl of HBSS to which 200µl of trypan blue solution (0.5% (v/v) trypan blue in 0.85% saline solution) was added (giving a dilution factor of 1:2). An Improved Neubauer haemocytometer (depth 0.1mm) was used to count viable cells. The total number of cells excluding trypan blue in the $1mm^2$ middle square was counted twice an average taken and the following equation used to calculate the number of cells per ml:

Viable cells per ml = Number of cells in middle square x dilution factor (2) x 10^4

Cells were then diluted in culture medium to the required density and plated down into appropriate dishes, plates or slides for experiments.

2.2.1.5 Long-term cryopreservation of cells

In order to build up stocks of cell lines, cells were preserved in liquid nitrogen and regenerated when necessary. Following trypsinisation of cell monolayer, the single cell suspension was centrifuged and the cell pellet resuspended in 1ml of culture medium containing 10% FBS and 10% dimethylsulphoxide (DMSO) which acted as a cryoprotectant. This cell suspension was then placed into a cryotube and chilled slowly to minimise cell damage, the tubes were wrapped in cotton wool and placed at -20°C for 30 minutes then -70°C overnight before placing in the liquid nitrogen storage tank at -180°C for long term cryogenic storage.

To regenerate frozen cells, prewarmed culture medium was pipetted into the cryotube to dilute the DMSO and rapidly thaw the cells. The defrosted cell suspension was then transferred to a new $80cm^3$ flask containing 20mls of medium and placed in the

incubator at 37°C. Cells were allowed to attach for 6 hours before changing the medium to remove any residual DMSO.

2.2.1.6 Serum starving and stimulation of cells with growth factors, growth factor inhibitors or sodium cromoglycate

Prior to experimental stimulation with EGF, HB-EGF, tyrphostin or sodium cromoglycate, cell cultures were serum starved for 24 hours using a serum free medium (UltraCulture containing 2mM L-glutamine, 50UI/ml penicillin and 50μg/ml streptomycin). This step aimed to render the cells quiescent by elimination of residual growth factors derived from the FBS in the medium. For primary cell cultures, which were not cultured in serum, cells were cultured in basal BEBM (BEBM containing 1% insulin-transferrin-sodium selenite) for 24 hours before experiments to deplete EGF and other growth factors.

For experiments cells were treated with 1nM (6ng/ml), 5nM (30ng/ml) or 17nM (100ng/ml) recombinant human epidermal growth factor or 1nM (9ng/ml) recombinant human heparin binding epidermal growth factor. The EGF receptor tyrosine kinase inhibitor, tyrphostin AG1478 was used at a concentration of 1μM where it is selective for the EGF receptor tyrosine kinase (85). When using tyrphostin, a DMSO treated control was also used as tyrphostin was dissolved in DMSO. For this control, DMSO was diluted to 1 in 20,000 in UltraCulture which is the equivalent concentration of DMSO in 1μM tyrphostin. Growth factors and inhibitors were diluted for experiments in UltraCulture or basal BEBM medium for cell lines or primary cells respectively. Sodium cromoglycate was first prepared as a 100mM solution in PBS before further diluting in UltraCulture or basal BEBM to 100μM for use in experiments.

2.2.2 Methylene blue assay

The methylene blue uptake assay was developed as a measure of proliferation following the observation that there is a linear correlation between absorbance of the dye and cell number (108). The assay was used here to determine the effect of FBS,

EGF, HB-EGF and tyrphostin AG1478 on the proliferation of 16HBE 14o- and NCI-H292 cells.

Cells were plated overnight with 10% FBS to allow cells to attach prior to starting the assay. 100µl of cell suspension ($2.5x10^5$ cells/ml of 16HBE 14o- cells and $6x10^4$ cells/ml of NCI-H292 cells) was used to seed each well of a 96-well plate. The following day, day 0 of the assay, the medium was changed to UltraCulture serum free medium +/- 10% FBS, 1nM EGF, 1uM tyrphostin (AG1478) or 1 in 20,000 DMSO control to assess the proliferative effect of these growth factors and the inhibitor.

Cells were fixed at days 0, 1, 3, 5 and 7, following removal of medium, with 200µl/well of formol saline (4% formaldehyde, 0.9% saline) for a minimum of 30 minutes. Fixative was removed and plates were blotted dry. Cells were then stained for 30 minutes with 100µl per well of 1% methylene blue dye in 0.01M borate buffer, pH 8.5. Excess dye was washed off with tap water before blotting dry on absorbent paper. To release bound dye from within cells, plates were incubated with 100µl per well of acidified ethanol, 1:1 (v/v) ethanol and 0.1M HCl, for 30 minutes. Plates were shaken gently before reading the absorbance of samples at 630nM on a microplate spectrophotometer. As this assay is linear up to 1.0 OD some samples were diluted into acidified ethanol appropriately, OD values were then multiplied by the dilution factor to normalise. Data was analysed using Sigma Plot and Microsoft Excel and Student's unpaired *t*-test used to determine differences between treatments.

In order to relate optical density to cell number a standard curve was generated (figure 2.1) by plating cells at a range of densities ($1x10^6$–$3x10^4$ cells/ml) on duplicate plates. One plate was assayed using the methylene blue method. The cells in the individual wells of the second plate were counted using the trypan blue exclusion method (see 2.2.1.4) to determine the number of viable cells. Cell number was then plotted on the x-axis, against absorbance at 630nm of methylene blue on the y-axis. The standard curve could then be used to estimate cell number from a value for absorbance at 630nm (see figure 2.1 for standard curve).

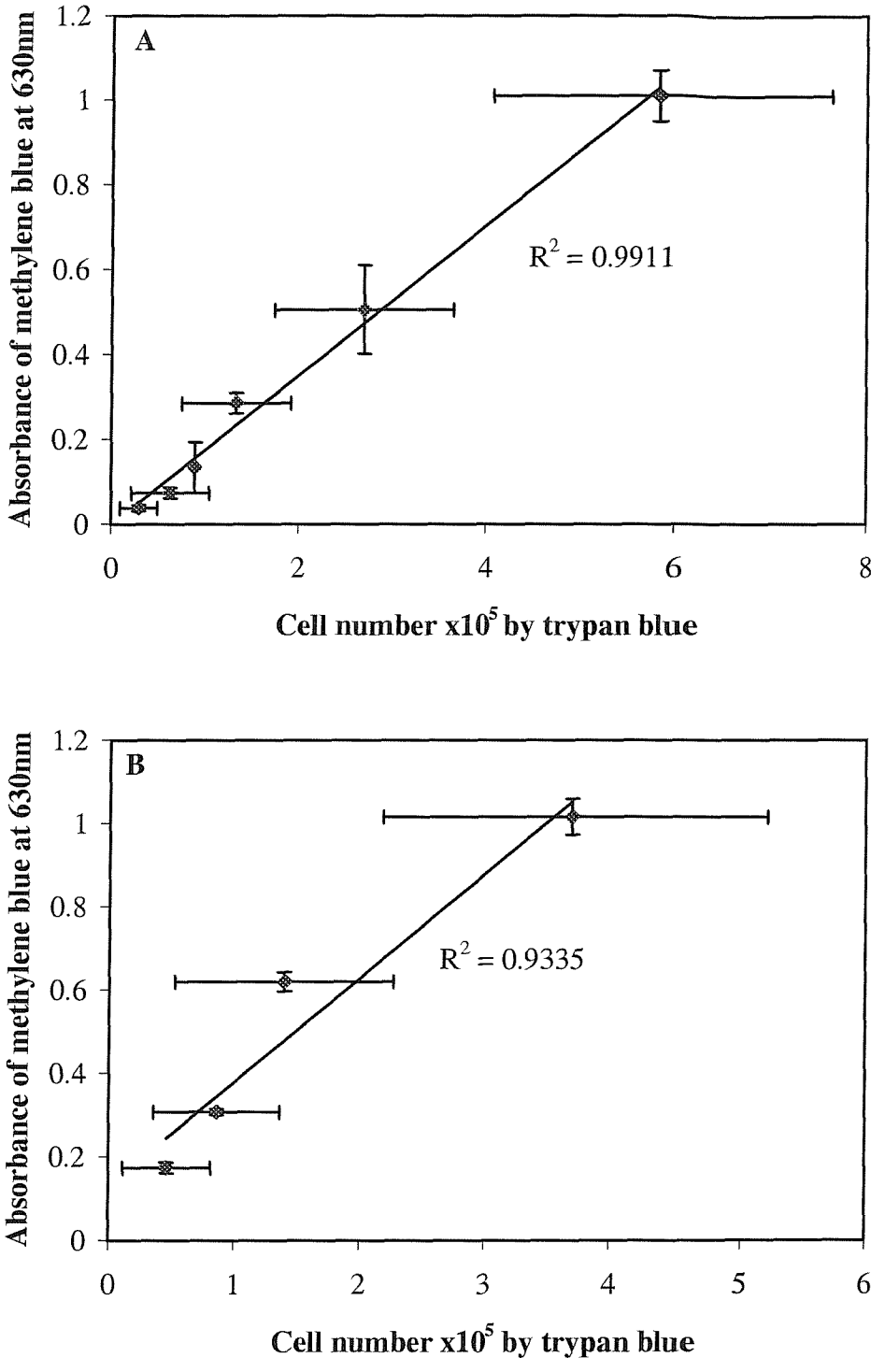

Figure 2.1. Methylene blue standard curves for NCI-H292 (A) and 16HBE 14o- (B) cells.

Absorbance of methylene blue at 630nm is plotted against cell number determined by exclusion of trypan blue dye. Data are the mean of three repeats within a single experiment+/– standard deviation.

2.2.3 Collagen coating of slides

Chamber slides were coated with collagen type I solution to assess the effect of extracellular matrix substrate on ezrin and moesin distribution. 0.1% collagen type I solution was diluted 100x with sterile PBS to give a solution of 0.001% (10μg/ml) collagen. Slides were coated with 200μl of this solution and incubated for 1 hour at 37°C. The collagen solution was pipetted off and discarded prior to plating cells on the coated slides.

2.2.4 Fixation of cells

Cells cultured on chamber slides for immunocytochemistry were treated with growth factors, inhibitors or sodium cromonoglycate then washed twice with PBS prior to fixation. Cells were fixed in cold (-20°C) methanol for 10 minutes and then left to air dry for approximately 10 minutes. After removal of the chamber from the slides, they could be wrapped in aluminium foil and stored at -20°C. Slides were stored for up to 2 months prior to staining.

2.2.5 Immunocytochemistry

Prior to staining for CD44, CD44v3, ezrin or moesin, cells were rehydrated in PBS and then blocked for 10 minutes with 1% BSA in PBS (50μl per chamber). Primary antibodies were diluted (see table 2.1) into 0.1% BSA in PBS and incubated with the fixed cells for 1 hour at room temperature in a humidified chamber. Two controls were carried out, firstly omission of primary antibody where cells were incubated with 50μl of 0.1% BSA in PBS and secondly incubation with an irrelevant antibody control at the equivalent IgG concentration of the primary antibody. Following incubation, cells were washed with PBS three times for 5 minutes each. The secondary anti-mouse FITC conjugate, diluted 1 in 80 into 0.1% BSA in PBS, was incubated for 1 hour in the dark. After PBS washes, slides were mounted using coverslips with a solution of 9% Mowiol, 23% glycerol and 0.09M Tris pH 8.5 containing 2.5% DABCO as an antifading agent. After the mountant had hardened overnight, slides could be observed

Table 2.1. Primary and secondary antibodies used for single staining immunocytochemistry

Antigen	Class	Source	Dilution	Secondary antibody
CD44 standard (clone 25-32)	Mouse monoclonal IgG_1	Hybridoma	1 in 100	FITC-conjugated $F(ab')_2$ fragment of Rabbit anti-mouse immunoglobulins (Dako) 1 in 80 dilution
CD44v3 (clone 3G5)	Mouse Monoclonal IgG_{2B}	R&D Systems, UK	1 in 100	
ezrin (clone 18)	Mouse Monoclonal IgG_1	Transduction Laboratories, UK	1 in 50	
moesin (clone 38)	Mouse monoclonal IgG_1	Transduction Laboratories, UK	1 in 100	

Table 2.2. Primary and secondary antibodies used for double immunocytochemical staining

Antigen	Class	Source	Dilution	Secondary antibody
CD44 standard (clone 25-32)	Mouse monoclonal IgG_1	Hybridoma	1 in 100	TRITC-conjugated Rabbit anti-mouse immunoglobulins (Dako) 1 in 80 dilution
ezrin (clone 15)	Goat polyclonal	Santa Cruz Biotechnology	1 in 25	FITC-conjugated AffiniPure $F(ab')_2$ fragment of Donkey anti-Goat immunoglobulins 1 in 100
moesin (clone 15)	Goat polyclonal	Santa Cruz Biotechnology	1 in 50	

Table 2.3 Typical double staining protocol indicating primary and secondary antibodies and relevant controls

Stain	Antigen A primary antibody	Antigen A secondary antibody	Antigen B primary antibody	Antigen B secondary antibody
Double stain CD44 and Ezrin	anti-CD44 antibody (25-32, mouse monoclonal, IgG1)	anti-mouse TRITC-conjugate	anti-Ezrin antibody (clone 15, goat polyclonal)	anti-goat FITC-conjugate
Isotype / serum controls	Mouse IgG1 negative control	anti-mouse TRITC-conjugate	anti-Ezrin antibody	anti-goat FITC-conjugate
	anti-CD44 antibody	anti-mouse TRITC-conjugate	Goat serum	anti-goat FITC-conjugate
Crossover controls	anti-CD44 antibody	0.1% BSA/PBS	0.1% BSA/PBS	anti-goat FITC-conjugate
	0.1% BSA/PBS	anti-mouse TRITC-conjugate	anti-Ezrin antibody	0.1% BSA/PBS
Omission of primary antibodies control	0.1% BSA/PBS	anti-mouse TRITC-conjugate	0.1% BSA/PBS	anti-goat FITC-conjugate
Single CD44 staining	anti-CD44 antibody	anti-mouse TRITC-conjugate	0.1% BSA/PBS	0.1% BSA/PBS
Single ezrin staining	0.1% BSA/PBS	0.1% BSA/PBS	anti-Ezrin antibody	anti-goat FITC-conjugate

under a Leica immunofluorescent microscope. Some experiments were viewed using a Leica confocal scanning laser microscope.

2.2.6 Double staining

Double immunocytochemistry was used to assess the co-localisation of two proteins and required the employment of primary antibodies directed against the individual proteins that were raised in different species. An appropriate secondary antibody against each species of primary antibody conjugated to either -FITC or -TRITC fluorochromes could then used to distinguish the molecules (see table 2.2 for primary and secondary antibodies utilised here). Several controls were also required to ensure specific staining of antigens (see table 2.3 for a typical double staining protocol and controls used). Isotype or serum controls were used to ensure that secondary antibodies did not bind non-specifically to other proteins in the cell preparation. The crossover control was carried out to check for cross-reactivity between a secondary antibody directed against one species and the primary antibody of another species, the use of pre-adsorbed secondary antibodies minimises cross-reactivity. Single staining was carried out to confirm that there was no merging of fluorochrome.

As for single immunofluorescent staining, cells fixed in methanol were rehydrated in PBS and then blocked for 10 minutes with 1% BSA in PBS (50µl per chamber). For double immunocytochemical staining the two primary antibodies against different proteins were diluted and prepared as a mixed solution in PBS containing 0.1% BSA (see table 2.2 for details), the relevant controls were also prepared in this way and incubated with the fixed cells for 1 hour at room temperature in a humidified chamber. Following incubation cells were washed with PBS three times for 5 minutes each. Secondary antibodies were diluted together in a solution of 0.1% BSA/PBS and incubated with the cells for 1 hour, in a humidified chamber in the dark. After PBS washes (3 times for 5 minutes each), slides were mounted using coverslips with a solution of 9% Mowiol, 23% glycerol and 0.09M Tris pH 8.5 containing 2.5% DABCO as an antifading agent. After the mountant had hardened overnight, slides could be observed on a Zeiss immunofluorescent microscope and images were taken using a colour video camera and the Zeiss Image analysis system software used to merge

images of the staining. Double staining was also observed using a Leica confocal scanning laser microscope.

2.2.7 Flow cytometry

Flow cytometry (FACS) analysis enabled the measurement of cell surface expression of CD44 and CD44v3. A suspension of single cells was prepared before incubation with an antigen specific primary antibody followed by a secondary FITC conjugated antibody. Samples could then be analysed by passing through a flow cytometer or FACS machine, which measures the fluorescent intensity of each individual cell. These intensities are converted to dot plots or histograms by the PC Lysys software, which is then able to calculate median fluorescent intensity values.

NCI-H292 and 16HBE 14o- cells grown in 57cm^2 petridishes to 60% confluence were serum starved for 24 hours before culturing for 24 hours in UltraCulture serum free medium with or without 10% FBS, 1nM EGF or HB-EGF at the end of which cells were around 90% confluent. To assess the affect of cell density NCI-H292 cells were plated at high cell density (1x10^5 cells per ml) or low cell density (1x10^4 cells per ml) and cultured for 3 days. A 24 hour period of serum starvation was followed by stimulation for 24 hours with UltraCulture serum free medium with or without 10% FBS, 1nM EGF or HB-EGF. At the end of the period of stimulation cells plated at high cell density were around 95% confluent and those plated at low cell density had reached around 60% confluency.

A single cell suspension was obtained by washing the cell monolayer with HBSS (w/o Ca^{2+} and Mg^{2+}) and incubating with cell dissociation solution (Sigma) for 20-30 minutes at 37°C, 5% (v/v) CO_2. Cells were collected and washed with FACS medium (HBSS with Ca^{2+} and Mg^{2+}, 2% FBS and 0.1% NaN_3) and the cell concentration adjusted to 2 x 10^6 cells/ml with FACS medium.

Throughout the following staining procedure all samples and buffers were stored on ice or at 4°C. 100µl of cell suspension was aliquoted into tubes for the immunostaining step. Primary antibodies to CD44 and CD44v3 were diluted into FACS medium (see

Table 2.4. Primary and secondary antibodies used for flow cytometry

Antigen	Class	Source	Dilution	Secondary antibody
CD44 standard (25-32)	Mouse Monoclonal IgG_1	Hybridoma	1 in 40	Rabbit α-mouse FITC conjugate (Dako) 1 in 80 dilution
CD44v3 (Clone 3G5)	Mouse Monoclonal IgG_{2B}	R&D Systems, UK	1 in 250	

Table 2.4) and 30µl aliquoted into appropriate tubes which were then incubated for 30-45 minutes on ice to allow antigen binding to take place. Following washing with FACS medium cells were incubated with 30µl of the secondary anti-mouse FITC conjugate, diluted in FACS medium (see Table 2.4), for 30-45 minutes on ice, in the dark. After washing, cells were resuspended in 300µl of FACS medium and analysed using a Becton Dickinson FACScan with LysisII and PC Lysys software. Statistical analysis of data was carried out using an unpaired Students *t*-test

2.2.8 Cell wounding assays

2.2.8.1 Time-lapse video microscopy

For preliminary experiments time-lapse video microscopy was used to determine the rate of repair of 16HBE 14o- and primary bronchial epithelial cell cultures following scrape wounding. Cells grown to confluence in small petridishes were serum starved for 24 hours before wounding with a 1ml pipette tip. Cells were then washed 1x with serum free medium before addition of serum free medium containing 100mM HEPES to buffer the medium and prevent fluctuations in pH in the absence of a CO_2 source along with 1nM EGF. Cells were then returned to the incubator for 30 minutes to allow cultures to stabilise before proceeding with time-lapse microscopy. Cells were placed in a humidified chamber at 37°C where wound closure was observed using a phase contrast microscope together with a black and white video camera. IP Lab software was used to capture a 125-millisecond image of the culture every 60 minutes for 6 hours (16HBE 14o-) or 20 hours (primary cells). At the end of the time-lapse period images were converted into TIFF files then imported into Scion Image analysis software. For each image a measurement of the wound area in pixels was determined using Scion Image and the data was then converted into mm^2. Data was then analysed using Microsoft Excel and the Student's unpaired *t*-test used to determine differences between treatments.

2.2.8.2 Chamber slide method

To investigate the effect of a range of stimuli on the rate of wound repair 16HBE 14o- cells were cultured in 4 well chamber slides to 95% confluence before serum starving

cells for 24 hours. Multiple straight wounds were then made using a comb before adding serum free medium (UltraCulture) with the addition of growth factors, inhibitors or sodium cromoglycate.

Cells were fixed immediately after wounding then at 3, 6 and 9 hours after wounding. After washing twice with PBS cells were fixed for 10 minutes with cold methanol, air-dried then stored at -20°C prior to staining.

To visualise cells and determine the wound edge nuclei were stained with filtered Mayer's Haematoxylin for 5 minutes and blued under running tap water for a further 5 minutes. Slides were mounted using a coverslip and crystal mount which was left to dry and set overnight.

Once the mountant had hardened slides were scanned using an Epson scanner and Epson Scan II! 32software. Images were then imported into Scion Image analysis software which was used to measure the area of individual wounds in pixels. Alongside the slides a ruler was also scanned to enable determination of the ratio of pixels to mm^2 by Scion Image. Using Microsoft Excel, data was then converted from pixels into mm^2 and statistically analysed using a Student's unpaired *t*-test.

2.2.9 Cell lysis

For SDS-PAGE analysis of proteins and denaturing immunoprecipitation, cells were cultured in 57cm^2 petridishes to around 80% confluence before serum starving for 24 hours. Following stimulation of cells, monolayers were washed twice with 5ml PBS containing protease and phosphatase inhibitors (PBS, 1mM sodium orthovanadate, 50mM sodium fluoride, 1mM PMSF, 1.54μM aprotinin and 21μM leupeptin, adjusted to pH 7.4). Cells were lysed with 200μl or 500μl hot 1 x denaturing lysis buffer containing protease and phosphatase inhibitors (1% (w/v) SDS, 10mM Tris pH 7.4, 1mM sodium orthovanadate, 50mM sodium fluoride, 1mM PMSF, 1.54μM aprotinin and 21μM leupeptin, 5mM EGTA, 5mM EDTA, adjusted to pH 7.4). The lysed cells were scraped off the plate and pipetted into an eppendorf tube and heated to 95°C for 5 minutes on a hotblock. Samples were sonicated for 15 seconds before clarifying by

centrifugation at 16,000xg, 10minutes at 4°C. The protein concentration in each sample was determined using the method described in section 2.2.12. Samples were stored at -80°C for up to one month before analysis by SDS-PAGE and Western blotting.

2.2.10 Preparation of soluble and particulate fractions

This procedure is a modification of the technique of Short *et al* (130). In summary, cellular homogenates were prepared and centrifuged at high speed to provide a pellet consisting of membrane and particulate material and a supernatant fraction of soluble proteins i.e. those not attached to membrane or cytoskeletal components.

Cells were cultured in 57cm^2 petridishes, serum starved for 24 hours and stimulated for 15 minutes with 1nM EGF or HB-EGF. Following stimulation cells were washed twice with 5ml PBS containing protease and phosphatase inhibitors (1mM sodium orthovanadate, 50mM sodium fluoride, 1mM PMSF, 1.54μM aprotinin and 21μM leupeptin, adjusted to pH 7.4).

During the preparation of fractions all buffers and samples were kept at 4°C or on ice. 700μl of homogenising buffer containing protease and phosphatase inhibitors (20mM NaCl, 5mM EDTA, 1mM EGTA, 20mM HEPES, 1mM sodium orthovanadate, 50mM NaF, 1mM PMSF, 1.54μM aprotinin, 21μM leupeptin, pH adjusted to 7.2) was pipetted onto the cells. Cells were then scraped off the dish and transferred into a glass homogeniser, the plate was washed twice with 300μl of homogenising buffer and these washes added to the homogeniser to give a final volume of 1300μl. The homogeniser was plunged six times to ensure consistent disruption of the cells between the samples. Whole cells and small cell debris was pelleted out at 100xg for 5 min before transferring the homogenate into an ultracentrifuge tube which was spun at 100,000xg for 1 hour at 4°C.

After centrifugation the supernatant was removed and the proteins in this soluble fraction were solubilised and denatured with hot 5x denaturing lysis buffer (5% (w/v) SDS, 50mM Tris pH 7.4, 1mM sodium orthovanadate, 50mM sodium fluoride, 1mM

PMSF, 1.54μM aprotinin and 21μM leupeptin, 5mM EGTA, 5mM EDTA, adjusted to pH 7.4) to give a final concentration of 1x lysis buffer.

The particulate fraction was dissolved in 500μl hot 1 x denaturing lysis buffer containing protease and phosphatase inhibitors (1% (w/v) SDS, 10mM Tris pH 7.4, 1mM sodium orthovanadate, 50mM sodium fluoride, 1mM PMSF, 1.54μM aprotinin and 21μM leupeptin, 5mM EGTA, 5mM EDTA, adjusted to pH 7.4).

Both fractions were heated at 95°C for 5 minutes on a hotblock, then sonicated for 15 seconds and clarified by centrifugation at 16,00xg, 10 minutes at 4°C (Sigma 4K10 Bench Centrifuge). If necessary the particulate fraction was vortexed or passed through a needle to disrupt and solubilise any remaining pellet/insoluble proteins.

The protein concentration in each sample was determined using the method described in section 2.2.12. Samples were stored at -80°C for up to one month before analysis by SDS-PAGE and Western blotting.

2.2.11 Preparation of soluble/cytoskeletal fractions

This cell fractionation technique relies on the relative insolubility of the actin cytoskeleton, compared to the remainder of the cellular components and is based on the technique of Crepaldi *et al* (33).

16HBE 14o- cells were cultured in 57cm^2 petridishes and primary cells in 6-well plates to around 80% confluence before serum starving or growth factor depletion with serum free medium or BEBM respectively for 24 hours. Following stimulation of cells, monolayers were washed twice with 5ml PBS containing protease and phosphatase inhibitors (PBS, 1mM sodium orthovanadate, 50mM sodium fluoride, 1mM PMSF, 1.54μM aprotinin and 21μM leupeptin, adjusted to pH 7.4).

The detergent-soluble fraction of the cells was extracted using the extraction buffer (50mM MES (2-[N-morpholino] ethanesulfonic acid, 3mM EGTA, 5mM $MgCl_2$, 0.5% Triton X-100, 1mM sodium orthovanadate, 50mM sodium fluoride, 1mM PMSF,

1.54μM aprotinin, 21μM leupeptin, 5mM EDTA, adjusted to pH 6.4). For 16HBE 14o- cells, 500µl of extraction buffer was pipetted onto the cells and incubated for one minute, cells were rinsed with this buffer twice before transferring the soluble proteins in extraction buffer to a cold eppendorf tube. This procedure was repeated with another 500µl of extraction buffer and this pipetted into the same tube. One final wash of the cells was carried out with 1ml extraction buffer to remove as much of the soluble fraction as possible and this wash discarded. To this soluble fraction 250µl of hot 5x denaturing lysis buffer was added (5% (w/v) SDS, 50mM Tris pH 7.4, 1mM sodium orthovanadate, 50mM sodium fluoride, 1mM PMSF, 1.54µM aprotinin and 21µM leupeptin, 5mM EGTA, 5mM EDTA, adjusted to pH 7.4) to give a final concentration of 1x lysis buffer. With primary cells wells were stimulated in duplicate and the volumes of buffer were reduced. Soluble proteins were extracted with 100µl extraction buffer, followed by 200µl buffer and these fractions pooled from duplicate wells and solubilised with 150µl hot 5x denaturing lysis buffer. A final wash of the cells was carried out with a further 500µl extraction buffer which was then discarded.

The remaining detergent-insoluble fraction (cytoskeleton) was solubilised with 500µl (100µl per well for primary cultures) hot 1x denaturing lysis buffer containing protease and phosphatase inhibitors (1% (w/v) SDS, 10mM Tris pH 7.4, 1mM sodium orthovanadate, 50mM sodium fluoride, 1mM PMSF, 1.54µM aprotinin and 21µM leupeptin, 5mM EGTA, 5mM EDTA, adjusted to pH 7.4).

Both fractions were heated at 95°C for 5 minutes on a hotblock, then sonicated for 15 seconds and clarified by centrifugation at 16,00xg, 10 minutes at 4°C. If necessary the detergent-insoluble/cytoskeletal fraction was vortexed or passed through a needle to disrupt and solubilise any remaining insoluble proteins.

The protein concentration in each sample was determined using the method described in section 2.2.12. Samples were stored at -80°C for up to 1 month before analysis by SDS-PAGE and Western blotting.

2.2.12 MicroBCA protein assay

The protein concentration of cell lysates and fractions was determined to ensure comparable protein loading onto SDS-PAGE gels and for immunoprecipitation experiments. Protein determination was carried out using the MicroBCA kit (Pierce) which has a minimum detection level of 0.5µg/ml and is a colourmetric protein determination assay. In an alkaline environment protein is able to reduce Cu^{2+} to Cu^{1+}. This reduction is detected by bicinchoninic acid (BCA) which chelates Cu^{1+} in a 2:1 ratio. A purple reaction product is formed which has a strong absorbance at 562nM and is linear with increasing protein concentration. Dilutions of a BSA standard are assayed alongside serial dilutions of samples and used to generate a standard curve which can be then be used to deduce the protein concentration of samples.

To allow accurate extrapolation of protein concentration from the standard curve all samples, standards and the diluent used in this assay are normalised to contain equivalent concentrations of denaturing lysis buffer to reduce any errors which may arise from the components of the lysis buffer. Substances known to interfere with the assay include detergents e.g. SDS, Triton X-100, buffer salts e.g. HEPES, NaCl, inhibitors e.g. EDTA, PMSF, aprotinin, leupeptin.

Cell lysates in denaturing lysis buffer were first diluted 1 in 25 with water in order to dilute out the above components well below the maximum recommended concentration so it should no longer interfere with the assay. Similarly, to prepare BSA standards 2mg/ml BSA were diluted 1 in 25 with 23 parts water, 1 part denaturing lysis buffer to 1 part 2mg/ml BSA to provide a 80µg/ml solution of BSA containing equivalent concentrations of detergents, buffer salts and inhibitors as test samples. Denaturing lysis buffer was diluted 25 times with distilled water for use as a diluent for serial dilutions and blank wells.

Following appropriate dilutions as described above, BSA standards (BSA Stds) and samples were assayed in duplicate and 200µl of each loaded into wells on row A of the microtiter plate. 100µl of diluent was pipetted into all other wells and standards/samples were serially diluted down the plate to row H, except for the BSA

standards which were diluted up to row G. Row H wells 1 and 2 contain diluent as an assay blank (see figure 2.2 for set up of 96-well plate).

Following serial dilutions of BSA standard and samples down the plate 100µl of MicroBCA reagent (prepared according to manufacturers instructions) was pipetted into each well. The plate was then covered with cellophane cover, shaken for 15 seconds and incubated at 60°C for 1 hour.

After allowing the plates to cool to room temperature absorbance of protein standards and samples was read at 562nm using a microplate spectrophotometer. A typical standard curve is shown in figure 2.3. Typical protein concentrations obtained were 5-7 µg/µl for 16HBE 14o- cells grown to 90% confluence on 57cm^2 petridishes and lysed in 200µl denaturing lysis buffer. For primary cells cultured on 6-well plates and lysed in 100µl of denaturing lysis buffer per well 2-3 µg/µl was a typical yield.

2.2.13 Immunoprecipitation

This technique was used to examine tyrosine phosphorylation of the EGF receptor, ezrin and moesin. Phosphotyrosine residues were immunoprecipitated using a phosphotyrosine (clone PY20)-agarose conjugate and immunoprecipitates were analysed using SDS-PAGE transferred onto nitrocellulose and Western blots were immunostained for EGFR, phosphotyrosine (PY20), ezrin and moesin.

Cells were stimulated with EGF, HB-EGF or sodium cromoglycate and lysed following the procedure in 2.2.9 with one exception; cells were lysed in 200µl of lysis buffer instead of 500µl in order that the sample was less dilute. Primary cells cultured in 6-well plates were treated in duplicate and lysed in 100µl of lysis buffer per well to provide 200µl lysate for each treatment. The protein concentration of lysates was determined using the method described in section 2.2.12.

1mg of cell lysate was mixed with an equal volume of 2x Triton buffer, (20mM Tris pH 7.4, 300mM NaCl, 10mM EGTA, 10mM EDTA, 2mM sodium orthovanadate, 100mM sodium fluoride, 140µM PMSF, 3.08µM aprotinin, 42µM leupeptin, pH to 7.4 then add

	1	2	3	4	5	6	7	8	9	10	11	12
A	BSA Stds 80µg/ml		Sample 1 Diluted x25		Sample 2 Diluted x25		Sample 3 Diluted x25		Sample 4 Diluted x25		Sample 5 Diluted x25	
B	BSA Stds 40µg/ml		Sample 1 Diluted x50		Sample 2 Diluted x50		Sample 3 Diluted x50		Sample 4 Diluted x50		Sample 5 Diluted x50	
C	BSA Stds 20µg/ml		Sample 1 Diluted x100		Sample 2 Diluted x100		Sample 3 Diluted x100		Sample 4 Diluted x100		Sample 5 Diluted x100	
D	BSA Stds 10µg/ml		Sample 1 x200		Sample 2 x200		Sample 3 x200		Sample 4 x200		Sample 5 x200	
E	BSA Stds 5µg/ml		Sample 1 x400		Sample 2 x400		Sample 3 x400		Sample 4 x400		Sample 5 x400	
F	BSA Stds 2.5µg/ml		Sample 1 x800		Sample 2 x800		Sample 3 x800		Sample 4 x800		Sample 5 x800	
G	BSA Stds 1.25µg/ml		Sample 1 x1600		Sample 2 x1600		Sample 3 x1600		Sample 4 x1600		Sample 5 x1600	
H	BLANK		Sample 1 x3200		Sample 2 x3200		Sample 3 x3200		Sample 4 x3200		Sample 5 x3200	

Figure 2.2. MicroBCA protein assay
Standard layout of 96-well plate used to determine the protein concentration of cell lysates and solubilised cellular fractions.

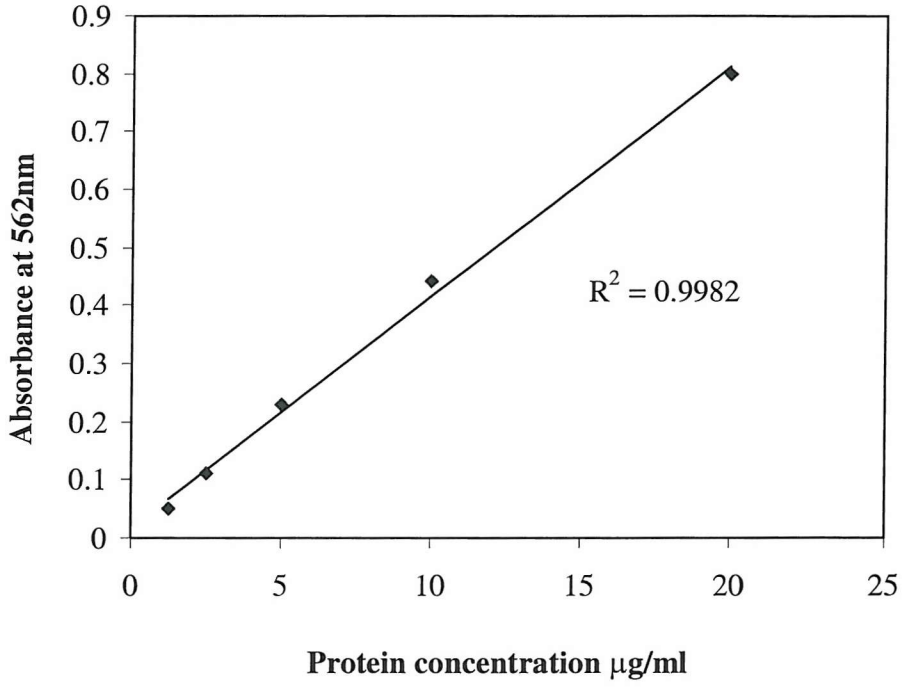

Figure 2.3. Typical standard curve obtained from MicroBCA protein assay kit.

2% (v/v) Triton X-100 and 1% (v/v) NP-40). The sample was then made up to 1ml with 1x Triton buffer (1:1 (v/v) 2xTriton buffer:dH_2O). This method gives 1mg of sample in a final concentration of 1x Triton buffer. To each tube 60µl of PY20-agarose conjugate was added and after briefly vortexing samples were incubated at 4°C, overnight on a rotary mixer to enable formation of immune complexes.

To precipitate immune complexes, tubes were centrifuged at 600xg, for 15 minutes at 4°C. The supernatant was retained and solubilised in 5x Sample buffer in a ratio of 4:1, heated to 95°C for 5 minutes and analysed by SDS-PAGE and Western blotting to determine the proportion of proteins which did not bind to the PY20-agarose. The immunoprecipitate pellet was washed three times with 1ml of 1x Triton buffer to remove unbound proteins. To wash the pellet, 1ml of 1x Triton buffer was added to the tubes which were briefly vortexed before centrifuging at 600xg for 5 minutes at 4°C followed by removal of the supernatant.

After the final wash as much of the supernatant as possible was removed without disrupting the bead pellet. Immune complexes were solubilised in 80µl hot 2x sample buffer containing protease and phosphatase inhibitors (0.1261M Tris-Cl pH 6.8, 4% SDS, 10% 2-mercaptoethanol, 20% glycerol, 0.01% bromophenol blue, 2mM sodium orthovanadate, 2mM sodium fluoride, 0.14mM PMSF).

Samples were analysed using 7.5% or 10% SDS-PAGE gels and Western blotting, blots were stained for phosphotyrosine (PY20), EGFR, ezrin and moesin.

2.2.14 SDS-PAGE

Separation of proteins on the basis of their molecular weight by SDS-PAGE and Western blotting was used to analyse proteins present in cell lysates, fractions and immunoprecipitates.

7.5% or 10% SDS-PAGE mini-gels were cast using the BioRad mini-protean II or III system. Firstly glass plates, spacers and combs were cleaned using a 10% SDS solution followed by 70% methanol to remove dirt and grease. Glass plates and spacers

were then set up in the casting stand ensuring correct alignment to minimise leakage of gel mix.

Separation gel and stacking gel solutions (see below) were prepared in advance and following filtration could be stored in a dark bottle for up to one month at 4°C.

Separation gel mix	**10% gel**	**7.5% gel**
Acrylamide/bis-acrylamide	30.0 ml	22.5 ml
1.5M Tris-Cl, pH 8.8	22.5 ml	22.5 ml
Distilled H_2O	37.1 ml	44.6 ml
20% SDS	0.45 ml	0.45 ml

Stacking gel mix	
Acrylamide/bis-acrylamide	12.5 ml
0.5M Tris-Cl pH 6.8	25.0 ml
H_2O	62.0 ml
20% SDS	0.5 ml

For two pairs of gels, 20ml separation gel mix was mixed with 66µl 10% ammonium persulphate (prepared fresh daily) and 10µl TEMED to catalyse polymerisation of the gel. The solution was then poured between the plates, overlaid with propan-2-ol to exclude air and left to set for 30 minutes.

After checking that the separation gel was fully set the propan-2-ol was washed off with distilled water and excess liquid blotted off with filter paper being careful not to touch the polymerised gel. Stacking gel solution for two pairs of gels was prepared by adding 33.4µl of ammonium persulphate and 7.6µl TEMED to 10ml of stacking gel mix. This was then pipetted over the separation gel up to the top of the glass plates and a plastic comb (10 or 15 lane) positioned between the glass plates to allow formation of lanes and to exclude air. The stacking gel was left to set for a further 30 minutes.

Once the gel had set combs were carefully removed and the gel plates set up in the running stand and tank. Cooled (4°C) running buffer (0.025M Tris, 0.192M glycine, 0.1% SDS, pH 8.3) was then poured between the gels.

Following calculation of the protein concentration cell lysates and fractions were diluted with 5x sample buffer (0.31525M Tris-Cl pH 6.8, 10% SDS, 25% 2-mercaptoethanol, 50% glycerol, 0.01% bromophenol blue) and distilled water to make each sample the same protein concentration in 1x sample buffer. Generally 8μg of protein in 20μl was loaded per lane and therefore a 0.4μg/μl solution was prepared. For example for 2 gels 50μl of sample was prepared from a lysate with a protein concentration of 6μg/μl and comprised 3.3μl lysate, 36.7μl distilled water and 10μl 5xSB. Following dilution samples were vortexed and then both samples and Kaleidoscope prestained gel markers were heated to 95°C for 5 minutes and centrifuged at 600xg for 1 minute.

20μl of each sample was loaded onto the stacking gel alongside 10μl of prestained molecular weight markers (BioRad) and the gels run at 160 volts, amps limit 300mA for approximately 1 hour until the bromophenol blue dye front had reached close to the bottom of the gel. Gels were then stained with Coomassie blue to check protein loading or transferred onto nitrocellulose membrane by Western blotting before immunostaining (see section 2.2.16).

2.2.15 Coomassie blue staining

Coomassie blue staining was used to visualise the proteins bands on a SDS-PAGE gel. Staining of the gel also enabled a check to be made on the protein loading of the gel and was also used to stain a gel after Western blotting as a control to ensure all proteins had been transferred onto the nitrocellulose.

The gel was placed in the staining solution (40% (v/v) methanol, 10% (v/v) acetic acid and 0.1% (w/v) Coomassie brilliant blue) and incubated for 2 hours with shaking. The gel was then transferred into destain (20% (v/v) methanol, 5% (v/v) acetic acid and

75% (v/v) water) and incubated overnight to reveal bands. Gels were then dried using a BioRad gel dryer according to the manufacturers instructions.

2.2.16 Western Blotting

Gels were transferred onto nitrocellulose using a wet, tank transfer system. At the completion of gel electrophoresis gels were carefully removed from between the glass plates and equilibrated in transfer buffer (25μM Tris, 192μM glycine, 20% v/v methanol in H_2O, with a final pH of 8.3) for 30 minutes. Nitrocellulose rectangles cut slightly larger than each mini-gel were pre-wetted in distilled water before soaking in transfer buffer for 15 minutes.

Filter papers and Scotch-brite pads were soaked in transfer buffer and a test-tube used to roll out any air bubbles. To set up the transfer, the gel and nitrocellulose were sandwiched between filter papers and Scotch brite pads in a plastic cassette and air bubbles were gently removed by rolling a test-tube over the top Scotch-brite pad before closing the cassette. This cassette was placed vertically into the transfer tank with the gel towards the negative terminal and the nitrocellulose towards the positive terminal (see figure 2.4).

Gels were transferred on the bench for 1 hour at 100 volts, 300 mAmps limit, using a mini-Trans-blot cell ensuring ice packs were positioned around the tank to minimise heating and with the tank on a magnetic stirrer. Alternatively a large Trans-blot cell with plate electrodes was used to transfer proteins at 30 volts, 200 mAmps limit for 18 hours in the cold room on a magnetic stirrer. Within the same experiment the transfer tank used was of the same type to minimise differences in protein transfer efficiency.

Following completion of electrophoretic transfer blots were dried on filter paper and the position of molecular weight calibrators marked with a pencil. Corners were cut off the blots or small slits made to mark and orientate the blots. Blots were either stained immediately or stored at 4°C wrapped in cling film for up to one week.

2.2.17 Immunostaining of Western blots

After drying, nitrocellulose blots were incubated in blocking buffer (5% milk in PBS, 0.5% Tween-20, 1mM sodium orthovanadate, 1mM sodium fluoride, 70uM PMSF) for 30 minutes. After washing blots for 15 minutes in PBS-Tween wash buffer (PBS, 0.5% (v/v) Tween-20, 1mM sodium orthovanadate, 1mM sodium fluoride, 70μM PMSF) blots were incubated for 1 hour with the primary antibody (see Table 2.5) diluted in antibody buffer (150nM NaCl, 50mM Tris, 0.25% BSA, 1mM sodium orthovanadate, 1mM sodium fluoride, 70μM PMSF, pH to 7.4 prior to addition of 0.5% Tween 20). Membranes were washed once for 15 minutes and twice for 5 minutes with fresh changes of PBS-Tween.

Incubation with secondary Horseradish peroxidase antibody (see Table 2.5) was carried out for 1 hour followed by washing with PBS-Tween once for 15 minutes and four times for 5 minutes. The chemiluminescence detection reagent, ECL Plus (Amersham) was applied to blots for 5 minutes according to the manufacturers instructions (see figure 2.5 for explanation of chemical reaction). Blots were then wrapped in cling film being careful to avoid creases or air bubbles and placed in a film cassette. In the dark room Hyperfilm ECL autoradiography film was placed on top of the blots and exposed for a range of time periods from 10 seconds to 5 minutes before developing the film. Bands were then analysed by densitometry using Kodak 1D software and statistical analysis carried out using an unpaired Students *t*-test.

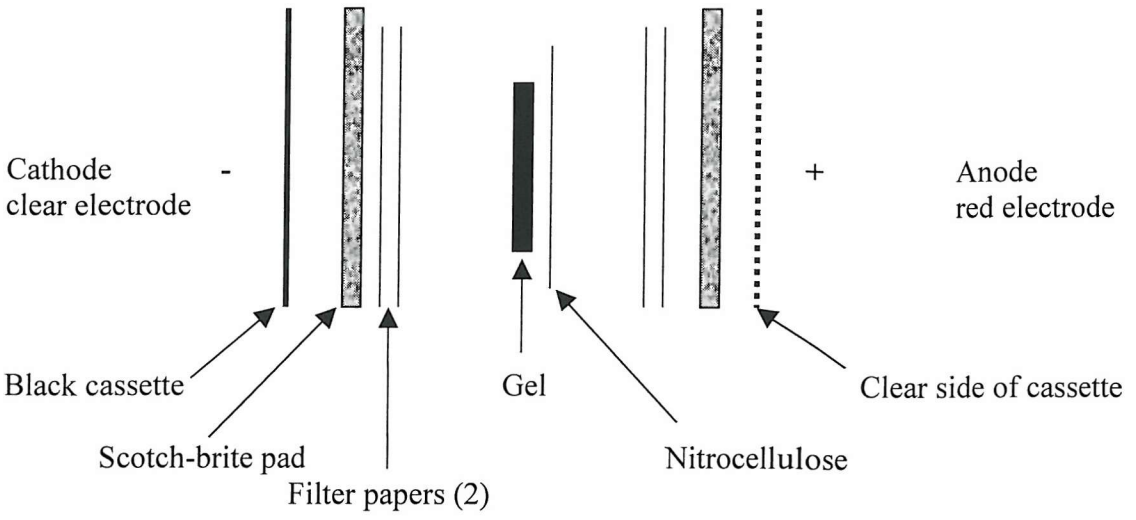

Figure 2.4. Set up of Western blotting transfer
Showing orientation of gel and nitrocellulose membrane in cassette and transfer tank for Western blotting in terms of the positive and negative electrodes

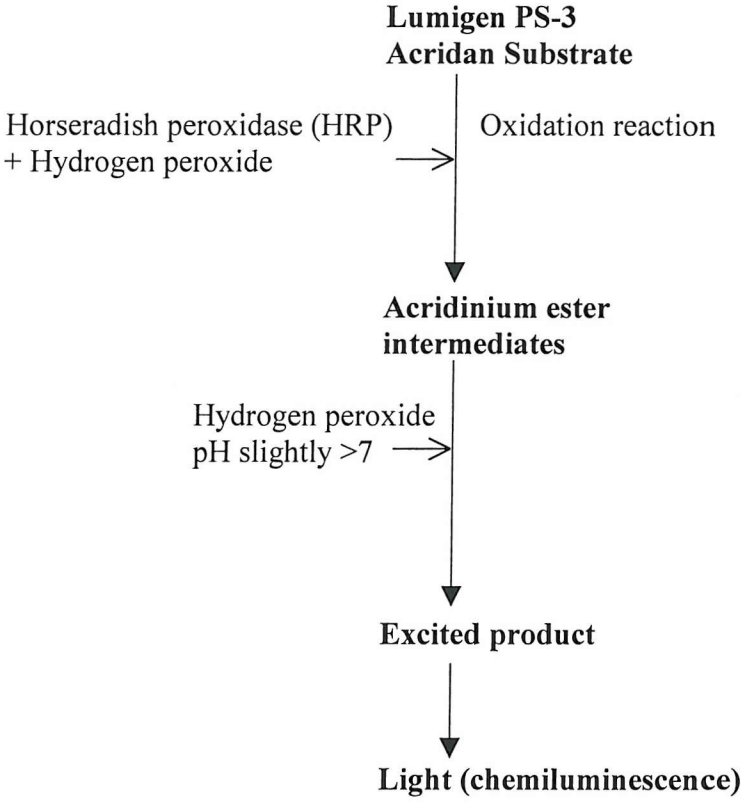

Figure 2.5. Reaction of ECL Plus with HRP-conjugated antibodies.
Detection of HRP-conjugated antibodies by ECL Plus involves oxidation of Lumigen PS-3 acridian substrate to acridinium ester intermediates which react with peroxide under slight alkaline conditions to produce an excited product with emission of light or chemiluminescence.

Table 2.5. Primary and secondary antibodies used for Western blotting.

Antigen	Class	Source	Dilution	Secondary antibody
CD44 standard (Hermes-3)	Mouse monoclonal IgG_{2A}	Gift	1 in 500	Rabbit anti-mouse HRP conjugate (Dako) 1 in 1000
CD44v3	Rabbit polyclonal Purified IgG	Chemicon International Inc.	1 in 500	Swine anti-rabbit HRP conjugate (Dako) 1 in 1000
Ezrin (Clone 18)	Mouse monoclonal IgG_1	Transduction Laboratories, UK	1 in 125	Rabbit anti-mouse HRP conjugate (Dako) 1 in 1000
Moesin (Clone 38)	Mouse monoclonal IgG_1	Transduction Laboratories, UK	1 in 1000	Rabbit anti-mouse HRP conjugate (Dako) 1 in 1000
Ezrin (C-15)	Goat polyclonal	Santa Cruz Biotechnology	1 in 2000	Rabbit anti-goat HRP conjugate (Dako) 1 in 1000
Moesin (C-15)	Goat polyclonal	Santa Cruz Biotechnology	1 in 2000	Rabbit anti-goat HRP conjugate (Dako) 1 in 1000
phosphotyrosine PY20:biotin	Mouse monoclonal IgG_{2B}	Transduction Laboratories, UK	1 in 1600	Streptavidin-biotinylated HRP complex (Amersham) 1 in 1000
EGFR (sheep 529)	Sheep polyclonal	Produced 'in-house'	1 in 16,000	Rabbit anti-sheep HRP conjugate (Dako) 1 in 1000
actin	Rabbit polyclonal	Sigma	1 in 4000	Swine anti-rabbit HRP conjugate (Dako) 1 in 1000

3 CHAPTER THREE

CD44 EXPRESSION IN BRONCHIAL EPITHELIAL CELL LINES

CD44 is expressed by a variety of cells including fibroblasts, endothelial and epithelial cells (41). Several cytokines and growth factors have been shown to influence expression of CD44 in different *in vitro* models. Both Interleukin-1 (40) and Hepatocyte growth factor/Scatter factor (HGF/SF) (57) have been shown to increase CD44 expression on endothelial cells. In mouse fibroblasts, EGF has been shown to induce CD44 expression through transcriptional regulation of CD44 mediated by an EGF-regulatory element in the upstream regulatory region of the CD44 gene (166). In human bone marrow fibroblasts CD44 expression was unchanged by GM-CSF, interleukin-3 or TGFβ1 (125) and human lung fibroblast expression of CD44 was not influenced by TGFβ1 or bFGF (124).

Bronchial biopsies from asthmatic patients show intense staining on basal cells for both EGF receptor (115) and CD44 (73) in areas of epithelial damage. Based on the observations described above it was hypothesised that the EGF receptor could be responsible for the upregulation of CD44 expression. Therefore the aim of this chapter was to determine whether the EGF receptor ligands, EGF and HB-EGF influenced the expression of CD44 and CD44v3 by bronchial epithelial cells. The effect of HB-EGF on CD44v3 expression has also been studied here as the availability of the heparan sulphate moiety on CD44v3 for HB-EGF binding could itself be controlled by HB-EGF modulation of CD44v3 expression.

3.1 CD44 expression by bronchial epithelial cell lines

CD44 and CD44v3 expression by NCI-H292 and 16HBE 14o- cells was first assessed by immunocytochemistry. This showed that both cell lines had immunoreactivity for a pan CD44 antibody (clone 25-32) and a specific antibody against CD44 proteins containing peptides encoded by exon v3 (figure 3.1i and ii). Additionally, both antibodies revealed a pattern of staining consistent with a plasma membrane distribution and their role as cell adhesion molecules. These results are in agreement with the previous cellular distribution of proteins detected with these antibodies to

a. panCD44

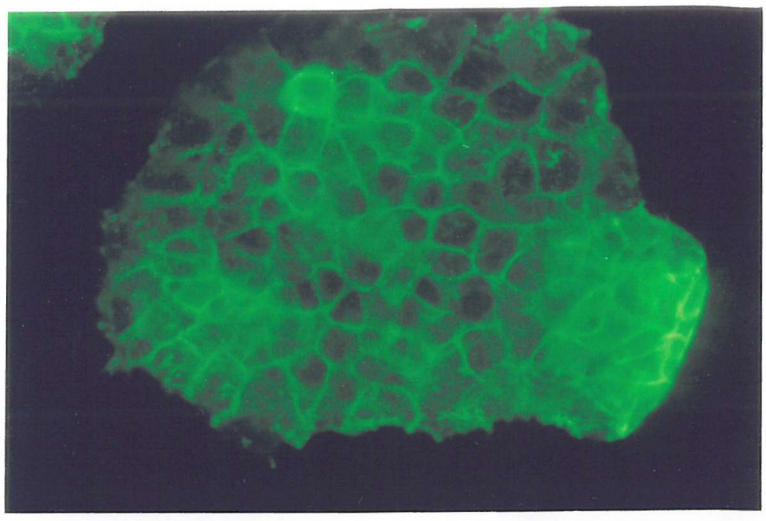

b. CD44v3

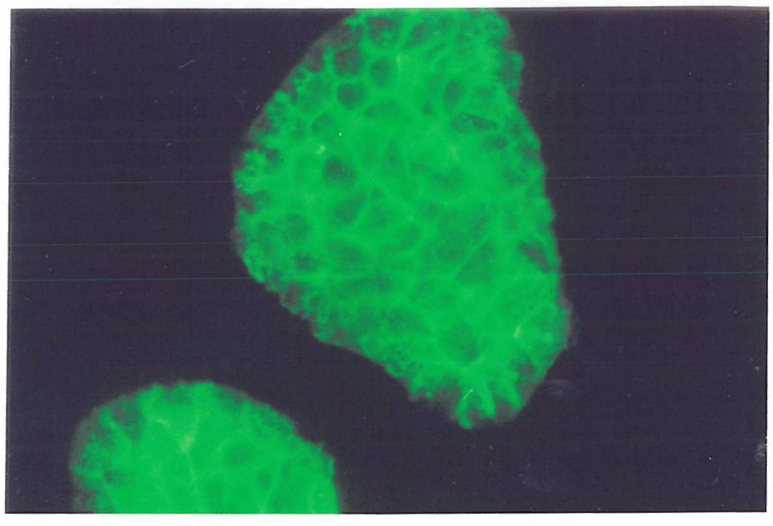

c. Control staining (without primary antibody)

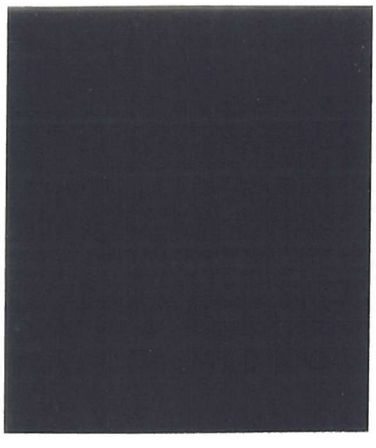

d. IgG1 negative control

e. IgG2B negative control

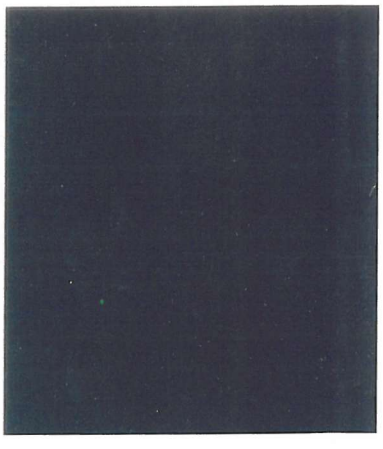

Figure 3.1i. CD44 Immunofluorescent staining.
NCI-H292 cells were stained with a pan-CD44 antibody (clone 25-32) (a) or CD44v3 specific antibody (clone 3G5, R&D Systems) (b) using a secondary anti-mouse FITC conjugate (Dako). Control plates are as follows, c shows control staining in the absence of primary antibody, d shows staining with a mouse IgG1 negative/irrelevant antibody control and e shows staining with a mouse IgG2B negative/irrelevant antibody control.

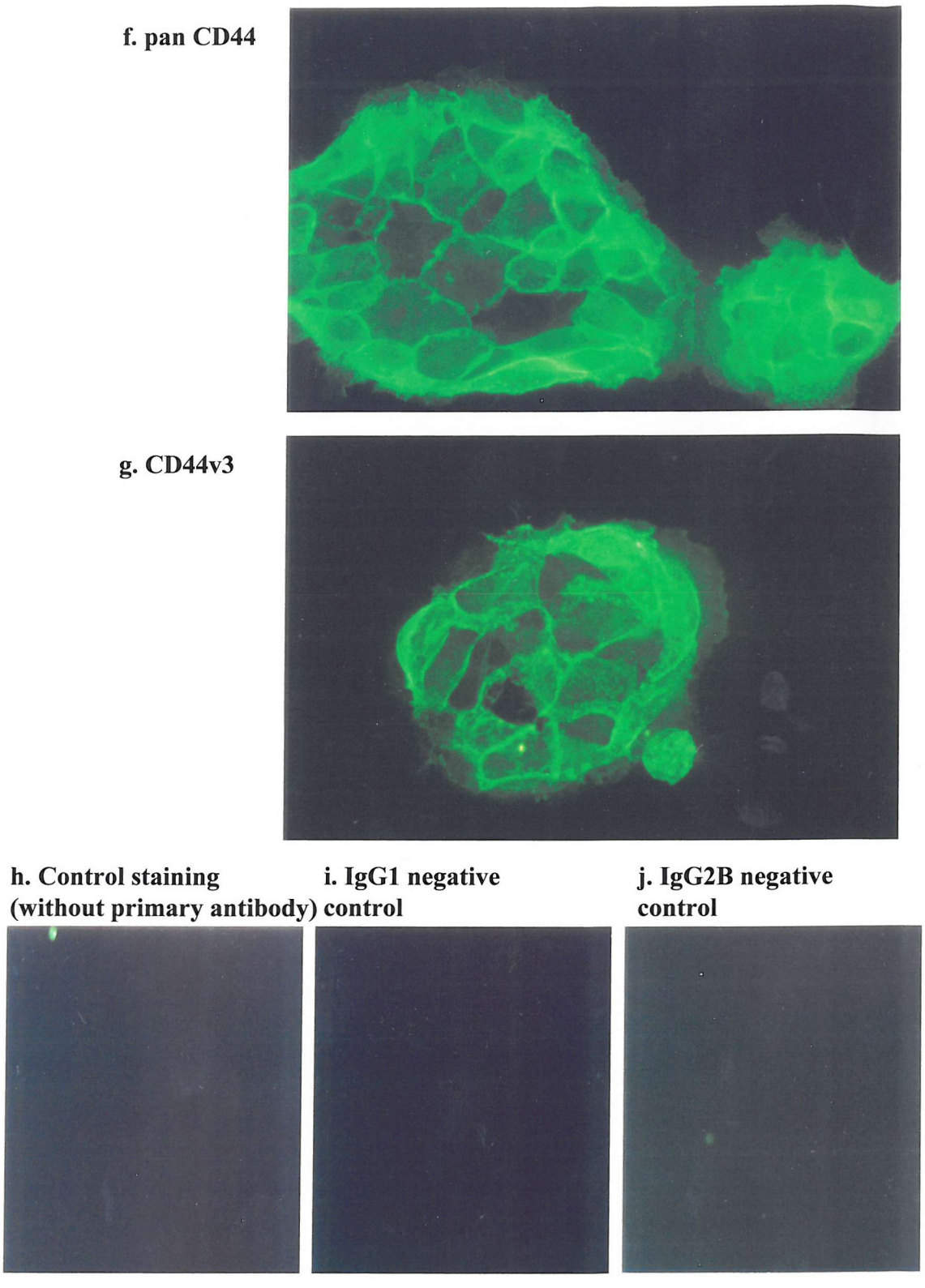

Figure 3.1ii. CD44 Immunofluorescent staining.
16HBE 14o- cells were stained with a pan-CD44 antibody (clone 25-32) (f) or CD44v3 specific antibody (clone 3G5, R&D Systems) (g) using a secondary anti-mouse FITC conjugate (Dako). Control plates are as follows, h shows control staining in the absence of primary antibody, i shows staining with a mouse IgG1 negative/irrelevant antibody control and j shows staining with a mouse IgG2B negative/irrelevant antibody control.

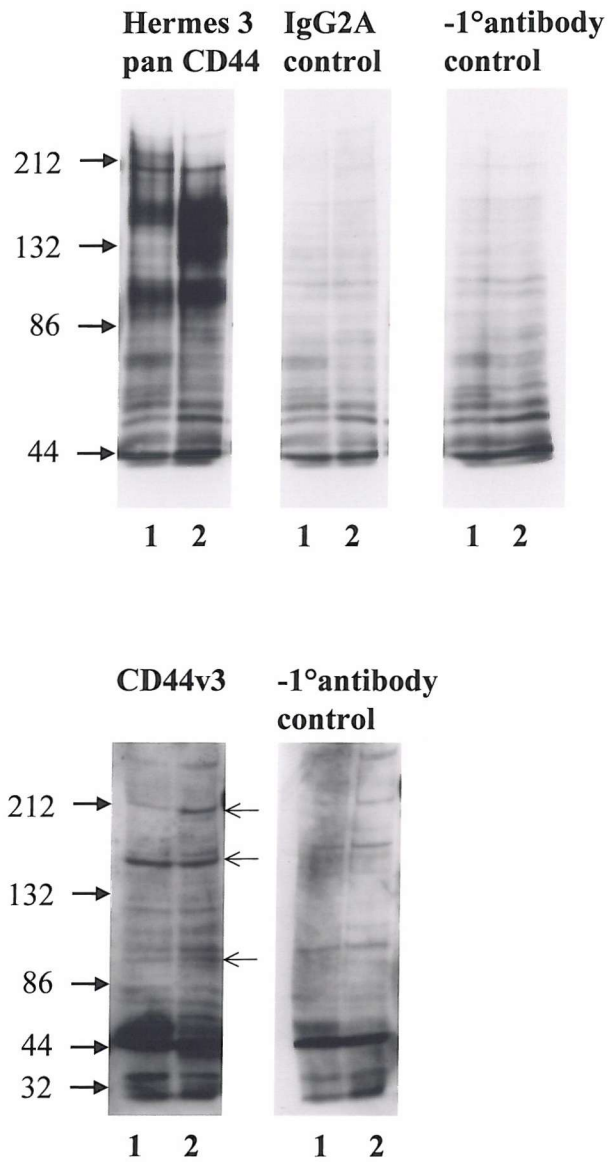

Figure 3.2. Analysis of CD44 and CD44v3 proteins by Western blotting. NCI-H292 (1) and 16HBE 14o- (2) whole cell lysates were separated by 7.5% SDS-PAGE and Western blots stained with antibodies against pan CD44 (Hermes 3) and exon v3 containing isoforms (Chemicon). An IgG_{2A} irrelevant control blot is shown corresponding to the pan-CD44 stained blot where in both cases 0.8μg/ml IgG_{2A} (either specific antibody or control IgG) was incubated in the primary antibody incubation step. Control blots where omission of primary antibody and incubation with antibody buffer alone was followed by incubation with anti-mouse or anti-rabbit HRP-conjugate secondary antibodies are also shown.

CD44 (89) and CD44v3 (41). Control staining with irrelevant antibodies of the same isotype and species as well as omission of the primary antibody gave very faint background staining just revealing the shape of colonies of cells.

Western blotting confirmed the expression of CD44 and CD44v3 by NCI-H292 and 16HBE 14o- cells (figure 3.2). The Hermes-3 antibody which recognises all forms of CD44 detects many bands on the Western blot not recognised by the isotype control in the range 90-220kDa with some differences observed between the cell lines. Both cell lines express a broad band at around 90kDa which probably represents the standard form of CD44. NCI-H292 cells express proteins with molecular weights of 150-220kDa whereas a large proportion of CD44 proteins expressed by 16HBE 14o- cells make up a broad band at 100-170kDa with another band at 210kDa. Isotype (IgG_{2A}) control and omission of primary antibody control with anti-mouse secondary-HRP blots show bands on the lower portion (44-70kDa) of the blots from both cell lines to be non-specific.

Using a specific antibody raised against the variant exon v3, Western blotting showed three major bands at approximately 90, 150 and 210kDa (indicated with arrows) as well as fainter bands within this range. Again control staining of one blot with omission of primary antibody followed by incubation with secondary anti-rabbit HRP showed bands which likely arose from non-specific binding. However when used for Western blotting the CD44v3 antibody is weaker than the CD44 pan antibody making it less easy to distinguish the specific bands.

The detection of proteins by Western blotting with a range of molecular weights suggests that the two bronchial epithelial cell lines probably expressed many alternatively spliced and glycosylated forms of CD44 and CD44v3 with molecular weights of between 90 and 220kD on the Western blot. These results are consistent with the initial characterisation of the antibodies (113), (51).

3.2 The effect of EGF on CD44 expression

To examine the effect of culture conditions on CD44 expression by NCI-H292 and 16HBE 14o- cell lines, cells were serum starved for 24 hours before changing the

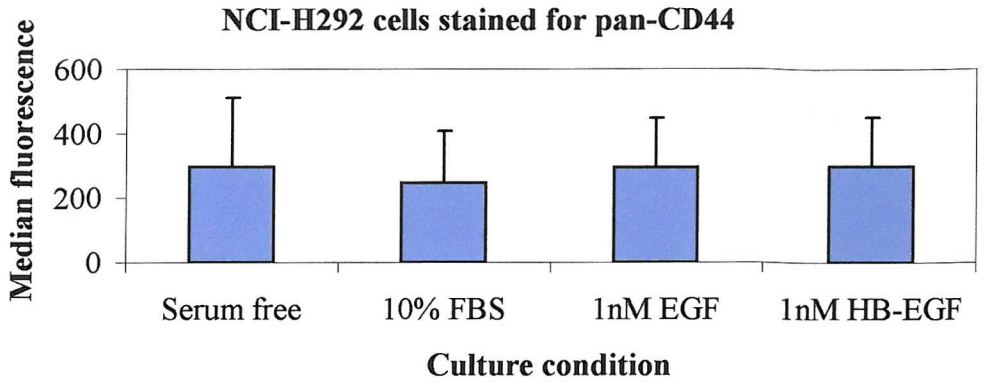

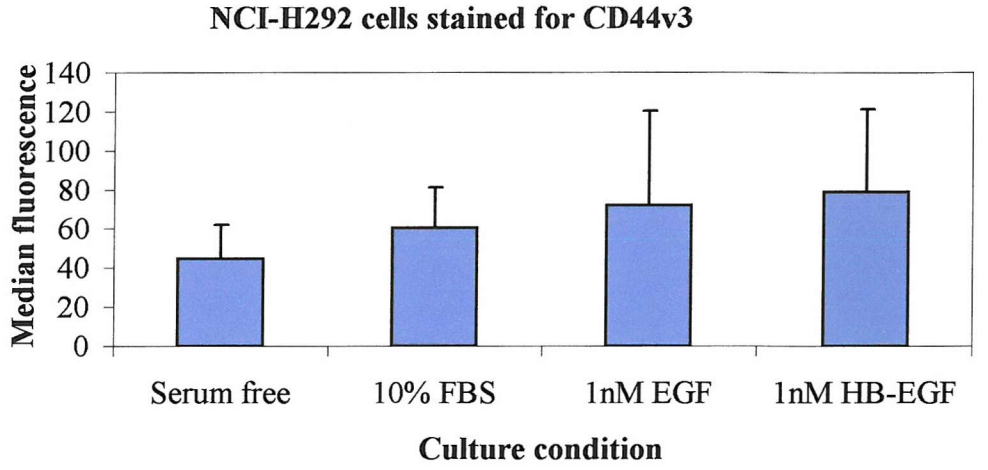

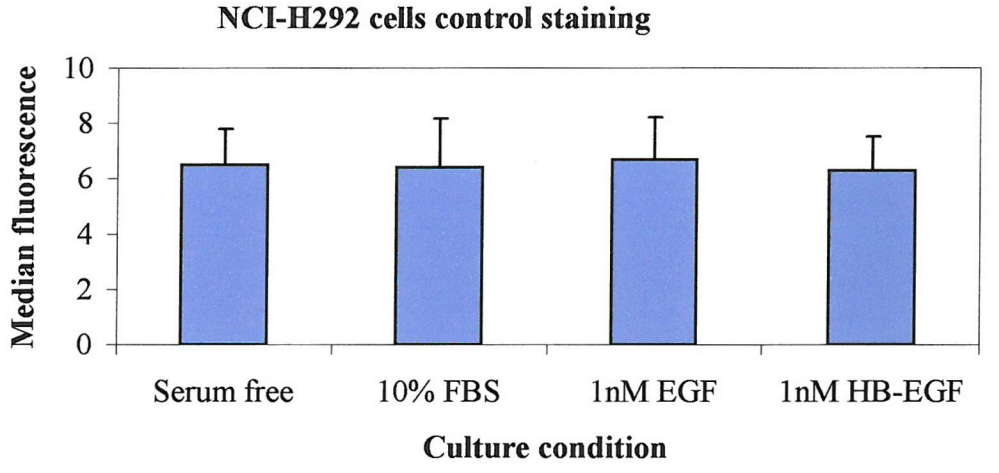

Figure 3.3i. Effect of culture conditions on surface CD44 expression. Flow cytometric measurement of surface expressed pan CD44 and CD44v3 specific proteins by NCI-H292 cells following 24 hour culture in serum free medium alone or supplemented with 10% FBS, 1nM EGF or 1nM HB-EGF. Data are the mean of three experiments +/-SD and Student's unpaired *t*-test was used to determine difference between serum free and supplemented medium (for all treatments $P>0.05$). NB: Scale differs between plots to allow clarity.

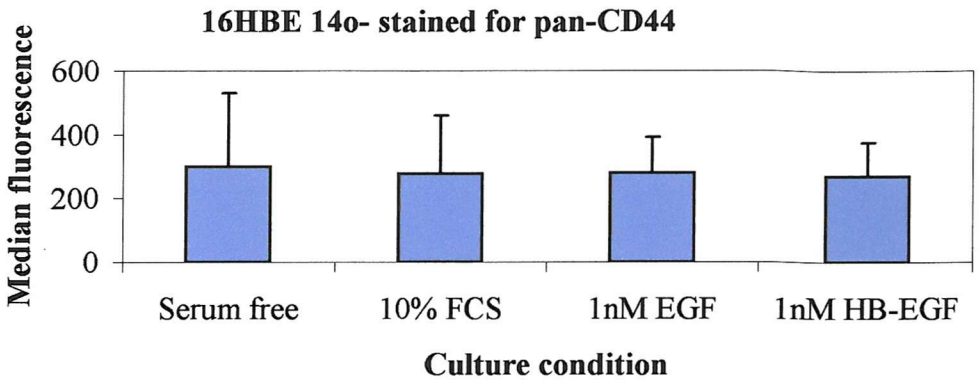

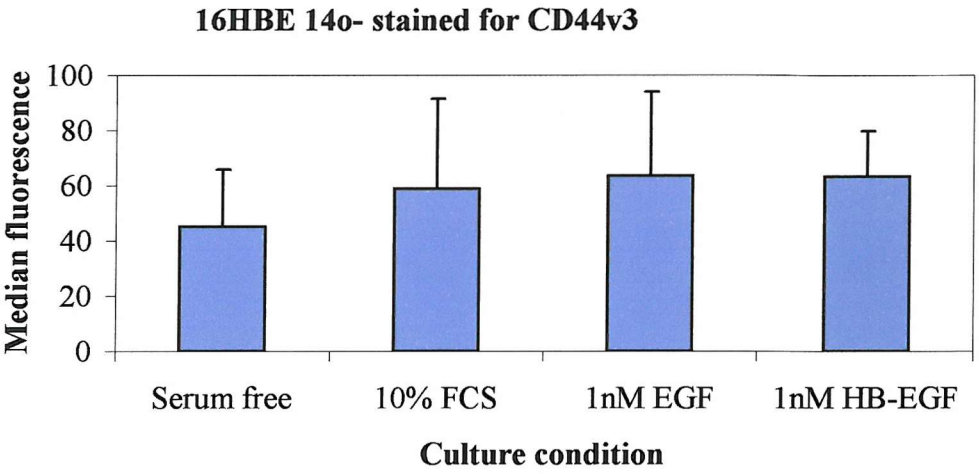

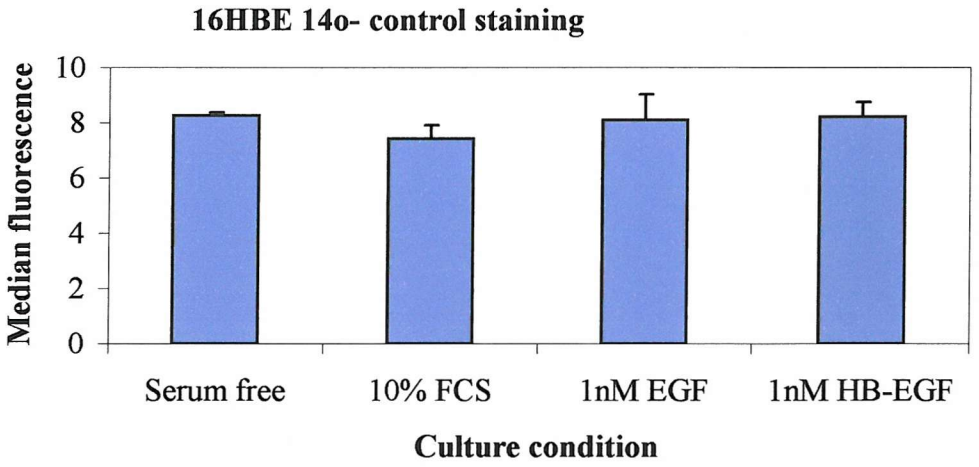

Figure 3.3ii. Effect of culture conditions on surface CD44 expression. Flow cytometric measurement of surface expressed pan CD44 and CD44v3 specific proteins by 16HBE 14o- cells following 24 hour culture in serum free medium alone or supplemented with 10% FBS, 1nM EGF or 1nM HB-EGF. Data are the mean of three experiments +/-SD and Student's unpaired *t* -test was used to determine difference between serum free and supplemented medium (for all treatments $P>0.05$). NB: Scale differs between plots to allow clarity.

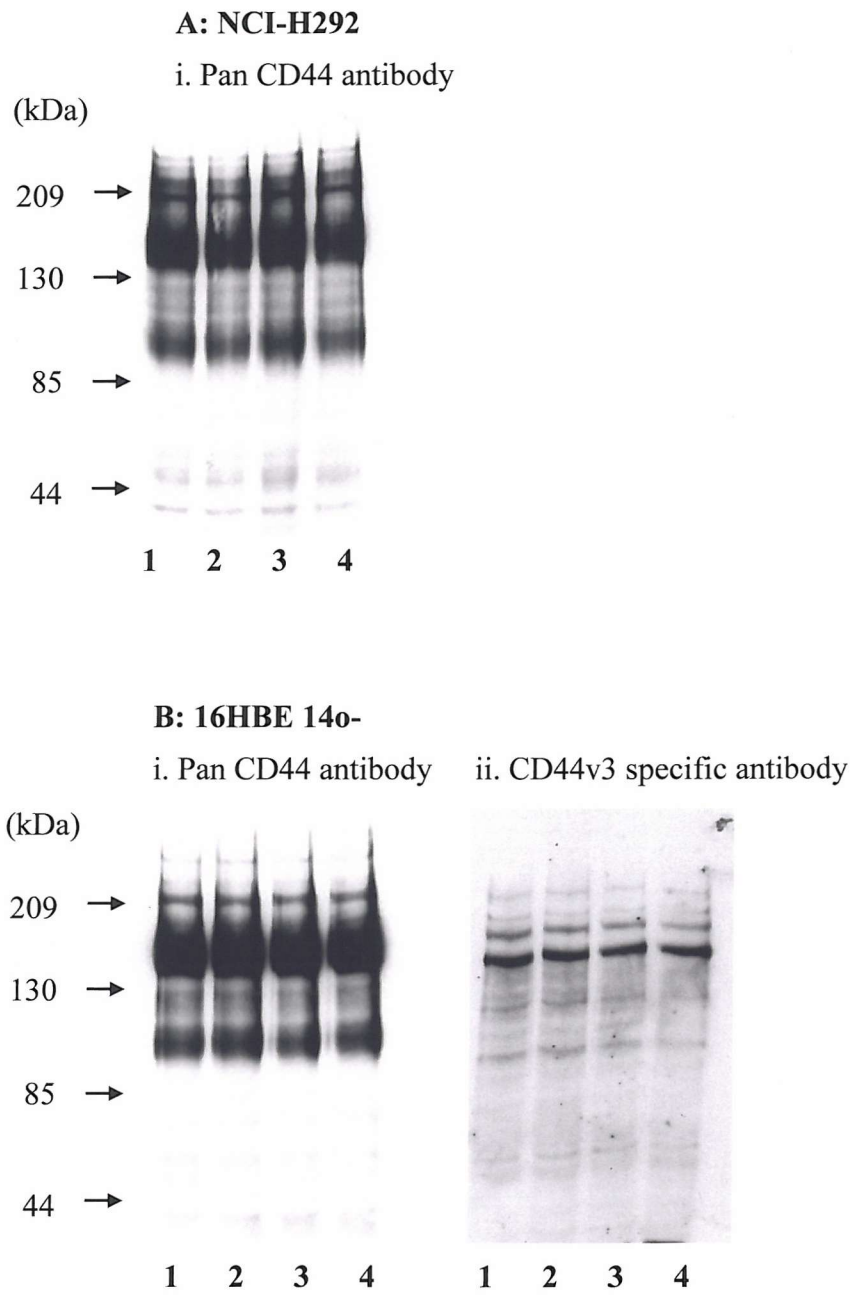

Figure 3.4. Effect of culture conditions on total CD44 expression. NCI-H292 (A) and 16HBE 14o- (B) cells were serum starved for 24 hours then cultured for 24 hours in serum free medium (lane 1) or serum free medium +/- 10% FBS (lane 2), 1nM EGF (lane 3) or 1nM HB-EGF (lane 4). Total cellular proteins were separated by 7.5% SDS-PAGE and Western blotting. Blots were stained with either (i) a pan CD44 antibody (Hermes 3) or (ii) a specific antibody which recognises exon v3 containing CD44 proteins.

medium to serum free medium with or without 10% FBS, 1nM EGF or 1nM HB-EGF for a further 24 hours. Surface expression of CD44 and CD44v3 immunoreactivity was measured by flow cytometry and total cellular CD44 and CD44v3 immunoreactivity was determined by SDS-PAGE and Western blotting.

Flow cytometric analysis indicated that the addition of 10% FBS, 1nM EGF or 1nM HB-EGF to the serum free culture medium had no significant effect on CD44 or CD44v3 surface protein expression (figure 3.3i and ii). Although small changes were seen, statistical analysis using an unpaired Students *t*-test showed that these were not significant ($P>0.05$). Total cellular CD44 was examined using SDS-PAGE and Western blotting and NCI-H292 and 16HBE 14o- cells were treated as for the flow cytometric analysis, lysed and the protein concentration determined. An equal amount of protein from each sample was then separated by SDS-PAGE, transferred onto nitrocellulose and Western blots were stained for CD44 and CD44v3 (figure 3.4). These blots do not reveal any significant changes in either total cellular CD44 or CD44v3 expression or the relative intensity of any specific band on the Western blots thus confirming the result obtained by flow cytometry.

3.3 The effect of culture conditions on the growth of bronchial epithelial cells

Results from the experiments described above showed that 24-hour treatment with EGF or HB-EGF did not significantly influence CD44 or CD44v3 expression in the cell lines tested. However it has been recorded that there is an inverse relationship between cell density and CD44 expression (81), an observation confirmed in the experiment shown in figure 3.5. This showed that cells plated at high cell density expressed less surface CD44 and CD44v3 per cell than cells plated at low cell density following a 5-day culture period. Consequently, if EGF was influencing proliferation (i.e. increasing cell density) then any increase in CD44 expression by EGF or HB-EGF could be masked by the parallel increase in cell density and accompanying reduction in CD44 or CD44v3 surface expression. Therefore the effect of the EGF on the proliferation of NCI-H292 and 16HBE 14o- cells over a 7-day period was tested in *in vitro* growth studies.

Cell proliferation was measured using the methylene blue assay method followed by construction of growth curves over a 7 day time course for NCI-H292 and 16HBE 14o-

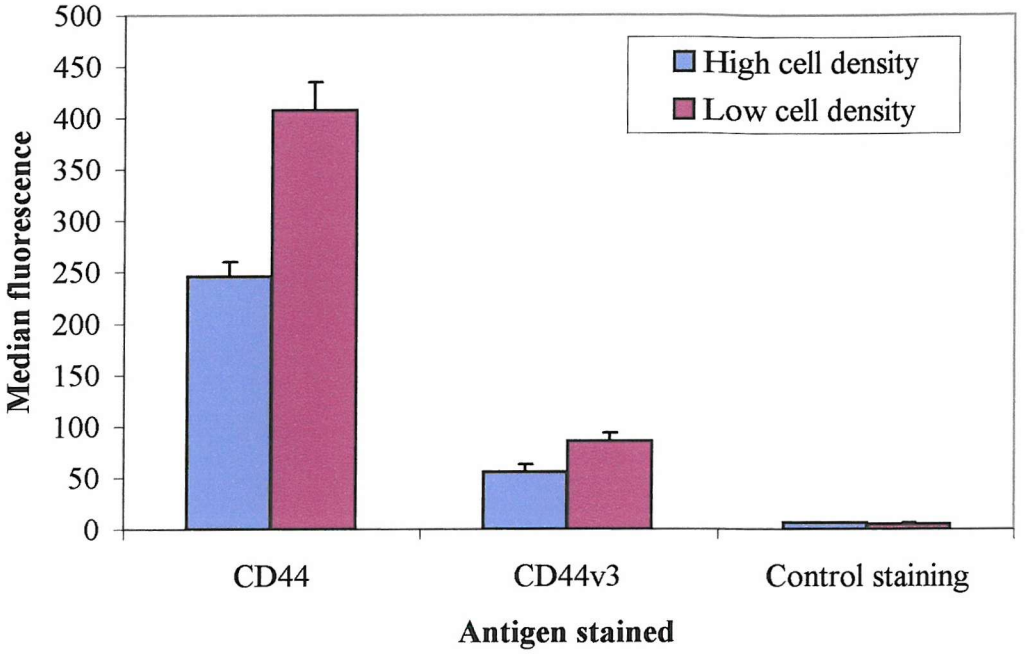

Figure 3.5. Effect of cell density on surface CD44 and CD44v3 expression. NCI-H292 cells were seeded onto 6-well plates at high ($3x10^5$ cells per well) and low ($3x10^4$ cells per well) cell density and cultured for 5 days before measurement of CD44 and CD44v3 surface expression using flow cytometry. Control staining is omission of primary antibody. Data are mean +/- SD of triplicates from a single experiment.

cells grown in a range of culture medium conditions. Over a 7 day growth period both cell lines exhibited similar patterns of proliferation; an initial, short lag phase after plating was followed by a sustained period of log growth and cell proliferation did not plateau in either of the cell lines grown in any culture medium condition (figure 3.6).

These preliminary experiments looking at culture conditions showed that both cell types were able to proliferate in serum free medium and that the addition of 1nM EGF to the culture medium had no significant stimulatory effect on the proliferation of either of the cell lines over the 7 day growth period (figure 3.6). Only the addition of 10% FBS to NCI-H292 cells significantly influenced proliferation where a reduced number of cells was seen at days 5 and 7 ($P<0.001$). In 16HBE 14o- cells 10% FBS shows a reduction in absorbance of methylene blue at day 7 although this is not significant ($P=0.14$).

The concentration of EGF has been shown to be important in regulating proliferation of A431 human epidermoid carcinoma cells, EGF stimulates cells proliferation but higher concentrations of EGF (greater than 5nM) inhibit proliferation (91). Therefore this initial study was followed up by an experiment to study the dose/response relationship of EGF on proliferation of NCI-H292 and 16HBE 14o- cells in case 1nM EGF was inhibitory. Figure 3.7 shows proliferation of NCI-H292 and 16HBE 14o- cells cultured in serum free medium containing EGF over the range 0.015nM-16nM. Here no enhancement of proliferation was seen with increasing doses of EGF compared to 1nM EGF suggesting that proliferation of both cell lines is independent of exogenous EGF.

As it was hypothesised that HB-EGF could have distinct or enhanced effects over EGF due to its co-localisation with CD44v3 at the plasma membrane, equivalent molar concentration of EGF and HB-EGF might have different effects on 16HBE 14o- and NCI-H292 cell growth. Therefore the addition of 1nM EGF or HB-EGF to serum free medium was compared but neither had any influence on proliferation when compared with serum free medium growth curves for each cell line (figure 3.8).

Supplementing culture medium of NCI-H292 or 16HBE 14o- cells with EGF or HB-EGF appeared to have no significant influence on the rate of proliferation of these cells, even though these cells respond to short term stimulation with 1nM EGF or 1nM HB-

EGF with changes in protein phosphotyrosine staining (figure 3.9). Since tumour cells such as NCI-H292 frequently exhibit autonomous growth due to autocrine ligand production (147), the role of the EGFR itself in proliferation was examined by measuring the effect of 1μM tyrphostin AG1478, a selective inhibitor of the EGF receptor tyrosine kinase (85), on proliferation of these cells. In NCI-H292 cells (figure 3.10) tyrphostin diminished the growth of cells cultured in serum free medium at days 3, 5 and 7 ($P<0.001$) and medium containing 10% FBS at days 3, 5 and 7 ($P<0.001$) by approximately 50%. Conversely tyrphostin was unable to inhibit the proliferation of cells when cultured in the presence of 1nM EGF except after 7 days of culture where there was a small but significant reduction in the proliferation of NCI-H292 cells cultured in 1nM EGF and 1μM tyrphostin ($P<0.03$). Proliferation of control cells cultured in serum free medium containing 1 in 20,000 DMSO was at the same rate as those cultured in serum free medium alone suggesting the tyrphostin itself is causing the effects seen and not the DMSO vehicle.

16HBE 14o- cells showed a greater variation in proliferative responses and a slight inhibitory effect of tyrphostin in all treatments only reached significance when added to 1nM HB-EGF containing medium at days 5 and 7 of growth (figure 3.11). Again as with NCI-H292 cells DMSO did not interfere with the proliferation of 16HBE 14o- cells when added in a 1 in 20,000 dilution to serum free medium.

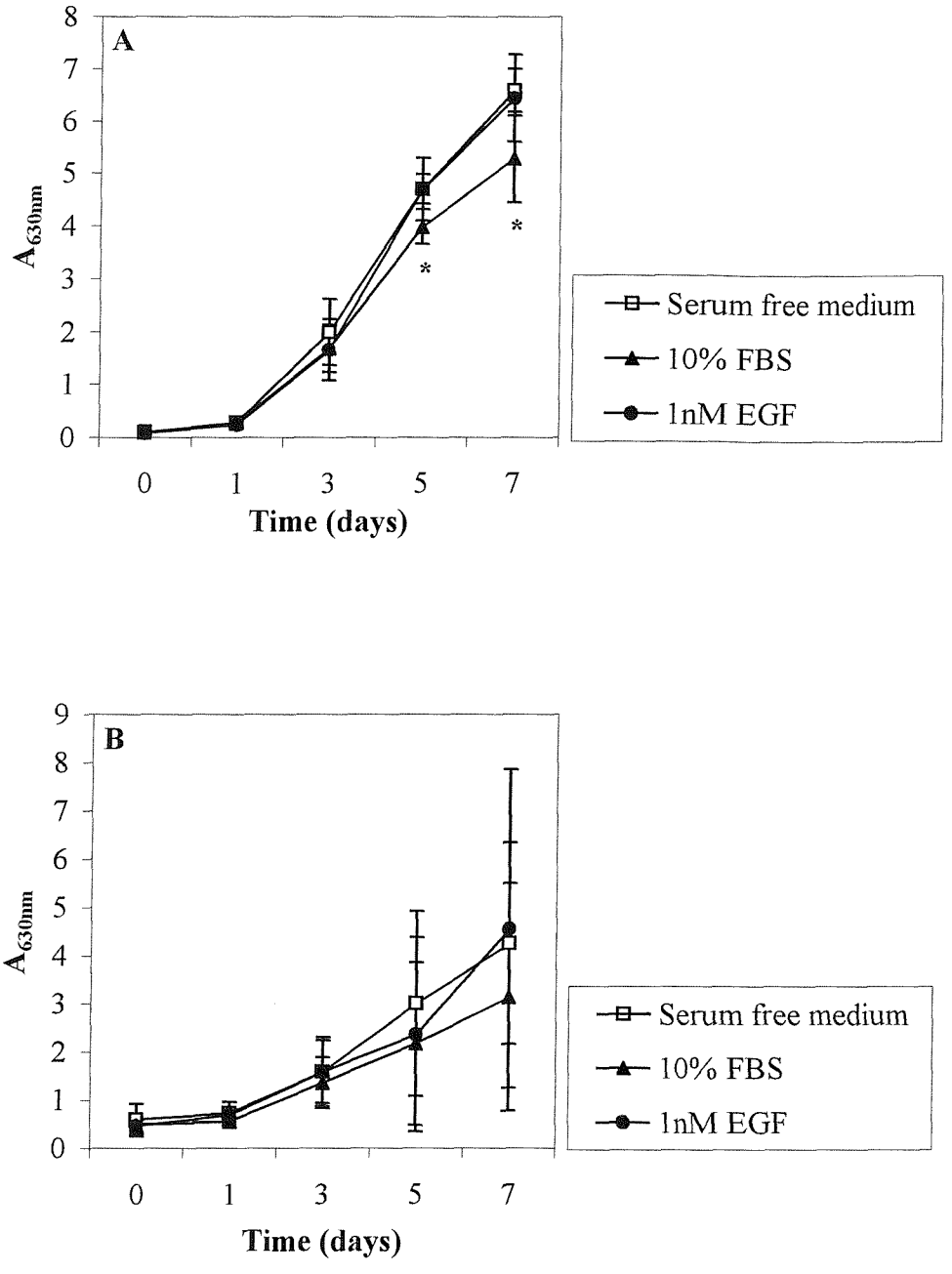

Figure 3.6. Effect of FBS and EGF on growth of bronchial epithelial cell lines.

The effect of serum free medium, 10% FBS or 1nM EGF on the growth of NCI-H292 (A, n=15) and 16HBE 14o- (B, n=18) cells was determined using methylene blue assay. Data are mean absorbance of methylene blue at 630nm +/– SD. *P<0.001 using an unpaired Student's *t*-test to compare serum free with 10% FBS or 1nM EGF culture conditions.

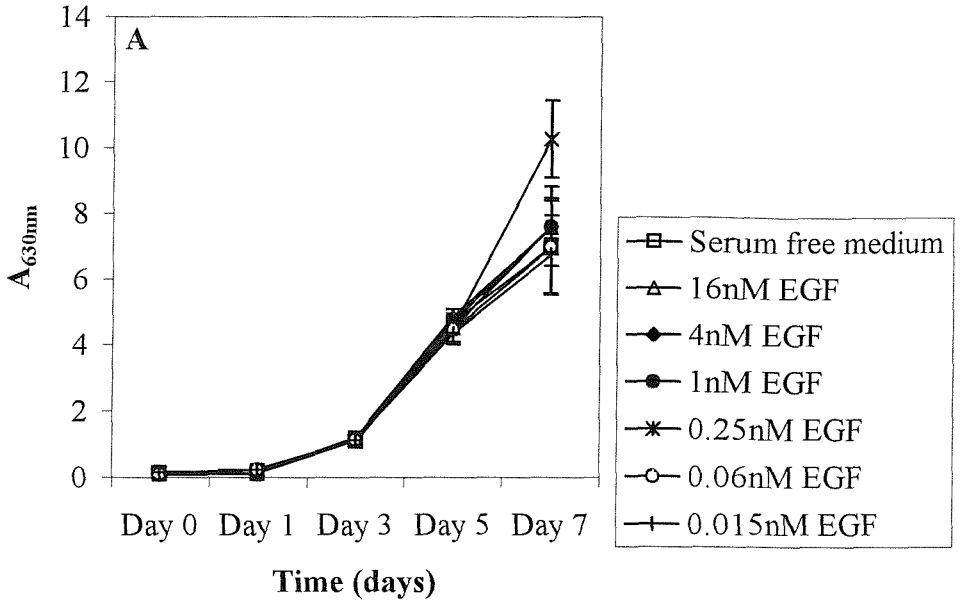

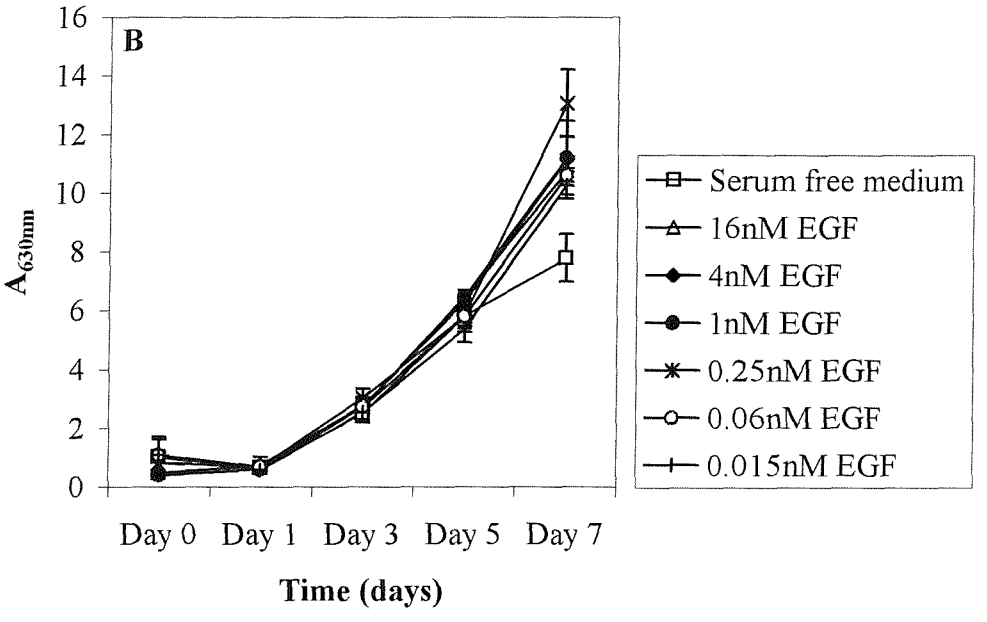

Figure 3.7. The effect of a range of concentrations of EGF (0.015nM-16nM) on the growth of cells.

NCI-H292 (A) and 16HBE 14o- (B) were cultured in a range of doses of EGF for 7 days and cell growth was determined using methylene blue assay. Data are mean methylene blue absorbance at 630nm over a 7 day growth period +/−SD derived from triplicates within a single experiment.

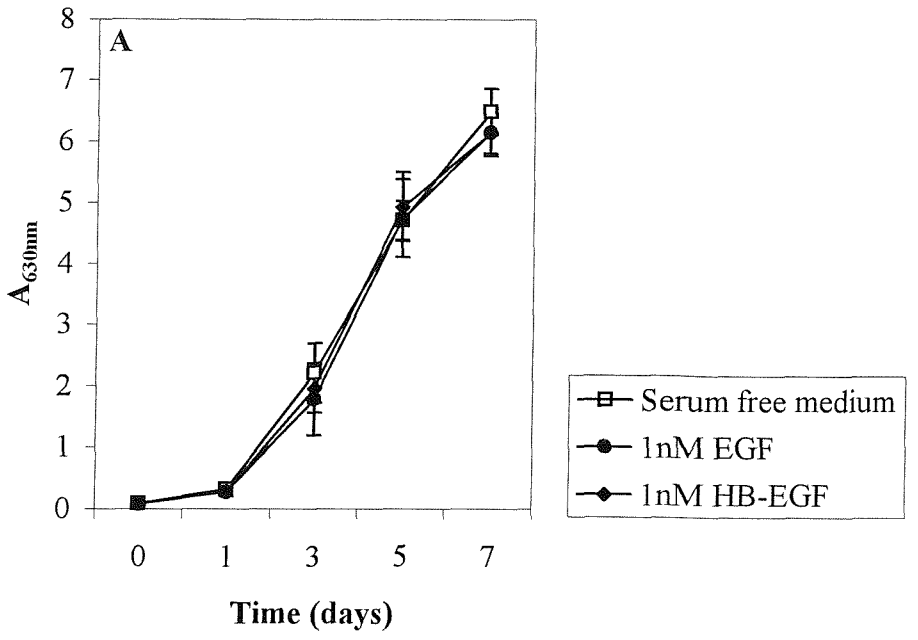

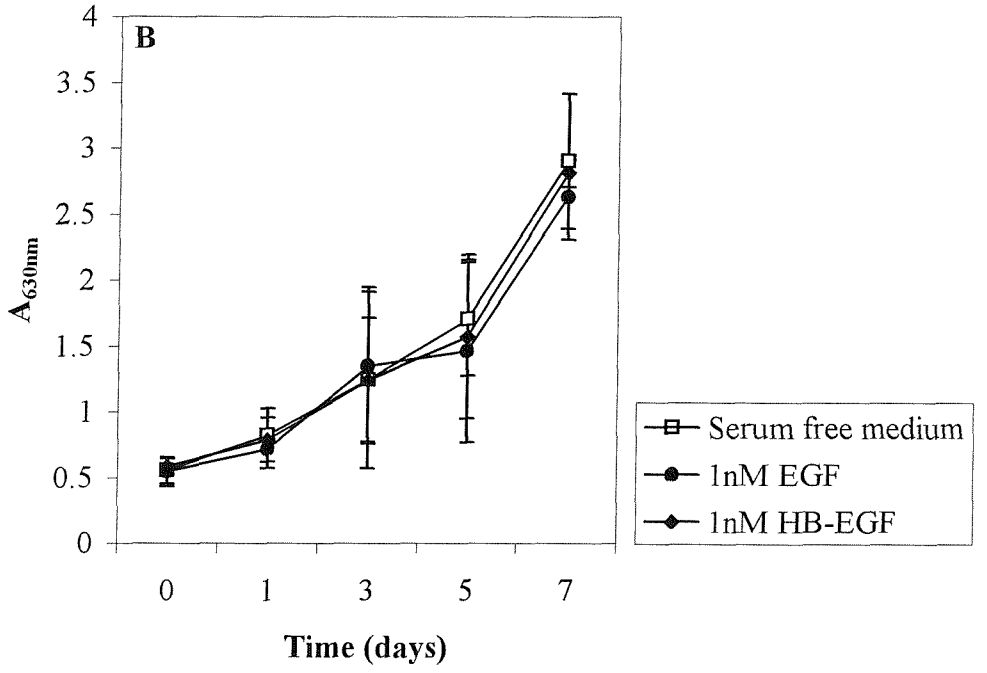

Figure 3.8. Comparison of the effect of 1nM EGF or 1nM HB-EGF on the growth of cells.

NCI-H292 (A) and 16HBE 14o- (B) cells were cultured for 7 days in medium containing 1nM EGF or 1nM HB-EGF and growth was determined using methylene blue assay. Data are mean methylene blue absorbance at 630nm +/– SD, n=12.

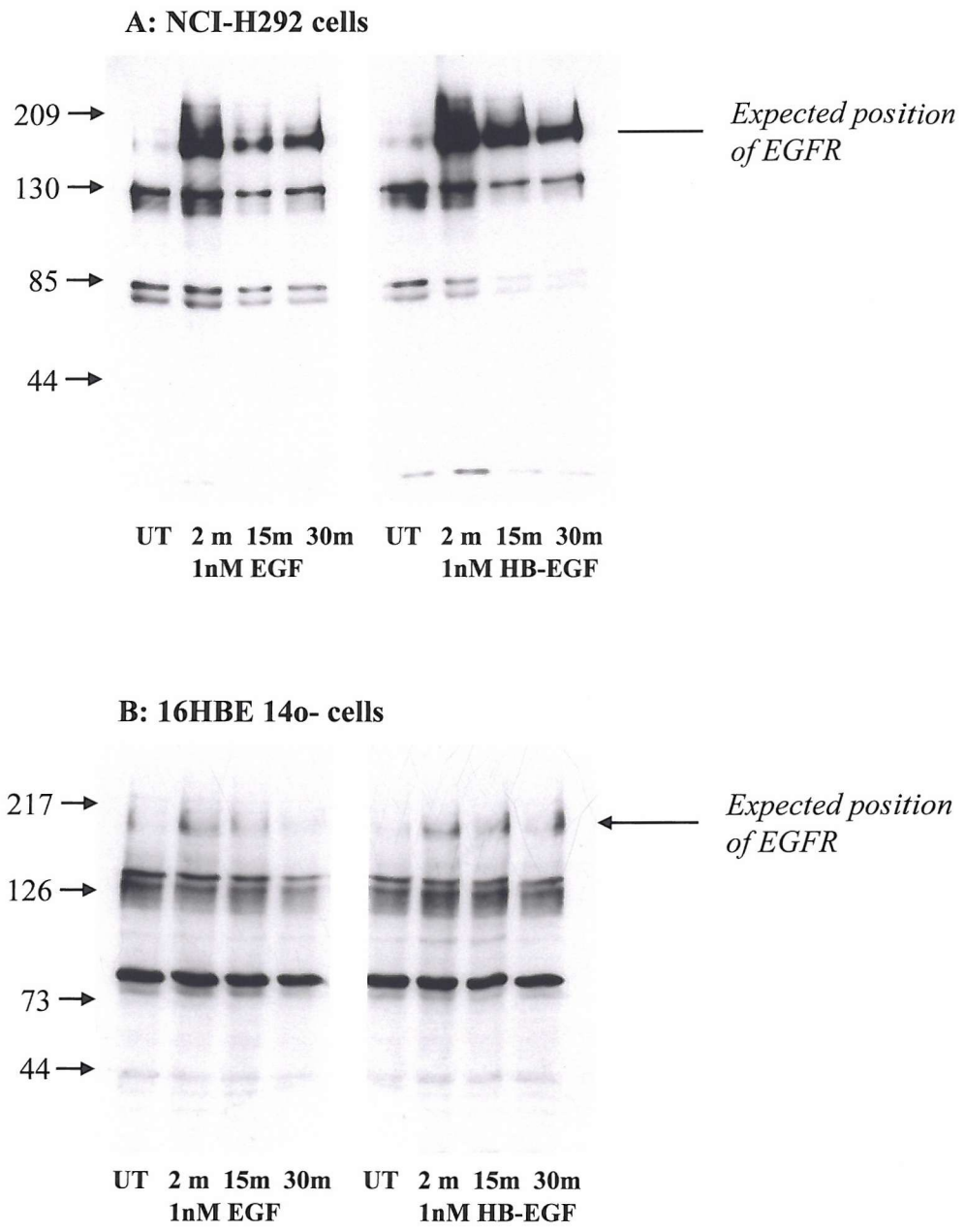

Figure 3.9. Effect of EGF and HB-EGF on phosphotyrosine levels. Phosphotyrosine stained Western blots of whole cell lysates of NCI-H292 (A) and 16HBE 14o- (B) cells serum starved for 24 hours then treated with 1nM EGF or HB-EGF for 2, 15 or 30 minutes (m) or left untreated (UT). Proteins were separated by 7.5% SDS-PAGE and transferred onto a nitrocellulose membrane before staining with an anti-phosphotyrosine (clone PY20) antibody.

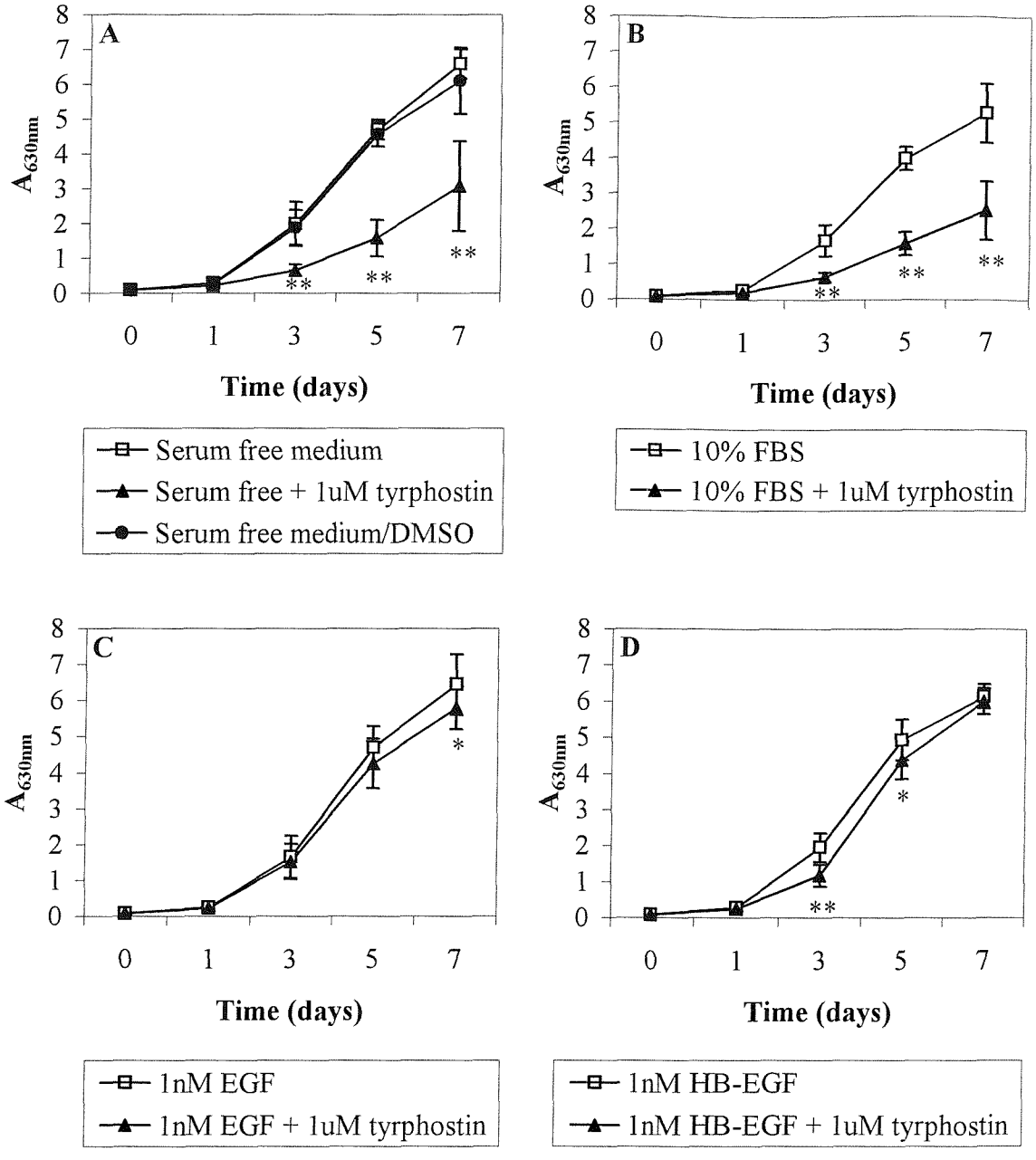

Figure 3.10. Effect of tyrphostin AG1478 on growth of NCI-H292 cells.
NCI-H292 cells were cultured for up to 7 days with the addition of 1μM tyrphostin AG1478 to serum free medium (A), 10% FBS (B), 1nM EGF (C) or 1nM HB-EGF (D). Data are mean absorbance of methylene blue at 630nm +/- SD. *P<0.05, **P<0.001 using Student's unpaired *t*- test to compare culture conditions +/- tyrphostin AG1478 (n=15 except HB-EGF graph where n=12)

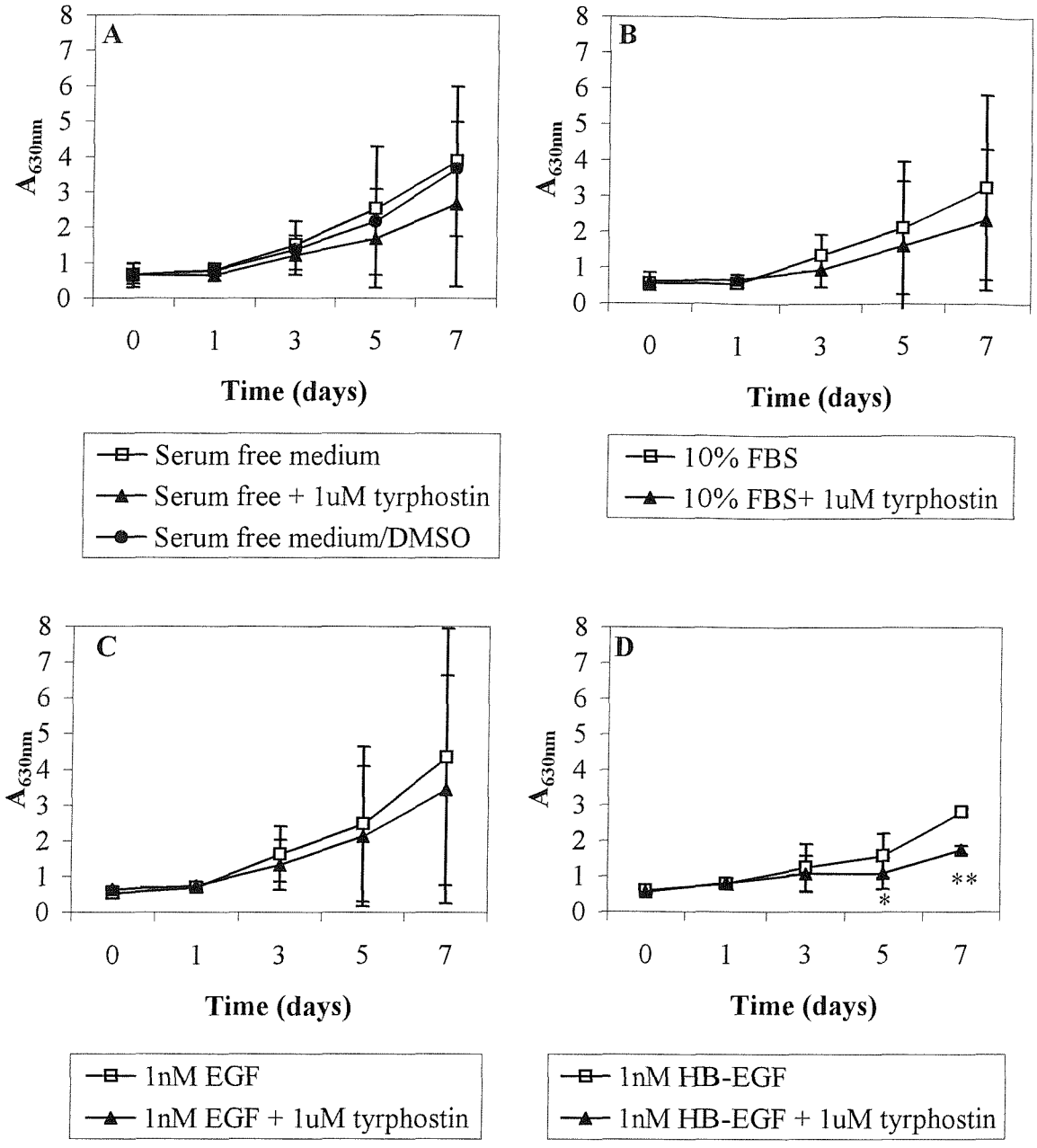

Figure 3.11. Effect of tyrphostin AG1478 on growth of 16HBE 14o- cells.
16HBE 140- cells were cultured for up to 7 days with the addition of 1μM tyrphostin AG1478 to serum free medium (A), 10% FBS (B), 1nM EGF (C) or 1nM HB-EGF (D). Data are mean absorbance of methylene blue at 630nm +/- SD. *P<0.05, **P<0.001 using Student's unpaired *t*- test to compare culture conditions +/- tyrphostin AG1478 (n=15 except HB-EGF graph where n=12)

3.4 Discussion

Cell adhesion molecules expressed on the cell surface are involved in a variety of functions including cell-cell and cell-extracellular matrix binding, ligand binding and cell migration (83). Shifts in the levels of cell adhesion molecules expressed on the cell surface along with alternative splicing of variant exons and variations in the pattern of glycosylation and sulphation allows dynamic control of adhesion molecule function. For example the combination of alternatively spliced CD44 variants along with overexpression of CD44 proteins has been shown to result in enhancement of hyaluronan mediated cell adhesion (168), (15). The enhanced staining for CD44 observed in the bronchial epithelium of asthmatic subjects (73) could provide a mechanism for increased adhesion to adjacent cells or to the extracellular matrix via hyaluronan or enhanced presentation of heparin binding growth factors such as HB-EGF by exon v3 containing CD44 proteins.

EGF receptor staining is also elevated in the epithelium of asthmatic bronchial biopsies (115) and EGF has been shown to increase CD44 expression in mice fibroblasts (166). Therefore the main aim of this chapter was to examine the effect of EGF on CD44 expression by human bronchial epithelial cell lines NCI-H292 and 16HBE 14o-. Expression of CD44 and CD44v3 by NCI-H292 and 16HBE 14o- cells was demonstrated and immunocytochemistry showed staining consistent with a plasma membrane distribution a finding compatible with the role of CD44 as a cell adhesion molecule. Western blotting analysis of CD44 and CD44v3 proteins expressed by the bronchial epithelial cell lines revealed multiple bands from 90kDa – 220kDa and 100-200kDa, respectively, suggesting that many alternatively spliced and glycosylated isoforms are expressed. These findings are consistent with an immunohistochemical study by Mackay *et al* 1994 (90) that described expression of multiple isoforms of CD44 (CD44s, v4, v6, v9) in human lung bronchial epithelium and also showed a Western blot profile with multiple bands ranging from 90-over 200kDa similar to that presented here in figure 3.2. Another large study by Fox *et al*, 1994 (41) described CD44s, v3, v4/5, v6 and v8/9 expression in respiratory epithelium using immunohistochemistry. The 90kD protein detected on Western blots in figure 3.2 probably corresponds to the standard form of CD44 whereas the higher molecular weight proteins are likely to correspond to isoforms containing alternatively spliced

exons and post-translational glycosylation. The absence of tight bands on the blot can probably be accounted for by the expected high glycosylation of the proteins run on the gel, as glycosylation reduces the mobility of proteins and heterogeneity in the extent of glycosylation results in smears of proteins rather than tight bands on the gel.

Quantification of CD44 and CD44v3 cell surface expression using flow cytometry showed that EGF and HB-EGF had no significant effect on the expression of these cell surface proteins by the bronchial epithelial cell lines, NCI-H292 and 16HBE 14o-. This was confirmed by Western blotting. This is in contrast to a study looking at CD44 expression by fibroblasts which demonstrated EGF induction of CD44 gene transcription and subsequent expression by mouse fibroblasts (166). One possible reason for the lack of effect seen here is that EGF could stimulate changes in gene transcription with no subsequent enhancement of translation into surface expressed protein. Alternatively EGF may play a role in the control of the complement of exons alternatively spliced and expressed. Epithelial cells predominantly express CD44 proteins containing the variant exons v8, v9 and v10 (referred as the epithelial forms of CD44 or CD44E) (30), and in the cell lines studied here EGF receptor ligands could influence these or other alternatively spliced forms and not total CD44 or CD44v3. EGF receptor ligands might modify CD44 function through changes in glycosylation or sulphation or its sub-cellular distribution, as has been shown for tumour necrosis factor-α (TNF-α) which stimulates CD44 sulphation on leukocytes and increased adhesion to the endothelium of blood vessels (92).

Factors other than cytokines and growth factors might also influence CD44 expression by these cells and it has previously been shown that cell density is a factor to be considered when measuring CD44 levels (81). It was therefore important to examine the possibility that in these cells EGF affected cell density with a concurrent down regulation of CD44 expression thus masking any EGF regulated changes in CD44 expression.

The effect of culture conditions on growth of NCI-H292 and 16HBE 14o- cells was quantified using the methylene blue assay. The growth curves presented in figure 3.6 showed that the addition of 1nM EGF to the growth medium of these cells has no significantly stimulatory effect on the growth of these cells. Thus it is unlikely that any

EGF stimulated increase in total CD44 or CD44v3 expression was masked by a parallel increase in cell density or proliferation. In addition to cell adhesion, CD44 might play other roles in the maintenance of the bronchial epithelium and its repair following damage for which its presence on the cell surface rather than the absolute values of CD44 expression is important.

Growth experiments described in this chapter showed how EGF was unable to induce an increase in proliferation above that measured when cells were cultured in serum free medium implying these cells have the ability to grow without any requirement for exogenous growth factor. The absence of an EGF mediated proliferative response in 16HBE 14o- cells could be accounted for by the fact that these cells are a virally transformed cell line and that their proliferation cannot be controlled by growth factors due to the absence of normal cell cycle controls (49). NCI-H292 cells are a tumour cell line (10) and like other tumour cells probably secrete their own growth factors such as transforming growth factor-alpha (TGFα) and amphiregulin (AR) (147) which stimulate proliferation of cells (18), (131) to grow at a maximal rate so the addition of further EGF has no stimulatory effect, as shown in figure 3.7. A comparison of the proliferation of cells cultured in EGF or HB-EGF (figure 3.8) showed that the effects of HB-EGF resembled that seen with EGF where no enhancement of growth was observed. Only the addition of 10% FBS to NCI-H292 cells resulted in any significant change as shown by a reduction in the growth of NCI-H292 cells cultured in 10% FBS for 7 days (figure 3.6), this could be due to the presence of factors in the serum such as transforming growth factor-β (TGFβ) which is known to inhibit growth of epithelial cells (18), (131). This inhibition was not observed in the virally transformed 16HBE 14o- cell line because these cells proceed through the cell cycle irrespective of the presence of growth factors.

Experiments further examining the role of the EGF receptor in proliferation of these cells utilised a selective inhibitor of the EGF receptor tyrosine kinase, tyrphostin AG1478. Proliferation of 16HBE 14o- cells was only significantly inhibited by 1μM tyrphostin when added to 1nM HB-EGF. The addition of tyrphostin to other treatments resulted in a slight reduction of growth at day 7 but the greater variation in data prevented this reaching significance. This and the observation that addition of 1nM

EGF has no stimulatory effect on 16HBE 14o- cells suggests that proliferation is not under the control of soluble factors. 16HBE 14o- cells are an SV40, Large-T antigen transformed cell line and this transformation process immortalises the cells by activation of the p53 oncogene and subsequent inhibition of proteins involved in senescence, allowing the cells to progress through the cell cycle without the need for activation by growth factors and their receptors. It would therefore be expected that the proliferation of these cells is not dependent on growth factors or significantly retarded by their inhibitors (49). Although transformation of these cells does not allow manipulation of proliferation these cells have the advantage that they have retained specific features of a normal differentiated epithelium as shown by their ability to be cultured in a confluent monolayer and display cilia under defined culture conditions. Unlike NCI-H292 cells 16HBE 14o- and other transformed cells also retain the ability to express and form tight junctions in culture (32) and hence a polarised epithelium with separate apical and basolateral compartments allowing regulated movement of ions, water and macromolecules in a defined direction across the epithelium (32), (49).

Conversely, cells like NCI-H292 cells which are a carcinoma derived cell line retain some growth control systems as shown by the ability of tyrphostin AG1478 to inhibit growth under certain defined conditions. Here, NCI-H292 cell proliferation was inhibited by tyrphostin AG1478 when cultured in serum free or serum containing medium but not when in the presence of 1nM EGF except at day 7. These data implicate the EGFR tyrosine kinase and imply the expression of autocrine ligand such as TGFα as a mediator of NCI-H292 cell proliferation. In the case of cells cultured in 1nM EGF and tyrphostin this concentration of tyrphostin was presumably insufficient to inhibit EGFR phosphorylation by exogenous and autocrine ligand except at 7 days of culture. Measuring EGFR tyrosine phosphorylation after treating cells with increasing doses of tyrphostin added to 1nM EGF containing medium could test this hypothesis. In conclusion, these data suggest that activation of the EGFR is required for the proliferation of NCI-H292 cells but that autocrine ligand such as TGFα is expressed and activates EGFR to stimulate proliferation sufficient for growth.

Cellular events during repair of bronchial epithelial cells probably require changes in cell adhesion, morphology and motility and as the initial stages of bronchial epithelial repair involve migration and spreading of the epithelial cells rather than proliferation

(71) the absence of any requirement of growth factors for proliferation is not so important as the retention of normal structural features of the epithelium. The EGFR and CD44 have been implicated in migration of 16HBE 14o- cells during epithelial repair following mechanical damage to confluent monolayers, further emphasising the suitability of 16HBE 14o- cells as an *in vitro* model of bronchial epithelial repair. The EGFR ligands EGF and HB-EGF have been shown to enhance the rate of repair (118) and expression of CD44 is increased after damage with brighter staining seen specifically at the wound edge of repairing cultures (80).

In addition to the adhesion properties of CD44 it has also been shown to bind the intracellular linker molecules, ezrin, radixin and moesin, belonging to the ERM protein family which crosslink actin filaments with proteins of the plasma membrane following EGF treatment as detailed in the introduction (see Section 1.6). Modulation of actin dynamics and CD44 localisation by ERM proteins could be an important feature of cell motility and morphology changes during bronchial epithelial repair and these events could be dynamically controlled by CD44 levels on the cell surface, ERM protein activation by EGFR ligands and the actin cytoskeleton.

4 CHAPTER FOUR

THE EFFECT OF EGF RECEPTOR LIGANDS ON EZRIN AND MOESIN IN HUMAN BRONCHIAL EPITHELIAL CELLS

EGF receptor ligands have previously been shown to induce pronounced changes in the morphology of epithelial cells and the distribution of ERM (ezrin, radixin and moesin) proteins. In A431 cells, EGF is able to induce formation of microvilli, then membrane ruffles followed by rounding up of cells. These distinct morphological changes are accompanied by redistribution of ezrin into microvilli and membrane ruffle structures and its phosphorylation on tyrosine residues (23). Other growth factors that act via receptor tyrosine kinases also modulate ezrin behaviour. Hepatocyte growth factor/scatter factor (HGF/SF) binding to its receptor tyrosine kinase, *c-met*, on epithelial cells stimulates tyrosine phosphorylation of ezrin and its enrichment in the detergent insoluble cytoskeletal fraction of these cells. Furthermore ezrin has been shown to play a role in HGF/SF mediated cell migration (33).

The aims of the work in this chapter were to examine the effect of the EGF receptor tyrosine kinase ligands, EGF and HB-EGF, on the distribution, binding and phosphorylation of the ERM proteins, ezrin and moesin, in bronchial epithelial cells. Furthermore as there may be local regulation of these effects by co-localisation of HB-EGF at the plasma membrane with CD44v3, the effects of EGF were compared with those of HB-EGF.

4.1 Western blotting using antibodies against ezrin and moesin

Antibodies raised against ezrin and moesin were tested by Western blotting to determine their reactivity. Staining of nitrocellulose blots with mouse monoclonal antibodies to ezrin and moesin showed immunoreactivity to proteins in the range 80-85kDa, the expected molecular weight of members of the ERM protein family (figure 4.1A). Furthermore both antibodies had immunoreactivity towards a single band on the Western blot implying specific detection of the individual protein. Control stained Western blots with omission of primary antibody showed little staining and no non-specific bands were seen at the expected molecular weight of ezrin or moesin (figure

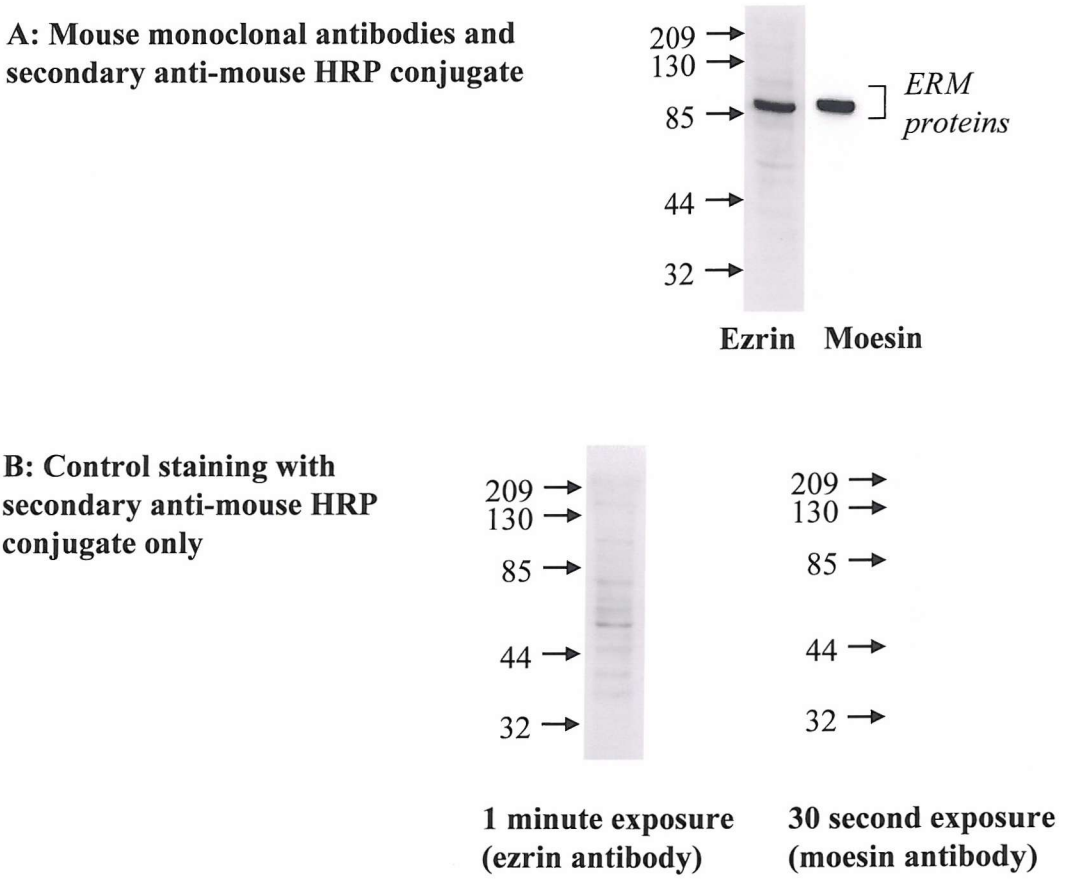

Figure 4.1. Western blotting for ezrin and moesin using mouse monoclonal antibodies.
Proteins in cell lysates from 16HBE 14o- cells were separated by 10% SDS-PAGE and transferred onto nitrocellulose. Antibodies against ezrin and moesin were mouse monoclonal from Transduction Laboratories (A). Panel B shows control staining of Western blots in the absence of primary antibody with secondary antibody incubation alone. Bands on all blots were developed with ECL Plus followed by exposure of autoradiography film for 1 minute for the ezrin antibody and 30 seconds for the moesin antibody, respective exposure times for the antibody controls are shown in panel B for comparison.

4.1B). The mouse monoclonal antibodies were used for further studies on the basis of their ability to detect a single band by Western blotting at the expected molecular weight of ezrin and moesin with no detectable non-specific binding by the secondary-HRP conjugated antibody.

4.2 Ezrin and moesin distribution in membrane and cytoskeletal fractions of 16HBE 14o- bronchial epithelial cells

It has previously been shown that tyrosine phosphorylation of ezrin and moesin by HGF/SF causes them to be associated with the cytoskeleton of bronchial epithelial cells (33). The aims of these experiments were to examine whether EGF was able to stimulate ezrin and moesin to become physically associated with plasma membrane proteins or sub-plasma membrane cytoskeletal proteins, to form protein complexes within the cytoplasm, of human bronchial epithelial cells.

Initial experiments involved preparing particulate and soluble fractions by homogenisation and ultracentrifugation to sediment the particulate membrane fraction that includes plasma membrane and cytoskeletal protein complexes.

16HBE 14o- cells were treated with serum free medium in the absence or presence of 1nM EGF for 15 minutes and then disrupted by homogenisation. Whole cells and large cell debris were pelleted and removed, prior to separation of the particulate fraction from the soluble (cytosolic) fraction of the cell homogenate using an ultracentrifuge. In order to examine changes in the relative amount of specific proteins, the concentration of protein was determined and normalised to 0.3μg/μl of protein. 20μl (6μg protein) of each fraction was then separated by SDS-PAGE and Western blotting was used to detect any changes in the relative amounts of ezrin and moesin in these fractions.

Western blots stained for ezrin and moesin from a preliminary experiment (figure 4.2a) showed that ezrin and moesin were present in both fractions in the untreated cells. When the cells were treated for 15 minutes with 1nM EGF both ezrin and moesin became enriched in the particulate fraction. Figure 4.2b shows semi-quantitative analysis of these blots to clarify changes in the intensity of bands on the Western blots.

The increased levels of ezrin and moesin in the particulate fraction suggests reduced solubility of ezrin and moesin and likely reflects an increase in the binding of ezrin and moesin to insoluble protein components of the plasma membrane and cytoskeleton of these cells.

As this preliminary experiment showed that treatment with EGF was able to stimulate an enrichment of ezrin and moesin in the particulate fraction of cells, it was next determined whether ezrin and moesin became differentially associated with the actin cytoskeleton after treatment of bronchial epithelial cells with EGF or HB-EGF. Cytoskeletal preparations were also a much more convenient method for larger experiments than the homogenisation/ultracentrifugation method of cell fractionation.

Following treatment of 16HBE 14o- cells with serum free medium without or with 1nM EGF or 1nM HB-EGF, cytoskeletal extracts were prepared using a method based on the relative insolubility of the actin cytoskeleton in mild detergents compared with other cellular proteins. Proteins in these extracts were analysed by SDS-PAGE and Western blotting (figure 4.3a). In untreated cells, both ezrin and moesin were present in the cytoskeletal fraction. Upon treatment with 1nM EGF for 15 minutes there was a significant increase in the levels of ezrin ($P<0.05$) and moesin ($P<0.003$) in the cytoskeletal fraction, as determined by semi-quantitative analysis of Western blots (figure 4.3b). However, when looking at the effect of HB-EGF on redistribution of ezrin and moesin variation in the data obtained was observed. The Western blot presented in figure 4.3a shows that HB-EGF appears to stimulate a small enrichment similar to that seen with EGF. However, when Western blots from three experiments were subjected to semi-quantitative analysis, enabling variability between experiments to be taken into account, there was no significant effect of HB-EGF on the distribution of ezrin and moesin between fractions of 16HBE 14o- cells (figure 4.3b).

To further examine the EGF stimulated changes in cytoskeletal binding 16HBE 14o- cells were treated with 1nM EGF for a range of time points between 2 minutes and 6 hours (figure 4.4). This time course of 1nM EGF treatment indicated that an enhancement of the binding of ezrin and moesin to the actin cytoskeleton occurred after 2 minutes of treatment. Enrichment of ezrin and moesin in the cytoskeleton gradually decreased after 15 minutes to untreated levels at 30 minutes, 1 hour and 6 hours. As a

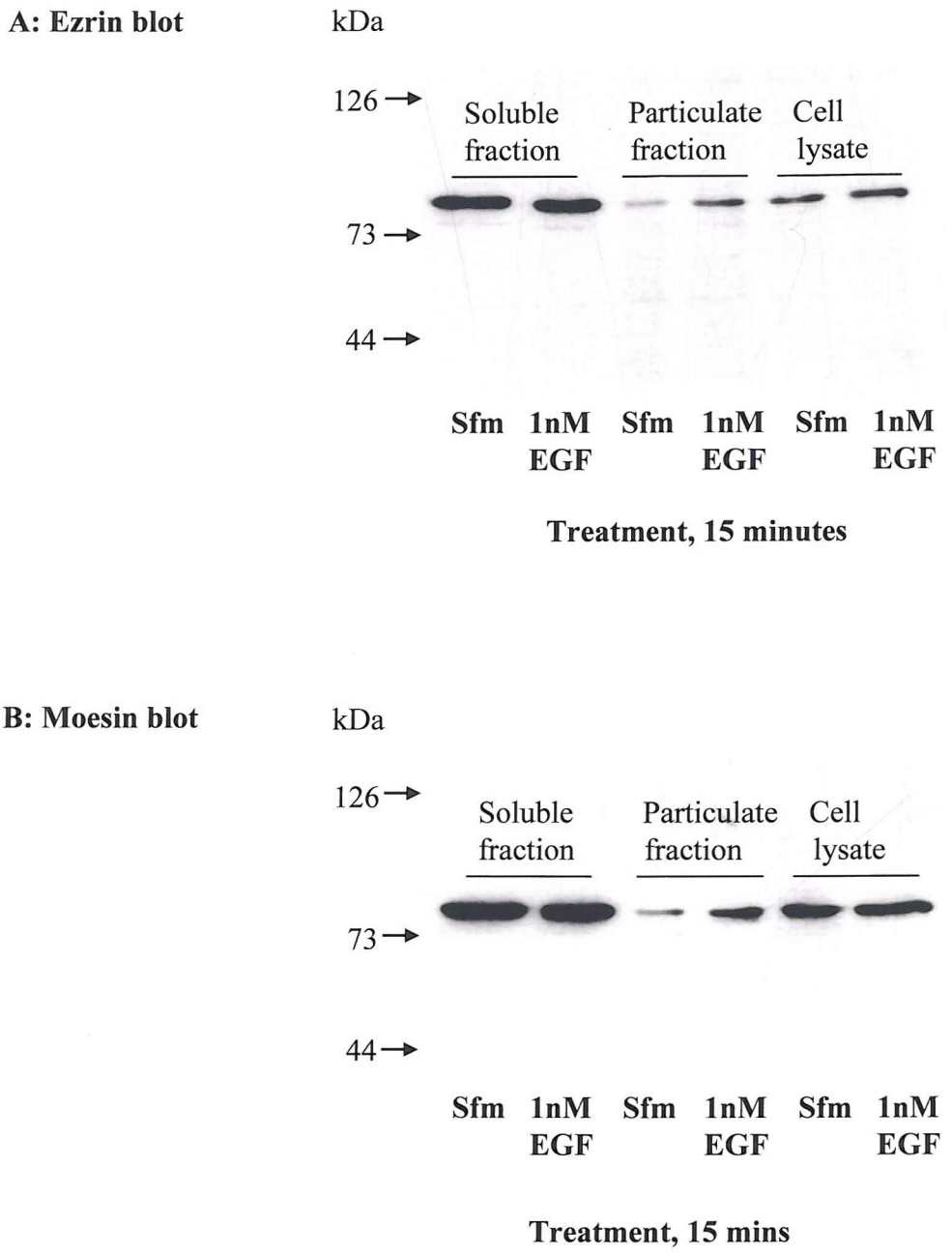

Figure 4.2a. Effect of EGF on the distribution of ezrin and moesin between particulate and soluble fractions of 16HBE 14o- cells.
Cells were serum starved for 24 hours then treated for 15 minutes with serum free medium (Sfm) +/- 1nM EGF prior to the preparation of particulate (membrane) and soluble fractions. Fractions were solubilised in denaturing lysis buffer and a protein assay carried out. 6μg of protein from each fraction/sample was separated by 7.5% SDS-PAGE and transferred onto a nitrocellulose membrane before staining with mouse monoclonal antibodies against (A) ezrin or (B) moesin (Transduction Labs).

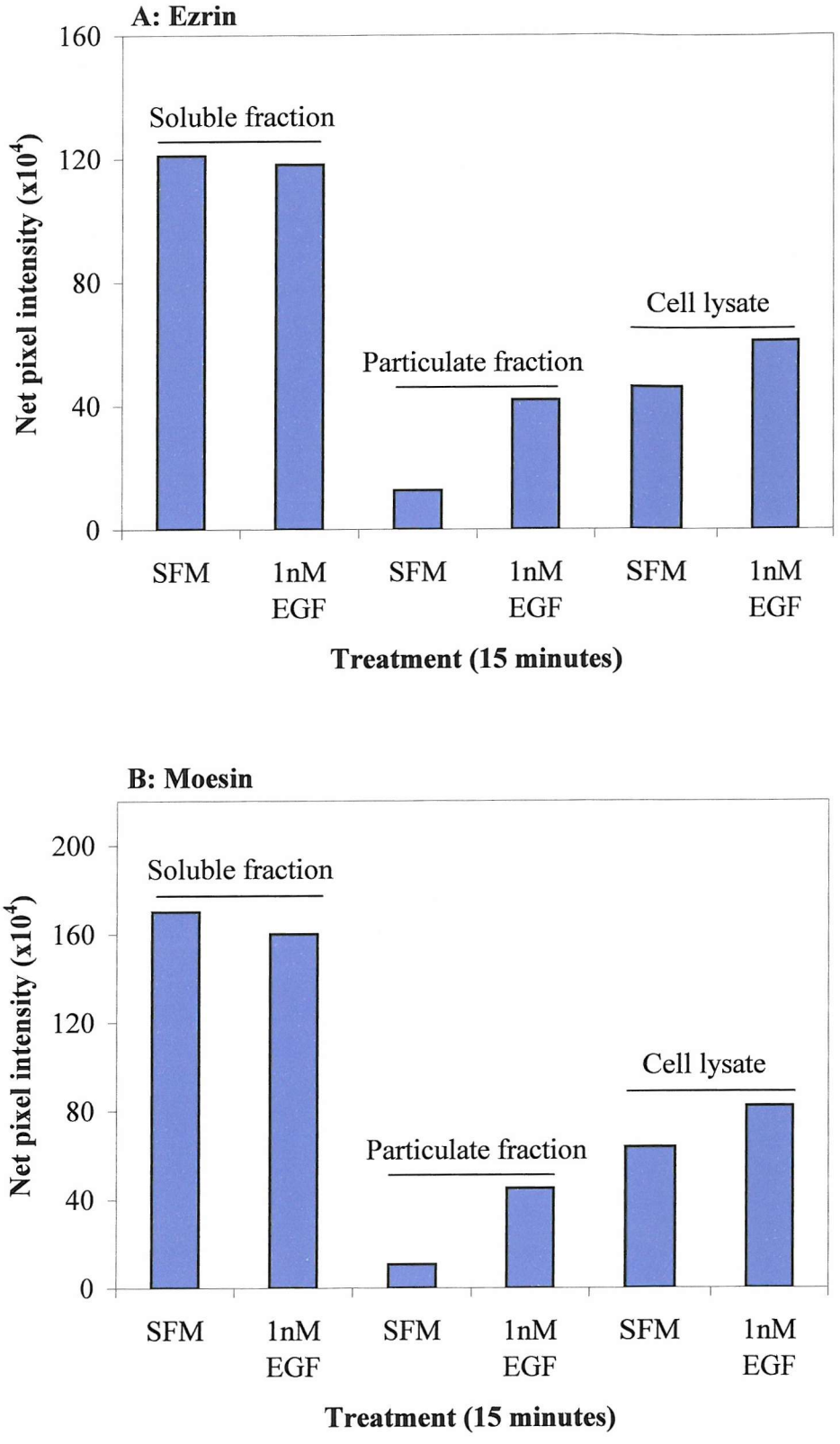

Figure 4.2b. Semi-quantitative densitometry of Western blots in figure 4.2a.

Western blots were scanned using a Hewlett Packard Deskscan and levels of immunoreactive ezrin and moesin measured using Kodak 1D software. Data are from a single experiment.

A: Ezrin blot

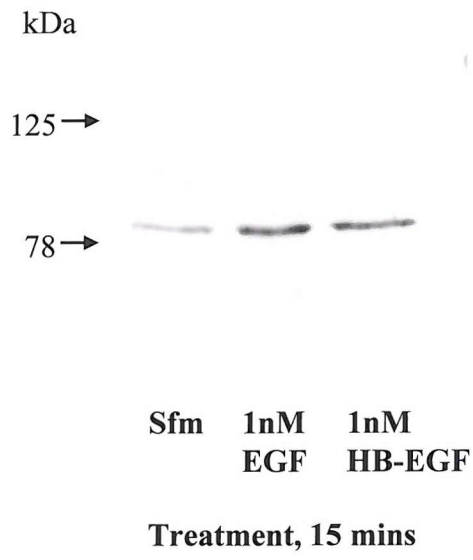

B: Moesin blot

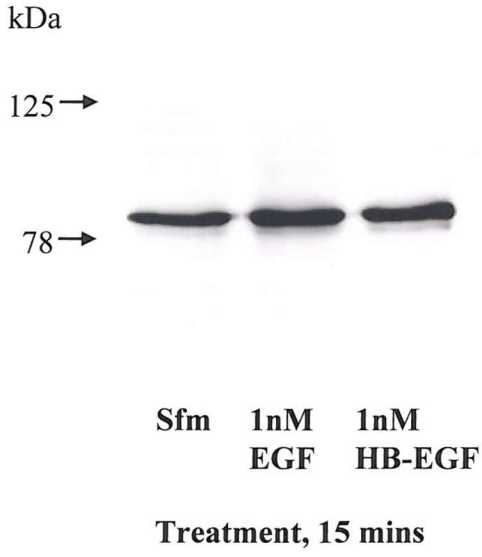

Figure 4.3a. Effect of EGF and HB-EGF on ezrin and moesin levels in cytoskeletal fractions from 16HBE 14o- cells.
Cells were serum starved for 24 hours then treated for 15 minutes with serum free medium (Sfm) +/– 1nM EGF or HB-EGF prior to extraction of the soluble fraction followed by lysis of the cytoskeletal fraction into hot denaturing lysis buffer. The protein concentration of samples was determined and 6μg of protein from each sample separated by 7.5% SDS-PAGE. Proteins were transferred onto a nitrocellulose membrane and stained with mouse monoclonal antibodies to ezrin or moesin (Transduction Labs). Blots are representative of three experiments.

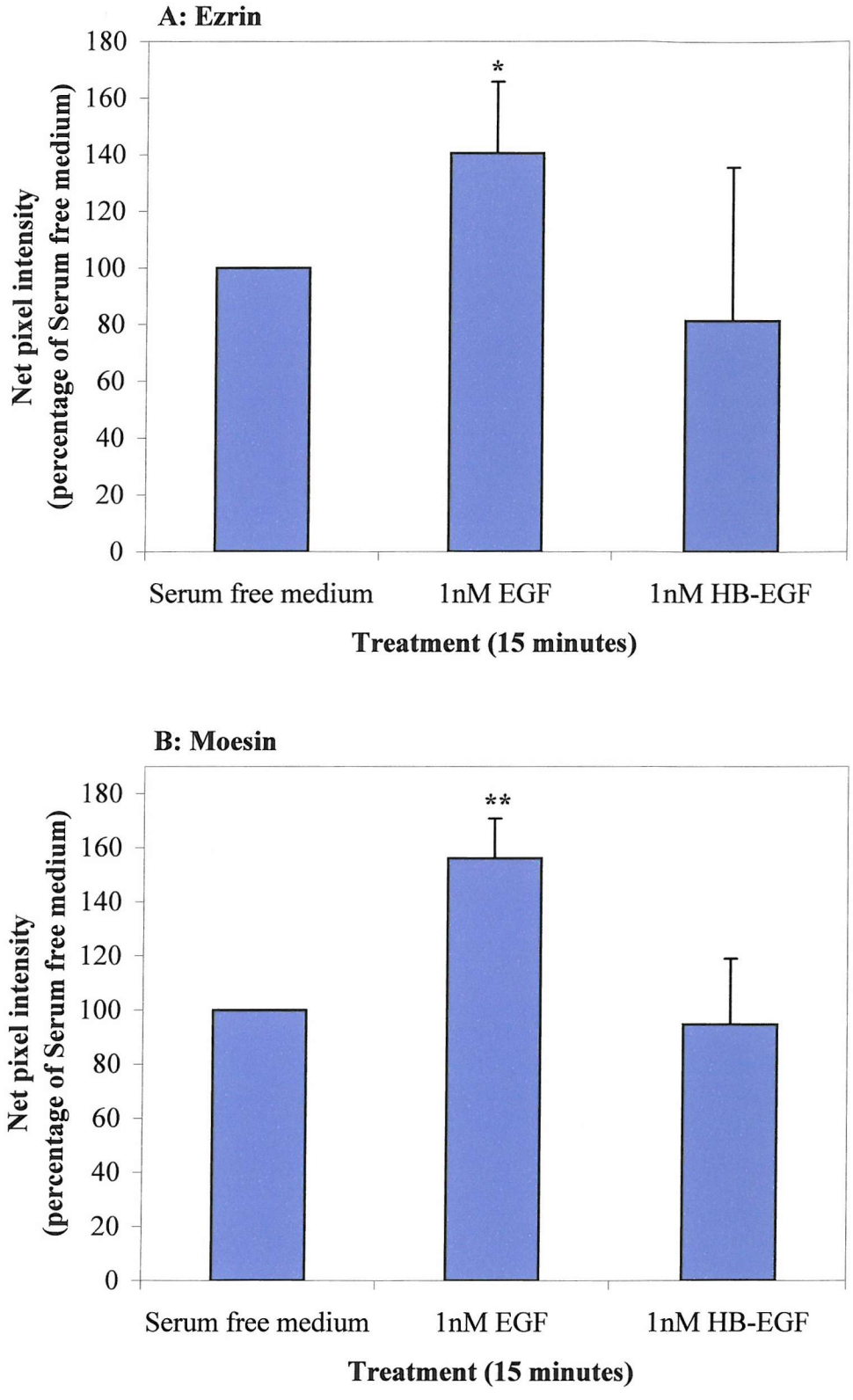

Figure 4.3b. Semi-quantitative densitometry of ezrin and moesin stained Western blots of cytoskeletal fractions from figure 4.3a. Levels of immunoreactive ezrin or moesin were measured using Kodak 1D software. Data are the mean +/– SD of net pixel intensity expressed as a percentage of the serum free medium treated control sample. Data from three individual experiments were statistically analysed using a Student's unpaired t-test *P=<0.05, **P<0.003.

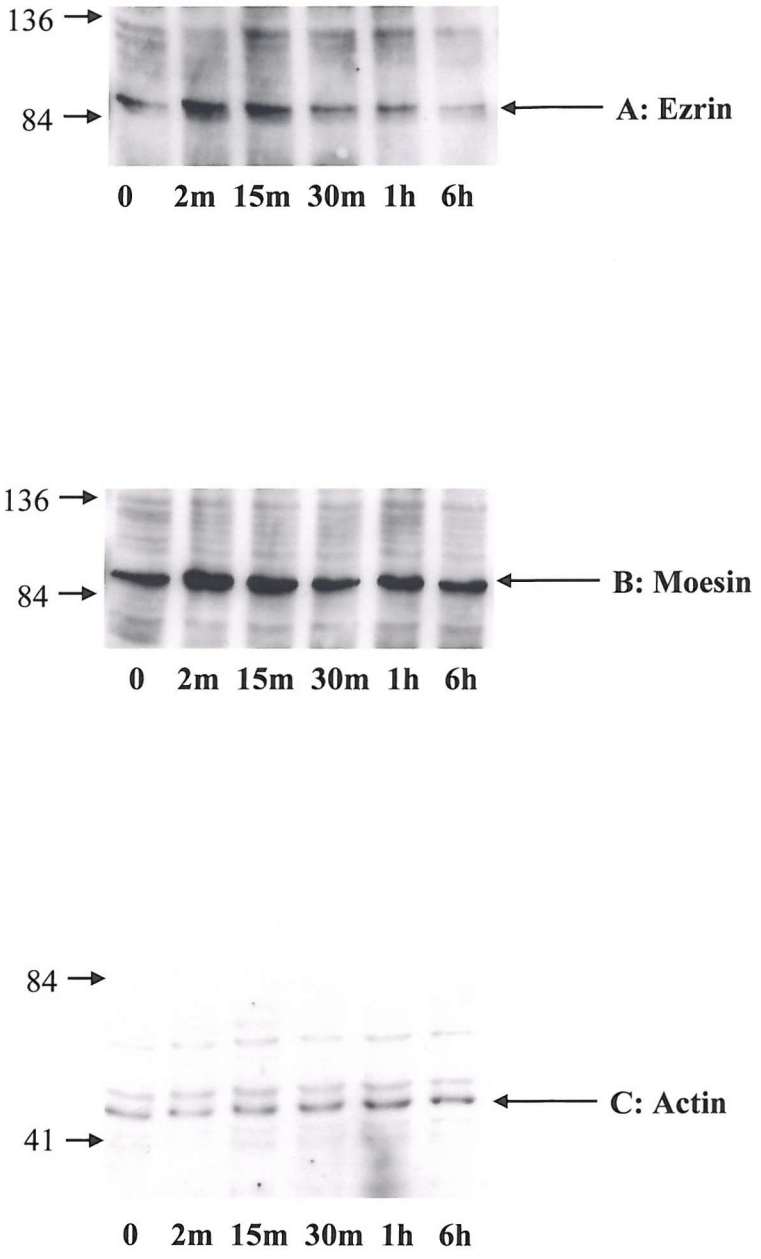

Figure 4.4. Cytoskeleton extracts of 16HBE 14o- cells treated with 1nM EGF for various time periods from between 2 minutes and 6 hours. 16HBE 14o- cells were serum starved for 24 hours before treating with serum free medium containing 1nM EGF for 2, 15, 30 minutes, 1 or 6 hours. Soluble proteins were extracted before solubilising cytoskeletons in hot denaturing lysis buffer. 5μg of protein was loaded onto each lane of a 7.5% SDS-PAGE gel and nitrocellulose Western blots were stained using mouse monoclonal anti-ezrin (A), anti-moesin (B) or rabbit polyclonal anti-actin (C) antibodies. Blots are representative of two experiments.

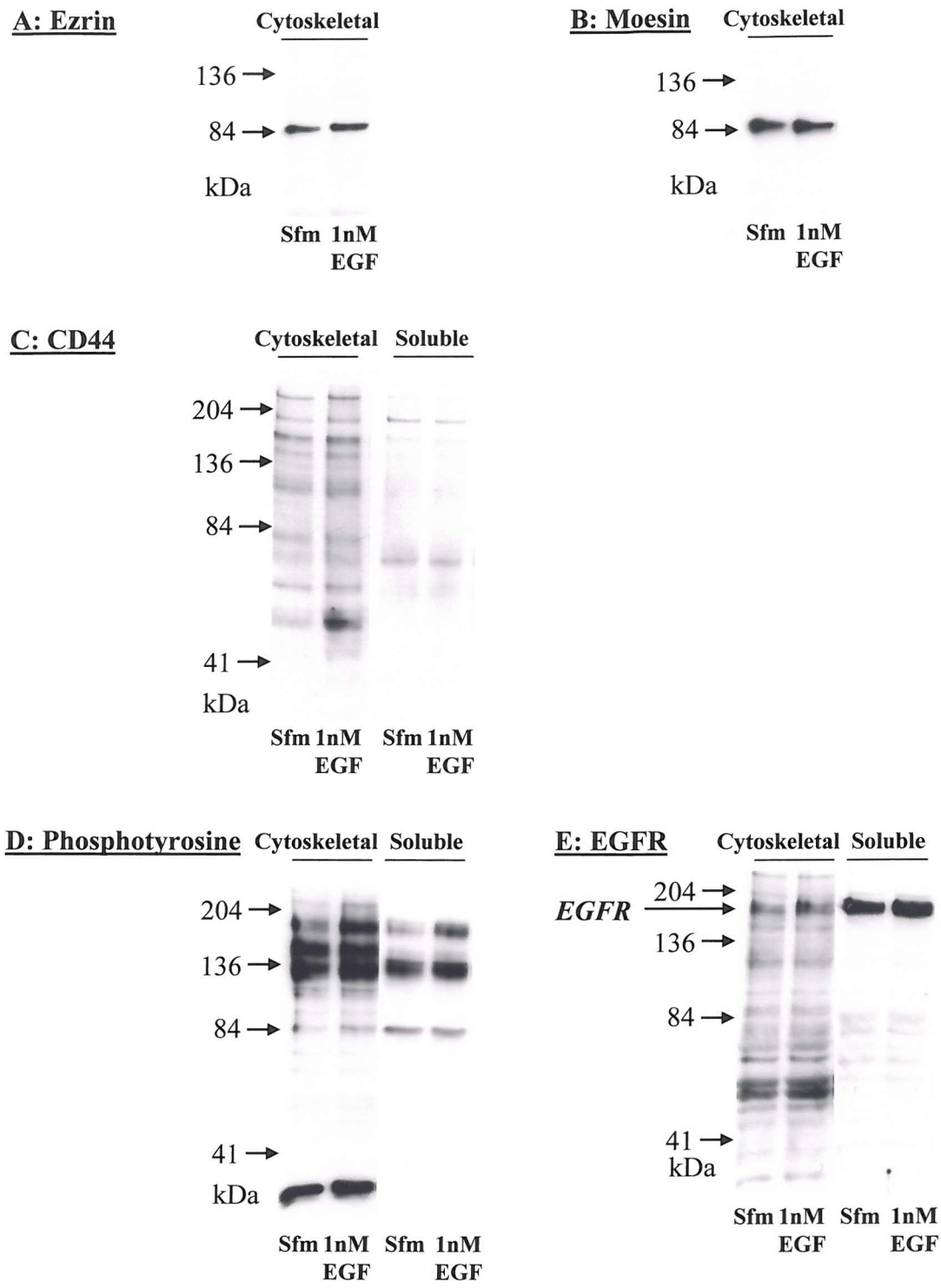

Figure 4.5. Effect of EGF on the distribution of ezrin, moesin, CD44, phosphotyrosine and EGF receptor in cytoskeletal and soluble fractions of 16HBE 14o- cells.

Cells were serum starved for 24 hours, treated with serum free medium (Sfm) +/– 1nM EGF for 15 minutes before preparation of soluble and cytoskeletal fractions. 8μg of protein was separated by 7.5% SDS-PAGE and elecrophoretically transferred onto nitrocellulose. Western blots were stained with antibodies against ezrin (A), moesin (B) (both mouse monoclonal), CD44 (C), phosphotyrosine (D) and EGF receptor (clone Ab-4) (E). Blots are representative of two experiments.

control, actin levels were also assessed by Western blotting and remained consistent throughout the time course.

Alongside staining for ezrin and moesin, CD44, phosphotyrosine and EGF receptor proteins were also detected in both the cytoskeletal and soluble fractions of these cells. As CD44 is known to be a binding partner for ERM proteins its distribution in cytoskeletal and soluble fractions of 16HBE 14o- cells was also assessed (figure 4.5C). CD44 was present in both fractions with the cytoskeletal fraction having more total CD44 per μg of protein as well as a greater number of bands than the soluble fraction. No effect on this distribution was observed with EGF treatment. EGF receptor proteins were also observed in both fractions, with no detectable changes occurring following treatment with EGF (figure 4.5E). An EGF stimulated increase in phosphotyrosine staining was detected in both fractions after treatment (figure 4.5D) and the enhancement of the major band at around 175kDa probably reflects an increase in tyrosine phosphorylation of EGF receptors following treatment with EGF.

4.3 Ezrin and moesin distribution in 16HBE 14o- bronchial epithelial cells

Following the observation that EGF was able to elicit a small increase in the association of ezrin and moesin with the insoluble cytoskeletal fraction, the next aim was to examine whether EGF was able to stimulate the redistribution of ezrin and moesin to associate with the actin cytoskeleton in surface structures such as microvilli. 16HBE 14o- cells were treated with serum free medium with or without 1nM EGF or 1nM HB-EGF then cells were fixed and stained for ezrin or moesin using immunocytochemistry.

Treatment of 16HBE 14o- cells with 1nM EGF or HB-EGF stimulated redistribution of ezrin and moesin to plasma membrane regions of the cell. 16HBE 14o- cells were serum starved for 24 hours before cells were treatment with 17, 5, 1nM EGF or 1nM HB-EGF for 2, 15 or 30 minutes. Ezrin and moesin distribution could then be observed following immunocytochemical staining of these cells. Unstimulated 16HBE 14o- cells expressed both ezrin and moesin and both proteins were found in a diffuse cytoplasmic distribution throughout the cells, sometimes both ezrin and moesin were also concentrated in plasma membrane as well as perinuclear regions (figure 4.6).

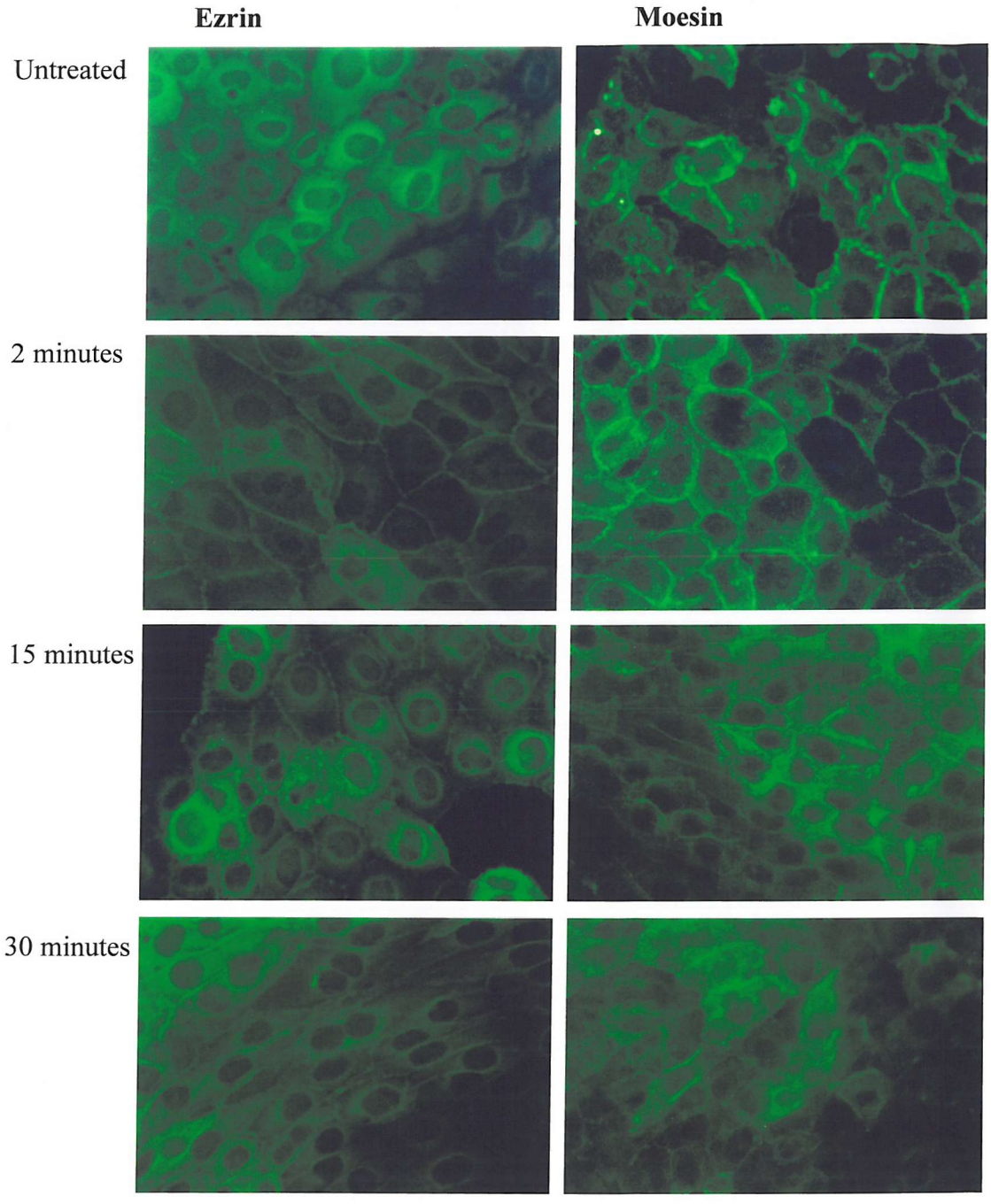

Figure 4.6. Effect of EGF on distribution of ezrin and moesin.
16HBE 14o- cells treated with 1nM EGF for a time course of between 2 and 30 minutes. Cells were serum starved for 24 hours before treating with serum free medium containing 1nM EGF for 2, 15 or 30 minutes or left untreated. Cells were washed twice with PBS before fixing and staining using mouse monoclonal primary antibodies against ezrin or moesin and a secondary anti-mouse FITC-conjugate antibody.

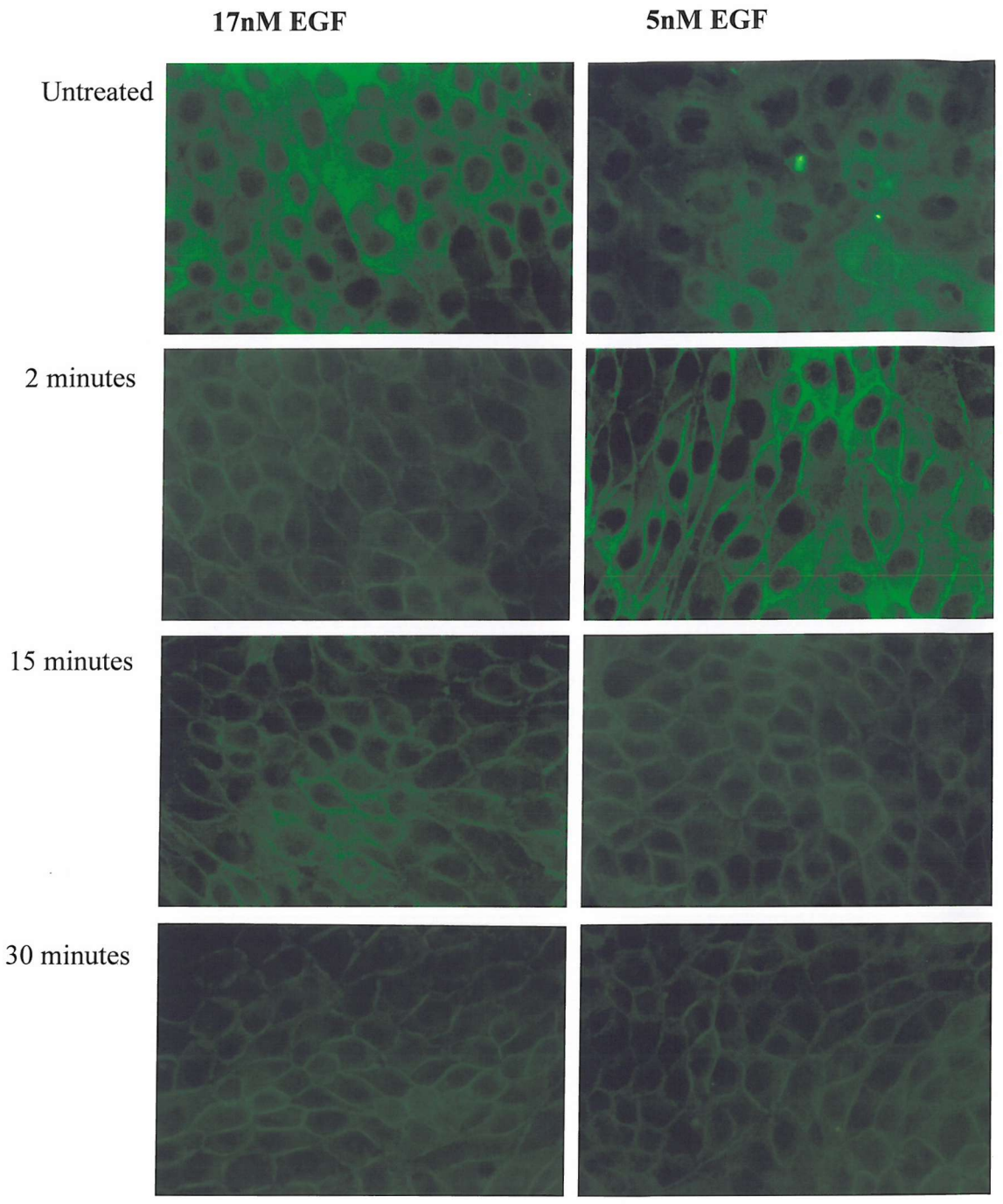

Figure 4.7. Effect of a range of doses of EGF and 1nM HB-EGF on ezrin distribution.
To observe the dose response relationship of EGF on the redistribution time course of ezrin distribution 16HBE 14o- cells were untreated or treated with serum free medium containing 17, 5, 1nM EGF or 1nM HB-EGF for 2, 15 or 30 minutes. Cells were fixed and stained with a mouse monoclonal primary antibody against ezrin and a secondary anti-mouse FITC-conjugated antibody.

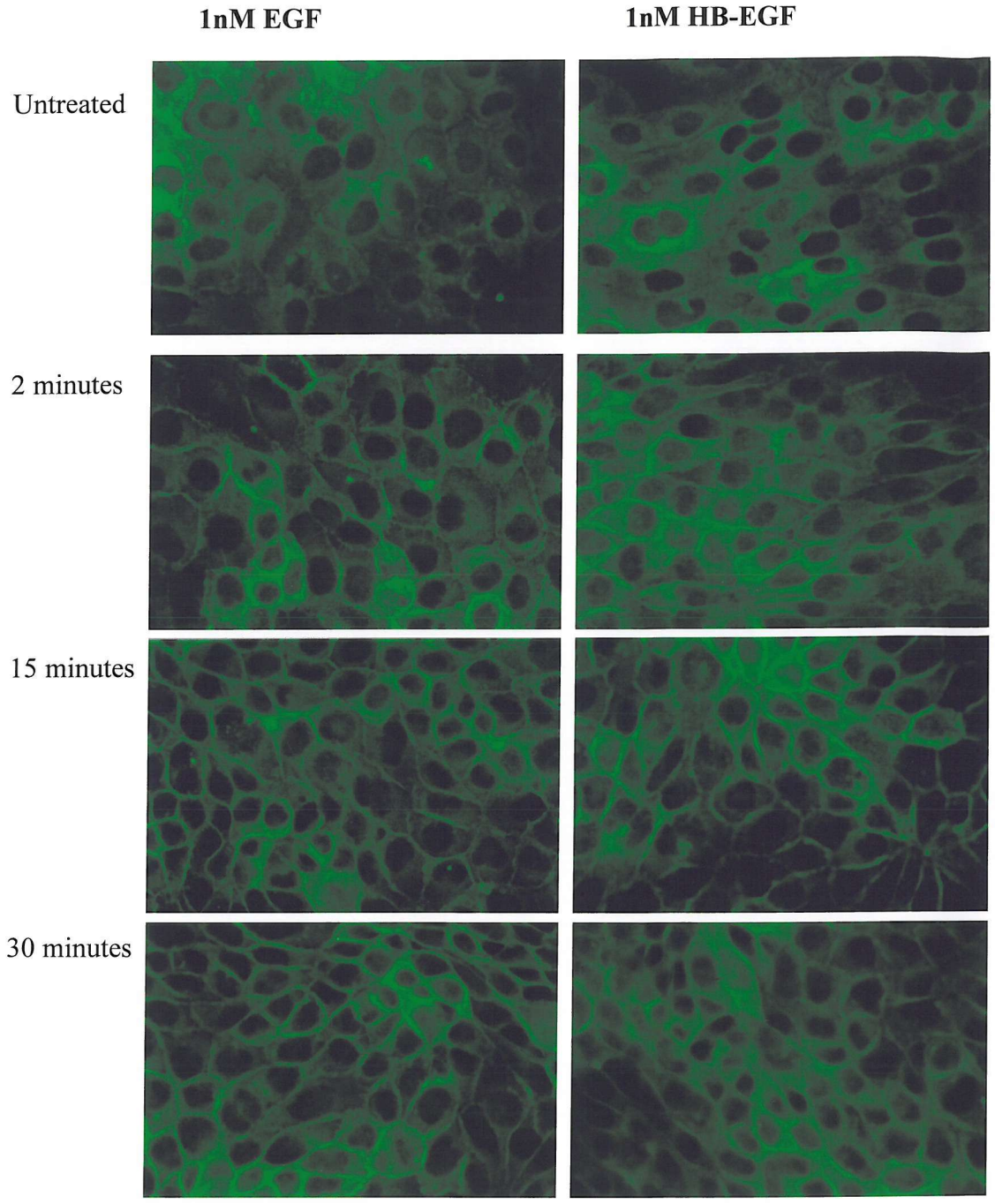
1nM EGF
1nM HB-EGF
Untreated
2 minutes
15 minutes
30 minutes

When 16HBE 14o- cells were treated with 1nM EGF, ezrin and moesin were redistributed to plasma membrane areas of the cell with a loss of some cytoplasmic staining (figure 4.6). This redistribution occurred when cells were treated for only 2 minutes with EGF and was still evident after 15 and 30 minutes of treatment. The redistribution of ezrin was examined in greater detail by looking at the dose response relationship of EGF on ezrin localisation (figure 4.7). 16HBE 14o- cells were treated with a range of doses of EGF (17, 5 or 1nM), and these experiments showed that the higher concentrations of EGF failed to further enhance the redistribution of ezrin and moesin, (i.e. there was incomplete redistribution of ezrin to the plasma membrane, with some residual cytoplasmic staining). However, when cells were treated with the higher doses of EGF membrane associated staining was observed more rapidly, but by 30 minutes ezrin distribution was similar with all doses of EGF. Additionally, 1nM EGF was compared with 1nM HB-EGF to determine whether HB-EGF might have a more potent effect on ezrin redistribution than a similar concentration of EGF (as co-localisation of HB-EGF by CD44v3 at the plasma membrane might potentiate effects). It was shown, (figure 4.7) that there were no differences between treatments either in terms of the pattern of staining or the rate of redistribution.

4.4 Detection of ezrin and moesin in primary bronchial epithelial cells

To further investigate the effects of EGF or HB-EGF on ezrin and moesin in bronchial epithelial cells, another *in vitro* model was employed. Primary bronchial epithelial cells obtained from bronchial brushings were cultured and stimulated with EGF or HB-EGF in the same way as 16HBE 14o- cells.

Initially, ezrin and moesin were detected in primary bronchial epithelial cell cultures using Western blotting. As in section 4.1, mouse monoclonal antibodies raised individually against ezrin and moesin were tested to determine reactivity and were able to detect protein bands at the expected molecular weight of ezrin and moesin (figure 4.8). The mouse monoclonal antibody raised against ezrin detected a single band in primary cells as seen in 16HBE 14o- cells (B). By comparison, the mouse monoclonal antibody raised against moesin detects 2 bands on the Western blot at the molecular weight expected, suggesting cross reactivity of the antibody with more than one member of the ERM protein family which have 75-80% homology with each other.

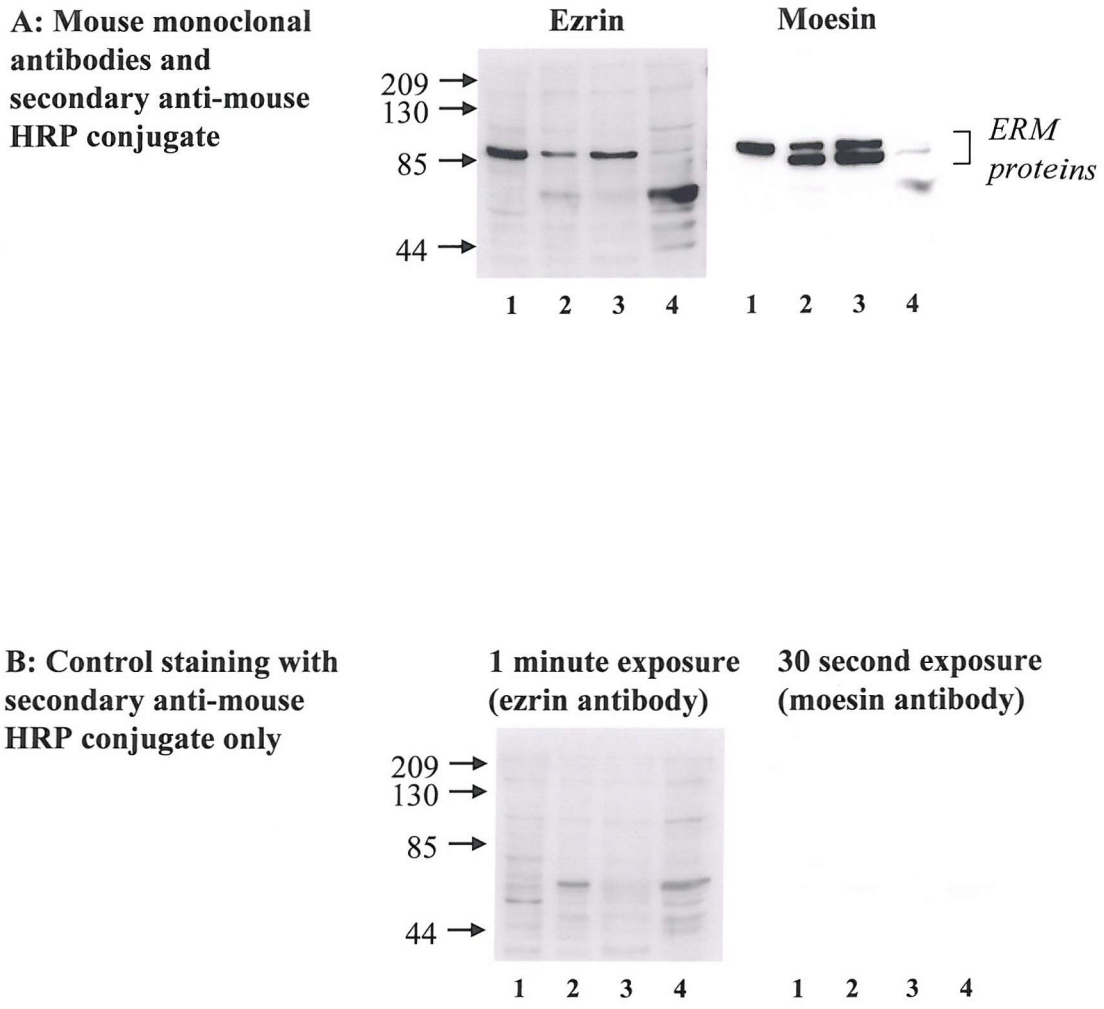

Figure 4.8. Comparison of cell lysates from 16HBE 14o- and primary bronchial epithelial cells using Western blotting for ezrin and moesin. Proteins in cell lysates from 16HBE 14o- cells (1), primary bronchial epithelial cells (2) and soluble (3) and cytoskeletal (4) fractions from primary bronchial epithelial cells were separated by 10% SDS-PAGE and transferred onto nitrocellulose. Antibodies against ezrin and moesin were mouse monoclonal from Transduction Laboratories (A). Panel B shows control staining of Western blots in the absence of primary antibody with secondary antibody incubation alone. Bands on all blots were developed with ECL Plus followed by exposure of autoradiography film for 1 minute for ezrin antibody and 30 seconds for moesin antibody, respective exposure times for the antibody controls are shown in panel B for comparison.

4.5 Effect of EGF on distribution of ezrin and moesin in cytoskeletal fractions of primary bronchial epithelial cells

The redistribution of ezrin and moesin in 16HBE 14o- cells was further examined in primary human bronchial epithelial cells. Cytoskeletal and soluble fractions were prepared as in section 4.2 to determine if ezrin and moesin association with the actin cytoskeleton is influenced by EGF as observed in 16HBE 14o- cells. As for 16HBE 14o- cells, ezrin and moesin were found in both the soluble and cytoskeletal fractions of primary bronchial epithelial cells and treatment with 1nM EGF for 15 minutes was able to induce an enrichment of ezrin and moesin in the cytoskeletal fraction (figure 4.9 A and B). As presented in figure 4.8 a double band was detected in Western blots stained for moesin and a single band observed on the ezrin blot. Western blot analysis of EGF receptor levels (figure 4.9D) again demonstrated the occurrence of soluble and cytoskeletal associated receptors. Proteins phosphorylated on tyrosine residues (figure 4.9C) could be detected in both fractions with an enhancement of a band at 175kDa in both fractions following EGF treatment likely reflecting increased tyrosine phosphorylation of the EGF receptor. These results are comparable with those observed in 16HBE 14o- cells.

4.6 Effect of EGF on ezrin and moesin distribution in primary bronchial epithelial cells

Ezrin and moesin distribution in primary cell cultures was observed by immunofluorescent staining. In untreated primary bronchial epithelial cells, all cells showed a similar pattern of cytoplasmic and perinuclear staining with some peripheral staining in plasma membrane structures (figure 4.10). Upon treatment with 1nM EGF for 15 minutes, both proteins showed enhanced staining in the periphery and appeared to be concentrated within plasma membrane structures resembling lamellipodia, microspike and microvilli-like membrane protrusions (figure 4.10). Ezrin distribution appeared to be of a more lamellipodia-type appearance resembling membrane ruffles whereas moesin appeared to redistribute to fine, projections of the peripheral plasma membrane as well as membrane ruffles.

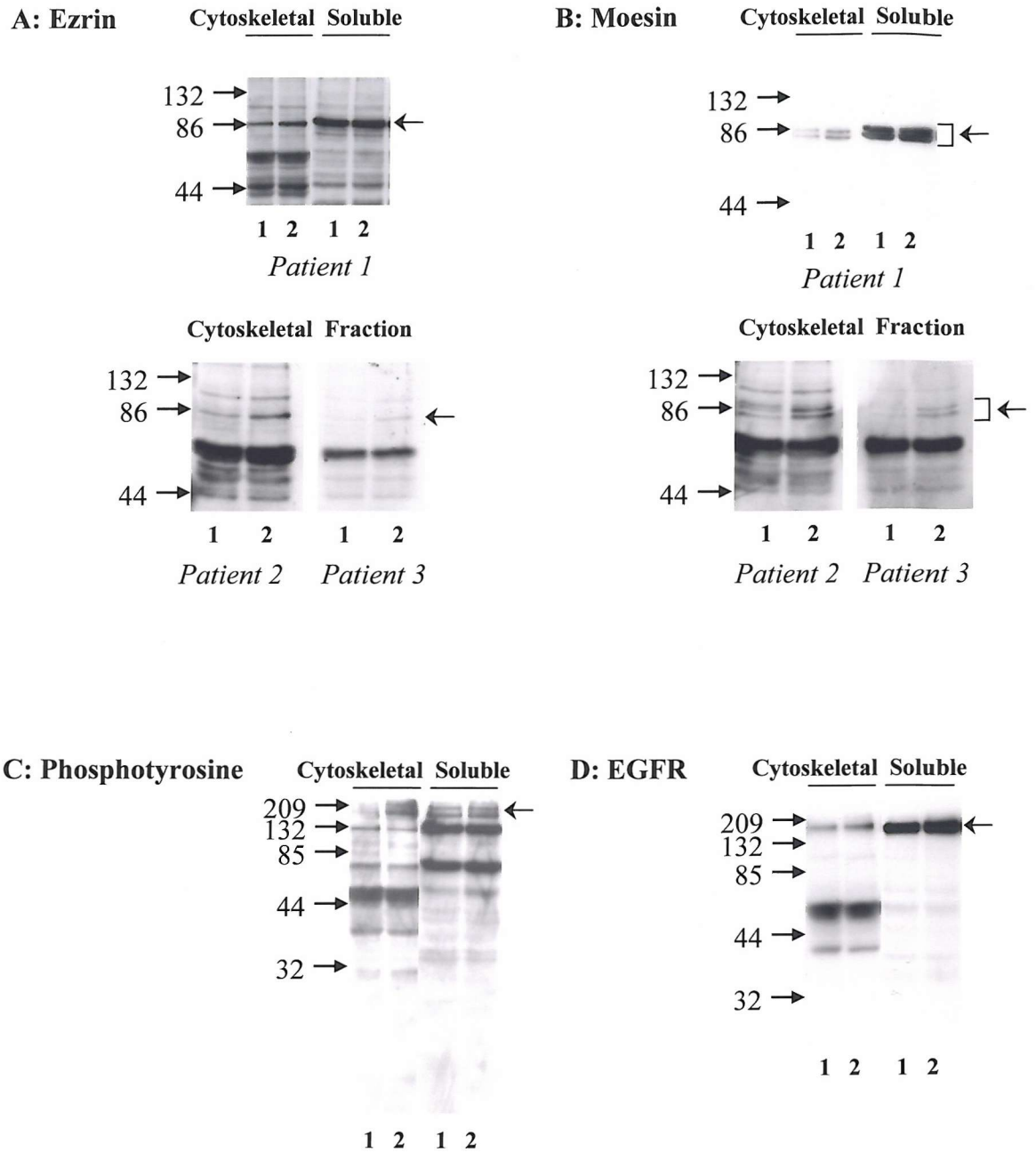

Figure 4.9. Effect of EGF on distribution of proteins in primary bronchial epithelial cells.

Primary bronchial epithelial cell monolayers were cultured in basal medium (BEBM) for 24 hours before treating with BEBM alone (1) or supplemented with 1nM EGF (2) for 15 minutes. Cultures were washed with PBS before extraction of soluble proteins and lysis of remaining cytoskeletons. The protein concentration of samples was determined and 6μg per lane loaded onto 10% SDS-PAGE gels. Nitrocellulose Western blots were stained with antibodies against ezrin (A), moesin (B) (both mouse monoclonal), phosphotyrosine (C) or EGF receptor (D). Cytoskeletal fraction samples from 3 different patients stained for ezrin and moesin are presented (A and B) to show responses between subjects. Arrows indicate band/s representing ERM proteins (A and B) and EGFR (C and D).

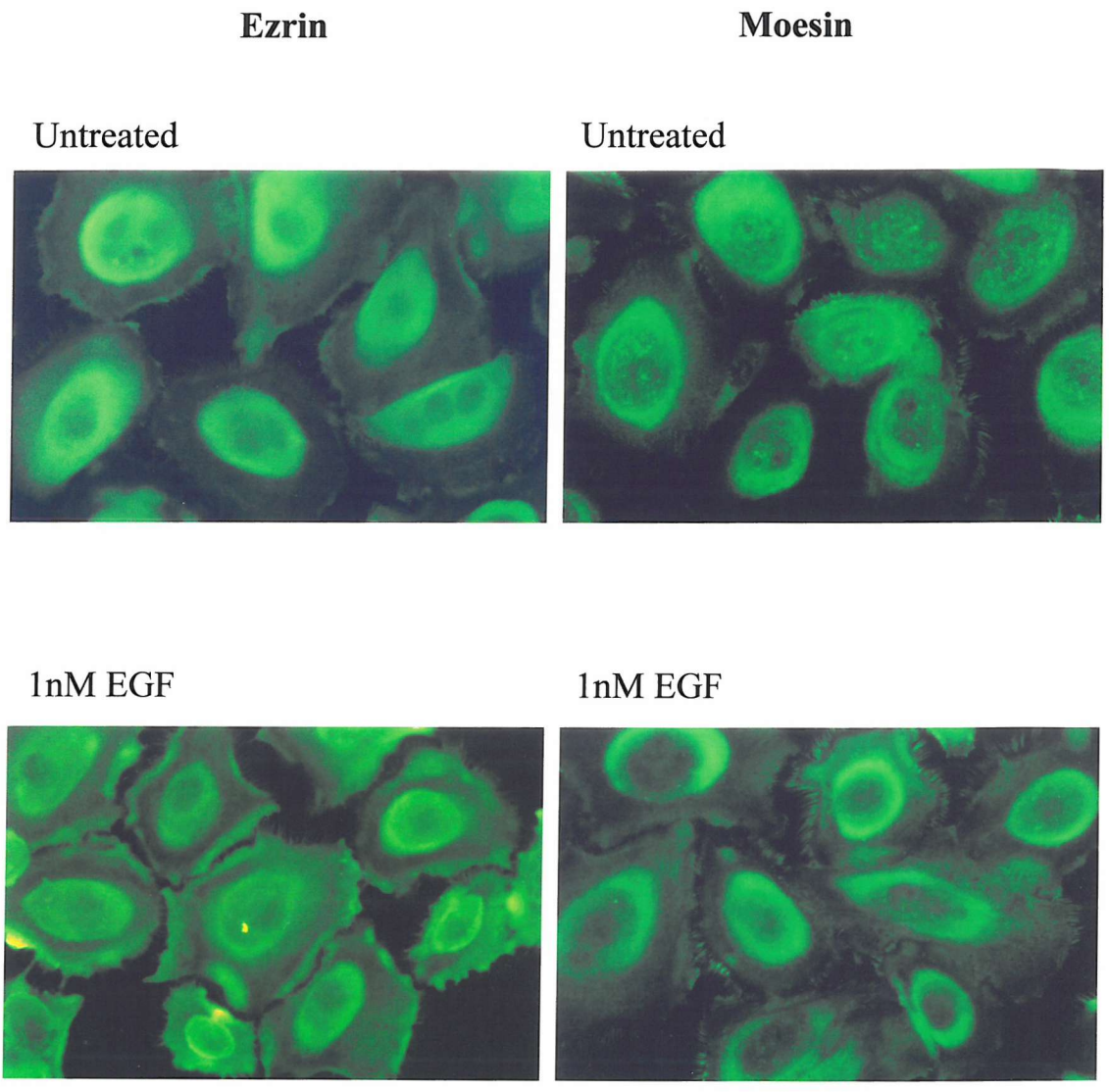

Figure 4.10. Effect of EGF on ezrin and moesin distribution in primary bronchial epithelial cells.
Primary bronchial epithelial cells were untreated or treated with serum free medium containing 1nM EGF for 15 minutes prior to fixation and fluorescent staining for ezrin and moesin using mouse monoclonal antibodies as previously.

The redistribution of ezrin and moesin, as described, to plasma membrane structures followed a time course comparable with the enhanced association of ezrin and moesin with the cytoskeletal fraction of primary cells. In order to examine whether this was also accompanied by binding to CD44 proteins, hence crosslinking of the ERM proteins, a double immunocytochemical staining method was employed to assess co-localisation of proteins (see Chapter 2, Materials and Methods, section 2.2.7 for method and details of controls used).

Double staining for CD44 and ezrin or moesin (figure 4.11) showed that these proteins appeared to be co-localised in cultures treated with basal medium. CD44 had a diffuse distribution with bright staining observed at the plasma membrane, which is co-localised with ezrin or moesin staining as indicated by the orange colour in the merged image and highlighted with an arrow in figure 4.11 (A). Ezrin and moesin proteins are seen predominantly in the cytoplasm, plasma membrane and in some extensions of the plasma membrane. Following treatment of cells with 1nM EGF (B) for 15 minutes cell edges not in contact with other cells show enhanced staining of ezrin and moesin in structures resembling lamellipodia and fine microvilli-like extensions of the membrane (highlighted with an arrow). The distribution of CD44 proteins in EGF treated cultures appears to be unaffected by EGF treatment and CD44 staining is observed at the plasma membrane but not in extensions of the plasma membrane observed here.

Co-localisation of CD44 with ezrin and moesin was examined more closely using laser scanning confocal microscopy (figure 4.12i and ii). These images show staining for both CD44 and the ERM proteins, ezrin and moesin, which are found in all sections of the cell from the apex to the base of the cells. The distribution of CD44, ezrin and moesin proteins along the vertical axis do not appear to be influenced by EGF treatment.

In cultures treated with basal medium (A), ezrin staining is seen in the cytoplasm, the plasma membrane and in fine extensions of the plasma membrane. Ezrin staining is co-localised with CD44 at the plasma membrane but CD44 proteins do not appear to be expressed in the microvilli-like structures. In EGF treated cells, ezrin staining at the plasma membrane is brighter than untreated cells and found in flat lamellipodia

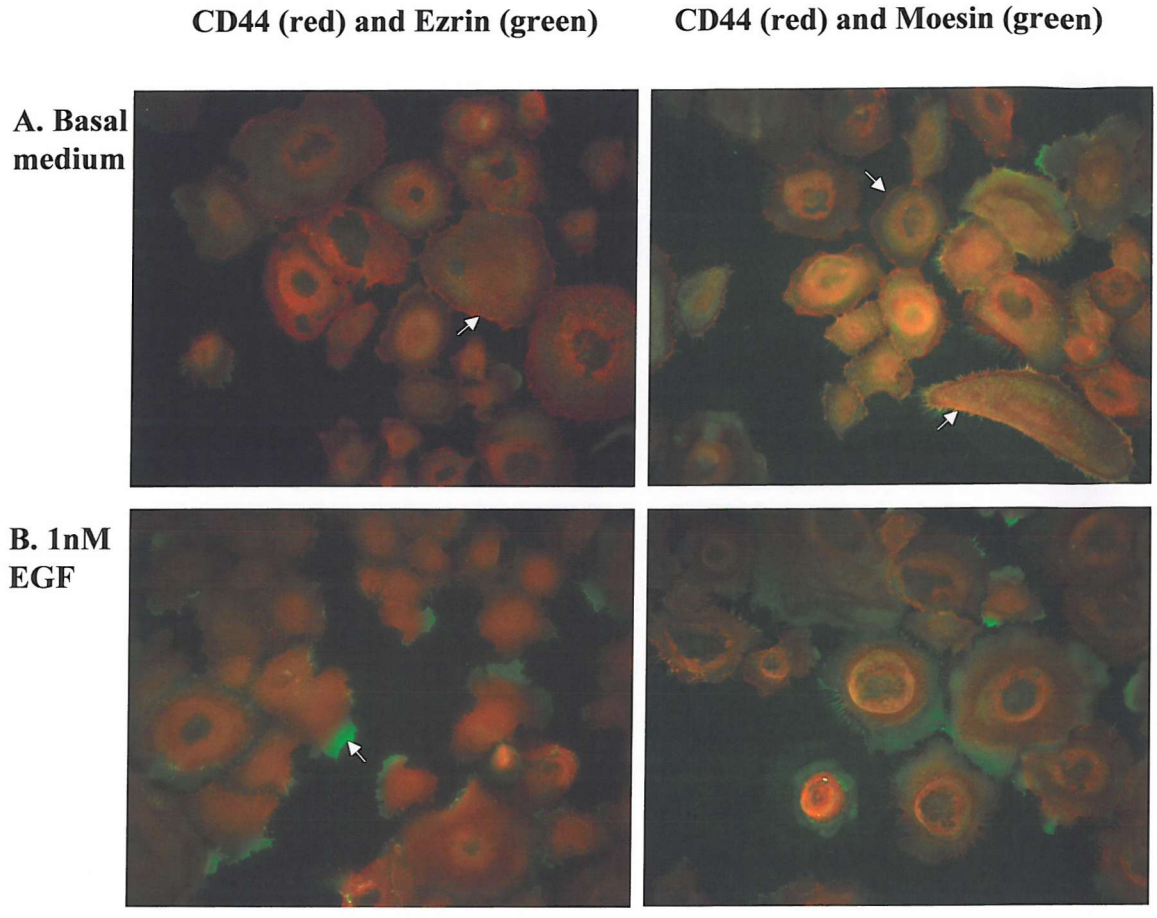

Figure 4.11. Double staining for CD44 and Ezrin/Moesin in primary bronchial epithelial cells to determine the effect of treatment on colocalisation of proteins. Primary bronchial epithelial cells were cultured in Basal medium (BEBM) for 24 hours to deplete growth factors before stimulation with basal medium (BEBM) alone (A) or containing 1nM EGF (B) for 15 minutes. Cells were fixed in cold methanol and double stained using the protocol described in Chapter 2, section 2.2.7. Briefly, mouse anti-CD44 and either goat anti-ezrin or goat anti-moesin were incubated together on fixed cells. Following PBS washes, cells were incubated with secondary antibodies raised against mouse or goat conjugated to TRITC and FITC fluorochromes respectively. Cells were visualised using a Zeiss immunoflourescent microscope and images captured using a colour video camera. Arrows refer to explanations in text of Chapter Four.

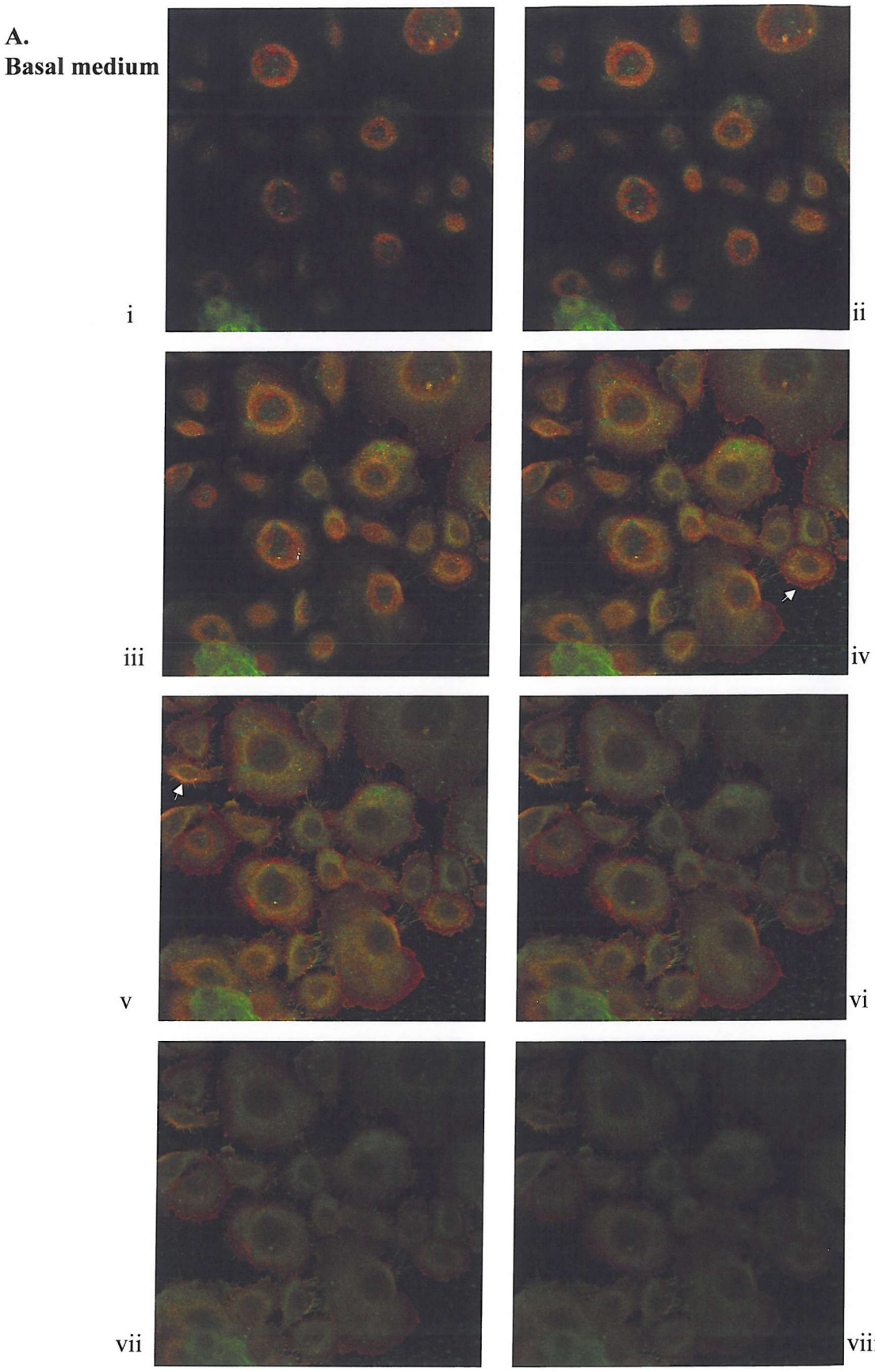

Figure 4.12i. Confocal microscopy of primary bronchial epithelial cells stained for CD44 (red) and Ezrin (green).

Cells were treated and stained as described in figure 4.11 and viewed using a Leica confocal scanning laser microscope. Panel A shows cells treated with basal medium (BEBM) and panel B (overpage) shows cells treated with 1nM EGF, both treatments were for 15 minutes before washing with PBS and fixing cells in cold methanol. Images are of 8 sections through the cell from top to bottom (images i-viii).

B.
1nM EGF

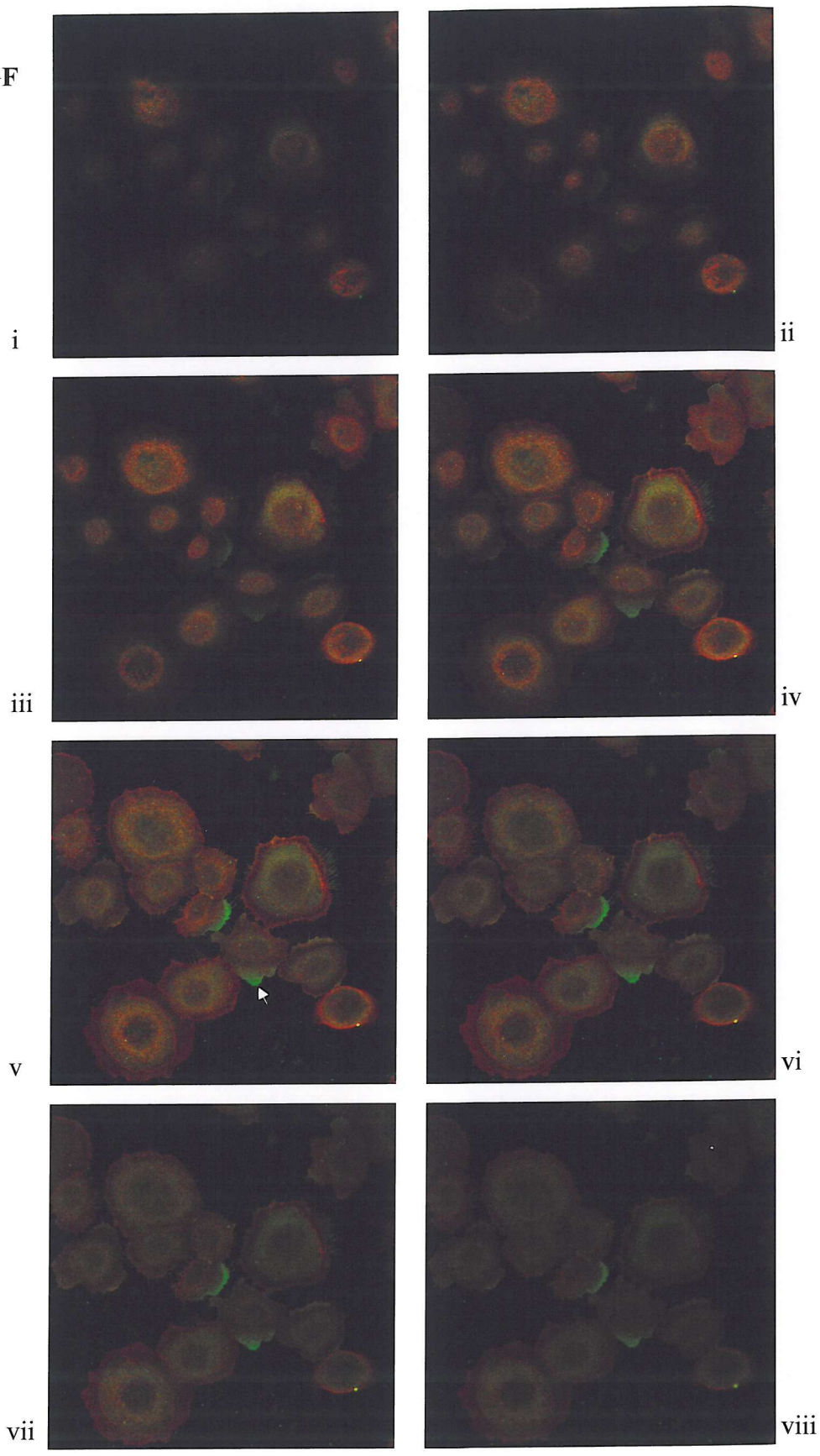

Figure 4.12i. continued

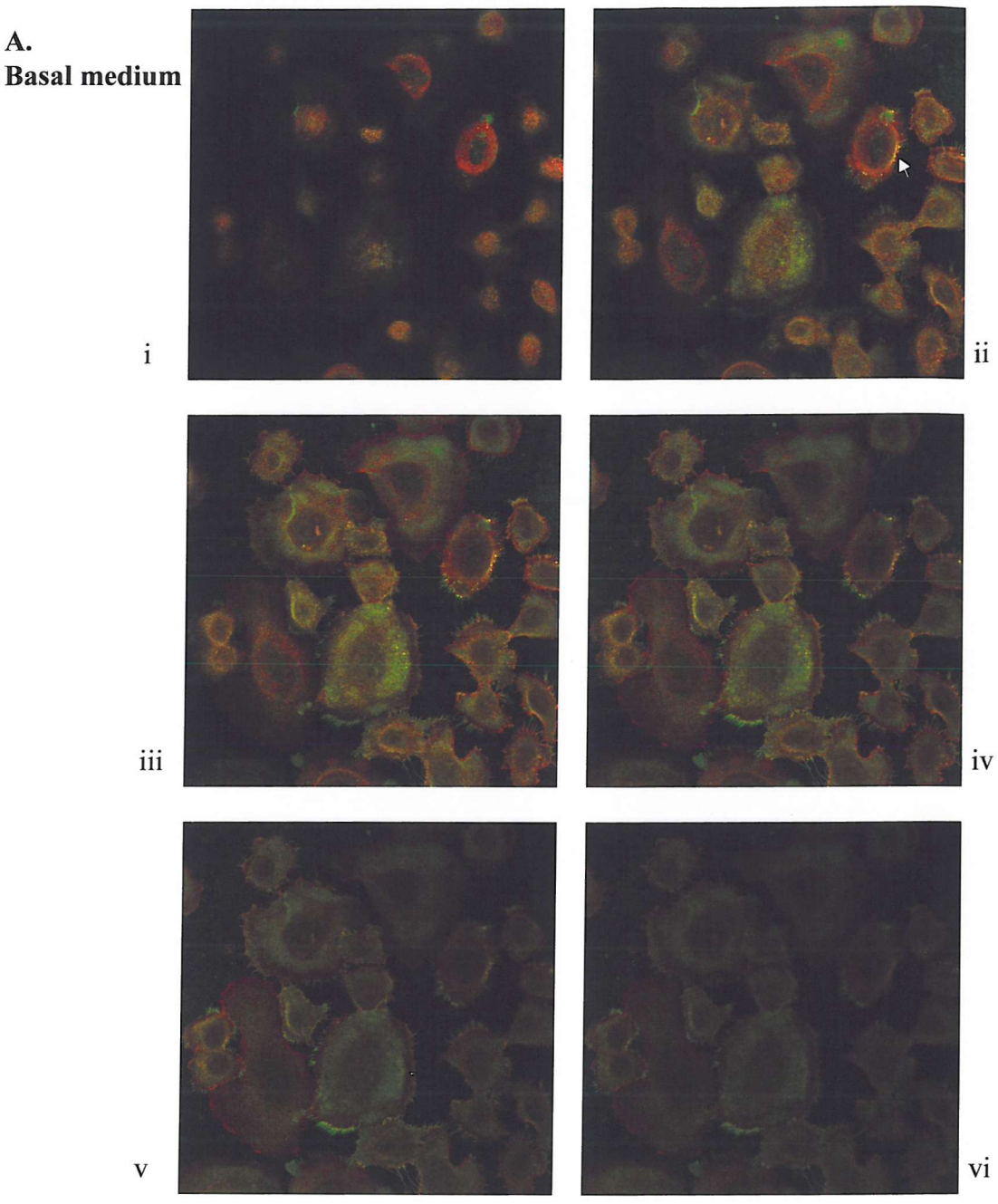

Figure 4.12ii. Confocal microscopy of primary bronchial epithelial cells stained for CD44 (red) and Moesin (green).
Cells were treated and stained as described in figure 4.11 and viewed using a Leica confocal scanning laser microscope. Panel A shows cells treated with basal medium (BEBM) and panel B (overpage) shows cells treated with 1nM EGF, both treatments were for 15 minutes before washing with PBS and fixing cells in cold methanol. Images are of 6 sections through the cell from top to bottom (images i-vi).

B.
1nM EGF

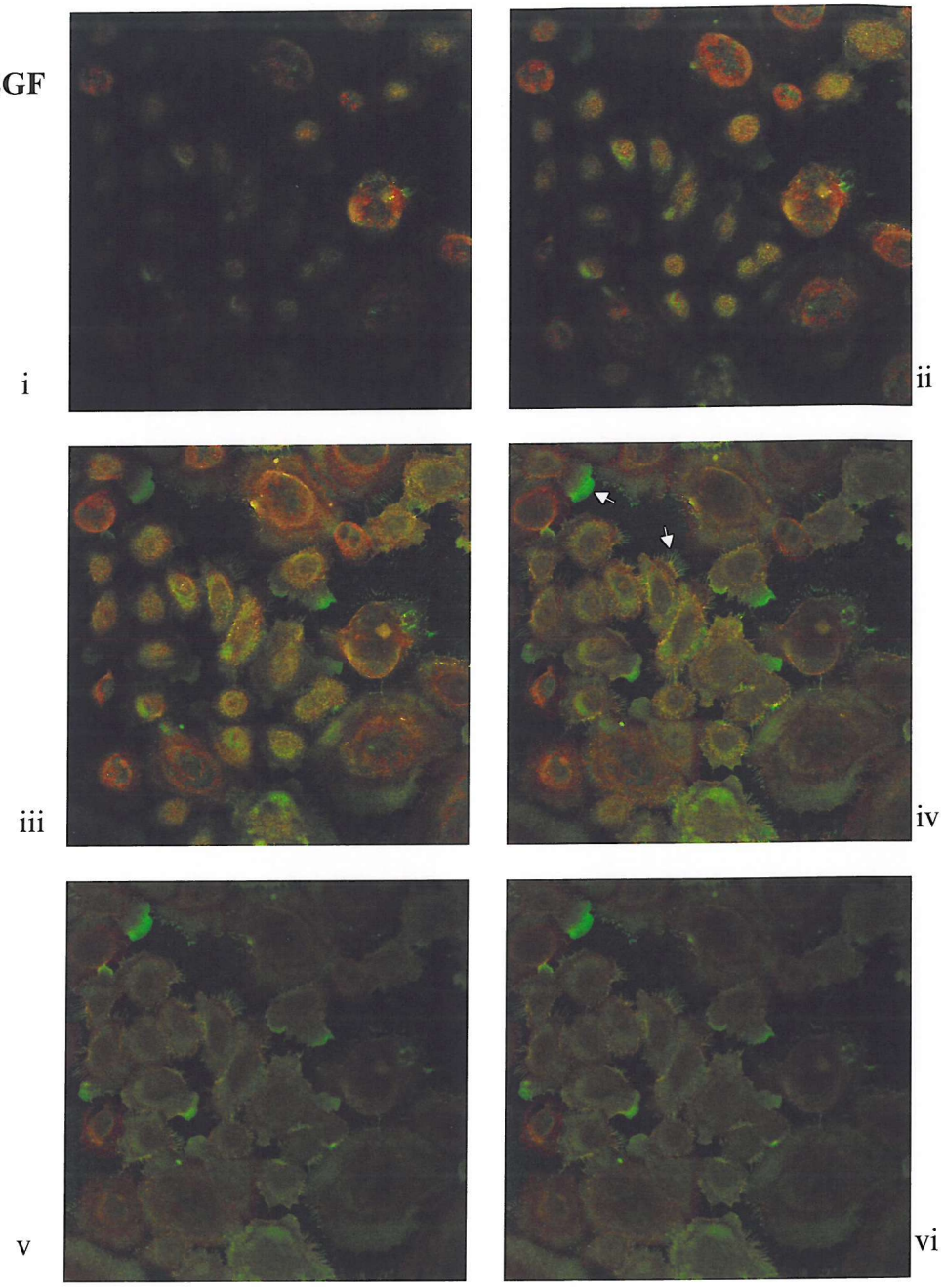

Figure 4.12ii. continued

extensions or ruffles of the plasma membrane. Staining in these structures is observed more so at the base of the cells with less staining observed apically.

Moesin staining is also seen throughout the cell in untreated cultures, in the cytoplasm, at the plasma membrane and within fine microvilli-like projections of the plasma membrane. Staining is co-localised with CD44 at the plasma membrane (indicated by an arrow, figure 4.12ii, panel A, image ii) but not in plasma membrane extensions where only moesin staining is observed. Upon treatment with 1nM EGF moesin staining in spikes and lamellipodia is enhanced whereas CD44 distribution remains unchanged. Staining in these structures is brighter towards the base of the cells and predominantly in areas of the plasma membrane not in contact with other cells.

4.7 Tyrosine phosphorylation of ezrin and moesin in epithelial cell cultures

EGF induced tyrosine phosphorylation of ERM proteins in epithelial cells has previously been reported and might play a role in EGF induced redistribution of ezrin and moesin. For example, tyrosine phosphorylation of ERM proteins may allow a conformational change in the structure of the protein to expose actin and plasma membrane protein binding sites, thus accounting for the changes in cellular distribution and cytoskeletal association.

Immunoprecipitation using a phosphotyrosine (clone PY20) specific agarose conjugate followed by SDS-PAGE and Western blotting analysis of the solubilised immunoprecipitate allowed changes in phosphorylation on tyrosine residues to be examined. 16HBE 14o- cells show small changes in total phosphotyrosine following treatment with 1nM EGF for 10 minutes as shown in figure 4.13i (A). Increased phosphorylation of the EGF receptor (B) was also detected but no proteins with immunoreactivity to antibodies against ezrin and moesin could be detected in the immunoprecipitate (C and D). Unbound proteins in the immunoprecipitation supernatant (collected after the initial centrifugation following the antibody binding incubation step) were also analysed by Western blotting as a control to confirm the presence and detection of ezrin and moesin in the cell lysate. In these blots bands at the expected molecular weight for ezrin and moesin were observed in the supernatant and no differences were observed between treatments (figure not shown). As a further

control to confirm the efficacy of the Western blotting run these blots were stained alongside blots of immunoprecipitate samples where no staining was observed.

Treatment of primary bronchial epithelial cultures with 1nM EGF for 10 minutes yielded comparable results (figure 4.13ii) with a significant increase in total phosphotyrosine, (A) including increased phosphorylation on tyrosine residues of the EGF receptor (B) being observed, but no detection of ezrin and moesin in the immunoprecipitate (C and D)

As a control, the reliability and sensitivity of the immunoprecipitation technique and reagents was tested using A431 cells which have previously been shown to respond to EGF with phosphorylation of ezrin on tyrosine residues (23). Figure 4.14i confirms this previously published observation. Treatment of A431 cells with 1nM EGF stimulated phosphorylation of the EGF receptor in a time dependent manner and with greater levels of phosphorylation than serum free medium (B). Activation of EGFR was further enhanced when cells were treated with 33nM EGF and here tyrosine phosphorylation of the EGFR was accompanied by ezrin and moesin phosphorylation (C and D). Ezrin and moesin phosphorylation was detected after 2 minutes of treatment with 33nM EGF, peaked after 5 minutes of treatment and was slightly reduced after 10 minutes of treatment.

A431 cells are a carcinoma cell line and express large numbers of EGF receptors. NCI-H292 cells, an epithelial cell line of lung carcinoma origin, were examined to see if phosphorylation of ERM proteins was restricted to A431 cells or could be detected in another carcinoma cell line (figure 4.14ii). NCI-H292 cells were treated with 1nM or 33nM EGF for the same time course as A431 cells and this induced phosphorylation of the EGF receptor (B) but not ezrin or moesin, even at the higher doses of EGF (C and D).

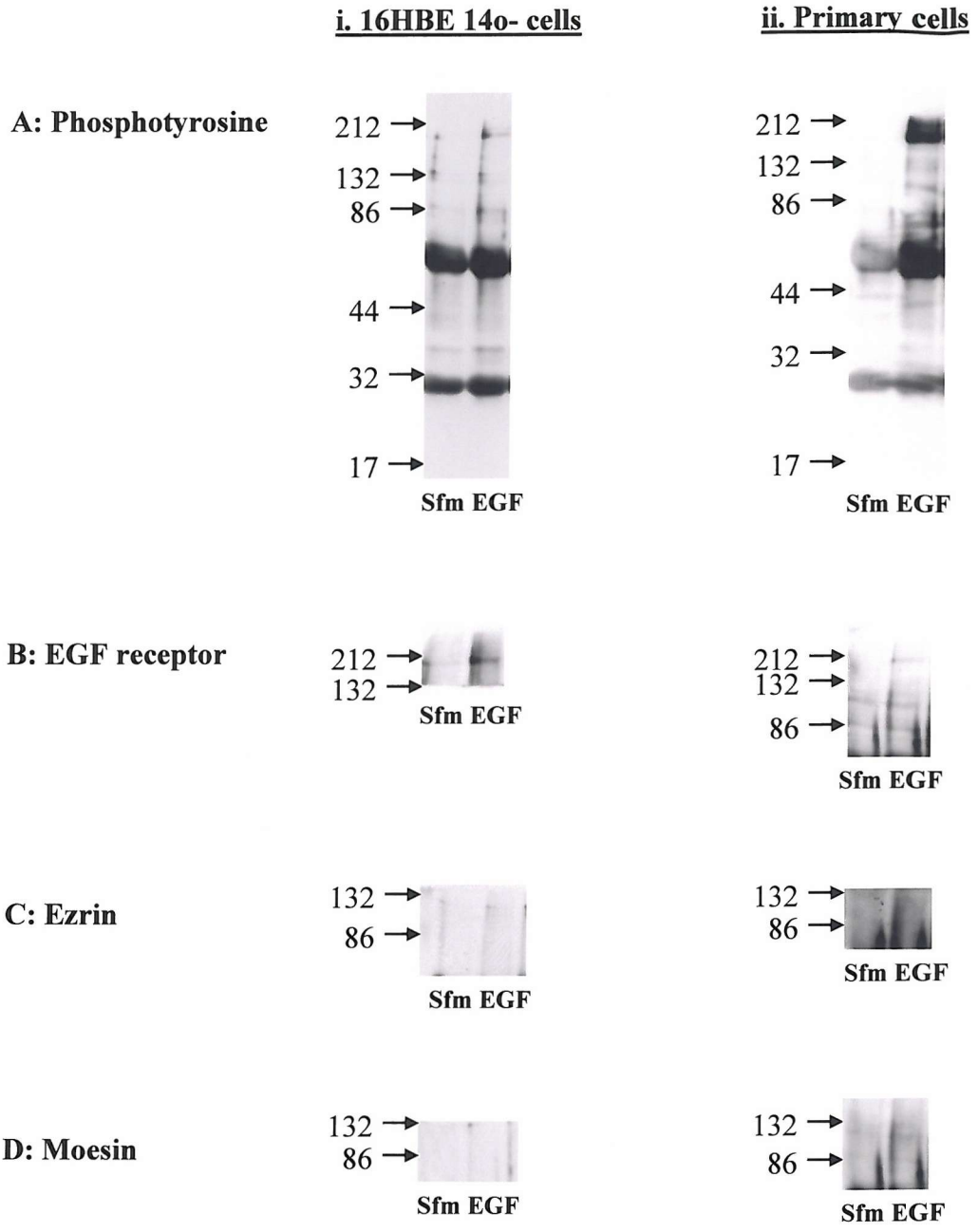

Figure 4.13. Analysis of tyrosine phosphorylated proteins in treated 16HBE 14o- and primary bronchial epithelial cells using immunoprecipitation.
16HBE 14o- (i) and primary (ii) bronchial epithelial cells were serum starved for 24 hours in serum free medium (sfm) or primary bronchial epithelial cell basal medium (BEBM) respectively. Cells were then treated with serum free medium or BEBM with or without 1nM EGF for 10 minutes. Following lysis of proteins in denaturing lysis buffer and a protein assay was performed. For the immunoprecipitation 1mg of protein (16HBE 14o-cells) or 0.3mg protein (primary cells) in Triton buffer was incubated with 60µl of phosphotyrosine (PY20)-agarose conjugate overnight. Following centrifugation to precipitate proteins the supernatant was removed and the immunoprecipitate washed before solubilising in hot sample buffer. Samples were analysed by 10% SDS-PAGE and Western blotting for phosphotyrosine (A), EGFR (B), ezrin (C) and moesin (D) (both goat polyclonal).

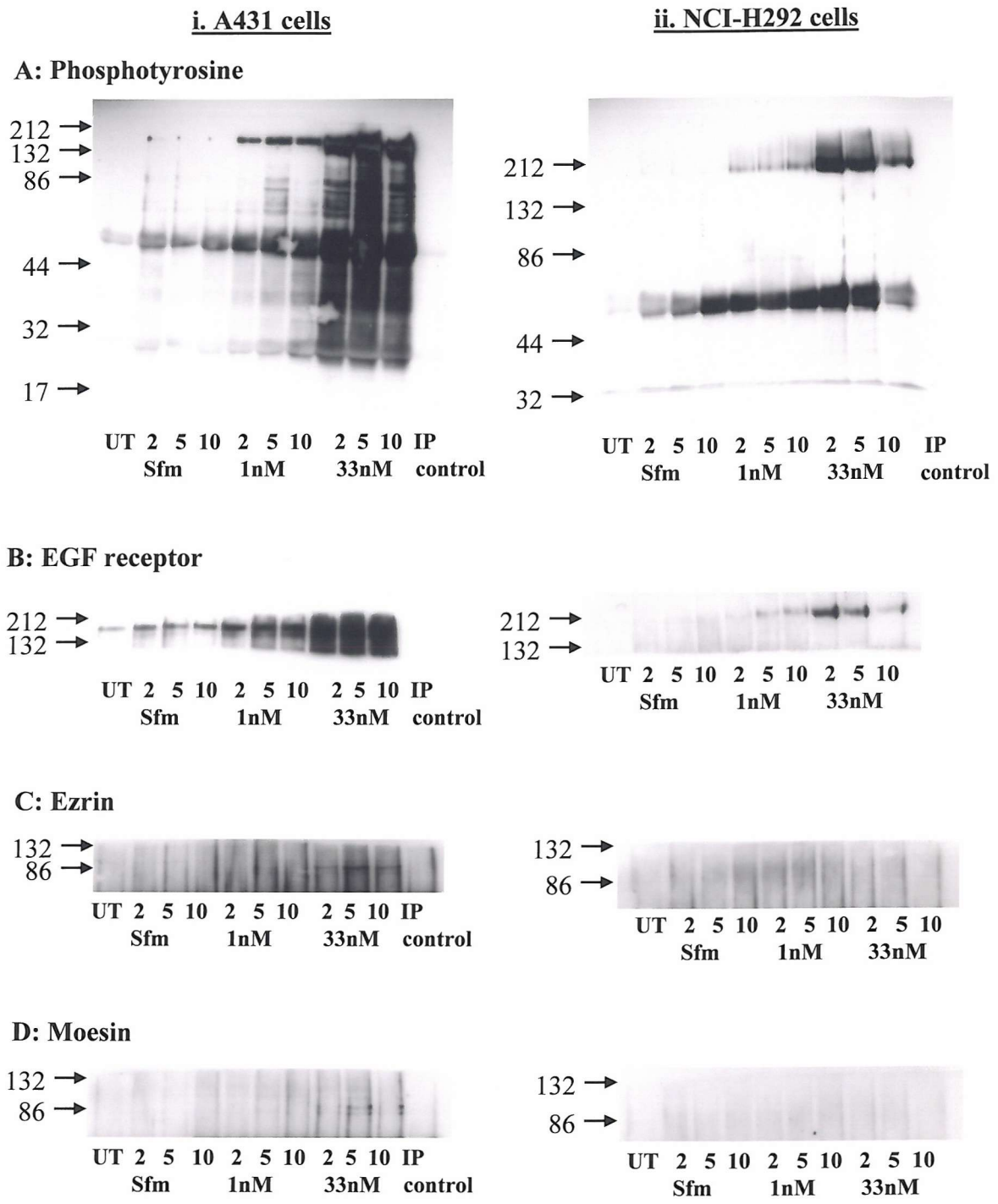

Figure 4.14. Analysis of tyrosine phosphorylated proteins in EGF treated A431 and NCI-H292 cells using immunoprecipitation.
A431 (i) and NCI-H292 (ii) cells were serum starved for 24 hours then treated with serum free medium (Sfm), 1nM EGF or 33nM EGF for 2, 5 or 10 minutes or left untreated (UT). Following lysis of proteins in denaturing lysis buffer and protein determination, 1mg of protein in Triton buffer was incubated with 60µl of phosphotyrosine(PY20)-agarose conjugate overnight. Following centrifugation to precipitate proteins the supernatant removed and the immunoprecipitate washed before solubilising in hot sample buffer. Samples were analysed by 10% SDS-PAGE and Western blotting using antibodies against phosphotyrosine (A), EGFR (B), ezrin (C) and moesin (D) (both goat polyclonal). IP control represents an immunoprecipitation with Triton buffer alone (without cell lysate).

4.8 Discussion

ERM proteins are expressed by a variety of cell types including the epithelial cells lining the airway, where they could be involved in a range of cellular functions including migration and adhesion as well as maintenance of epithelial integrity and wound repair. Their distribution and pleiotropic functions can be modulated by a variety of stimuli including tyrosine kinases such as the EGF receptor (23), (72), and the HGF receptor (*c-met*) (33), (68). Furthermore tyrosine phosphorylation sites on ERM proteins have been identified (72).

The aims of this chapter were to investigate the ERM proteins, ezrin and moesin, in bronchial epithelial cell lines and to examine their distribution and how they might be modulated to begin to elucidate their role. Modulation of ERM proteins by EGF was investigated here as the EGF receptor tyrosine kinase has been implicated in the modulation of ERM proteins (23), (72). Furthermore, as previously discussed EGF receptors are over-expressed in asthmatic airways with enhanced staining being observed in the basal cells underlying columnar cell (115). In addition, as there may be local regulation of these effects by co-localisation of HB-EGF at the plasma membrane with CD44v3, the effects of EGF were compared with that of HB-EGF.

The distribution of ERM proteins was examined by Western blotting of cellular fractions as well as visually by immunofluorescent staining of fixed cells. Initial observations that ezrin and moesin protein increased in particulate fractions of 16HBE 14o- cells following EGF treatment were further investigated by the preparation of cytoskeletal fractions. Here it was shown that, EGF stimulated a modest increase in binding of ezrin and moesin to components of the insoluble cytoskeletal fraction which might include membrane proteins and actin filaments (figure 4.3). A time course experiment showed that enhanced binding of ezrin and moesin to the cytoskeleton could be observed after 2 minutes of treatment, but was reduced back to baseline levels at all time points after 30 minutes (figure 4.4) implying this association is a transient one. EGF has been shown to play a role in activation of migration and here this transient association of ERM proteins with the actin cytoskeleton, which is stimulated by EGF, could be an initial event in reorganisation of the actin cytoskeleton to allow changes in cell migration to occur.

EGF receptor protein was detected in both fractions and their position on the Western blot (figure 4.5E) corresponds to a same molecular weight band on a Western blot stained for phosphotyrosine, which changes in intensity following EGF treatment (figure 4.5D). This band is brighter in both fractions in EGF treated cultures, although the relative amounts of EGF receptor proteins are unchanged within the fractions following treatment. Cytoskeletal fractions stained for EGFR show a number of bands below the expected molecular weight of EGFR (170kDa) particularly below the 84kDa marker, these bands probably relate to cytokeratin and other cytoskeletal proteins, which are enriched in the cytoskeletal fraction and not detected in the soluble fraction.

Data from cytoskeletal fractions suggested a redistribution of ezrin and moesin following EGF treatment and immunocytochemistry was used to look more specifically at redistribution in cells. Immunofluorescent staining showed there to be a change in the cellular localisation of ezrin and moesin from a diffuse cytoplasmic distribution to being more concentrated at the plasma membrane following EGF treatment. This observation reflects Western blotting data where increased proteins were detected in insoluble and cytoskeletal fractions of the cells and taken together these data suggest that EGF stimulates the binding of ezrin and moesin to the actin cytoskeleton in 16HBE 14o- cells.

Primary cell cultures were used to confirm observations in 16HBE 14o- cells. Although cultured as monolayers and not differentiated cultures, their phenotype is more closely related to that of the epithelial cells lining the airway than the transformed cell line. Data from cytoskeletal fractions confirmed that seen in 16HBE 14o- cells with a small increase in ezrin and moesin protein in the cytoskeletal fraction following treatment with 1nM EGF. Immunocytochemistry again showed an enhancement of staining at the plasma membrane following treatment with EGF.

Data from 16HBE 14o- and primary cells suggests that EGF is able to modulate ERM proteins in bronchial epithelial cells as it stimulates increased binding to the actin cytoskeleton and their redistribution to the plasma membrane, although differences between 16HBE 14o- and primary bronchial epithelial cultures were observed.

Primary bronchial epithelial cells exhibited actin-rich lamellipodia and microvilli-like plasma membrane structures, which were not observed in 16HBE 14o- cells, and these structures showed enhanced staining for ezrin and moesin following treatment. Actin staining (using specific antibodies or rhodamine phalloidin) would enable clarification of whether these extensions were present prior to treatment or developed as a result of EGF treatment. Using phase-contrast microscopy, primary human bronchial epithelial cells as well as the cell line BEAS-2B, show morphological changes characterised by extension of filopodia following EGF treatment (1-2 hours) (13) further evidence of a role for EGF in bronchial epithelial cell morphology. Previously published data from A431 (23) and HT115 colon carcinoma (68) epithelial cells shows that treatment with EGF or HGF/SF, respectively, induced translocation of ezrin to membrane structures as shown by immunocytochemical staining for actin proteins.

Additionally, unlike 16HBE 14o- cells where both ezrin and moesin became concentrated at the plasma membrane following EGF treatment, in primary cells ezrin and moesin themselves showed distinct staining patterns in EGF treated primary cultures. Following EGF treatment, enhanced staining for ezrin in lamellipodia structures occurred in areas of the plasma membrane not in contact with other cells where cells appeared to be spreading to cover the cell culture substrate. Conversely, moesin as well as being observed in lamellipodia was found also in microvilli-like structures of the cell. EGF has previously been shown to cause changes in cell shape as well as initiate cell spreading and migration, and these differences between the distribution of ezrin and moesin might imply distinct roles for these proteins in bronchial epithelial cells. Alternatively ezrin and moesin may become reorganised into different compartments of the membrane where they crosslink with a different membrane protein to serve a variety of functions.

To investigate CD44 as a possible plasma membrane binding partner for ezrin and moesin, their co-localisation was observed by double immunocytochemistry employing two distinct fluorophores. Staining showed that in untreated primary bronchial epithelial cells CD44 and ezrin or moesin were co-localised at the plasma membrane and upon treatment ezrin and moesin proteins redistributed to plasma membrane extensions resembling actin cytoskeletal based microvilli and lamellipodia. CD44 distribution remained in a pattern resembling cell surface staining and was not observed

in the cell projections. In cytoskeletal fractions of 16HBE 14o- cells no changes in the relative amounts of CD44 proteins were observed between fractions although CD44 proteins could be detected in both cytoskeletal and soluble fractions. In other cell types association of CD44 with both fractions has been reported with between 30-80% of CD44 proteins being found in the detergent insoluble fraction of fibroblasts (27) and baby hamster kidney cells (142).

In untreated cells the presence of CD44-ERM-actin complexes as suggested by cytoskeletal and immunocytochemical data presented here could be involved in stabilisation of CD44 proteins within the plasma membrane with the actin cytoskeleton. In mouse fibroblasts and baby hamster kidney cells CD44 and ERM proteins are co-localised just beneath the plasma where they are proposed to act as molecular linkers between the cytoplasmic domain of CD44 and the actin cytoskeleton (148).

EGF treatment appears to promote dissociation of this complex as evidenced by the observation that co-localisation of CD44 with ezrin or moesin is no longer observed and also that CD44 protein levels in cytoskeletal fractions are not enhanced along with ezrin and moesin. Upon treatment with EGF, the cells might adopt a more migratory phenotype as evidenced by development of lamellipodia and microvilli-like cell projections where ERM proteins might become dissociated from CD44 to associate with another of its binding partners. Association of ERM proteins with other known binding proteins expressed in actin cytoskeleton cell extensions such as CD43, ICAM-1, -2, -3 or EBP-50 could be tested by the same double co-localisation staining method used here. Alternatively the use of immunoprecipitation techniques to pull down ezrin and moesin to determine its phosphorylation state (denaturing immunoprecipitation) or binding partners (non-denaturing immunoprecipitation) was explored here. Unfortunately commercially available antibodies against ERM proteins were tested but found to be unsuitable reagents for immunoprecipitation (data not shown).

As EGF was able to elicit changes in ERM protein distribution it was hypothesised that these changes were enabled by tyrosine phosphorylation of ezrin and moesin, resulting in conformational changes to the protein structure and redistribution within the cell. Changes in tyrosine phosphorylation of proteins following EGF treatment was examined in cell lysates using immunoprecipitation to pull down proteins

phosphorylated on tyrosine and Western blotting of these precipitates. Although EGF stimulated tyrosine phosphorylation of ezrin and moesin and accompanying changes in protein distribution have been observed in A431 cells (23) tyrosine phosphorylation could not be detected in bronchial epithelial cells following EGF treatment. Western blotting of PY20 agarose immunoprecipitates for phosphotyrosine (figure 4.13A) showed enhanced phosphorylated proteins following EGF treatment and phosphorylated forms of the EGF receptor could be detected in the immunoprecipitate (figure 4.13 B) giving confidence to the immunoprecipitation process as well as the efficacy of the exogenous EGF ligand. Phosphorylated forms of ezrin and moesin could not be detected although control blots showed detection of proteins in the unbound supernatant. In case this was related to the use of a transformed cell line, immunoprecipitates from EGF treated primary bronchial epithelial cells were also examined.

Primary cell cultures exhibited low basal levels of total tyrosine phosphorylation as shown in lane 1 of figure 4.13A and when stimulated with EGF a bright, wide band was detected at the expected molecular weight of the EGF receptor. However when blotting for the EGFR only a small band was detected in the treated sample. This observation suggests the EGFR (c-erbB1) is not the only protein that is phosphorylated at this molecular weight. For example other members of the EGF receptor family are phosphorylated and as c-erbB2, a 180kDa protein, is expressed in bronchial epithelial cells (116) it could be phosphorylated here. Despite detection of tyrosine phosphorylation ezrin and moesin could not be detected in the immunoprecipitate by Western blotting.

As a control to confirm the reagents and techniques used here would allow for the detection of phosphorylated ERM proteins, A431 cells were treated with EGF and, as reported previously (23) ezrin and moesin could be detected in the phosphotyrosine immunoprecipitate. However these small levels of phosphorylation were only detected when cells were treated with a high dose (33nM) of EGF and a large smear of EGFR were seen on the Western blot. Phosphorylated ezrin and moesin were not observed in A431 cells treated with 1nM EGF although EGF receptor phosphorylation was evident, but at much lower levels and comparable with those seen with NCI-H292 cells treated with 33nM EGF. Furthermore when these treated cells were examined under the

microscope, the cells had rounded up following the formation of microvilli so it seems unlikely in this situation that ezrin and moesin phosphorylation and redistribution contribute to a migratory phenotype and hence an involvement in wound repair.

A431 cells are a vulval, epidermoid carcinoma cell line (44) and express high levels of EGF receptor protein and so have been used extensively to study EGF and its receptors. The bronchial epithelial cell line, NCI-H292 is a lung, epithelial carcinoma cell line also expressing large numbers of EGF receptors so was tested here to see if ezrin and moesin phosphorylation could be detected in another carcinoma cell line. EGF receptor phosphorylation was detected when cells were treated with 1nM EGF and levels were enhanced with 33nM EGF but phosphorylated forms of ezrin and moesin could not be detected in the immunoprecipitate. The levels of EGF receptor protein in the immunoprecipitate were much lower than those in A431 cells implying a requirement for much higher EGF receptor phosphorylation for ERM protein phosphorylation to be observed. EGF receptor phosphorylation levels in NCI-H292 cells treated with 33nM EGF are comparable with those seen in A431 cells treated with 1nM EGF where ezrin and moesin phosphorylation could not be detected.

In conclusion, in the bronchial epithelial cell lines, 16HBE 14o- and NCI-H292, and primary bronchial epithelial cell lines EGF stimulates phosphorylation of its receptor (EGFR). However, there were no detectable changes in tyrosine phosphorylation of ezrin and moesin, at least under conditions described here, which included a range of doses of EGF and a time course. One hypothesis, which could have been tested here, is that EGF causes phosphorylation on serine/threonine residues of ezrin and moesin. Following ligand activation of the EGFR and receptor dimerisation, phospholipase C-γ (PLC-γ) an intracellular signalling molecule is able to bind phosphorylated tyrosine residues of the EGFR via its SH2 domains. Activated PLC-γ then catalyses the breakdown of phosphatidylinositol-bisphosphate (PIP2) into diacylglycerol (DAG) and inositol-trisphosphate (IP3) and DAG in turn activates protein kinase C (PKC) which has been shown to be a mediator of ERM protein phosphorylation on threonine residues at the carboxy-terminal of the ERM protein molecule (106), (114).

A comparison of 16HBE 14o- cells with primary cells enabled any differences in ERM protein distribution between the transformed cell line and primary cells to be examined. Cytoskeletal data showed that both proteins became slightly enriched in the insoluble cytoskeletal fraction after treatment with EGF and also redistributed to membrane regions of the cell as observed by immunocytochemistry.

In 16HBE 14o- cells, ezrin and moesin behaved similarly when treated with EGF in that both proteins had a cytoplasmic distribution prior to treatment with EGF and following treatment staining was enhanced at the plasma membrane but cells were treated at confluence and did not exhibit cell surface projections. Conversely, primary cells were treated sub-confluence and upon treatment with EGF ezrin redistributed to lamellipodia cell projections and moesin to microvilli-like cell extensions as well as lamellipodia cell projections.

Western blotting for ezrin and moesin showed a further difference in 16HBE 14o- cells compared to primary cell cultures. Immunostaining of Western blots of whole cell lysate, cytoskeletal and soluble fractions from primary cells using a mouse monoclonal antibody against moesin proteins detected 2 bands in the molecular weight range of that expected for moesin (figure 4.8). This double band was not observed with 16HBE 14o- cell lysates or fractions and was not observed when staining for ezrin.

Further examination of the protein structure for ezrin and moesin and the immunogens used to raise antibodies, detailed in figure 4.15, indicated the potential for crossreactivity of the anti-moesin antibody with other members of the ERM protein family. The protein sequence used as an immunogen to raise the anti-moesin antibody only spans ten amino acids (554-564) the identical sequence of which is found in all three members of the ERM protein family and makes up the F-actin binding domain common to all ERM proteins (149). Therefore, this antibody does not specifically recognise moesin but cross-reacts with all members of the ERM protein family despite the data sheet implying this was a specific anti-moesin antibody as opposed to a pan-ERM protein family antibody.

ERM proteins share 75-80% homology with each other but have different molecular weights; ezrin 69.4kDa, radixin 68.5kDa and moesin 67.8kDa enabling the elucidation

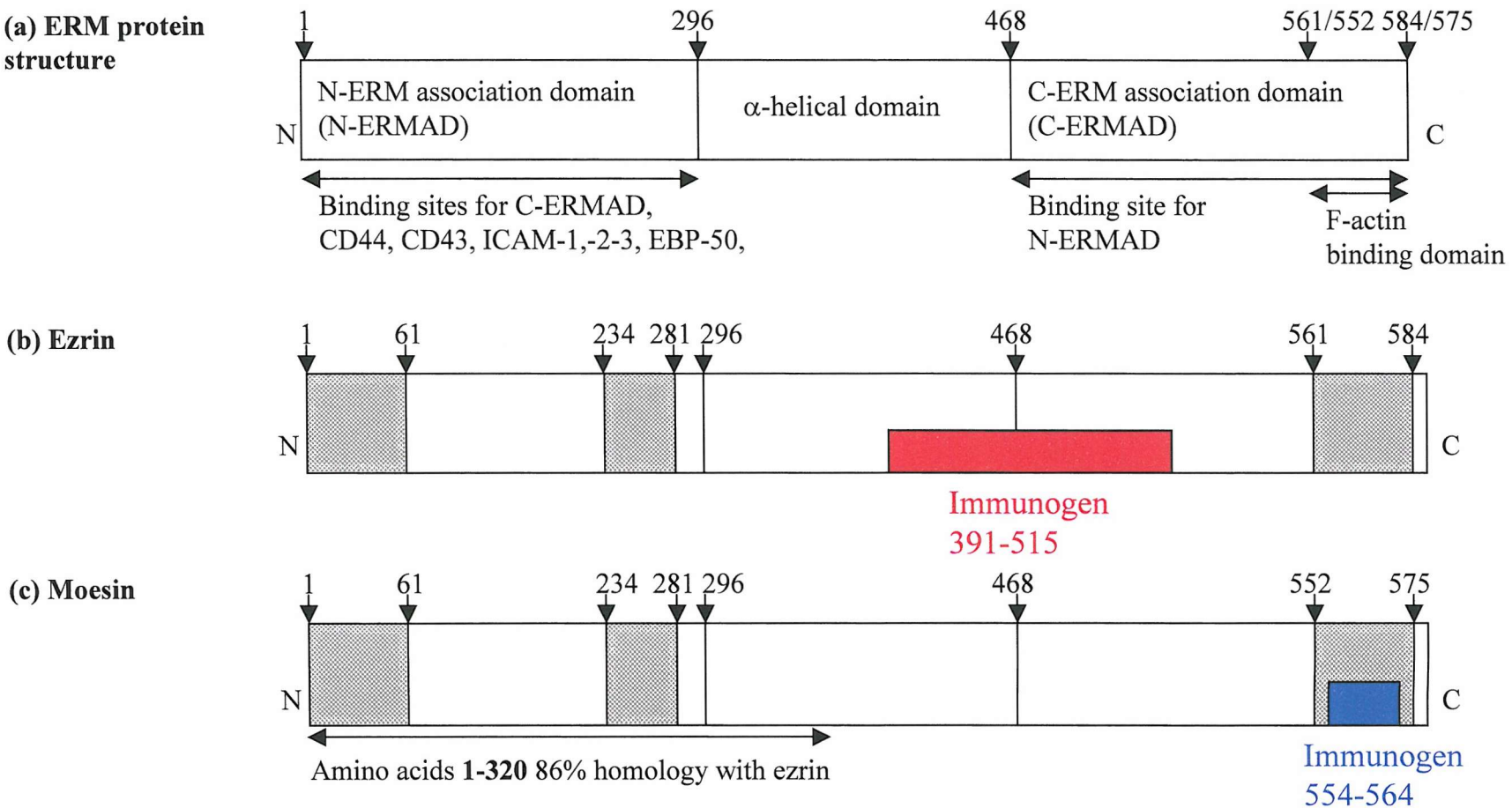

Figure 4.15. ERM protein structure indicating main functional domains and antibody binding sites.
ERM protein structure indicating structural domains common to all members of the ERM protein family (a). (b) and (c) indicate the regions used as immunogens to raise mouse monoclonal antibodies (Transduction Laboratories) against ezrin and moesin, respectively and hence indicate the binding site of the resultant antibodies. Shaded areas (▨) indicate regions which have identical sequences in ezrin and moesin.

of which bands correspond to which member of the ERM protein family. A charged alpha-helical region on ERM proteins causes them to migrate at approximately 80kDa and appear to have a higher molecular weight. It is likely that in primary cells the higher molecular weight band corresponds to ezrin as this is detected with the anti-ezrin mouse monoclonal antibody which recognises a sequence of 124 amino acids (391-515) which is unique to ezrin (figure 4.15). The lower molecular weight band could correspond to either moesin or radixin. As 16HBE 14o- cells only reveal one band when blotted for moesin and this corresponds in size with the upper band detected in primary cells (figure 4.8 B) it appears that 16HBE 14o- cells express undetectable levels of moesin or radixin, as indicated by the absence of a lower band and that the antibody is in fact cross reacting with ezrin.

Immunocytochemistry data showed that in 16HBE 14o- cells ezrin and moesin had a similar distribution whereas in primary cells differences were seen. This can be explained by the fact that by Western blotting 16HBE 14o- cells appear to only express ezrin proteins whereas primary cells express ezrin and one other member of the family, either radixin or moesin. Differences in staining patterns observed in figure 4.10 suggest that ezrin has a distinct function to the protein detected using the anti-moesin antibody. These distinct staining patterns were not so clear in the double staining experiments (figure 4.11) where ezrin and moesin were both found in lamellipodia and microvilli-like extensions of the plasma membrane with no observable differences between ezrin and moesin distribution. Here, goat polyclonal antibodies which more than likely detect all ERM protein members were utilised, necessitated by the fact that only antibodies raised in mouse against CD44 proteins were available.

Loss of expression of moesin by the transformed cell line might be one of the many changes induced during the transformation and subsequent immortalisation. Following crisis (where most cells die and only stably transformed cells survive) cells tend to have differing growth and phenotypic properties to the native cell (reviewed in (48)). Additionally, the origin of the 16HBE 14o- cell line could be from a more distal part of the lung than those cells harvested during the bronchoscopy procedure which come from the proximal airways and hence vary in their phenotype, with more distal cells showing a more squamous phenotype with loss of cilia. The likelihood of expression of ezrin, radixin and moesin in 16HBE 14o- and primary cells could have been checked

by RT-PCR to confirm which members of the ERM protein family are expressed by primary cells and the 16HBE 14o- cell line.

My original hypothesis stated that co-localisation of HB-EGF with CD44v3 at the plasma membrane might potentiate its effects. In this set of experiments I have shown no evidence for this; whereas EGF was able to significantly stimulate an enrichment of ezrin ($P<0.05$) and moesin ($P<0.003$) into the cytoskeletal fraction of 16HBE 14o- cells there was no stimulatory effect of HB-EGF on the distribution of ezrin or moesin. Also the experiments that examined ezrin and moesin distribution by immunocytochemistry showed that HB-EGF had the same effect as EGF.

This chapter has examined the regulation of ERM proteins in cultured bronchial epithelial cells under normal conditions. The involvement of ERM proteins during migratory phases of repair is well documented and therefore ERM proteins might be involved in bronchial epithelial repair. The distribution of ERM proteins to membrane extensions and in areas of the cell which are not in contact with other cells, as shown here, suggests a possible involvement of these proteins in cell migration as the development of lamellipodia are essential for cell motility (reviewed in (133)). Furthermore, EGF which has been shown here to stimulate changes in ERM protein distribution has been shown to initiate repair of bronchial epithelial cells following scrape wounding as well as stimulate migration of epithelial cells (71), (84), (118). Therefore, the next chapter will examine the role of EGF in cell migration and ERM protein distribution using an *in vitro* wound/repair assay. Changes in the cellular distribution and binding of ERM proteins by EGF might enable modulation of the actin cytoskeleton and cell adhesion molecules through its effects on ERM proteins and this might be relevant in terms of modulating cell morphology, motility and adhesion during repair of bronchial epithelium.

5 CHAPTER FIVE

THE ROLE OF ERM PROTEINS IN EGF STIMULATED MIGRATION OF BRONCHIAL EPITHELIAL CELLS FOLLOWING MECHANICAL DAMAGE

Epithelial cell spreading and migration are highly controlled cell processes shown to occur in the early stages of repair following damage to the skin, gut and lung epithelium. Epithelial cell migration is a dynamic process requiring reorganisation of the cellular cytoskeleton as well as changes to cell-cell and cell-extracellular matrix adhesions.

The involvement of growth factors and cytokines in both cell migration and more specifically in actin cytoskeleton reorganisation has been described in numerous *in vivo* and *in vitro* studies. Furthermore enhanced expression of growth factors in wounds has been described further supporting a role for these soluble factors in regeneration of tissues.

ERM proteins through their crosslinking with the actin cytoskeleton and cell adhesion molecules could play a role in regulation of cell migration and adhesion in bronchial epithelial cells as has been shown for other epithelial cells. Modulation of ERM protein binding and their sub-cellular distribution by growth factors, such as EGF as described in the previous chapter, could be involved in EGF stimulated cell migration to allow regeneration of the damaged epithelium. Data presented in Chapter 4 showed that EGF was able to stimulate redistribution of ERM proteins into actin cytoskeleton based membrane extensions resembling the leading edge of a spreading and migrating cell and this redistribution was especially prominent in cells that were not in direct contact with another cell. This chapter aims firstly to further characterise the role of EGFR ligands in repair following wounding of epithelial cell monolayers and secondly the effect of EGF on the distribution of ERM proteins and CD44 in repairing cultures. In addition the influence of the mast cell stabiliser, sodium cromoglycate, will be studied here as it has been shown to induce phosphorylation of moesin in mast cells as well as promote dermal wound repair (unpublished observations, Alan Edwards).

5.1 Factors affecting 16HBE 14o- cell migration following mechanical damage

After mechanical damage with a pipette tip cell migration of epithelial monolayers of 16HBE 14o- cells was observed by time-lapse microscopy over a 6-hour time course with images captured every hour. Figure 5.1 shows the appearance of the cells during this migratory phase and a visible difference in wound area between the conditions was observed. Here the cells appear to move forward in a sheet or monolayer of closely packed cells rather than individual cells at the wound edge moving forward, as there seemed to be very little change in the appearance and formation of the cells at the migrating edge of the wound. Image analysis software, Scion Image, was then used to measure the area of the culture plate not covered by cells on each of these images and hence determine wound area. These data are plotted in figure 5.2 and indicate that under both culture conditions cell migration is linear over the 6-hour time course. When cultured in basal serum free medium, cells migrate in an attempt to cover the denuded substrate resulting in partial closure of the wound at the end of the time course (from a wound area of $0.45mm^2$ at T=0 to $0.27mm^2$ at 6 hours post damage). Supplementing the medium with 1nM EGF appears to enhance this process with near closure of the wound at the end of the 6-hour time, as well as a significant difference in wound area between treatments at 4, 5 and 6 hours ($P<0.04$, 0.04, 0.03 respectively). Data plotted in figure 5.2 suggests the rate of repair may be enhanced in the presence of 1nM EGF with a steeper slope indicating a more rapid migration of the cells in the presence of 1nM EGF.

In order to assess the influence of a range of factors on cell migration, 16HBE 14o- cells cultured in 4-well chamber slides were wounded using a comb to create a reproducible series of wounds that could then be measured individually. Using this technique, cells migrated under serum free conditions as in Figure 5.1 and had almost fully repaired 9 hours after damage (figure 5.3i). The addition of 1μM tyrphostin AG1478 to the medium inhibited the basal repair at 6 and 9 hours after wounding with significantly greater wound area at these time points when compared to serum free medium alone (P values <0.01 and <0.001 respectively).

EGF has previously been shown to enhance repair of 16HBE 14o- cell cultures after mechanical damage (118) and comparable data are presented in figure 5.3ii. Addition

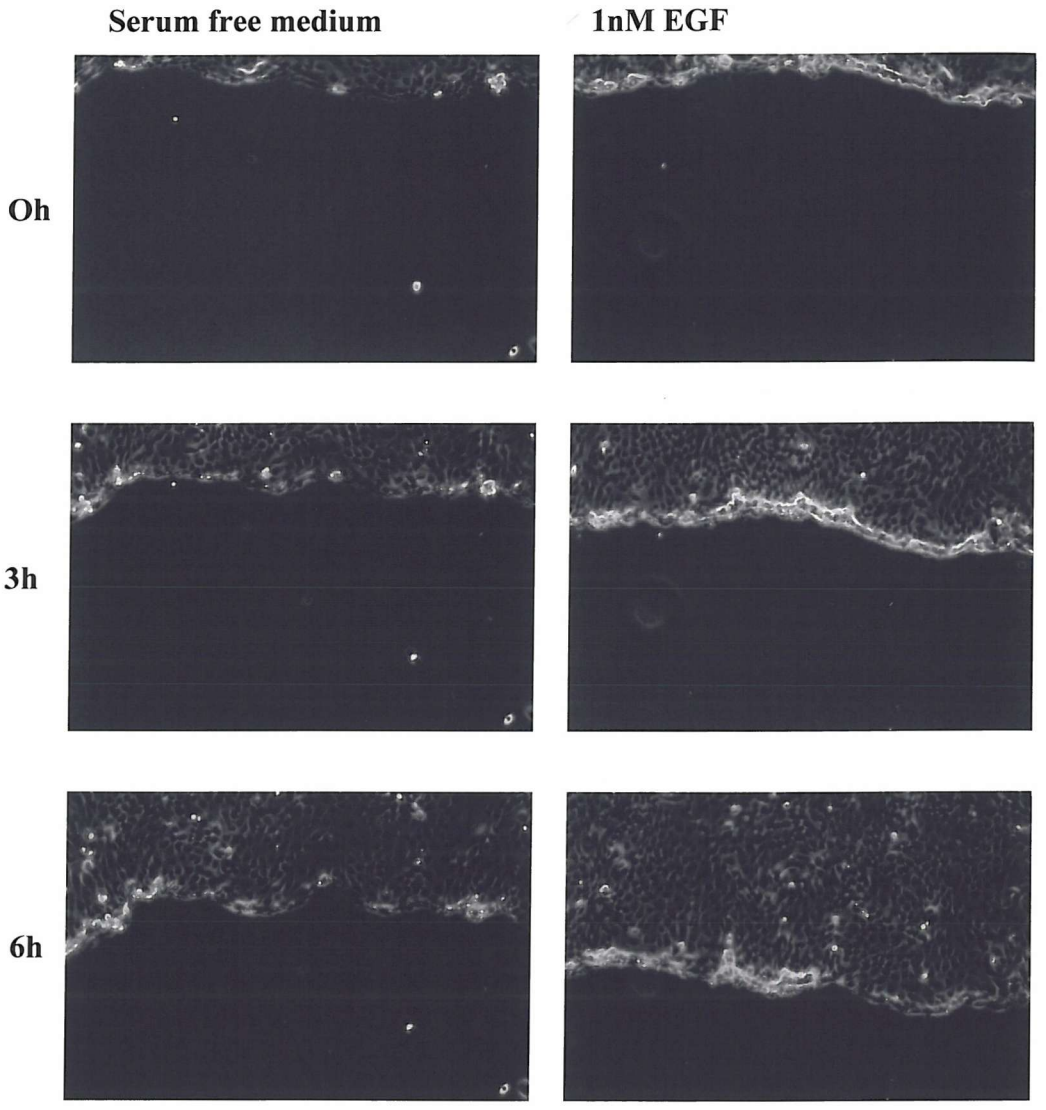

Figure 5.1. Microscopic images of repairing 16HBE 14o- cells.
Time lapse video microscopy capture of wounded 16HBE 14o- cells treated with serum free medium alone or with the addition of 1nM EGF were used to observe the rate of cell migration. Cells were left to recover in an incubator for 30 minutes after wounding then viewed using a time-lapse video microscopy system and images captured at 0, 3 and 6 hours after the start of the time lapse.

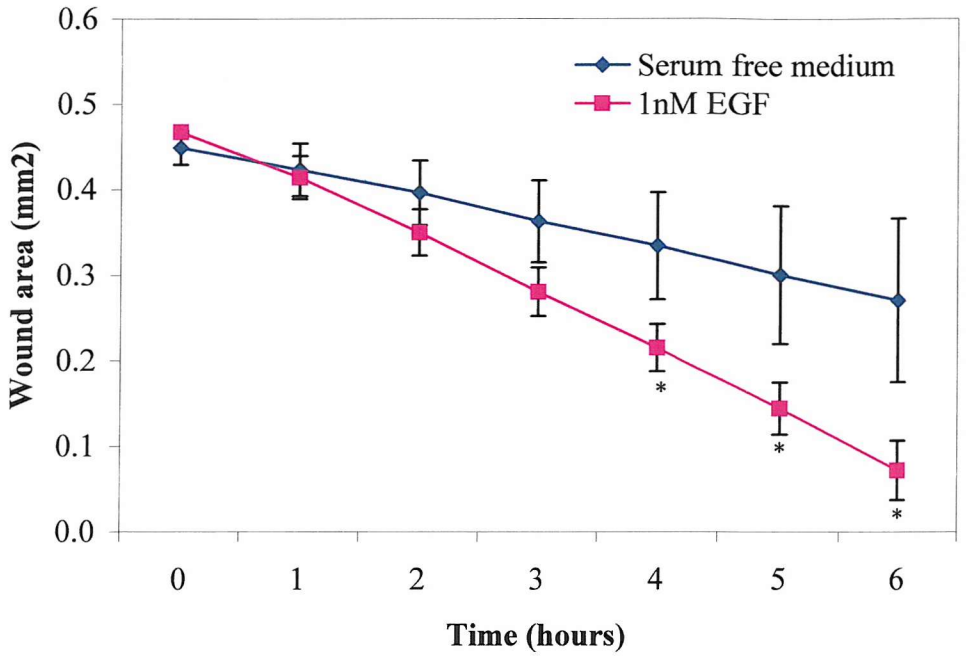

Figure 5.2. Effect of EGF on restitution of 16HBE 14o- cell monolayers. The effect of serum free medium and 1nM EGF on 16HBE 14o- wound repair following mechanical damage was measured using a time lapse video microscopy method. Cell movement was observed over a 6 hour time period and an image captured every hour using IP Lab software. Wound area was measured using Scion Image and data are mean wound area +/– Standard deviation from 3 individual experiments and were statistically analysed using a Student's unpaired *t* -test, P=<0.05.

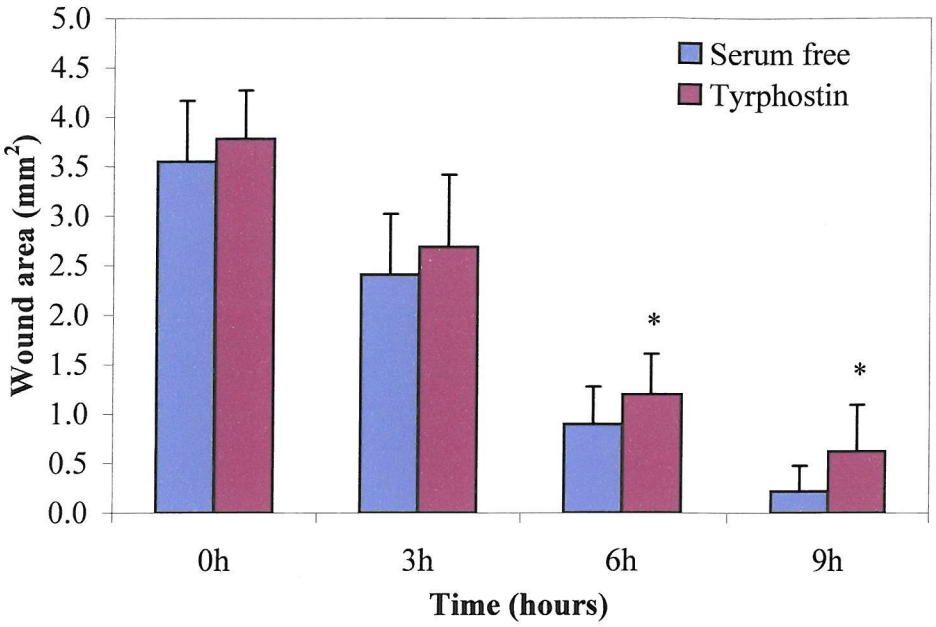

Figure 5.3i. Effect of tyrphostin AG1478 on repair of 16HBE 14o- cells. The effect of 1μM tyrphostin AG1478 on basal repair of scrape wounded 16HBE 14o- cells was measured using the chamber slide method. Data are mean +/- Standard deviation of 25 wounds measured in 3 individual experiments and were statistically analysed using a Student's unpaired *t* -test. *P<0.05 comparing the addition of 1μM tyrphostin with serum free medium alone.

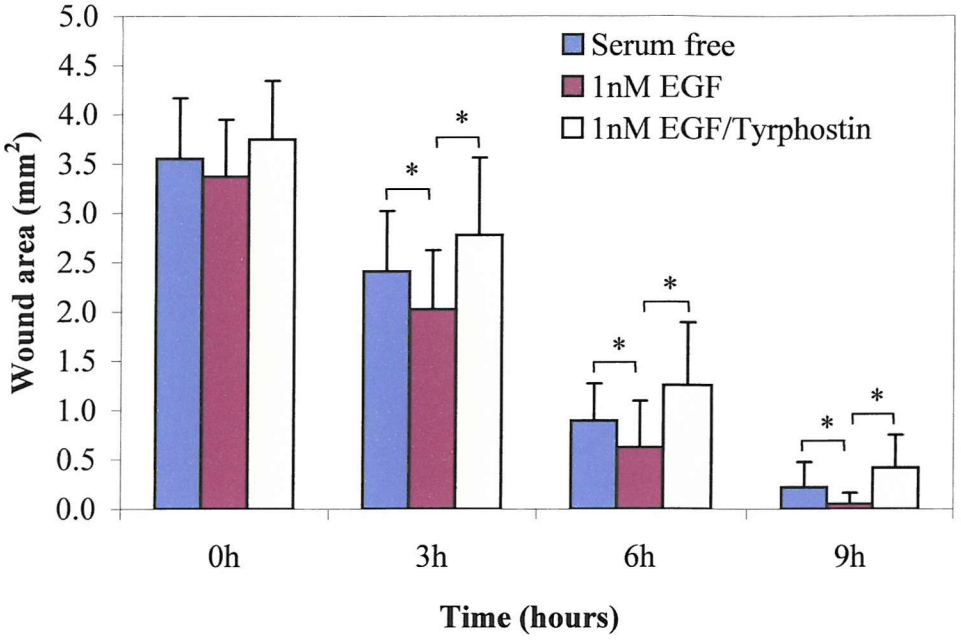

Figure 5.3ii. Effect of 1μM tyrphostin AG1478 on 1nM EGF stimulated repair of scrape wounded 16HBE 14o- cells.
Data are mean +/- Standard deviation of 25 wounds from 3 individual experiments and were statistically analysed using a Student's unpaired *t* -test. *P<0.05 comparing serum free medium vs EGF and EGF vs EGF/tyrphostin.

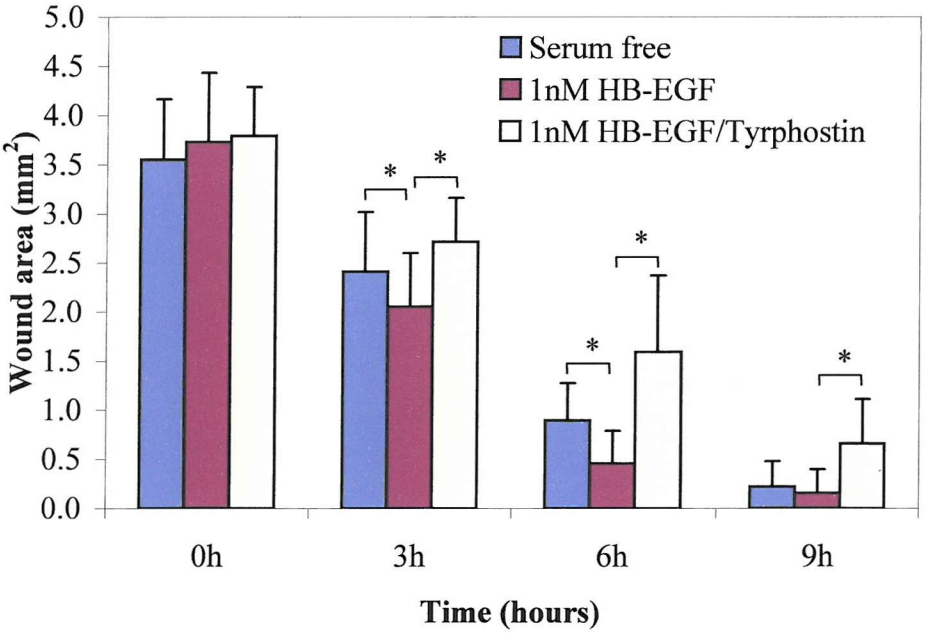

Figure 5.3iii. Effect of 1μM tyrphostin AG1478 on 1nM HB-EGF stimulated repair of scrape wounded 16HBE 14o- cells.
Data are mean +/- Standard deviation of 25 wounds from 3 individual experiments and were statistically analysed using a Student's unpaired *t* -test. *P<0.05 comparing serum free medium vs HB-EGF and HB-EGF vs HB-EGF/tyrphostin.

of 1nM EGF to serum free medium was able to significantly increase the rate of repair of cells at 3, 6 and 9 hours ($P<0.03$, $P<0.03$ and $P<0.005$ respectively). 1nM HB-EGF was also able to enhance repair at 3 and 6 hours ($P<0.04$ and $P<0.0001$, respectively) (figure 5.3iii), but at 9 hours the wound area was not statistically different to that of cells cultured in serum free medium ($P=0.36$). Co-incubation of cells with tyrphostin AG1478 at 1μM along with EGF (figure 5.3ii) or HB-EGF (figure 5.3iii), inhibited both EGF and HB-EGF stimulated repair at 3, 6 and 9 hours after damage, when comparing incubation with growth factor alone with growth factor and tyrphostin AG1478 together.

5.2 Distribution of ezrin in migrating bronchial epithelial cells following scrape wounding

As previously described, the actin cytoskeleton and its associated proteins play a major role in cell migration. The distribution of ezrin in repairing cultures treated with serum free medium and EGF was therefore observed using fluorescent immunocytochemical staining. Immediately after wounding, (figure 5.4), the staining pattern for ezrin was predominantly cytoplasmic both in cells at the wound edge and in undamaged areas. Figure 5.5 shows the distribution of ezrin at the damaged edge during the early stages of repair and the influence of treatment with 1nM EGF on this. 15 minutes after wounding the distribution of ezrin is unchanged with cells having a mainly cytoplasmic distribution of ezrin, this is irrespective of treatment with serum free medium or EGF containing medium and this pattern continues to be seen 30 minutes and 1 hour after treatment. At 30 minutes and 1 hour after wounding, cells at the wound edge appeared to spread into the gap with flat lamellipodia projections of the plasma membrane exhibiting only faint ezrin staining. This data is in contrast to that presented in Chapter 4, Section 4.3, where 15-minute EGF treatment of 16HBE 14o- cells induced redistribution of ezrin to plasma membrane structures with untreated cells displaying a mainly cytoplasmic distribution. However, this observation is not seen here even in confluent areas of cells distant from the wound edge (figure 5.6) an observation, which is inconsistent with previous data.

Control experiments were carried out to determine the cause of these differences. A dose response experiment was carried out but no changes in ezrin and moesin

Wound edge

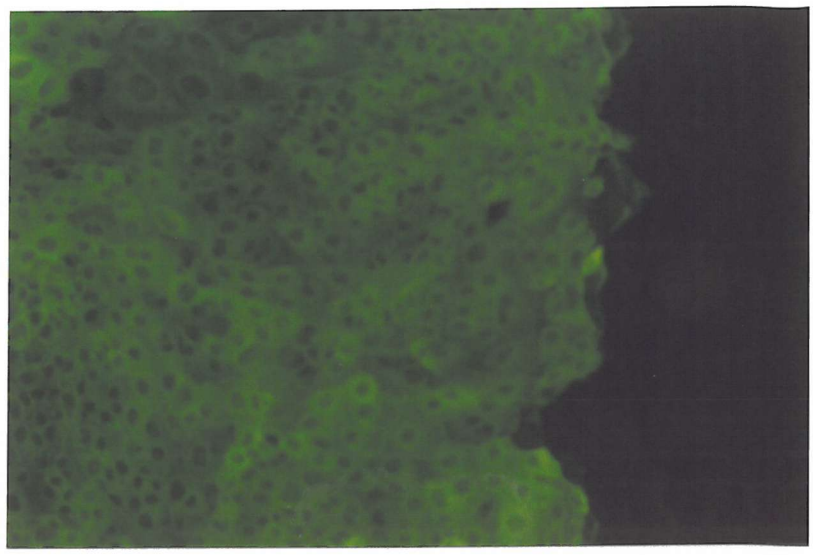

Confluent area

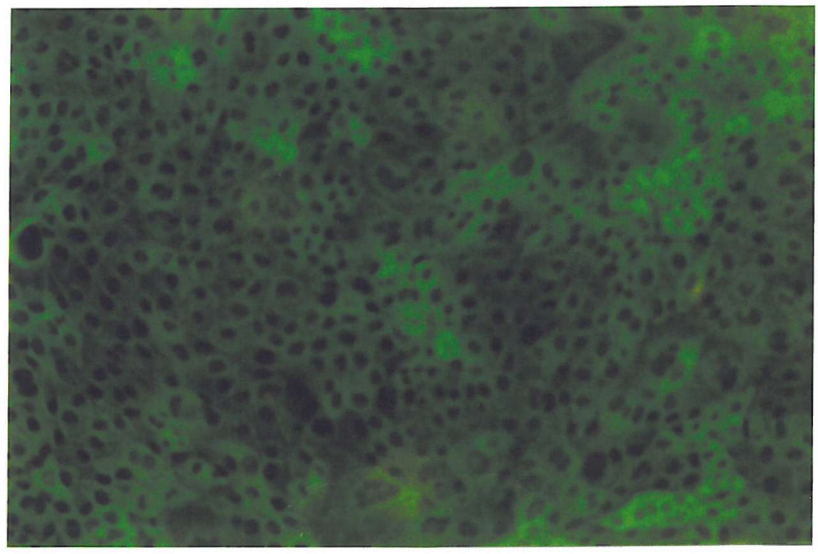

Figure 5.4. Ezrin distribution in 16HBE 14o- cells fixed immediately after scrape wounding.

Serum starved cell monolayers, were scrape wounded and fixed in cold methanol for 10 minutes before staining for ezrin using a mouse monoclonal primary antibody and a secondary anti-mouse FITC conjugate. Cells were visualised using a Leica fluorescent microscope and images taken of a damaged area and a confluent area distant from the damaged area.

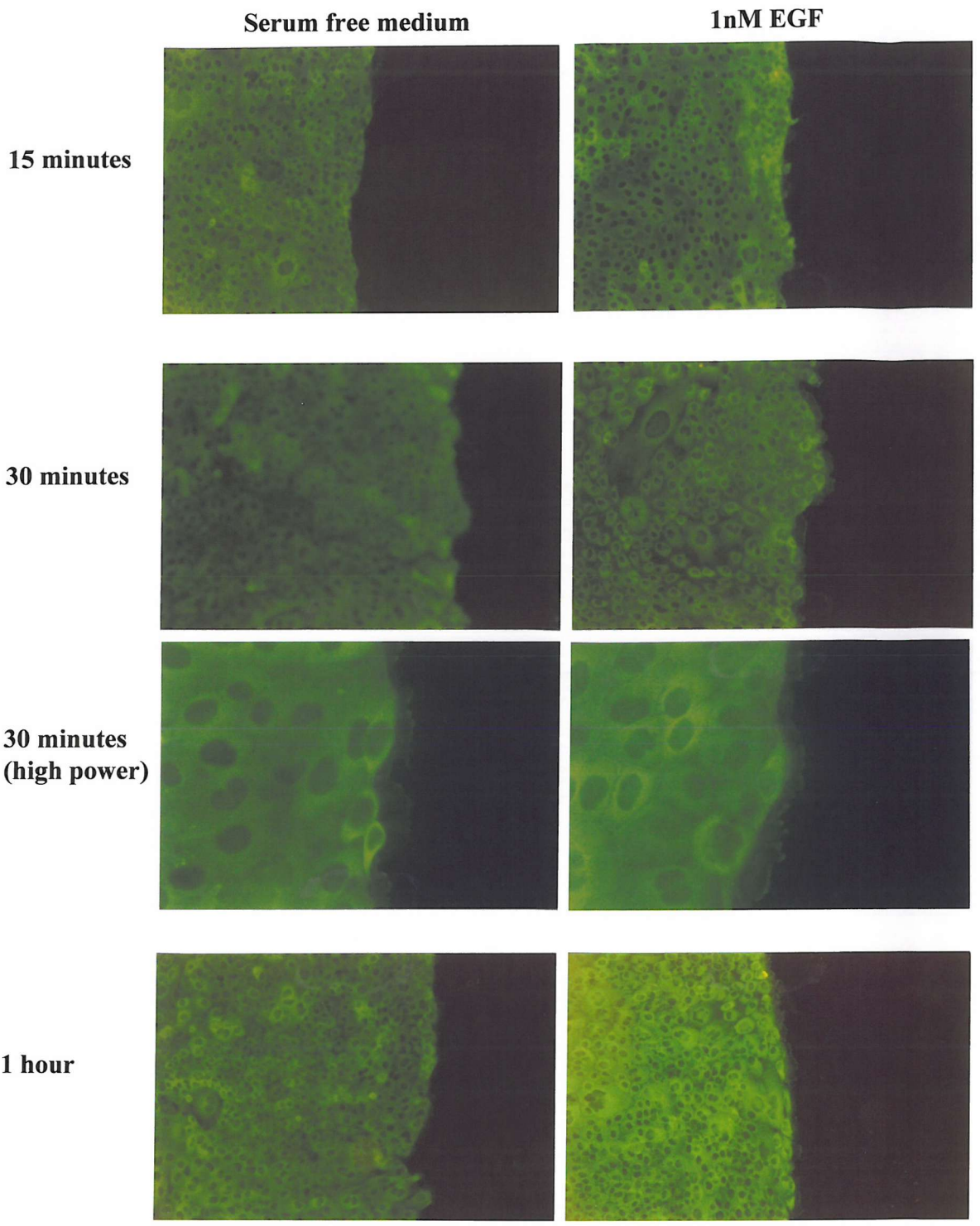

Figure 5.5. Ezrin distribution in repairing 16HBE 14o- bronchial epithelial cell cultures.
16HBE 14o- cell monolayers cultured in 8-well chamber slides were serum starved for 24 hours before scrape wounding with a 1ml pipette tip. Cells were briefly washed with serum free medium before adding serum free medium +/- 1nM EGF. Cells were fixed in cold methanol for 10 minutes immediately after wounding and at 15, 30 minutes and 1 hour after wounding. Fluorescent immunocytochemical staining for ezrin was carried out using the standard protocol.

Serum free medium

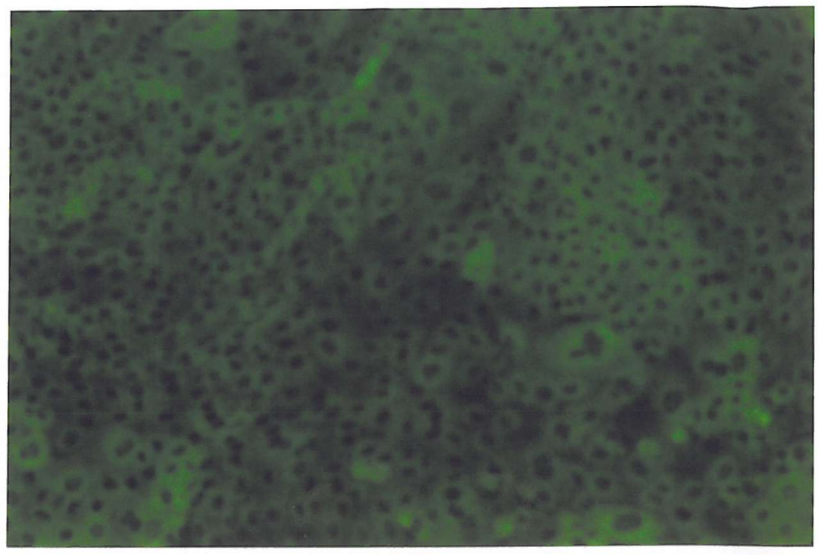

1nM EGF

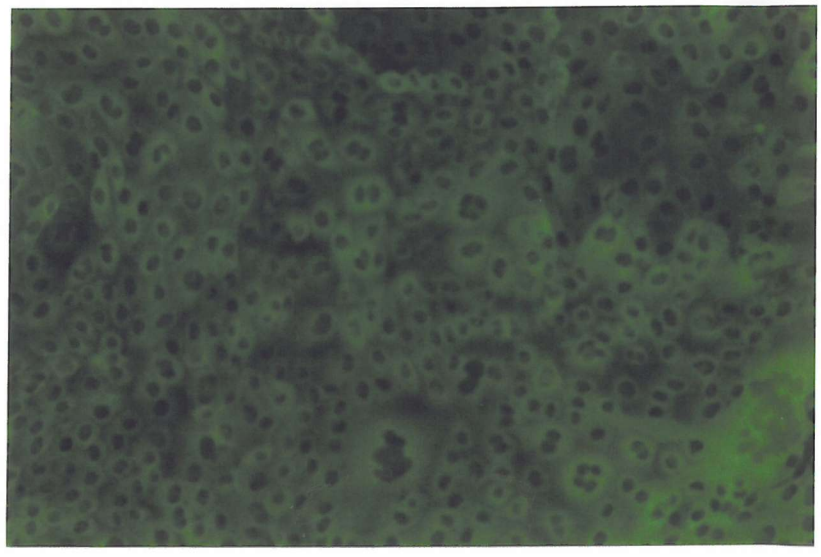

Figure 5.6. Ezrin distribution in confluent areas of EGF treated 16HBE 14o- cells after scrape wounding.
Serum starved 16HBE 14o- cells were scrape wounded and washed briefly with serum free medium before incubating with serum free medium +/- 1nM EGF for 15 minutes. Cells fixed in cold methanol for 10 minutes were stained for ezrin and staining was visualised using a Leica immunofluorescent microscope.

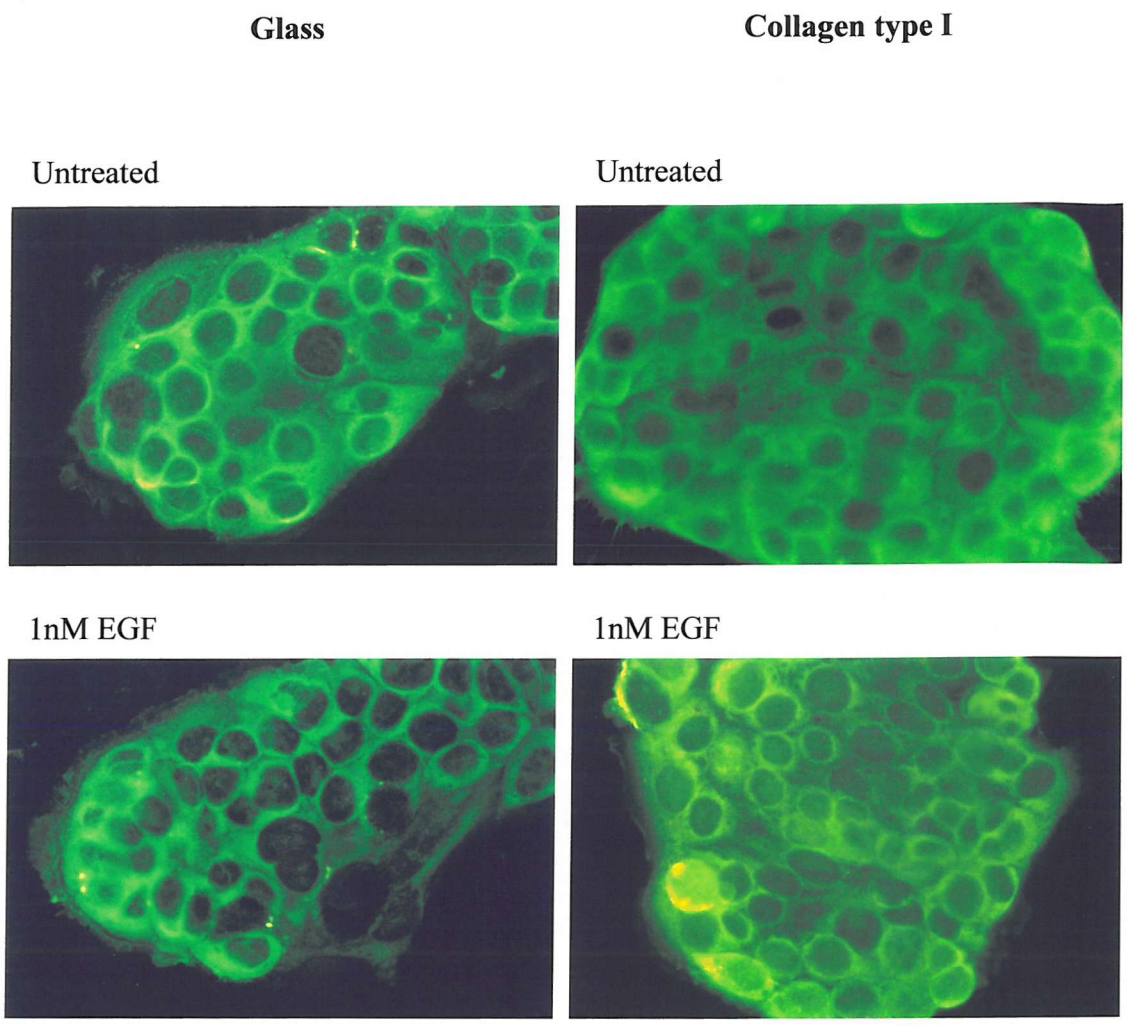

Figure 5.7. The effect of growth substrate on ezrin distribution.
16HBE 14o- cells were cultured on uncoated or collagen type I coated glass chamber slides to determine the influence of substrate on ezrin distribution before and after treatment with 1nM EGF for 15 minutes. Cells were then fixed in cold methanol for 10 minutes before staining for ezrin using a mouse monoclonal primary antibody and a secondary anti-mouse FITC conjugate. Cells were visualised using a Leica fluorescent microscope.

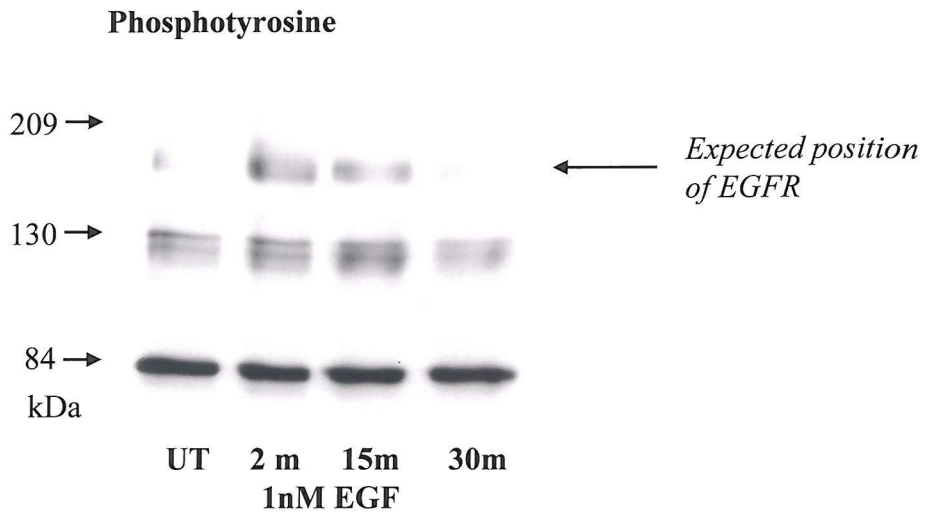

Figure 5.8. Tyrosine phosphorylation response of 16HBE 14o- cells following treatment with 1nM EGF.
Cells were serum starved for 24 hours then treated with 1nM EGF for 2, 15 or 30 minutes (m) or left untreated (UT). Following cell lysis 8μg protein per lane was separated by 7.5% SDS-PAGE and transferred onto a nitrocellulose membrane before staining Western blots with an anti-phosphotyrosine (clone PY20) antibody.

distribution were observed with EGF treatment (data not shown). The influence of cell density at the time of treatment and varying the time course was also investigated and even the addition of 17nM EGF failed to stimulate a redistribution of ezrin and moesin in these cells. Different stocks of EGF and 16HBE 14o- cells preserved in liquid nitrogen were also checked. Other factors that could affect the cells were also examined. All the chamber slides used were of the same batch number eliminating variability of the substrate the cells were cultured on. All cell culture and stimulation of cells was carried out in an air-conditioned environment thus controlling for seasonal differences in the temperature. Additional experiments were carried out to assess the influence of culturing cells on an extracellular matrix substrate. 16HBE 14o- cells were cultured on collagen type I coated slides prior to stimulation with InM EGF for 15 minutes and staining for ezrin using immunocytochemistry (figure 5.7) but this appeared to have no influence on ezrin distribution irrespective of treatment and in all conditions ezrin was mainly cytoplasmic.

As a final test, the responsiveness of the cells to EGF was tested in a tyrosine phosphorylation assay. Figure 5.8 shows that EGF was able to cause changes in the tyrosine phosphorylation profile of 16HBE 14o- cells and in particular an enhancement of a band around 170kDa was observed following EGF treatment. This suggests that the EGF receptor tyrosine kinase is still functional in these cells and not responsible for the inconsistent results observed.

In summary despite following the same protocol for all the experiments and carrying out numerous checks on cell stocks, growth factor stocks, chamber slides and the influence of extracellular matrix substrate no explanation was found for the discrepancies between the two otherwise identical sets of experiments.

5.3 Effect of EGF on repair of primary bronchial epithelial cells

To further investigate the role of EGF in stimulating repair of bronchial epithelial cells and the role of ERM proteins and CD44 in this process, primary bronchial epithelial cells were used as an *in vitro* model as these cells were found to respond to EGF in a consistent manner with regards to changes in ezrin and moesin distribution as monitored by by immunofluorescence. An initial control experiment measured the

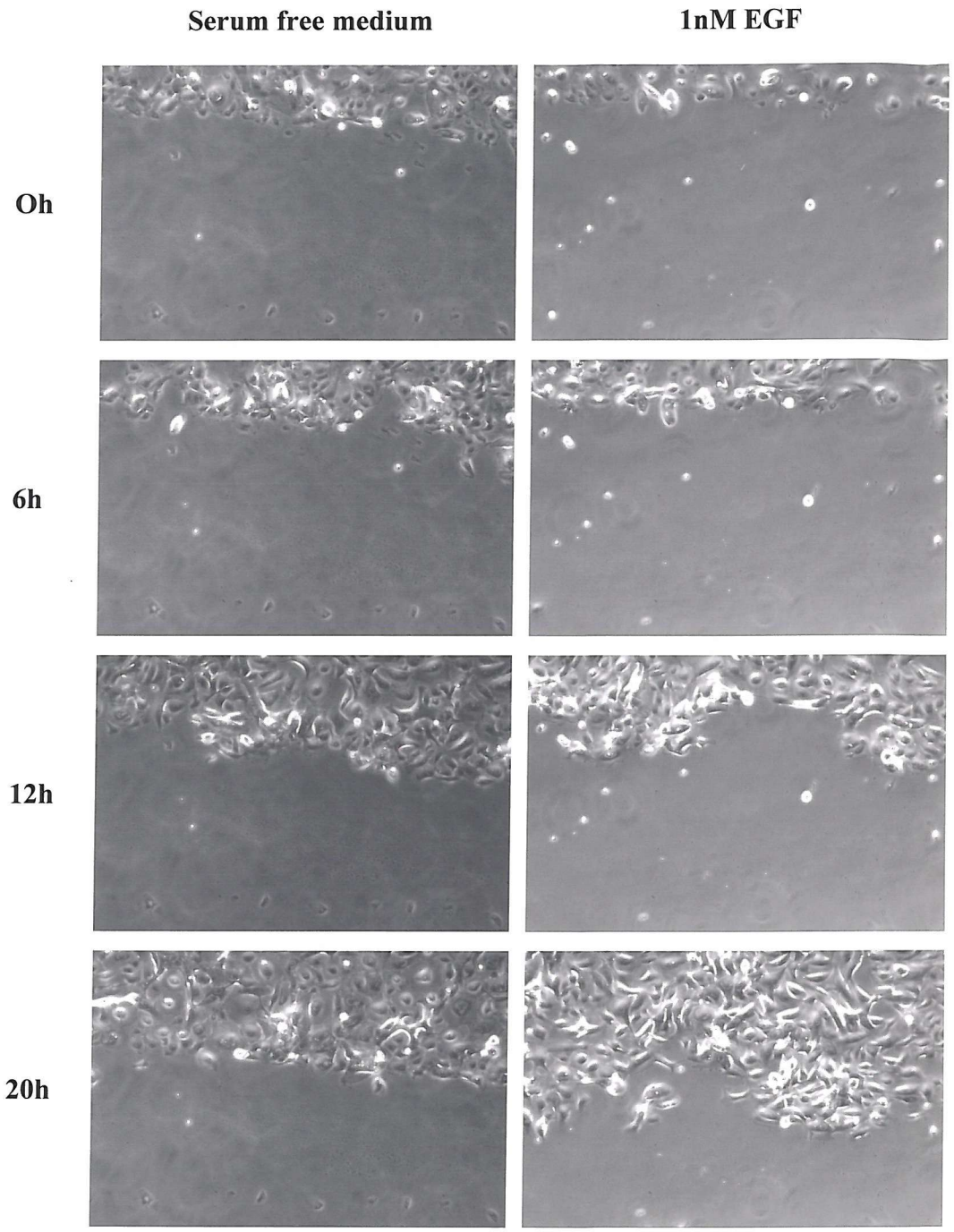

Figure 5.9. Microscopic images of repairing primary bronchial epithelial cells.

Time lapse video microscopy capture of wounded primary bronchial epithelial cell monolayers treated with serum free medium alone or with the addition of 1nM EGF was used to measure cell migration. Cells were left to recover in an incubator for 1 hour after wounding then viewed using a time-lapse video microscopy system and images captured at 0, 6, 12 and 24 hours after the start of the time lapse.

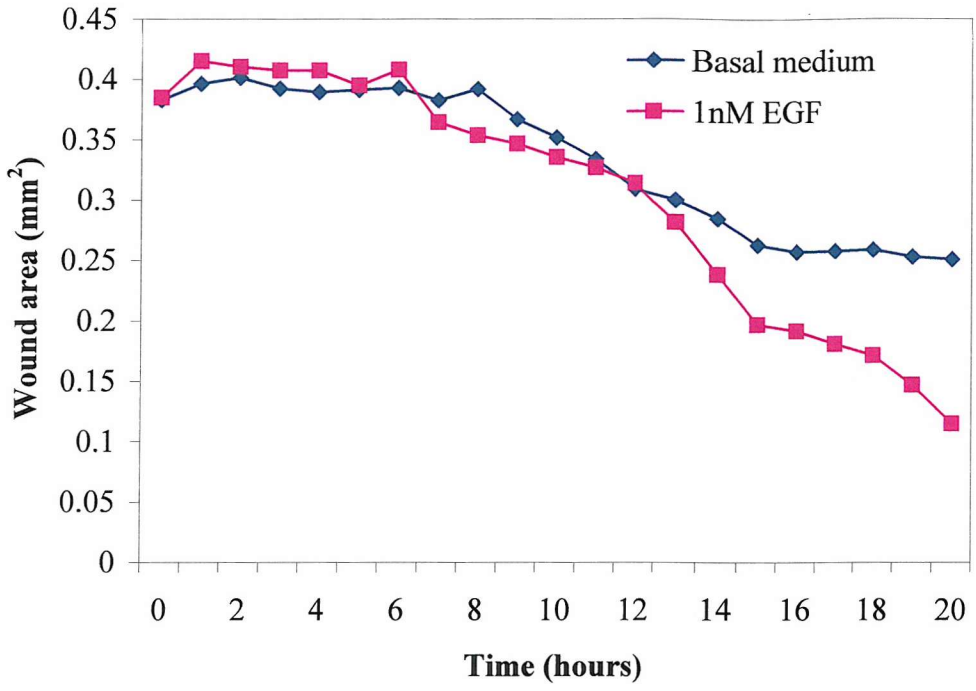

Figure 5.10. Effect of 1nM EGF on restitution of scrape wounded primary bronchial epithelial cell monolayers.
The effect of BEBM basal medium and 1nM EGF on migration of primary bronchial epithelial cells following mechanical damage was assessed using a time lapse video microscopy method. Cell movement was observed over a 20 hour time period and an image captured every hour using IP Lab software. Wound area was measured using Scion Image and converted from pixels to area (mm^2). Data are from a single experiment.

effect of EGF on the rate of repair following scrape wounding in the primary cell model using the time-lapse system. Figure 5.9 shows the appearance of cells during a wound healing time-lapse assay. In comparison to 16HBE 14o- cells, here the cells appeared to have a more spread phenotype with gaps observed between cells distant from the wound edge. Whilst the monolayer appeared to be moving forward to cover the denuded substrate as observed with 16HBE 14o- cells (figure 5.1) a number of cells were seen to be migrating free of the monolayer irrespective of treatment. Measurement of wound area, figure 5.10, indicates a result consistent with 16HBE 14o- cells as cells cultured in basal medium migrated to cover the denuded substrate, and treatment with 1nM EGF was able to enhance cell migration with a change in the rate of migration occurring after approximately 12 hours. The overall rate of repair was significantly slower in primary cells compared to 16HBE 14o- with the wound still being present at the end of the 20-hour time course.

5.4 Distribution of ERM proteins in repairing cultures of primary bronchial epithelial cells

Following confirmation that EGF was able to stimulate migration of primary bronchial epithelial cells, the distribution of ezrin and moesin in repairing cultures was investigated in these cells using fluorescent immunocytochemical dual staining for CD44 and ezrin or moesin. Primary bronchial epithelial cells were wounded then treated with basal medium alone or with 1nM EGF for 15 minutes, 1 hour and 3 hours, fixed and then stained to examine the distribution of the proteins in the initial stages of migration (figure 5.11). At the earliest time point, 15 minutes, as shown in figure 5.11A, CD44 staining had a surface distribution the intensity and distribution of which was unaffected by EGF and did not vary at the wound edge from cells distance from the wound. Ezrin and moesin were both found in the cytoplasm and in plasma membrane structures irrespective of treatment, although slightly more intense staining of plasma membrane structures was observed in 1nM EGF treated cells. Additionally, staining of membrane ruffles looked brighter and featured on more cells in cultures treated with EGF.

To confirm that the primary cell cultures were responding to EGF consistently, figure 5.12 shows staining for ezrin in a confluent area distant from the wound in untreated

A. Ezrin and CD44

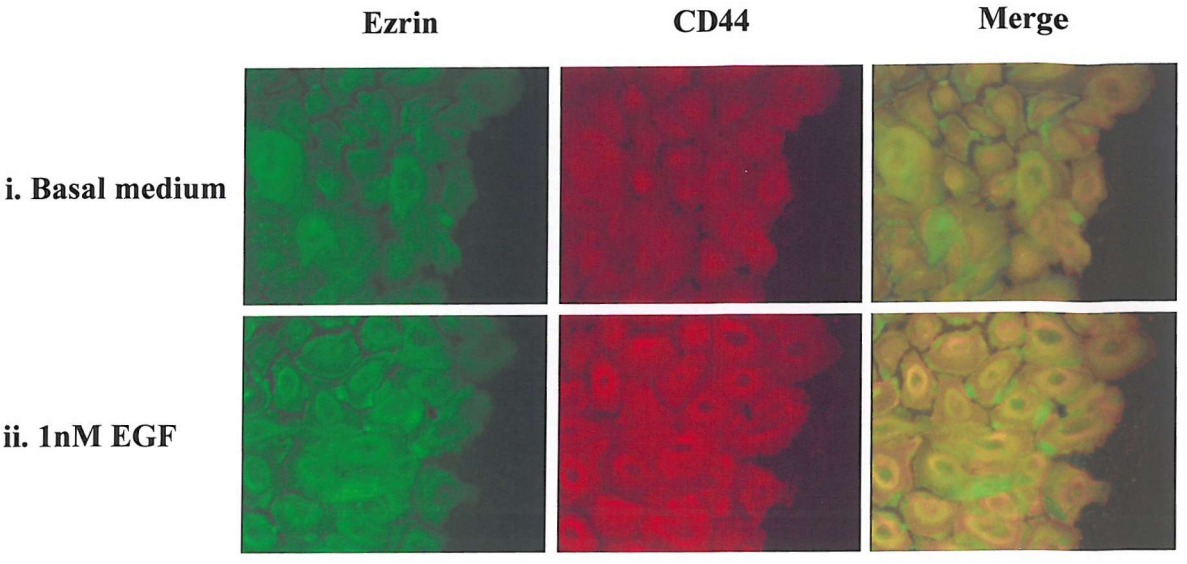

B. Moesin and CD44

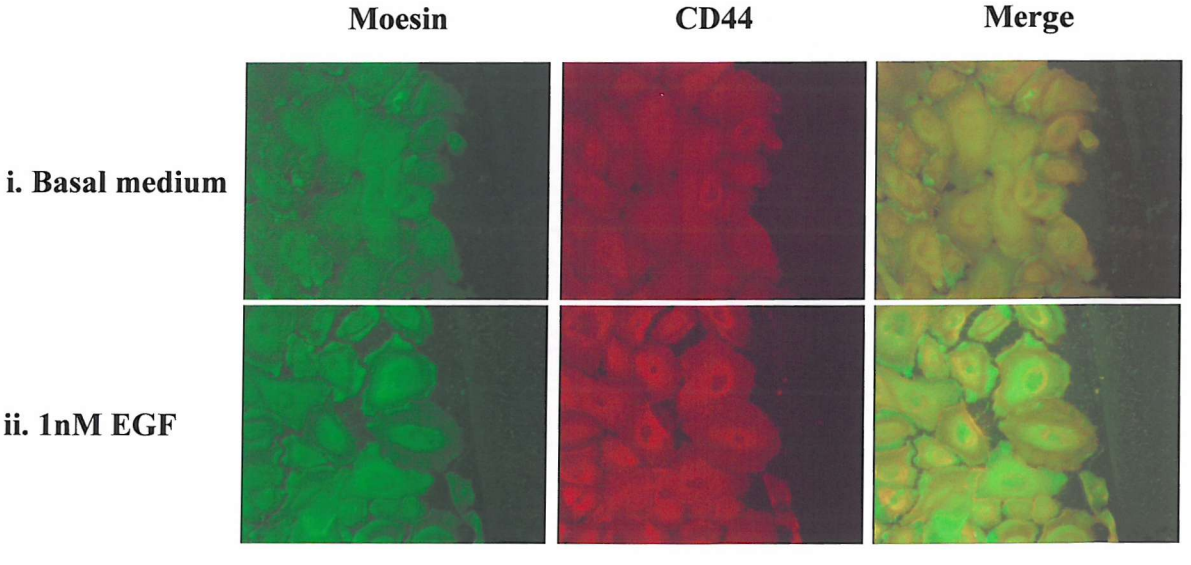

Figure 5.11A. Double immunocytochemistry staining for CD44 and ezrin or moesin in primary bronchial epithelial cells 15 minutes post-wounding.
Primary bronchial epithelial cells were cultured in Basal medium (BEBM) for 24 hours to deplete growth factors before scrape wounding. Cells were then treated with basal medium alone (i) or containing 1nM EGF (ii) for 15 minutes. Cells were fixed and double stained for CD44 and ezrin (A) or moesin (B) using the protocol described in Chapter 2, section 2.2.7. Cells were visualised using a Zeiss immunoflourescent microscope and images captured using a colour video camera.

A. Ezrin and CD44

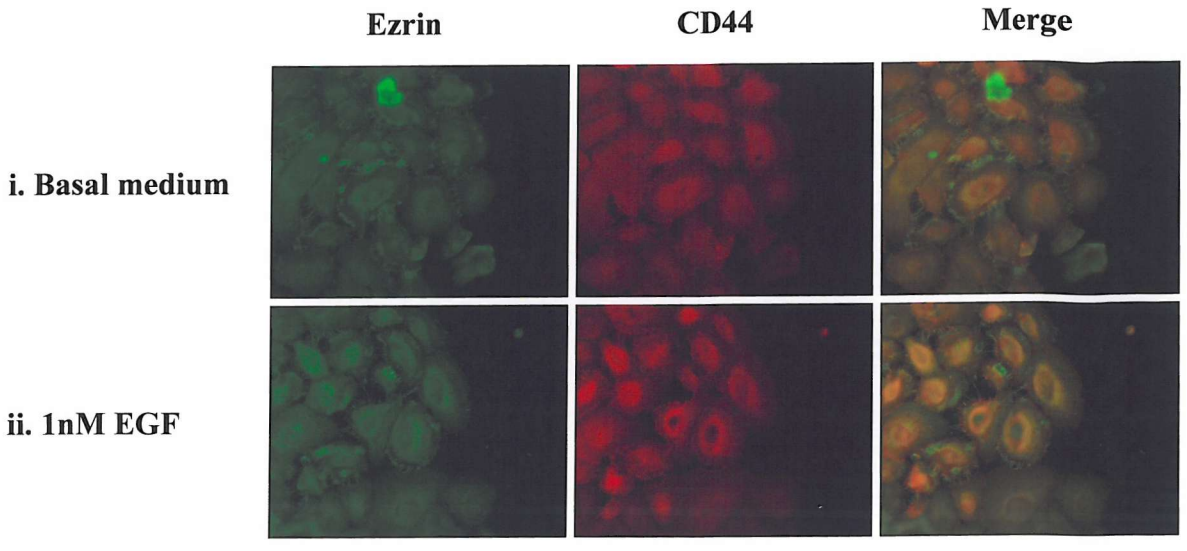

B. Moesin and CD44

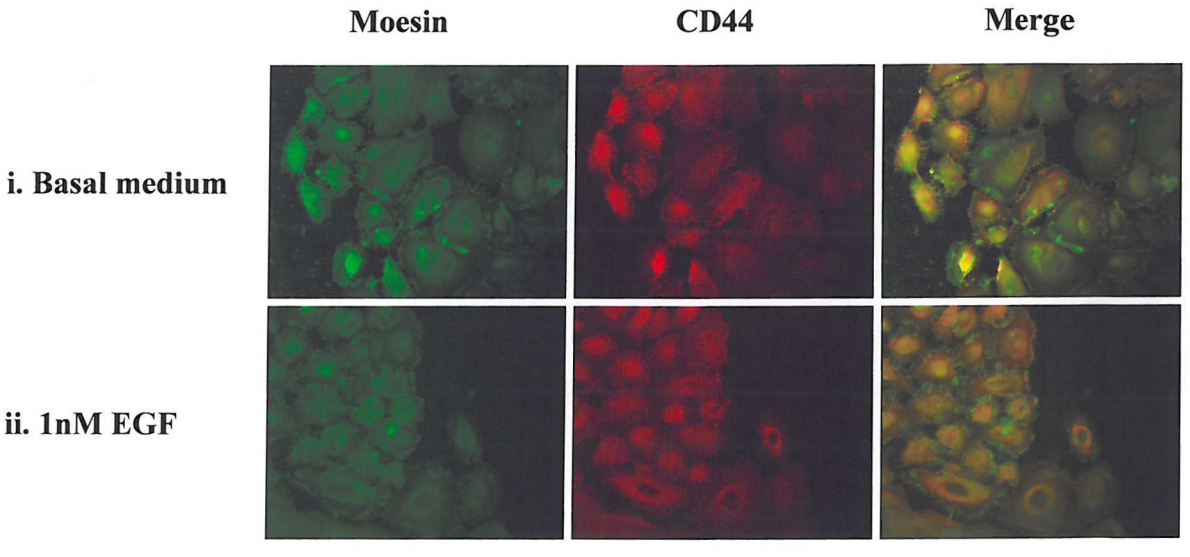

Figure 5.11B. Double immunocytochemistry staining for CD44 and ezrin or moesin in primary bronchial epithelial cells 1 hour post-wounding.
Primary bronchial epithelial cells were cultured in Basal medium (BEBM) for 24 hours to deplete growth factors before scrape wounding. Cells were then treated with basal medium alone (i) or containing 1nM EGF (ii) for 1 hour. Cells were fixed and double stained for CD44 and ezrin (A) or moesin (B) using the protocol described in Chapter 2, section 2.2.7. Cells were visualised using a Zeiss immunoflourescent microscope and images captured using a colour video camera.

A. Ezrin and CD44

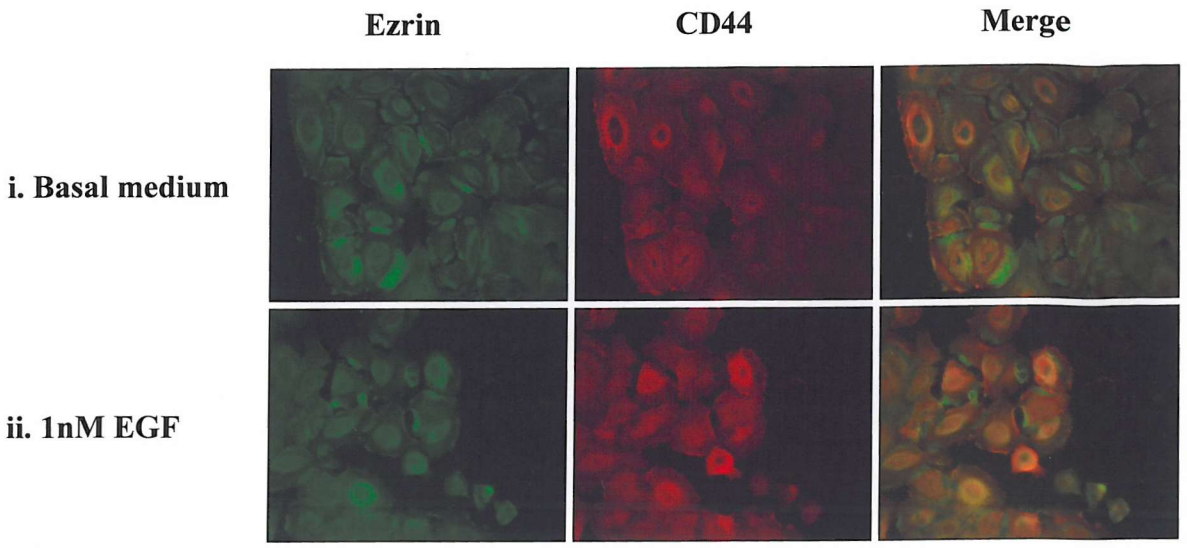

B. Moesin and CD44

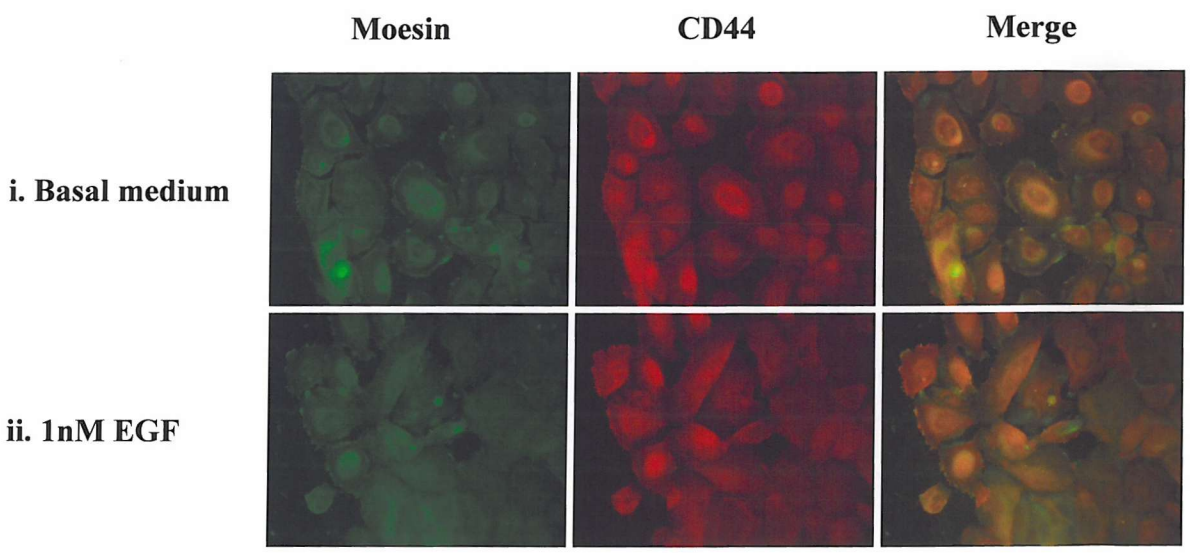

Figure 5.11C. Double immunocytochemistry staining for CD44 and ezrin or moesin in primary bronchial epithelial cells 3 hours post-wounding.
Primary bronchial epithelial cells were cultured in Basal medium (BEBM) for 24 hours to deplete growth factors before scrape wounding. Cells were then treated with basal medium alone (i) or containing 1nM EGF (ii) for 3 hours. Cells were fixed and double stained for CD44 and ezrin (A) or moesin (B) using the protocol described in Chapter 2, section 2.2.7. Cells were visualised using a Zeiss immunoflourescent microscope and images captured using a colour video camera.

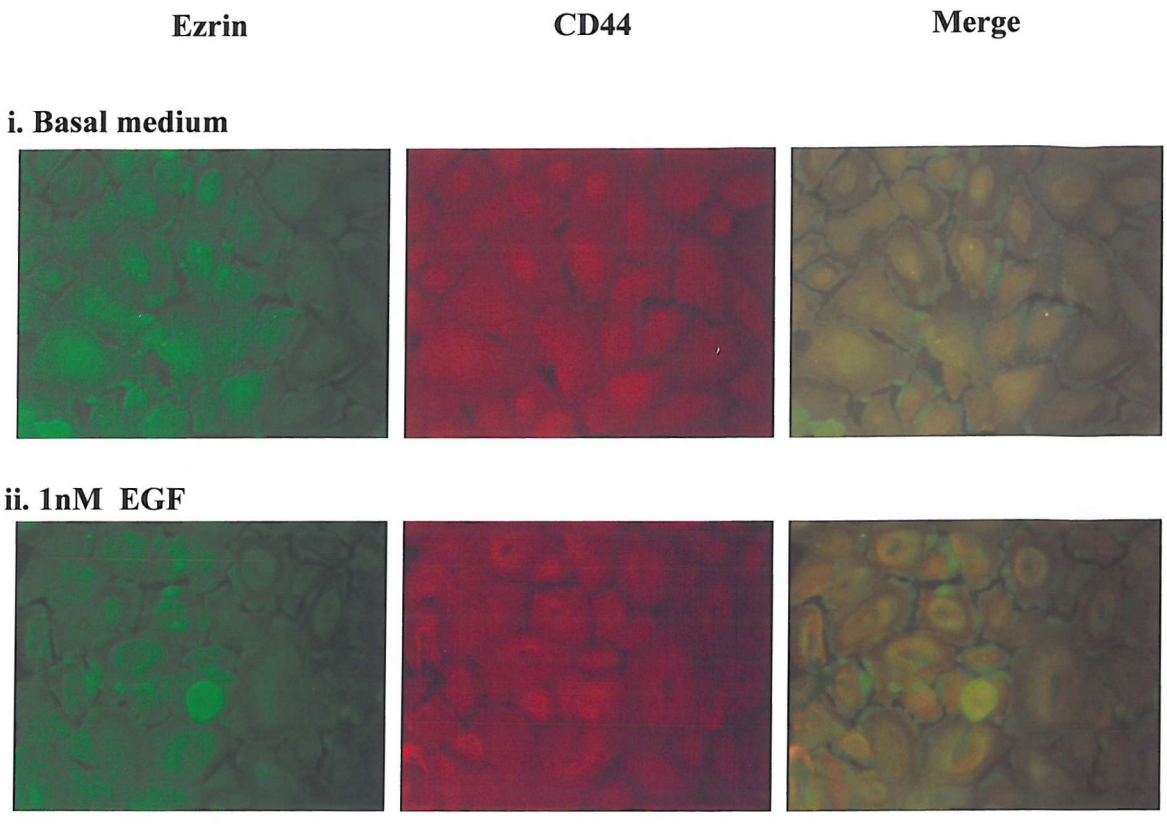

Figure 5.12. Double immunocytochemistry staining for CD44 and ezrin in confluent areas of scrape wounded primary bronchial epithelial cell cultures. Primary bronchial epithelial cells were cultured in Basal medium (BEBM) for 24 hours to deplete growth factors before scrape wounding. Cells were then treated with basal medium alone (i) or containing 1nM EGF (ii) for 15 minutes. Cells were fixed and double stained for CD44 and ezrin using the protocol described in Chapter 2, section 2.2.7. Cells were visualised using a Zeiss immunoflourescent microscope and images captured using a colour video camera. Confluent areas distant from the migrating wound edge are pictured here.

and EGF treated cultures. Although the differences between treatments are not as striking as previously shown (Chapter 4) and cultures exhibit staining of membrane structures when treated with basal medium, staining of membrane ruffles appears brighter and more prominent in those treated with 1nM EGF.

Figure 5.11B shows the distribution of ezrin and moesin in cultures 1 hour after wounding, here both ezrin and moesin are found in the cytoplasm of the cell and in small microspike extensions of the cell. Unlike the 15-minute time point, cells did not exhibit lamellipodia or ruffle structures of the plasma membrane. CD44 staining was also observed in these spikes and was co-localised with ezrin and moesin in spike structures and at the plasma membrane in both EGF and non-EGF treated cultures. Both ezrin and moesin staining in spikes was less prominent at the wound edge and occurred between cells, which were not in as close proximity to neighbouring cells with spaces between cells being larger and more prevalent.

3 hours after wounding (figure 5.11C) microspike structures had largely disappeared from repairing cultures and ezrin and moesin had a more cytoplasmic distribution, with some staining in membrane structures such as lamellipodia, ruffles and microspikes. These structures were less prominent at the wound edge and more commonly seen between cells away from the wound edge. Again no differences were seen between cells cultured in medium containing EGF compared to basal medium.

5.5 Effects of sodium cromoglycate on bronchial epithelial cells

As the mast cell stabiliser and anti-asthma drug, sodium cromoglycate has previously been reported to enhance dermal wound repair, its effect on 16HBE 14o- cell migration was also assessed. When added to serum free medium at a concentration of 100μM, sodium cromoglycate appeared to enhance repair at 3 and 9 hours ($P<0.03$ and $P<0.02$, respectively); wound area at 6 hours was smaller but not significantly different from serum free conditions ($P=0.27$). Sodium cromoglycate however was unable to stimulate repair in the presence of 1μM tyrphostin AG1478 at 9 hours, this inhibitory effect was not significant at the earlier time points (figure 5.13i).

Figure 5.13ii shows the effect of co-incubation of 100μM sodium cromoglycate with 1nM EGF. This combination is able to enhance repair at 3 and 6 hours when compared to serum free conditions ($P<0.02$ and $P<0.04$) but does not decrease wound area beyond that observed with EGF or sodium cromoglycate alone. At 9 hours cells treated with EGF and sodium cromoglycate together do not show enhanced repair when compared to serum free basal conditions or either stimuli alone.

As sodium cromoglycate stimulated repair was not enhanced by the addition of EGF but could be inhibited by the EGF receptor tyrosine kinase inhibitor, tyrphostin AG1478, it was hypothesised that sodium cromoglycate might be inducing bronchial epithelial repair through (direct or indirect) activation of the EGF receptor, and hence the same signalling pathway as EGF itself.

Analysis of tyrosine phosphorylated proteins in 16HBE 14o- cells by immunoprecipitation using an anti-phosphotyrosine agarose conjugate showed that treatment of cells for 10 minutes with sodium cromoglycate was able to induce enhanced tyrosine phosphorylation (figure 5.14A). Phosphorylated proteins included a band at around the molecular weight of the EGF receptor (170kDa) and EGFR phosphorylation was confirmed by staining Western blots of immunoprecipitates for EGFR (figure 5.14B). Treatment with 100μM sodium cromoglycate together with 1nM EGF showed increased phosphorylation above that seen when treated with each of the stimuli alone. This enhancement was not observed with the higher, 200μM concentration, of sodium cromoglycate when combined with 1nM EGF.

To observe whether other effects of EGF on bronchial epithelial cells described earlier in this thesis can be elicited by sodium cromoglycate, the distribution of ezrin, moesin and CD44 in primary bronchial epithelial cell cultures was observed by double fluorescent immunocytochemistry (figure 5.15). In cultures treated with basal medium cells had some staining of ezrin and moesin in membrane projections resembling microvilli and ruffles as observed previously. This staining of membrane structures did not appear to be enhanced in cells treated for 15 minutes with 100μM sodium cromoglycate. Ezrin and moesin were co-localised with CD44 at the periphery of the cell as described in Chapter 4.

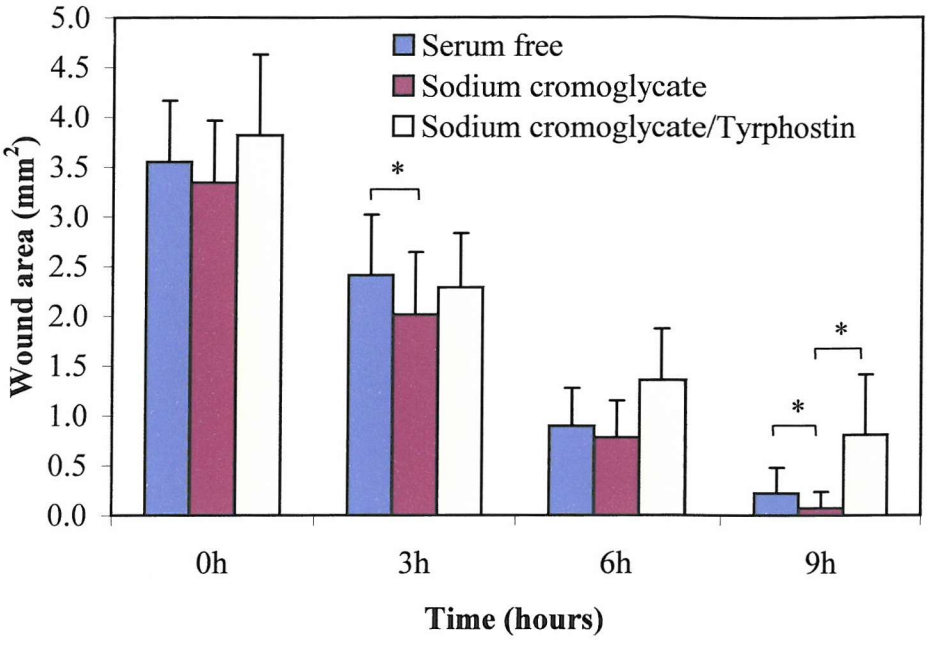

Figure 5.13i. Effect of 100μM sodium cromoglycate alone or in combination with 1μM tyrphostin AG1478 on repair of 16HBE 14o- cells. Data are mean +/- Standard deviation of 25 wounds from 3 individual experiments measured using Scion Image. *P<0.05 using a Student's unpaired *t* - test.

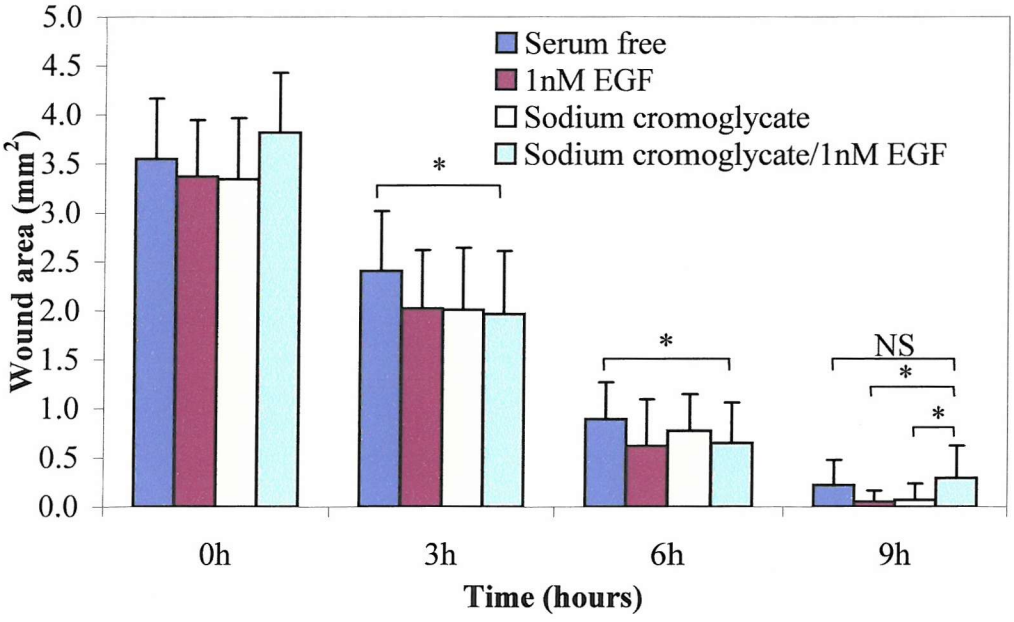

Figure 5.13ii. Comparison of the effect of 100μM sodium cromoglycate in the absence or presence of 1nM EGF on repair of 16HBE 14o- cells. Data are mean +/- Standard deviation of 25 wounds from 3 individual experiments measured using Scion Image. *P<0.05 using a Student's unpaired *t* - test.

A: Phosphotyrosine

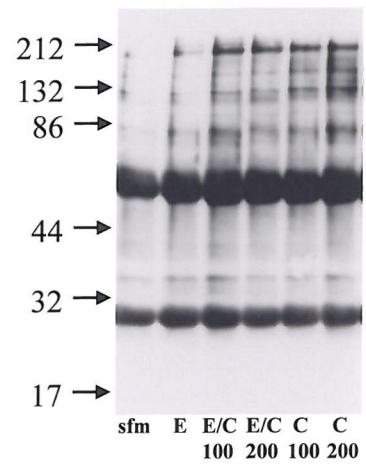

B: EGF receptor

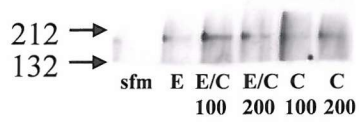

Figure 5.14. Analysis of tyrosine phosphorylated proteins in sodium cromoglycate treated 16HBE 14o- cells using immunoprecipitation.
16HBE 14o- cells were serum starved for 24 hours then treated for 10 minutes with serum free medium (sfm), 1nM EGF (E), 1nM EGF and 100μM sodium cromoglycate (E/C 100), 1nM EGF and 200μM sodium cromoglycate (E/C 200), 100μM sodium cromoglycate (C 100) or 200μM sodium cromoglycate (C 200). Following lysis of cells in denaturing lysis buffer and protein determination, 1mg of protein in Triton buffer was incubated with 60μl of anti-phosphotyrosine (PY20)-agarose conjugate overnight. Following centrifugation to precipitate immune complexes the supernatant was removed and the pellet washed before solubilising bound proteins in hot sample buffer. Samples were analysed by 10% SDS-PAGE and Western blotting for phosphotyrosine (A) and EGF receptor (B). Blots are representative of two individual experiments.

A. Ezrin and CD44

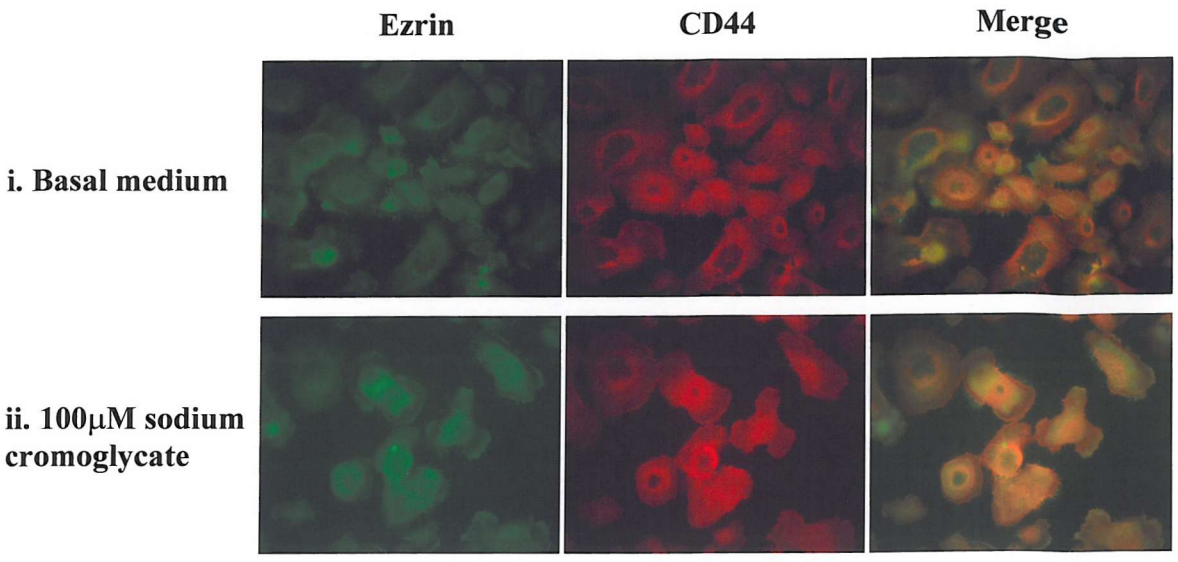

B. Moesin and CD44

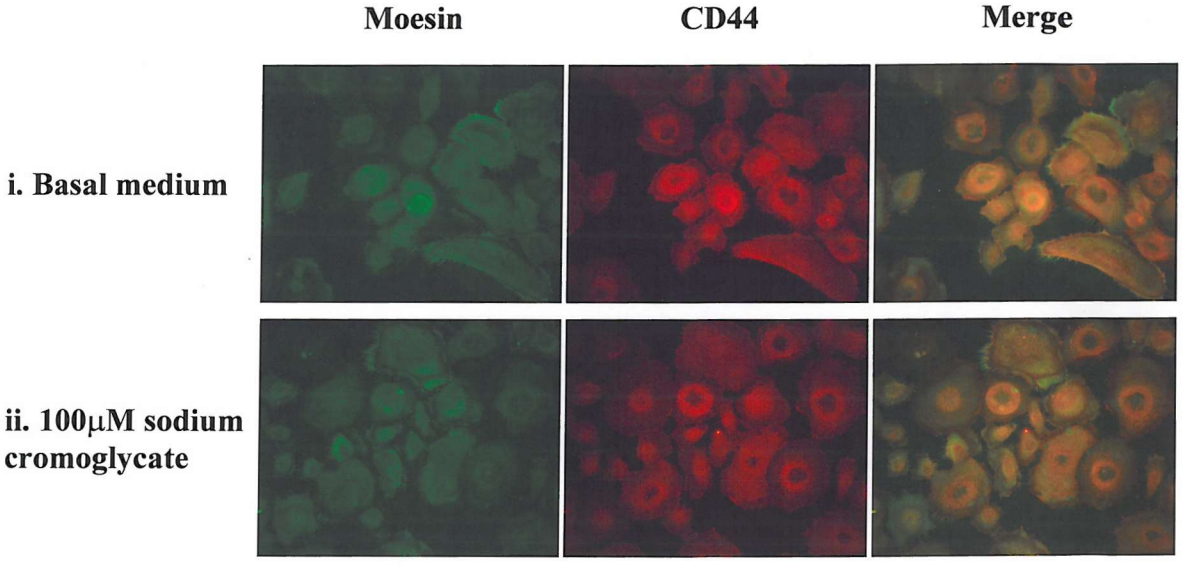

Figure 5.15. Double immunocytochemistry staining for CD44 and ezrin or moesin in primary bronchial epithelial cells treated with sodium cromoglycate. Primary bronchial epithelial cells were cultured in Basal medium (BEBM) for 24 hours to deplete growth factors. Cells were then treated with basal medium alone (i) or containing 100μM sodium cromoglycate (ii) for 15 minutes. Cells were fixed and double stained for CD44 and ezrin (A) or moesin (B) using the protocol described in Chapter 2, section 2.2.7. Cells were visualised using a Zeiss immunoflourescent microscope and images captured using a colour video camera.

5.6 Discussion

EGF receptor ligands such as EGF and HB-EGF have been shown to play a role in the regulation of cellular repair following wounding in numerous tissues including the gut, skin and lung. The mechanism of action whereby EGF can modulate repair is not fully elucidated but on a more cellular level EGF can influence the morphology of cells, the actin cytoskeleton and cellular migration through activation of a number of intracellular signalling molecules following EGFR tyrosine kinase activation.

Cellular migration following damage to bronchial epithelial monolayers has been examined here with the aim of determining the effect of growth factors on the rate of repair and the influence of these factors on ERM protein and CD44 distribution during repair which could be examined using immunocytochemistry.

Initial experiments using time lapse video microscopy enabled measurement of wound area over a time course and also allowed the morphology and arrangement of cells to be studied. In 16HBE 14o- cells, treatment of cells with 1nM EGF enhanced the repair seen with basal medium as shown by significantly reduced wound area at 4, 5 and 6 hours after damage. The appearance of the cells did not appear to change over the time course with the cells moving forward in a complete sheet (figure 5.1). The 16HBE 14o- cells were tightly packed at the start of wounding probably allowing the cells to spread a certain amount to cover the wound rapidly. The movement of cells in a sheet-like manner could be a mechanism to maintain epithelial integrity of the undamaged area and allowed by the presence of firm contacts between cells within the monolayer. In contrast, primary cell monolayers show gaps between cells and this would likely enable a greater movement of individual cells into the free area exposed following scrape wounding. This is shown in Figure 5.9 where individual cells move forward and the appearance of the wound front changes between images taken along the time course as cells move into the damaged area in a somewhat random fashion.

Another difference between primary and 16HBE 14o- cells is seen in terms of the rate of cell migration. 6 hours following damage 16HBE 14o- cells have almost repaired whereas the primary cell cultures show very little change in wound area at this time point and it takes 20 hours to migrate the equivalent distance of that moved by 16HBE

14o- cells after 6 hours of treatment. As 16HBE 14o- cell proliferation was not enhanced by EGF (Chapter 3) it seems unlikely that this observation is related to a greater ability of 16HBE 14o- cells to proliferate. Experiments which showed a stimulatory effect of keratinocyte growth factor (KGF) on migration of a variety of bronchial epithelial cell lines and primary cells also highlighted a difference in the rates of repair (156). Here, primary cells were compared with the bronchial epithelial cell lines 1HAEo- (another SV40 transformed airway epithelial cell line) and Calu-3 (derived from human lung adenocarcinoma). In control medium, 1HAEo- cells were able to migrate to cover 50% of the original wound size within approximately 10 hours whereas for primary cells this took over 20 hours and for Calu-3 cells the time taken was extended to 50 hours. These data suggest the differences in rates between the SV40 transformed cell lines 16HBE 14o- and 1HAEo- and primary cells are as a result of the immortalisation process. Along with disregulated proliferation as discussed in Chapter 3 this might also influence other cell processes such as protein expression and cytoskeleton turnover.

Repair of both primary and 16HBE 14o- cultures occurred under basal medium conditions (i.e. without the addition of growth factors). It has been shown previously that following damage there is release of growth factors known to enhance repair including HB-EGF (93), TGF-β (60) and KGF (1). Additionally Puddicombe *et al* (118) showed phosphorylation of the EGF receptor following scrape wounding in the absence of exogenous growth factor. Data from 16HBE 14o- cells presented in figure 5.3i supports the existence of either production of growth factor or endogenous receptor phosphorylation following wounding. The addition of an inhibitor of the EGF receptor tyrosine kinase, tyrphostin AG1478, to culture medium inhibits migration of cells at 6 and 9 hours after damage when cultured in basal medium. Here the inhibitor could be blocking tyrosine kinase activation occurring as a result of EGFR ligand or endogenous receptor activation.

To rapidly determine the effect of a range of factors on epithelial repair another method was utilised whereby cells in chamber slides were damaged using a comb to generate a uniform series of wounds which when the cells were fixed and stained could be measured using image analysis software. Data generated here for EGF was comparable to that seen with the time-lapse system giving confidence in the data.

EGF has been shown to stimulate repair of bronchial epithelial cells when compared to basal medium. This observation implies that EGF must therefore be modulating the actin cytoskeleton or cell adhesion mechanisms to enable the cell shape changes, de-adhesion and re-adhesion mechanisms required for repair. Therefore the distribution of ERM proteins along with CD44 and the differences between basal medium and EGF treated cells was examined using immunofluorescent staining of wounded cultures.

Results presented in Chapter 4 showed that in 16HBE 14o- bronchial epithelial cells the ERM proteins ezrin and moesin appeared to be regulated and influenced by EGF, as seen by increased association of ezrin and moesin with membrane and cytoskeletal fractions. The localisation of ezrin and moesin in 16HBE 14o- cells also appeared to be influenced by EGF and HB-EGF as these proteins redistributed to the plasma membrane and actin cytoskeletal structures however these observations could not be consistently repeated as described in Chapter 4. Using primary bronchial epithelial cells, ezrin and moesin redistribution to cell surface structures after EGF treatment was a consistent, repeatable effect. Several published observations have shed some light on this discrepancy. In normal fibroblasts, ezrin staining is very faint and cytoplasmic and staining is also observed in the nucleus. However in transformed, immortalised fibroblasts staining is much more intense and is also found at the plasma membrane as well as the cytoplasm, the intense staining prevents the nuclear staining from being observed (70). In primary rat fibroblasts ezrin is cytoplasmic, in fos oncogene transformed rat fibroblasts ezrin is found at the leading edge of cells and there is increased ezrin expression and phosphorylation compared to the primary cells. Here ezrin is hypothesised to be involved in cell morphology and motility (76).

Taken together these observations suggest that the 16HBE cells, which are transformed, immortalised cells, could have more ezrin and moesin than primary cells and any shift in protein distribution actually affects only a small proportion of the total protein and so is difficult to detect. Whereas, in primary cells, EGF stimulated redistribution of ezrin and moesin is always observed because less total protein is present. Additionally, an increase in ezrin phosphorylation at baseline could explain the fact that sometimes 16HBE 14o- cells already exhibited membrane staining for ezrin.

Despite the difficulties described above, the observations that in primary cells CD44 and ERM proteins are co-localised and that EGF is able to stimulate changes in ezrin and moesin localisation to cell surface structures, and in both primary and 16HBE cells stimulate an enrichment in the cytoskeletal fraction suggest that ezrin and moesin, in this system, are regulated by EGF to form a crosslinking structure with the plasma membrane and actin cytoskeleton.

Primary bronchial epithelial cultures were used to determine the distribution of ezrin and moesin in repairing cultures. Images presented in figure 5.11 firstly indicated there to be little difference between EGF treated cells and those cultured in growth factor-free basal medium with redistribution of ezrin and moesin present in all cultures. This effect is likely to be an effect of wounding as cells not wounded show comparable effects of EGF as already described (Figure 5.12) where cells cultured in basal medium show some staining in membrane structures which is enhanced by EGF.

The absence of a difference between treatments could be explained by the observations that following wounding growth factors are released into the surrounding medium or wound fluid following injury as described above. Additionally EGFR activation following scrape wounding of 16HBE 14o- cells irrespective of the presence of EGF has been previously described (118). These data suggest that following scrape wounding direct activation, or by endogenously released ligand, of the EGFR stimulates ezrin and moesin redistribution which is not enhanced by exogenous EGF. To test this hypothesis supplementing media with tyrphostin AG1478 would inhibit the EGF receptor tyrosine kinase and hence inhibit redistribution of ERM proteins to plasma membrane structures.

Despite no differences being observed between treatment, protein distribution changed with time possibly reflecting the involvement of ezrin and moesin in cellular events following damage. At the time points examined cells did not appear to have a polarised phenotype where there is a distinction between the leading edge and rear of the cell at least in terms of ezrin and moesin distribution. This implies the cells are not migrating consistent with time lapse data which only shows a reduction in wound size after 6-8 hours implying little migration occurs before this time point. As a consequence of damage and to protect the already compromised epithelial monolayer, ERM proteins

might serve a role in adhesion, in anchoring cell adhesion molecules to the actin cytoskeleton to stabilise cell-matrix and cell-cell adhesion and hence their distribution in microvilli-like membrane projections.

The anti-asthma drug, sodium cromoglycate, was examined here for its effect on cell migration as it has previously been reported to enhance dermal wound repair. Cell wounding data suggested it has a stimulatory effect on bronchial epithelial cell migration following damage and this effect appeared to be inhibited in the presence of tyrphostin AG1478. This observation could imply that sodium cromoglycate is acting through the EGF receptor to stimulate repair either that or the EGF receptor is the primary drive of cell migration and sodium cromoglycate stimulates through another mechanism which works in synergy with and requires EGF receptor activation. Phosphorylation data (figure 5.14) suggests that sodium cromoglycate works by, itself directly stimulating the EGFR or indirectly through release of EGFR ligand which then goes on to phosphorylate the EGFR. Phosphorylation of the EGFR by agents other than its cognate ligands has been previously reported and oxidants (e.g. hydrogen peroxide), ultraviolet (UV) radiation as well as other receptors including those for cytokines and other G-protein-coupled receptors have been shown to transactivate the EGFR (reviewed in (50), (169), (26)). In addition sodium cromoglycate could act independently of the EGFR to stimulate bronchial epithelial repair through production of inducible nitric oxide synthase (iNOS-2) as previously demonstrated *in vivo* (155) which is able to stimulate migration of renal tubular epithelial cells (107). These authors also demonstrated that EGF was able to enhance migration that could be inhibited by eliminating iNOS activity suggesting an additive effect. A synergistic effect of EGF and sodium cromoglycate was not observed here implying they act on the same signal transduction pathway/s.

6 CHAPTER SIX

FINAL DISCUSSION

In the airways of asthmatic subjects the stratified bronchial epithelium has an altered phenotype with shedding of the columnar cells reflecting areas of epithelial damage. In addition, this is also accompanied by permanent structural changes termed airway remodelling which include goblet cell hyperplasia, sub-epithelial fibrosis and increased smooth muscle. The altered phenotype of the airway epithelium in asthma implies an aberrant response to recurrent inflammation, as well as inefficient or disordered repair mechanisms following epithelial damage. Regeneration of a differentiated epithelium has been documented to involve an ordered sequence of cellular events including morphological changes, migration, proliferation and differentiation that is likely to require the co-ordinated control of a range of cell adhesion molecules, growth factors, cytoskeletal proteins, proteases and extracellular matrix components.

Growth factors and their cognate receptors have the ability to have pleiotropic effects on cells and tissues by the integration of signals from other growth factors, cell adhesion molecules and extracellular matrix components. Growth factors such as EGF (11), (118), HGF (165), TGFβ (60) and KGF (156) have all been shown to stimulate repair of the bronchial epithelium using both *in vivo* and *in vitro* techniques, however the mechanisms involved are yet to be fully elucidated. In this thesis, EGF has been shown to enhance repair of bronchial epithelial cell cultures following damage. Growth factor activity is regulated at many levels reflecting their central role in cell signalling. This complexity begins at the level of growth factor availability and presentation at receptors, with further regulation of their activity being modulated by the ability of growth factors to bind to the cell surface and extracellular matrix. Following synthesis, EGF and HB-EGF are present on the cell surface as pro-peptides where they can act on receptors in a juxtacrine manner or can be proteolytically cleaved by matrix metalloproteinases (MMPs) to act in an autocrine or paracrine way (35). In a cell-free *in vitro* assay MMP-3 was found to cleave HB-EGF at an extracellular site of the protein close to the transmembrane domain of the full length protein (137). More complex situations arise in whole-cell assay systems where a complex chain of events

may control ligand availability. In this case, activation of specific G-protein coupled receptors (GPCR) has been shown to stimulate metalloproteinases and release of soluble EGFR ligand from the cell surface. For example, in human lung cells, a bacterial wall polysaccharide (lipoteichoic acid) has been shown to activate the EGFR (82), which in turn is a potent inducer of mucin production by bronchial epithelial cells (139). This activation occurred via direct activation of the platelet-activating factor receptor (PAFR), a G-protein coupled receptor (GPCR), which in turn activates a disintegrin and metalloproteinase 10 (ADAM 10) to cleave and release soluble HB-EGF from the plasma membrane, this then goes on to activate the EGFR (82). In cardiomyocytes, phenylephrine, angiotensin II and endothelin-1 all enhance EGFR phosphorylation via activation of their respective GPCR's to cause ADAM 12 activation also leading to cleavage of HB-EGF (8). As scrape wounded bronchial epithelial cells also show increased tyrosine phosphorylation even in the absence of exogenous ligand this implies release of autocrine ligand (118) possibly involving metalloproteinase mediated shedding of surface bound ligand. In this thesis, sodium cromoglycate was shown to stimulate tyrosine phosphorylation of the EGFR through an unknown mechanism. It would be of interest to determine whether sodium cromoglycate also activates the EGFR by causing activation of a metalloproteinase via a GPCR. In an *in vivo* rat model, sodium cromoglycate has been shown to increase the expression of inducible nitric oxide synthase-2 (iNOS-2) (155). As reactive oxygen has also been shown to cause transactivation of the EGFR (reviewed in (117)), this may be the mechanism that leads to ADAM activation or it may act independently of the ADAM proteins, for example by inhibition of phosphotyrosine phosphatases.

Another method by which ligands can be regulated occurs by their binding to proteoglycans present on the cell surface, HB-EGF is able to bind CD44v3 (14) and TGFβ1 binds betaglycan (21). Cell surface bound ligand provides local reservoirs of ligand and also protects the ligand from degradation, which could enable potentiation of their effects. These surface bound ligands may stimulate adjacent receptors or be released into the surrounding extracellular matrix to act in a paracrine fashion. An increase in soluble growth factor after damage and the presence of ligand bound to the cell surface and extracellular matrix could provide a high local concentration of growth factor, thus enabling rapid recruitment to surface receptors when required. However, comparison of the effects of EGF and HB-EGF on bronchial epithelial cells presented

in this thesis has shown no preferential effect of HB-EGF over EGF on stimulating CD44 expression, changes in ERM protein redistribution or cell migration following scrape wounding. Similarly in a wound repair model, HB-EGF was no more potent than EGF (118). In contrast, studies of smooth muscle cell migration have shown that HB-EGF is significantly more potent than EGF even though both ligands have the same affinity for the EGF receptor and this is dependent upon the interaction of HB-EGF with heparan sulphate proteoglycans on the cell surface (53). This difference between cell types probably reflects differences in expression of heparan sulphate proteoglycans, which preferentially influences the localisation and presentation of HB-EGF to the EGFR on smooth muscle cells. Thus, the expression of accessory molecules can make a significant contribution to the biological potency of a growth factor, without the need for modulation of the level of growth factor expression.

By virtue of its complex signalling pathways, activation of the EGFR has the ability to have pleiotropic effects on bronchial epithelial cells, which could be important in cell migration. Following binding of ligand to its cognate receptor, dimerisation and cross-phosphorylation on tyrosine residues of the cytoplasmic domain of the two EGF receptor monomers occurs and this itself creates divergence of signalling depending on whether homo- or hetero-dimerisation of receptors occurs as different receptor sub-types can transduce the phosphorylation through different signalling pathways. This activation of the intracellular domain of receptors can then lead to transfer of phosphates to numerous signalling molecules by their binding phosphorylated tyrosines on the EGFR via SH2 domains on the signalling molecules. For example, activation of PLCγ by tyrosine phosphorylation, allows the breakdown of its substrate PIP2 into the second messengers DAG and IP3. DAG can then go and activate PKC. PKC has been shown to be essential for migration (86) and more specifically, EGF stimulated cell motility (28), as well as being responsible for threonine phosphorylation of ezrin and moesin (106), (114), (132). PI3-kinase is another signalling molecule which binds phosphorylated tyrosine residues of the activated EGFR and is involved in cell motility and is also required for PKC mediated ERM protein phosphorylation on threonine residues (106). Figure 6.1 highlights parts of the EGFR signalling cascade involved in EGF effects on cell migration.

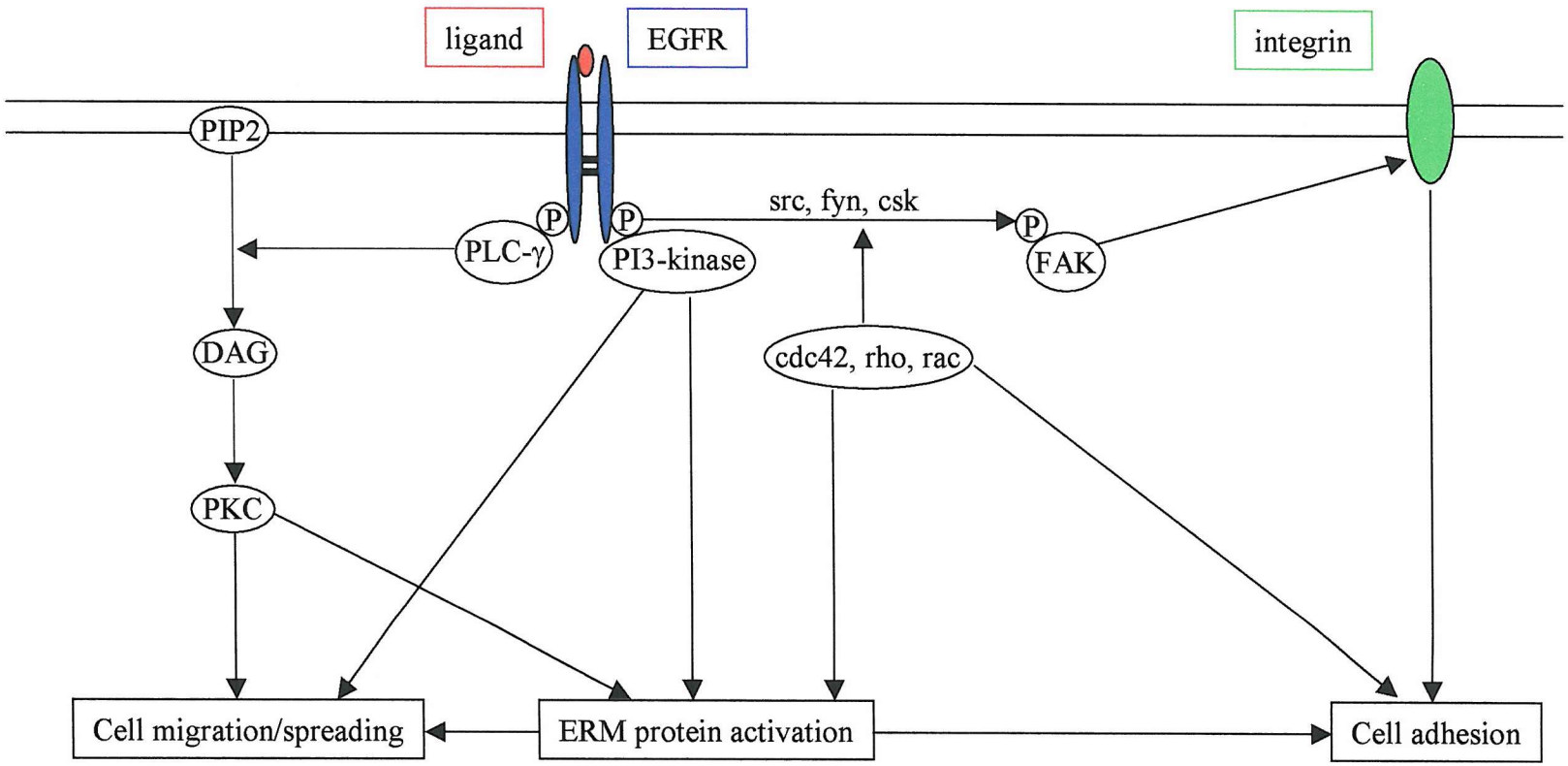

Figure 6.1. EGF receptor signalling pathway.
Indicating activation of EGFR and its intermediary signalling molecules involved in cell migration, spreading and adhesion. ERM protein activation refers to phosphorylation on serine/threonine residues.

In vivo models of epithelial repair have shown that the initial or early phase of repair involves the columnar cells surrounding the wound, which dedifferentiate, spread and migrate to cover the wound and reform a physical barrier without any specialised cell function (38). These cells then presumably proliferate and differentiate into ciliated and goblet columnar cells. In terms of the actin cytoskeleton, two models of wound healing have been proposed. Firstly, in embryonic wounds (95) and also in *in vitro* circular wounds (34), actin cables which form a ring around the circumference of the wound are proposed to contract to provide a 'purse string' like closer of the wound. Other studies have shown that repair occurs by co-ordinate migration of the epithelial sheet by extension of lamellipodia and filopodia cell processes (reviewed in (133)). This extension and migration of cells flanking the wound edge is an early event following wounding and requires the reorganisation of the actin cytoskeleton and cellular adhesions at the leading edge of the cell. Cell adhesion molecules at the periphery of cells, which are not adherent to a neighbouring cell, or exposure of the lateral edge of the cell to growth factors in the culture medium or wound fluid, could initiate this process.

Redistribution of ERM proteins along with recruitment of other actin-plasma membrane binding proteins to the periphery of the cells might allow for the co-ordinated organisation of an actin-scaffold at the leading edge (illustrated in figure 6.2). Flat structures of the plasma membrane at the leading edge of cells are often referred to as lamellipodia. Data presented in Chapter 4 of this thesis has shown that EGF stimulates an increased association with the actin cytoskeleton as well as redistribution of ezrin and moesin into lamellipodia-like membrane structures. These observations might represent the reorganisation of ezrin and moesin into the actin-rich structure at the leading edge of cells. This staining is seen, in particular, in cells not in direct contact with neighbouring cells implying a role for these proteins during colonisation and formation of a confluent monolayer. Furthermore, this staining pattern might be expected at the leading edge of cells at the wound edge suggesting a role for ERM proteins in cell migration. However, images from wounded cells stained for ezrin and moesin presented in this thesis did not provide any evidence for this and ERM protein staining was seen in microvilli-like structures rather than flat lamellipodia structures with no differences seen at the wound edge. Analysis of the kinetics of repair following mechanical damage to primary bronchial epithelial cells showed no

change in wound area until 6 hours after damage indicating little or no migration of the cells had occurred. Therefore lamellipodia formation might not have occurred in the time frame examined here, hence no ERM protein staining was observed in lamellipodia structures. Longer time course studies with cells at the migratory stage along with confocal microscopy of wounded cultures might suggest further roles for CD44 and ERM proteins in migratory processes during repair.

For migration to occur, as well as morphological changes at the leading alterations in adhesion must take place (see figure 6.2). De-adhesion at the rear of the cell has to occur to allow net cell movement along with formation of new adhesions at the leading edge of the cell. These processes require changes in cell-extracellular matrix adhesion. As indicated in figure 6.2, CD44 might be regulated during repair in the formation of new adhesion at the leading edge and de-adhesion at the rear of the cells as described in intestinal epithelial restitution where redistribution of integrins occurs to allow cell movement (88) and reviewed in (59). In untreated bronchial epithelial cells CD44 is distributed at sites associated with a plasma membrane distribution where it is co-localised with ERM proteins throughout and at the base of the cell as shown by confocal microscopy. This distribution suggests a role for the CD44-ERM protein complex in cell-substrate adhesion. This hypothesis could be further applied in wounded cultures, where CD44 and ERM proteins are found to be co-localised in microvilli-like structures of cells which do not appear to have a polarised, migrating phenotype but might represent enhanced points of adhesion following damage. Following treatment with EGF, ezrin and moesin redistribute to lamellipodia and microvilli-like projections and co-localisation with CD44 is lost. Here cells appear to adopt a more migratory phenotype as characterised by the formation of plasma membrane extensions. Thus it would appear that under normal conditions CD44 and ERM proteins are associated for stabilisation of cell adhesions with the actin cytoskeleton. Following treatment with EGF, ezrin and moesin have increased association with the actin cytoskeleton and are found in lamellipodia structures which are associated with cell migration, here ERM proteins might have another plasma membrane binding partner such as syndecan which has been found to be associated with ezrin in structures of the plasma membrane (46). This hypothesis is summarised in figure 6.3. In carcinoma cells, CD44 has been implicated in cell migratory processes but is not expressed in lamellipodia structures only at the plasma membrane of the

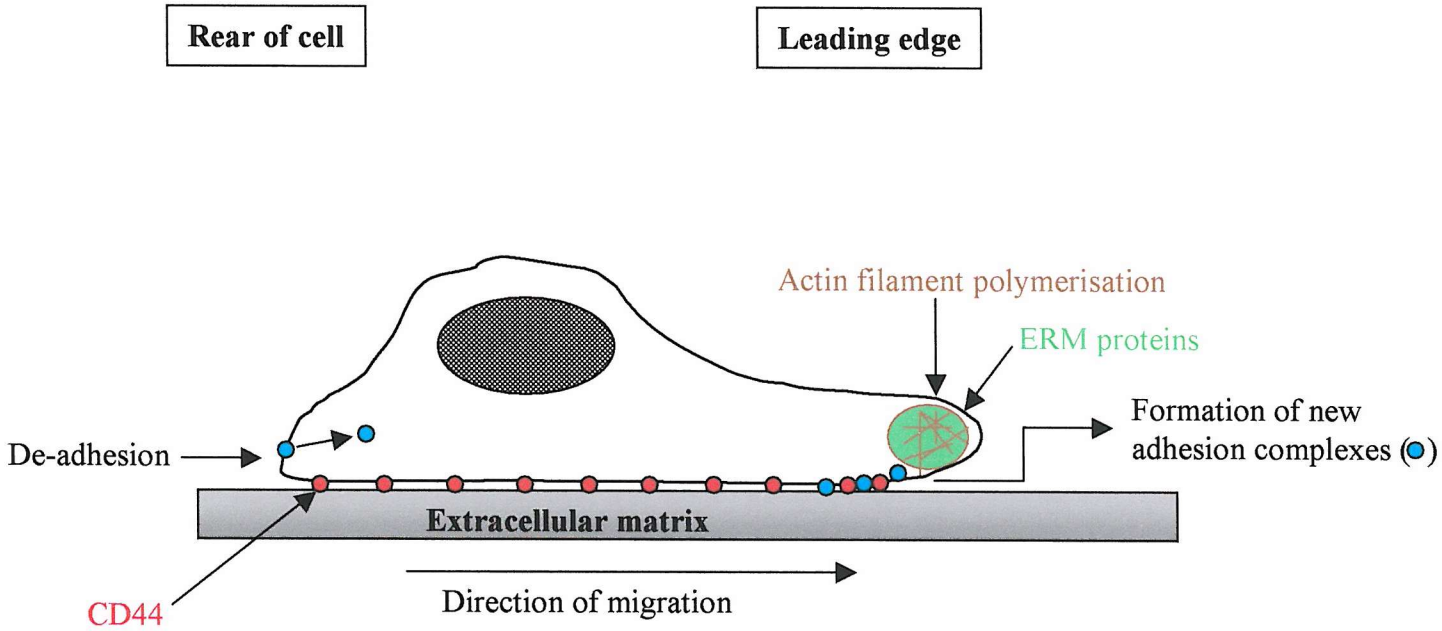

Figure 6.2. Cell migration and its associated processes and molecules.
Initiation of cell migration occurs by polarisation of the cell following actin filament polymerisation and formation of lamellipodia structures. Spreading is followed by formation of new cell-matrix adhesion complexes at the leading edge and de-adhesion at the rear of the cell which allows net movement of the cell. Extracellular matrix components (laminin, collagen, fibronectin, hyaluronic acid) act as ligands for integrins and other surface expressed cell adhesion molecules. This figure also highlights potential sites of CD44 and ERM protein localisation during migration of epithelial cells.

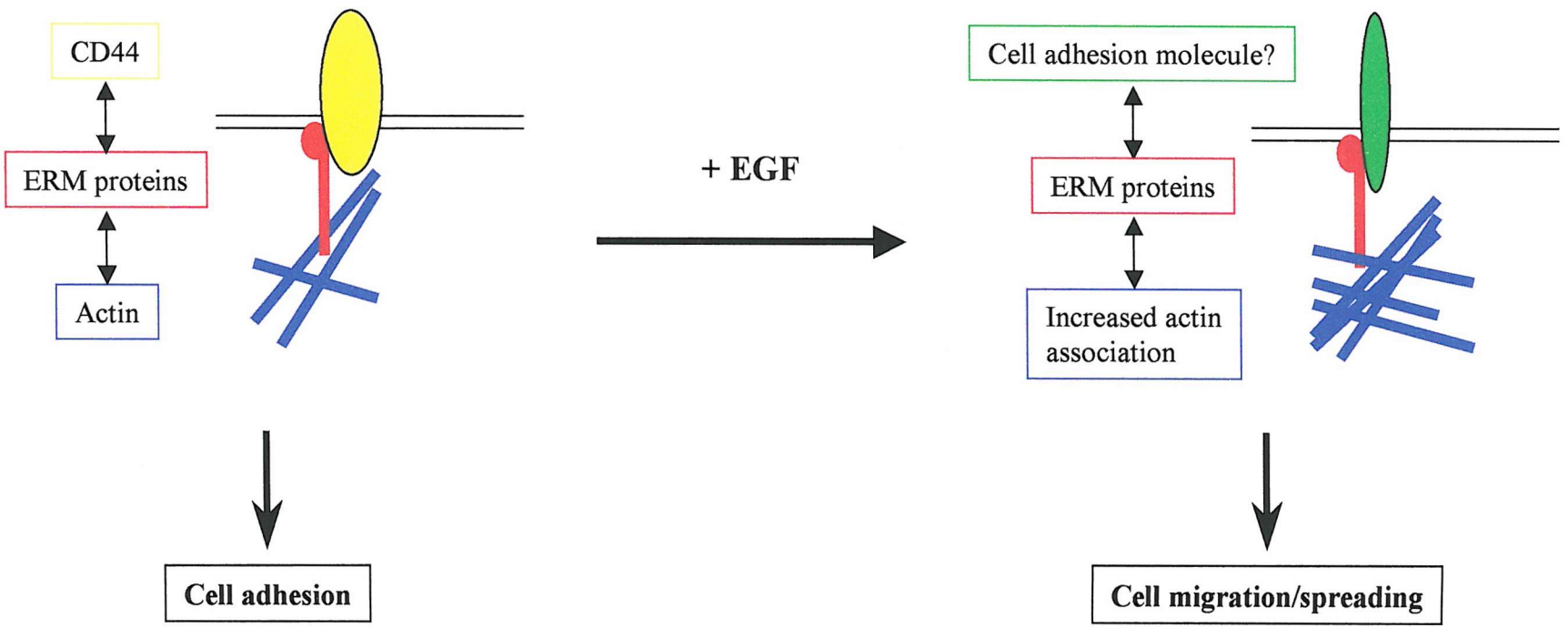

Figure 6.3. Proposed role of ERM proteins and CD44 in bronchial epithelial cells and regulation by EGF.
In untreated cells (left side of figure) CD44 and ERM proteins are colocalised and there is some association of ERM proteins with the actin cytoskeleton, here a function in cell adhesion is proposed. Following treatment with EGF (right side of figure), ERM proteins redistribute to actin containing lamellipodia structures with enhanced binding to the actin cytoskeleton and loss of colocalisation with CD44. EGF stimulates migration and development of lamellipodia reflect a migratory phenotype suggesting a function for ERM proteins in cell spreading and migration.

leading and trailing edges of migrating cells, here a role for CD44 in transient cell adhesions prior to stable adhesions was suggested (74). Additionally, cleavage of CD44 by membrane-type 1 matrix metalloproteinase (MT1-MMP) at the trailing edge has been shown to be necessary for migration to occur, further evidence that CD44 is directly regulated and involved in cell-matrix adhesion during repair (69).

In terms of EGF effects on adhesion, focal adhesion kinase (FAK) is a cytoskeleton associated protein found in newly formed adhesion complexes and assumed to participate in their formation through its association with numerous structural and cytoskeletal proteins. FAK is phosphorylated on tyrosine residues, by EGF (140), through its SH2 binding domains for fyn, csk and src and can then transduce this signal to other cytoskeletal-associated substrates, such as paxillin as well as bind structural proteins such as integrins. These data implicate FAK as a major player in cell adhesion and migratory processes during repair. Adding further complexity, cdc42, rac and rho are members of the ras family of GTP-binding proteins which play a major role in formation of lamellipodia, focal adhesions and cytoskeletal structures by acting as intermediary signalling molecules. EGF induces phosphorylation of FAK and paxillin which is dependent upon rho as well as PI3-kinase but independent of PKC (140). With regard to ERM proteins their activation and functions are regulated by rho (56) (110) and PKC (106), (114), (132) but no role has been shown yet for FAK. These numerous divergent signalling pathways (figure 6.1) serve to illustrate how EGF might be involved in the regulation of cell repair, which requires modification of cell adhesion and migratory processes.

Following migration of cells to cover the denuded area, proliferation of cells followed by differentiation to reform a polarised function epithelium and in the case of the lung epithelium, differentiation into specialised cells such as ciliated and goblet cells must occur. In the differentiated epithelium, ezrin is often found concentrated at the apical membrane of and in microvilli structures. In polarised bronchial epithelial cell cultures ezrin is localised to the apical membrane domain (101), (136) and EBP50 (ERM-binding phosphoprotein-50) a binding partner for ezrin is found concentrated at the apical cell surface but not in cilia of sections of bronchial biopsies (130). The apical distribution of ezrin in normal undamaged tissue and polarised cell cultures has lead to suggestions of a function in anchoring the apically expressed CFTR (cystic fibrosis

transmembrane conductance regulator) to the cytoskeleton (130) or ERM proteins may also play a role in cilia formation or their stabilisation with the plasma membrane. In human nasal epithelial cell cultures, examination of cells undergoing IL-13 stimulated differentiation from a ciliated to a predominantly secretory phenotype implied a role for ezrin in cilia formation. This loss of cilia was accompanied by a reduction in ezrin expression at the apical compartment with no expression by cells expressing MUC5AC (a mucin secreted by airway secretory cells) suggesting ezrin may be important in the maintaining the structure of cilia (77). Greater elucidation of the roles of ezrin, moesin and CD44 in repair of bronchial epithelial cultures would be enabled by the use of primary cells grown on an air-liquid interface to generate a differentiated as well as polarised cell layer with cilia structures and mucus producing cells as utilised by Laoukili *et al* (77). Additionally a study to examine the expression of ERM proteins in airway tissue in both healthy and asthmatic subjects would provide useful information regarding their function in the normal epithelium and damaged or repairing areas.

A greater understanding of the regulation and mechanism of lung repair might reveal new pharmacological targets. Sodium cromoglycate was one of the first asthma therapeutics with a known mode of action as mast cell stabiliser and its other anti-asthmatic mechanisms unexplained. Data presented in this thesis suggests sodium cromoglycate might also function to improve lung function by stimulating restitution of the airways providing a novel mechanism of action. Current therapeutic interventions for the treatment of asthma fall into two main groups firstly, those which target smooth muscle to promote relaxation of the bronchial lumen (β2 adrenoreceptor agonists such as salbutamol) and secondly anti-inflammatory drugs (corticosteroids, leukotriene antagonists). Neither of these therapies prevents the recurrent tissue injury including epithelial damage, the chronic and irreversible remodelling of the airways nor promotes regeneration of an intact and functional bronchial epithelium.

REFERENCES

1. Adamson,I.Y. and Bakowska,J., Relationship of keratinocyte growth factor and hepatocyte growth factor levels in rat lung lavage fluid to epithelial cell regeneration after bleomycin. *Am.J.Pathol.* **155**, 949-954, 1999.

2. Alberts,B., Bray,A., Lewis,J., Raff,M., Roberts,K., and Watson,J.D., "Molecular Biology of the Cell," 1994.

3. Algrain,M., Turunen,O., Vaheri,A., Louvard,D., and Arpin,M., Ezrin contains cytoskeleton and membrane binding domains accounting for its proposed role as a membrane-cytoskeletal linker. *J.Cell Biol.* **120**, 129-139, 1993.

4. Alonso-Lebrero,J.L., Serrador,J.M., Dominguez-Jimenez,C., Barreiro,O., Luque,A., del Pozo,M.A., Snapp,K., Kansas,G., Schwartz-Albiez,R., Furthmayr,H., Lozano,F., and Sanchez-Madrid,F., Polarization and interaction of adhesion molecules P-selectin glycoprotein ligand 1 and intercellular adhesion molecule 3 with moesin and ezrin in myeloid cells. *Blood* **95**, 2413-2419, 2000.

5. Amishima,M., Munakata,M., Nasuhara,Y., Sato,A., Takahashi,T., Homma,Y., and Kawakami,Y., Expression of epidermal growth factor and epidermal growth factor receptor immunoreactivity in the asthmatic human airway. *Am.J.Respir.Crit Care Med.* **157**, 1907-1912, 1998.

6. Arpin,M., Algrain,M., and Louvard,D., Membrane-actin microfilament connections: an increasing diversity of players related to band 4.1. *Curr.Opin.Cell Biol.* **6**, 136-141, 1994.

7. Aruffo,A., Stamenkovic,I., Melnick,M., Underhill,C.B., and Seed,B., CD44 is the principal cell surface receptor for hyaluronate. *Cell* **61**, 1303-1313, 1990.

8. Asakura,M., Kitakaze,M., Takashima,S., Liao,Y., Ishikura,F., Yoshinaka,T., Ohmoto,H., Node,K., Yoshino,K., Ishiguro,H., Asanuma,H., Sanada,S., Matsumura,Y., Takeda,H., Beppu,S., Tada,M., Hori,M., and Higashiyama,S., Cardiac hypertrophy is inhibited by antagonism of ADAM12 processing of HB-EGF: metalloproteinase inhibitors as a new therapy. *Nature Medicine* **8**, 35-40, 2002.

9. Aviezer,D. and Yayon,A., Heparin-dependent binding and autophosphorylation of epidermal growth factor (EGF) receptor by heparin-binding EGF-like growth factor but not by EGF. *Proc.Natl.Acad.Sci.U.S.A* **91**, 12173-12177, 1994.

10. Banks-Schlegel,S.P., Gazdar,A.F., and Harris,C.C., Intermediate filament and cross-linked envelope expression in human lung tumor cell lines. *Cancer Res.* **45**, 1187-1197, 1985.

11. Barrow,R.E., Wang,C.Z., Evans,M.J., and Herndon,D.N., Growth factors accelerate epithelial repair in sheep trachea. *Lung* **171**, 335-344, 1993.

12. Beasley,R., Roche,W.R., Roberts,J.A., and Holgate,S.T., Cellular events in the bronchi in mild asthma and after bronchial provocation. *Am.Rev.Respir.Dis.* **139**, 806-817, 1989.

13. Beckmann,J.D., Stewart,A., Kai,M., and Keeton,T.P., Controls of EGF-induced morphological transformation of human bronchial epithelial cells. *Journal of Cellular Physiology* **189**, 171-178, 2001.

14. Bennett,K.L., Jackson,D.G., Simon,J.C., Tanczos,E., Peach,R., Modrell,B., Stamenkovic,I., Plowman,G., and Aruffo,A., CD44 isoforms containing exon V3 are responsible for the presentation of heparin-binding growth factor. *J.Cell Biol.* **128**, 687-698, 1995.

15. Bennett,K.L., Modrell,B., Greenfield,B., Bartolazzi,A., Stamenkovic,I., Peach,R., Jackson,D.G., Spring,F., and Aruffo,A., Regulation of CD44 binding to hyaluronan by glycosylation of variably spliced exons. *J.Cell Biol.* **131**, 1623-1633, 1995.

16. Berryman,M., Gary,R., and Bretscher,A., Ezrin oligomers are major cytoskeletal components of placental microvilli: a proposal for their involvement in cortical morphogenesis. *J.Cell Biol.* **131**, 1231-1242, 1995.

17. Boland,S., Boisvieux-Ulrich,E., Houcine,O., Baeza-Squiban,A., Pouchelet,M., Schoevaert,D., and Marano,F., TGF beta 1 promotes actin cytoskeleton reorganization and migratory phenotype in epithelial tracheal cells in primary culture. *J.Cell Sci.* **109 (Pt 9)**, 2207-2219, 1996.

18. Booth,C., Evans,G.S., and Potten,C.S., Growth factor regulation of proliferation in primary cultures of small intestinal epithelium. *In Vitro Cell Dev.Biol.Anim* **31**, 234-243, 1995.

19. Borland,G., Ross,J.A., and Guy,K., Forms and functions of CD44. *Immunology* **93**, 139-148, 1998.

20. Bousquet,J., Jeffery,P.K., Busse,W.W., Johnson,M., and Vignola,A.M., Asthma. From bronchoconstriction to airways inflammation and remodeling. *Am.J.Respir.Crit Care Med.* **161**, 1720-1745, 2000.

21. Boyd,F.T., Cheifetz,S., Andres,J., Laiho,M., and Massague,J., Transforming growth factor-beta receptors and binding proteoglycans. *J.Cell Sci.Suppl* **13**, 131-138, 1990.

22. Bretscher,A., Purification of an 80,000-dalton protein that is a component of the isolated microvillus cytoskeleton, and its localization in nonmuscle cells. *J.Cell Biol.* **97**, 425-432, 1983.

23. Bretscher,A., Rapid phosphorylation and reorganization of ezrin and spectrin accompany morphological changes induced in A-431 cells by epidermal growth factor. *J.Cell Biol.* **108**, 921-930, 1989.

24. Brown,K.J., Hendry,I.A., and Parish,C.R., Acidic and basic fibroblast growth factor bind with differing affinity to the same heparan sulfate proteoglycan on BALB/c 3T3 cells: implications for potentiation of growth factor action by heparin. *J.Cell Biochem.* **58**, 6-14, 1995.

25. Brown,T.A., Bouchard,T., St.John,T., Wayner,E., and Carter,W.G., Human keratinocytes express a new CD44 core protein (CD44E) as a heparan-sulfate intrinsic membrane proteoglycan with additional exons. *J.Cell Biol.* **113**, 207-221, 1991.

26. Carpenter,G., Employment of the epidermal growth factor receptor in growth factor- independent signaling pathways. *J.Cell Biol.* **146**, 697-702, 1999.

27. Carter,W.G. and Wayner,E.A., Characterization of the class III collagen receptor, a phosphorylated, transmembrane glycoprotein expressed in nucleated human cells. *Journal of Biological Chemistry* **263**, 4193-2011, 1988.

28. Chen,P., Xie,H., Sekar,M.C., Gupta,K., and Wells,A., Epidermal growth factor receptor-mediated cell motility: phospholipase C activity is required, but mitogen-activated protein kinase activity is not sufficient for induced cell movement. *J.Cell Biol.* **127**, 847-857, 1994.

29. Chen,Z., Fadiel,A., Feng,Y., Ohtani,K., Rutherford,T., and Naftolin,F., Ovarian epithelial carcinoma tyrosine phosphorylation, cell proliferation, and ezrin translocation are stimulated by interleukin 1alpha and epidermal growth factor. *Cancer* **92**, 3068-3075, 2001.

30. Cooper,D.L., Dougherty,G., Harn,H.J., Jackson,S., Baptist,E.W., Byers,J., Datta,A., Phillips,G., and Isola,N.R., The complex CD44 transcriptional unit; alternative splicing of three internal exons generates the epithelial form of CD44. *Biochem.Biophys.Res.Commun.* **182**, 569-578, 1992.

31. Correia,I., Wang,L., Pang,X., and Theoharides,T.C., Characterization of the 78 kDa mast cell protein phosphorylated by the antiallergic drug cromolyn and homology to moesin. *Biochem.Pharmacol.* **52**, 413-424, 1996.

32. Cozens,A.L., Yezzi,M.J., Kunzelmann,K., Ohrui,T., Chin,L., Eng,K., Finkbeiner,W.E., Widdicombe,J.H., and Gruenert,D.C., CFTR expression and chloride secretion in polarized immortal human bronchial epithelial cells. *Am.J.Respir.Cell Mol.Biol.* **10**, 38-47, 1994.

33. Crepaldi,T., Gautreau,A., Comoglio,P.M., Louvard,D., and Arpin,M., Ezrin is an effector of hepatocyte growth factor-mediated migration and morphogenesis in epithelial cells. *J.Cell Biol.* **138**, 423-434, 1997.

34. Danjo,Y. and Gipson,I.K., Actin 'purse string' filaments are anchored by E-cadherin-mediated adherens junctions at the leading edge of the epithelial wound, providing coordinated cell movement. *J.Cell Sci.* **111 (Pt 22)**, 3323-3332, 1998.

35. Dong,J., Opresko,L.K., Dempsey,P.J., Lauffenburger,D.A., Coffey,R.J., and Wiley,H.S., Metalloprotease-mediated ligand release regulates autocrine signaling through the epidermal growth factor receptor. *Proc.Natl.Acad.Sci.U.S.A* **96**, 6235-6240, 1999.

36. Edwards,A.M. and Howell,J.B., The chromones: history, chemistry and clinical development. A tribute to the work of Dr R. E. C. Altounyan. *Clin.Exp.Allergy* **30**, 756-774, 2000.

37. Ellis,P.D., Hadfield,K.M., Pascall,J.C., and Brown,K.D., Heparin-binding epidermal-growth-factor-like growth factor gene expression is induced by scrape-wounding epithelial cell monolayers: involvement of mitogen-activated protein kinase cascades. *Biochem.J.* **354**, 99-106, 2001.

38. Erjefalt,J.S., Korsgren,M., Nilsson,M.C., Sundler,F., and Persson,C.G., Prompt epithelial damage and restitution processes in allergen challenged guinea-pig trachea in vivo. *Clin.Exp.Allergy* **27**, 1458-1470, 1997.

39. Faull,R.J., Stanley,J.M., Fraser,S., Power,D.A., and Leavesley,D.I., HB-EGF is produced in the peritoneal cavity and enhances mesothelial cell adhesion and migration. *Kidney International* **59**, 614-624, 2001.

40. Fitzgerald,K. and O'Neill,L.A., Induction of the adhesion molecule CD44 by the pro-inflammatory cytokine interleukin-1 in endothelial cells. *Biochem.Soc.Trans.* **25**, 185S, 1997.

41. Fox,S.B., Fawcett,J., Jackson,D.G., Collins,I., Gatter,K.C., Harris,A.L., Gearing,A., and Simmons,D.L., Normal human tissues, in addition to some tumors, express multiple different CD44 isoforms. *Cancer Res.* **54**, 4539-4546, 1994.

42. Gary,R. and Bretscher,A., Ezrin self-association involves binding of an N-terminal domain to a normally masked C-terminal domain that includes the F-actin binding site. *Mol.Biol.Cell* **6**, 1061-1075, 1995.

43. Gautreau,A., Poullet,P., Louvard,D., and Arpin,M., Ezrin, a plasma membrane-microfilament linker, signals cell survival through the phosphatidylinositol 3-kinase/Akt pathway. *Proc.Natl.Acad.Sci.U.S.A* **96**, 7300-7305, 1999.

44. Giard,D.J., Aaronson,S.A., Todaro,G.J., Arnstein,P., Kersey,J.H., Dosik,H., and Parks,W.P., In vitro cultivation of human tumors: establishment of cell lines derived from a series of solid tumors. *Journal of the National Cancer Institute* **51**, 1417-1423, 1973.

45. Gould,K.L., Cooper,J.A., Bretscher,A., and Hunter,T., The protein-tyrosine kinase substrate, p81, is homologous to a chicken microvillar core protein. *J.Cell Biol.* **102**, 660-669, 1986.

46. Granes,F., Urena,J.M., Rocamora,N., and Vilaro,S., Ezrin links syndecan-2 to the cytoskeleton. *J.Cell Sci.* **113 (Pt 7)**, 1267-1276, 2000.

47. Green,K.J. and Gaudry,C.A., Are desmosomes more than tethers for intermediate filaments? *Nat.Rev.Mol.Cell Biol.* **1**, 208-216, 2000.

48. Gruenert,D., Differentiated properties of human epithelial cells transformed *in vitro*. *BioTechniques* **5**, 740-749, 1987.

49. Gruenert,D.C., Finkbeiner,W.E., and Widdicombe,J.H., Culture and transformation of human airway epithelial cells. *Am.J.Physiol* **268**, L347-L360, 1995.

50. Hackel,P.O., Zwick,E., Prenzel,N., and Ullrich,A., Epidermal growth factor receptors: critical mediators of multiple receptor pathways. *Curr.Opin.Cell Biol.* **11**, 184-189, 1999.

51. Heider,K.H., Hofmann,M., Hors,E., van den,B.F., Ponta,H., Herrlich,P., and Pals,S.T., A human homologue of the rat metastasis-associated variant of CD44 is expressed in colorectal carcinomas and adenomatous polyps. *J.Cell Biol.* **120**, 227-233, 1993.

52. Heiska,L., Alfthan,K., Gronholm,M., Vilja,P., Vaheri,A., and Carpen,O., Association of ezrin with intercellular adhesion molecule-1 and -2 (ICAM-1 and ICAM-2). Regulation by phosphatidylinositol 4, 5-bisphosphate. *Journal of Biological Chemistry* **273**, 21893-21900, 1998.

53. Higashiyama,S., Abraham,J.A., and Klagsbrun,M., Heparin-binding EGF-like growth factor stimulation of smooth muscle cell migration: dependence on interactions with cell surface heparan sulfate. *J.Cell Biol.* **122**, 933-940, 1993.

54. Higashiyama,S., Abraham,J.A., Miller,J., Fiddes,J.C., and Klagsbrun,M., A heparin-binding growth factor secreted by macrophage-like cells that is related to EGF. *Science* **251**, 936-939, 1991.

55. Higashiyama,S., Lau,K., Besner,G.E., Abraham,J.A., and Klagsbrun,M., Structure of heparin-binding EGF-like growth factor. Multiple forms, primary structure, and glycosylation of the mature protein. *J.Biol.Chem.* **267**, 6205-6212, 1992.

56. Hirao,M., Sato,N., Kondo,T., Yonemura,S., Monden,M., Sasaki,T., Takai,Y., and Tsukita,S., Regulation mechanism of ERM (ezrin/radixin/moesin) protein/plasma membrane association: possible involvement of phosphatidylinositol turnover and Rho-dependent signaling pathway. *J.Cell Biol.* **135**, 37-51, 1996.

57. Hiscox,S. and Jiang,W.G., Regulation of endothelial CD44 expression and endothelium-tumour cell interactions by hepatocyte growth factor/scatter factor. *Biochem.Biophys.Res.Commun.* **233**, 1-5, 1997.

58. Hishiya,A., Ohnishi,M., Tamura,S., and Nakamura,F., Protein Phosphatase 2C Inactivates F-actin Binding of Human Platelet Moesin. *J.Biol.Chem.* **274**, 26705-26712, 1999.

59. Horwitz,A.R. and Parsons,J.T., Cell migration--movin' on. *Science* **286**, 1102-1103, 1999.

60. Howat,W.J., Holgate,S.T., and Lackie,P.M., TGF-beta isoform release and activation during in vitro bronchial epithelial wound repair. *American Journal of Physiology - Lung Cellular & Molecular Physiology* **282**, L115-L123, 2002.

61. Hudson,L.G. and McCawley,L.J., Contributions of the epidermal growth factor receptor to keratinocyte motility. *Microsc.Res.Tech.* **43**, 444-455, 1998.

62. Ichikawa,T., Masumoto,J., Kaneko,M., Saida,T., Sagara,J., and Taniguchi,S., Moesin and CD44 expression in cutaneous melanocytic tumours. *Br.J.Dermatol.* **138**, 763-768, 1998.

63. Jackson,D.G., Bell,J.I., Dickinson,R., Timans,J., Shields,J., and Whittle,N., Proteoglycan forms of the lymphocyte homing receptor CD44 are alternatively spliced variants containing the v3 exon. *J.Cell Biol.* **128**, 673-685, 1995.

64. Jalkanen,S., Bargatze,R.F., de los,T.J., and Butcher,E.C., Lymphocyte recognition of high endothelium: antibodies to distinct epitopes of an 85-95-kD glycoprotein antigen differentially inhibit lymphocyte binding to lymph node, mucosal, or synovial endothelial cells. *J.Cell Biol.* **105**, 983-990, 1987.

65. Jalkanen,S. and Jalkanen,M., Lymphocyte CD44 binds the COOH-terminal heparin-binding domain of fibronectin. *J.Cell Biol.* **116**, 817-825, 1992.

66. Jeffery,P.K., Wardlaw,A.J., Nelson,F.C., Collins,J.V., and Kay,A.B., Bronchial biopsies in asthma. An ultrastructural, quantitative study and correlation with hyperreactivity. *Am.Rev.Respir.Dis.* **140**, 1745-1753, 1989.

67. Jeon,S., Kim,S., Park,J.B., Suh,P.G., Kim,Y.S., Bae,C.D., and Park,J., RhoA and Rho-kinase dependent phosphorylation of moesin at Thr-558 in hippocampal neuronal cells by glutamate. *J.Biol.Chem.* 2002.

68. Jiang,W.G., Hiscox,S., Singhrao,S.K., Puntis,M.C., Nakamura,T., Mansel,R.E., and Hallett,M.B., Induction of tyrosine phosphorylation and translocation of ezrin by hepatocyte growth factor/scatter factor. *Biochem.Biophys.Res.Commun.* **217**, 1062-1069, 1995.

69. Kajita,M., Itoh,Y., Chiba,T., Mori,H., Okada,A., Kinoh,H., and Seiki,M., Membrane-type 1 matrix metalloproteinase cleaves CD44 and promotes cell migration. *J.Cell Biol.* **153**, 893-904, 2001.

70. Kaul,S.C., Kawai,R., Nomura,H., Mitsui,Y., Reddel,R.R., and Wadhwa,R., Identification of a 55-kDa ezrin-related protein that induces cytoskeletal changes and localizes to the nucleolus. *Exp.Cell Res.* **250**, 51-61, 1999.

71. Kim,J.S., McKinnis,V.S., Nawrocki,A., and White,S.R., Stimulation of migration and wound repair of guinea-pig airway epithelial cells in response to epidermal growth factor. *Am.J.Respir.Cell Mol.Biol.* **18**, 66-74, 1998.

72. Krieg,J. and Hunter,T., Identification of the two major epidermal growth factor-induced tyrosine phosphorylation sites in the microvillar core protein ezrin. *J.Biol.Chem.* **267**, 19258-19265, 1992.

73. Lackie,P.M., Baker,J.E., Gunthert,U., and Holgate,S.T., Expression of CD44 isoforms is increased in the airway epithelium of asthmatic subjects. *Am.J.Respir.Cell Mol.Biol.* **16**, 14-22, 1997.

74. Ladeda,V., Aguirre Ghiso,J.A., and Bal de Kier,J.E., Function and expression of CD44 during spreading, migration, and invasion of murine carcinoma cells. *Exp.Cell Res.* **242**, 515-527, 1998.

75. Laitinen,L.A., Heino,M., Laitinen,A., Kava,T., and Haahtela,T., Damage of the airway epithelium and bronchial reactivity in patients with asthma. *Am.Rev.Respir.Dis.* **131**, 599-606, 1985.

76. Lamb,R.F., Ozanne,B.W., Roy,C., McGarry,L., Stipp,C., Mangeat,P., and Jay,D.G., Essential functions of ezrin in maintenance of cell shape and lamellipodial extension in normal and transformed fibroblasts. *Curr.Biol.* **7**, 682-688, 1997.

77. Laoukili,J., Perret,E., Willems,T., Minty,A., Parthoens,E., Houcine,O., Coste,A., Jorissen,M., Marano,F., Caput,D., and Tournier,F., IL-13 alters mucociliary differentiation and ciliary beating of human respiratory epithelial cells. *Journal of Clinical Investigation* **108**, 1817-1824, 2001.

78. Lee,T.Y. and Gotlieb,A.I., Early stages of endothelial wound repair: conversion of quiescent to migrating endothelial cells involves tyrosine phosphorylation and actin microfilament reorganization. *Cell & Tissue Research* **297**, 435-450, 1999.

79. Legg,J.W. and Isacke,C.M., Identification and functional analysis of the ezrin-binding site in the hyaluronan receptor, CD44. *Curr.Biol.* **8**, 705-708, 1998.

80. Leir,S.H., Baker,J.E., Holgate,S.T., and Lackie,P.M., Increased CD44 expression in human bronchial epithelial repair after damage or plating at low cell densities. *American Journal of Physiology - Lung Cellular & Molecular Physiology* **278**, L1129-L1137, 2000.

81. Leir,S.H., Holgate,S.T., and Lackie,P.M., Cell density and CD44 isoform expression on human bronchial epithelial cells. *Mol.Biol.Cell* **8**, 2399, 1997.

82. Lemjabbar,H. and Basbaum,C., Platelet-activating factor receptor and ADAM10 mediate responses to Staphylococcus aureus in epithelial cells. *Nature Medicine* **8**, 41-46, 2002.

83. Lesley,J., Hyman,R., and Kincade,P.W., CD44 and its interaction with extracellular matrix. *Adv.Immunol.* **54**, 271-335, 1993.

84. Lesur,O., Arsalane,K., and Lane,D., Lung alveolar epithelial cell migration in vitro: modulators and regulation processes. *Am.J.Physiol* **270**, L311-L319, 1996.

85. Levitzki,A. and Gazit,A., Tyrosine kinase inhibition: an approach to drug development. *Science* **267**, 1782-1788, 1995.

86. Li,W., Nadelman,C., Gratch,N.S., Li,W., Chen,M., Kasahara,N., and Woodley,D.T., An important role for protein kinase C-delta in human keratinocyte migration on dermal collagen. *Experimental Cell Research* **273**, 219-228, 2002.

87. Lokeshwar,V.B., Fregien,N., and Bourguignon,L.Y., Ankyrin-binding domain of CD44(GP85) is required for the expression of hyaluronic acid-mediated adhesion function. *J.Cell Biol.* **126**, 1099-1109, 1994.

88. Lotz,M.M., Rabinovitz,I., and Mercurio,A.M., Intestinal restitution: progression of actin cytoskeleton rearrangements and integrin function in a model of epithelial wound healing. *Am.J.Pathol.* **156**, 985-996, 2000.

89. Mackay,C.R., Maddox,J.F., Wijffels,G.L., Mackay,I.R., and Walker,I.D., Characterization of a 95,000 molecule on sheep leucocytes homologous to murine Pgp-1 and human CD44. *Immunology* **65**, 93-99, 1988.

90. Mackay,C.R., Terpe,H.J., Stauder,R., Marston,W.L., Stark,H., and Gunthert,U., Expression and modulation of CD44 variant isoforms in humans. *J.Cell Biol.* **124**, 71-82, 1994.

91. MacLeod,C.L., Luk,A., Castagnola,J., Cronin,M., and Mendelsohn,J., EGF induces cell cycle arrest of A431 human epidermoid carcinoma cells. *Journal of Cellular Physiology* **127**, 175-182, 1986.

92. Maiti,A., Maki,G., and Johnson,P., TNF-alpha induction of CD44-mediated leukocyte adhesion by sulfation. *Science* **282**, 941-943, 1998.

93. Marikovsky,M., Breuing,K., Liu,P.Y., Eriksson,E., Higashiyama,S., Farber,P., Abraham,J., and Klagsbrun,M., Appearance of heparin-binding EGF-like growth factor in wound fluid as a response to injury. *Proc.Natl.Acad.Sci.U.S.A* **90**, 3889-3893, 1993.

94. Martin,M., Andreoli,C., Sahuquet,A., Montcourrier,P., Algrain,M., and Mangeat,P., Ezrin NH2-terminal domain inhibits the cell extension activity of the COOH-terminal domain. *J.Cell Biol.* **128**, 1081-1093, 1995.

95. Martin,P. and Lewis,J., Actin cables and epidermal movement in embryonic wound healing. *Nature* **360**, 179-183, 1992.

96. Matsui,T., Maeda,M., Doi,Y., Yonemura,S., Amano,M., Kaibuchi,K., and Tsukita,S., Rho-kinase phosphorylates COOH-terminal threonines of ezrin/radixin/moesin (ERM) proteins and regulates their head-to-tail association. *J.Cell Biol.* **140**, 647-657, 1998.

97. Matsui,T., Yonemura,S., and Tsukita,S., Activation of ERM proteins in vivo by Rho involves phosphatidyl- inositol 4-phosphate 5-kinase and not ROCK kinases. *Curr.Biol.* **9**, 1259-1262, 1999.

98. Mazzarella,G., Grella,E., Romano,L., Perna,A., Marzo,C., Guarino,C., Cammarata,A., Bianco,A., and Liccardo,G., Protective effects of nedocromil sodium on cellular and biohumoral components present in the bronchial alveolar lavage fluid and in peripheral blood in atopic asthmatics. *Respiration* **61**, 207-213, 1994.

99. McCarthy,D.W., Downing,M.T., Brigstock,D.R., Luquette,M.H., Brown,K.D., Abad,M.S., and Besner,G.E., Production of heparin-binding epidermal growth factor-like growth factor (HB-EGF) at sites of thermal injury in pediatric patients. *J.Invest Dermatol.* **106**, 49-56, 1996.

100. Mitic,L.L., Van Itallie,C.M., and Anderson,J.M., Molecular physiology and pathophysiology of tight junctions I. Tight junction structure and function: lessons from mutant animals and proteins. *Am.J.Physiol Gastrointest.Liver Physiol* **279**, G250-G254, 2000.

101. Mohler,P.J., Kreda,S.M., Boucher,R.C., Sudol,M., Stutts,M.J., and Milgram,S.L., Yes-associated protein 65 localizes p62(c-Yes) to the apical compartment of airway epithelia by association with EBP50. *J.Cell Biol.* **147**, 879-890, 1999.

102. Montefort,S., Baker,J., Roche,W.R., and Holgate,S.T., The distribution of adhesive mechanisms in the normal bronchial epithelium. *Eur.Respir.J.* **6**, 1257-1263, 1993.

103. Montefort,S., Roberts,J.A., Beasley,R., Holgate,S.T., and Roche,W.R., The site of disruption of the bronchial epithelium in asthmatic and non- asthmatic subjects. *Thorax* **47**, 499-503, 1992.

104. Nagafuchi,A., Molecular architecture of adherens junctions. *Curr.Opin.Cell Biol.* **13** , 600-603, 2001.

105. Nakamura,H. and Ozawa,H., Immunolocalization of CD44 and the ezrin-radixin-moesin (ERM) family in the stratum intermedium and papillary layer of the mouse enamel organ. *J.Histochem.Cytochem.* **45**, 1481-1492, 1997.

106. Ng,T., Parsons,M., Hughes,W.E., Monypenny,J., Zicha,D., Gautreau,A., Arpin,M., Gschmeissner,S., Verveer,P.J., Bastiaens,P.I., and Parker,P.J., Ezrin is a downstream effector of trafficking PKC-integrin complexes involved in the control of cell motility. *EMBO Journal* **20**, 2723-2741, 2001.

107. Noiri,E., Peresleni,T., Srivastava,N., Weber,P., Bahou,W.F., Peunova,N., and Goligorsky,M.S., Nitric oxide is necessary for a switch from stationary to locomoting phenotype in epithelial cells. *Am.J.Physiol* **270**, C794-C802, 1996.

108. Oliver,M.H., Harrison,N.K., Bishop,J.E., Cole,P.J., and Laurent,G.J., A rapid and convenient assay for counting cells cultured in microwell plates: application for assessment of growth factors. *J.Cell Sci.* **92 (Pt 3)**, 513-518, 1989.

109. Ordonez,C.L., Khashayar,R., Wong,H.H., Ferrando,R., Wu,R., Hyde,D.M., Hotchkiss,J.A., Zhang,Y., Novikov,A., Dolganov,G., and Fahy,J.V., Mild and Moderate Asthma Is Associated with Airway Goblet Cell Hyperplasia and Abnormalities in Mucin Gene Expression. *Am.J.Respir.Crit Care Med.* **163**, 517-523, 2001.

110. Oshiro,N., Fukata,Y., and Kaibuchi,K., Phosphorylation of moesin by rho-associated kinase (Rho-kinase) plays a crucial role in the formation of microvilli-like structures. *J.Biol.Chem.* **273**, 34663-34666, 1998.

111. Paglini,G., Kunda,P., Quiroga,S., Kosik,K., and Caceres,A., Suppression of radixin and moesin alters growth cone morphology, motility, and process formation in primary cultured neurons. *Journal of Cell Biology* **143**, 443-455, 1998.

112. Peppelenbosch,M.P., Tertoolen,L.G., Hage,W.J., and de Laat,S.W., Epidermal growth factor-induced actin remodeling is regulated by 5- lipoxygenase and cyclooxygenase products. *Cell* **74**, 565-575, 1993.

113. Picker,L.J., Nakache,M., and Butcher,E.C., Monoclonal antibodies to human lymphocyte homing receptors define a novel class of adhesion molecules on diverse cell types. *J.Cell Biol.* **109**, 927-937, 1989.

114. Pietromonaco,S.F., Simons,P.C., Altman,A., and Elias,L., Protein kinase C-theta phosphorylation of moesin in the actin-binding sequence. *J.Biol.Chem.* **273**, 7594-7603, 1998.

115. Polosa,R., Krishna,M.T., Howarth,P.H., Lackie,P.M., Holgate,S.T., and Davies,D.E., Elevated epidermal growth factor receptor expression in bronchial epithelium of mild and severe asthmatics. *Eur.Respir.J.* **12**, 56s, 1998.

116. Polosa,R., Prosperini,G., Leir,S.H., Holgate,S.T., Lackie,P.M., and Davies,D.E., Expression of c-erbB receptors and ligands in human bronchial mucosa. *Am.J.Respir.Cell Mol.Biol.* **20**, 914-923, 1999.

117. Prenzel,N., Fischer,O.M., Streit,S., Hart,S., and Ullrich,A., The epidermal growth factor receptor family as a central element for cellular signal transduction and diversification. *Endocrine-Related Cancer* **8**, 11-31, 2001.

118. Puddicombe,S.M., Polosa,R., Richter,A., Krishna,M.T., Howarth,P.H., Holgate,S.T., and Davies,D.E., Involvement of the epidermal growth factor receptor in epithelial repair in asthma. *FASEB J.* **14**, 1362-1374, 2000.

119. Reczek,D., Berryman,M., and Bretscher,A., Identification of EBP50: A PDZ-containing phosphoprotein that associates with members of the ezrin-radixin-moesin family. *J.Cell Biol.* **139**, 169-179, 1997.

120. Redington,A.E., Madden,J., Frew,A.J., Djukanovic,R., Roche,W.R., Holgate,S.T., and Howarth,P.H., Transforming growth factor-beta 1 in asthma. Measurement in bronchoalveolar lavage fluid. *Am.J.Respir.Crit Care Med.* **156**, 642-647, 1997.

121. Ridley,A.J. and Hall,A., The small GTP-binding protein rho regulates the assembly of focal adhesions and actin stress fibers in response to growth factors. *Cell* **70** , 389-399, 1992.

122. Ridley,A.J., Paterson,H.F., Johnston,C.L., Diekmann,D., and Hall,A., The small GTP-binding protein rac regulates growth factor-induced membrane ruffling. *Cell* **70**, 401-410, 1992.

123. Roche,W.R., Montefort,S., Baker,J., and Holgate,S.T., Cell adhesion molecules and the bronchial epithelium. *Am.Rev.Respir.Dis.* **148**, S79-S82, 1993.

124. Romaris,M., Bassols,A., and David,G., Effect of transforming growth factor-beta 1 and basic fibroblast growth factor on the expression of cell surface proteoglycans in human lung fibroblasts. Enhanced glycanation and fibronectin-binding of CD44 proteoglycan, and down-regulation of glypican. *Biochem.J.* **310 (Pt 1)**, 73-81, 1995.

125. Schmitz,B., Park,I.A., Kaufmann,R., Thiele,J., and Fischer,R., Influence of cytokine stimulation (granulocyte macrophage-colony stimulating factor, interleukin-3 and transforming growth factor-beta- 1) on adhesion molecule expression in normal human bone marrow fibroblasts. *Acta Haematol.* **94**, 173-181, 1995.

126. Screaton,G.R., Bell,M.V., Jackson,D.G., Cornelis,F.B., Gerth,U., and Bell,J.I., Genomic structure of DNA encoding the lymphocyte homing receptor CD44 reveals at least 12 alternatively spliced exons. *Proc.Natl.Acad.Sci.U.S.A* **89**, 12160-12164, 1992.

127. Serrador,J.M., Alonso-Lebrero,J.L., del Pozo,M.A., Furthmayr,H., Schwartz-Albiez,R., Calvo,J., Lozano,F., and Sanchez-Madrid,F., Moesin interacts with the cytoplasmic region of intercellular adhesion molecule-3 and is redistributed to the uropod of T lymphocytes during cell polarization. *J.Cell Biol.* **138**, 1409-1423, 1997.

128. Shapiro,G.G. and Konig,P., Cromolyn sodium: a review. *Pharmacotherapy* **5**, 156-170, 1985.

129. Shaw,R.J., Henry,M., Solomon,F., and Jacks,T., RhoA-dependent phosphorylation and relocalization of ERM proteins into apical membrane/actin protrusions in fibroblasts. *Mol.Biol.Cell* **9**, 403-419, 1998.

130. Short,D.B., Trotter,K.W., Reczek,D., Kreda,S.M., Bretscher,A., Boucher,R.C., Stutts,M.J., and Milgram,S.L., An apical PDZ protein anchors the cystic fibrosis transmembrane conductance regulator to the cytoskeleton. *J.Biol.Chem.* **273**, 19797-19801, 1998.

131. Siegfried,J.M., Detection of human lung epithelial cell growth factors produced by a lung carcinoma cell line: use in culture of primary solid lung tumors. *Cancer Res.* **47**, 2903-2910, 1987.

132. Simons,P.C., Pietromonaco,S.F., Reczek,D., Bretscher,A., and Elias,L., C-terminal threonine phosphorylation activates ERM proteins to link the cell's cortical lipid bilayer to the cytoskeleton. *Biochem.Biophys.Res.Commun.* **253**, 561-565, 1998.

133. Small,J.V., Stradal,T., Vignal,E., and Rottner,K., The lamellipodium: where motility begins. *Trends Cell Biol.* **12**, 112-120, 2002.

134. Stamenkovic,I., Amiot,M., Pesando,J.M., and Seed,B., A lymphocyte molecule implicated in lymph node homing is a member of the cartilage link protein family. *Cell* **56**, 1057-1062, 1989.

135. Stevenson,B.R. and Keon,B.H., The tight junction: morphology to molecules. *Annu.Rev.Cell Dev.Biol.* **14**, 89-109, 1998.

136. Sun,F., Hug,M.J., Lewarchik,C.M., Yun,C.H., Bradbury,N.A., and Frizzell,R.A., E3KARP mediates the association of ezrin and protein kinase A with the cystic fibrosis transmembrane conductance regulator in airway cells. *Journal of Biological Chemistry* **275**, 29539-29546, 2000.

137. Suzuki,M., Raab,G., Moses,M.A., Fernandez,C.A., and Klagsbrun,M., Matrix metalloproteinase-3 releases active heparin-binding EGF-like growth factor by cleavage at a specific juxtamembrane site. *J.Biol.Chem.* **272**, 31730-31737, 1997.

138. Takeuchi,K., Sato,N., Kasahara,H., Funayama,N., Nagafuchi,A., Yonemura,S., Tsukita,S., and Tsukita,S., Perturbation of cell adhesion and microvilli formation by antisense oligonucleotides to ERM family members. *J.Cell Biol.* **125**, 1371-1384, 1994.

139. Takeyama,K., Dabbagh,K., Lee,H.M., Agusti,C., Lausier,J.A., Ueki,I.F., Grattan,K.M., and Nadel,J.A., Epidermal growth factor system regulates mucin production in airways. *Proc.Natl.Acad.Sci.U.S.A* **96**, 3081-3086, 1999.

140. Tapia,J.A., Camello,C., Jensen,R.T., and Garcia,L.J., EGF stimulates tyrosine phosphorylation of focal adhesion kinase (p125FAK) and paxillin in rat pancreatic acini by a phospholipase C- independent process that depends on phosphatidylinositol 3-kinase, the small GTP-binding protein, p21rho, and the integrity of the actin cytoskeleton. *Biochim.Biophys.Acta* **1448**, 486-499, 1999.

141. Tarnawski,A.S. and Jones,M.K., The role of epidermal growth factor (EGF) and its receptor in mucosal protection, adaptation to injury, and ulcer healing: involvement of EGF-R signal transduction pathways. *Journal of Clinical Gastroenterology* **27 Suppl 1**, S12-S20, 1998.

142. Tarone,G., Ferrancini,R., Galetto,G., and omoglio,P., A cell surface integral membrane glycoprotein of 85,000 mol wt (gp85) associated with the Triton X-100-insoluble cell skeleton. *Journal of Cell Biology* **99**, 512-519, 1984.

143. Theoharides,T.C., Sieghart,W., Greengard,P., and Douglas,W.W., Antiallergic drug cromolyn may inhibit histamine secretion by regulating phosphorylation of a mast cell protein. *Science* **207**, 80-82, 1980.

144. Theoharides,T.C., Wang,L., Pang,X., Letourneau,R., Culm,K.E., Basu,S., Wang,Y., and Correia,I., Cloning and cellular localization of the rat mast cell 78-kDa protein phosphorylated in response to the mast cell "stabilizer" cromolyn. *J.Pharmacol.Exp.Ther.* **294**, 810-821, 2000.

145. Thompson,A.B., Robbins,R.A., Romberger,D.J., Sisson,J.H., Spurzem,J.R., Teschler,H., and Rennard,S.I., Immunological functions of the pulmonary epithelium. *Eur.Respir.J.* **8**, 127-149, 1995.

146. Thompson,S.A., Higashiyama,S., Wood,K., Pollitt,N.S., Damm,D., McEnroe,G., Garrick,B., Ashton,N., Lau,K., and Hancock,N., Characterization of sequences within heparin-binding EGF-like growth factor that mediate interaction with heparin. *J.Biol.Chem.* **269**, 2541-2549, 1994.

147. Tsao,M.S., Zhu,H., and Viallet,J., Autocrine growth loop of the epidermal growth factor receptor in normal and immortalized human bronchial epithelial cells. *Exp.Cell Res.* **223**, 268-273, 1996.

148. Tsukita,S., Oishi,K., Sato,N., Sagara,J., and Kawai,A., ERM family members as molecular linkers between the cell surface glycoprotein CD44 and actin-based cytoskeletons. *J.Cell Biol.* **126**, 391-401, 1994.

149. Turunen,O., Wahlstrom,T., and Vaheri,A., Ezrin has a COOH-terminal actin-binding site that is conserved in the ezrin protein family. *J.Cell Biol.* **126**, 1445-1453, 1994.

150. van,d., V, Taher,T.E., Wielenga,V.J., Spaargaren,M., Prevo,R., Smit,L., David,G., Hartmann,G., Gherardi,E., and Pals,S.T., Heparan sulfate-modified CD44 promotes hepatocyte growth factor/scatter factor-induced signal transduction through the receptor tyrosine kinase c-Met. *J.Biol.Chem.* **274**, 6499-6506, 1999.

151. Velden,V.H. and Versnel,H.F., Bronchial epithelium: morphology, function and pathophysiology in asthma. *Eur.Cytokine Netw.* **9**, 585-597, 1998.

152. Vignola,A.M., Chanez,P., Campbell,A.M., Bousquet,J., Michel,F.B., and Godard,P., Functional and phenotypic characteristics of bronchial epithelial cells obtained by brushing from asthmatic and normal subjects. *Allergy* **48**, 32-38, 1993.

153. Vignola,A.M., Chanez,P., Chiappara,G., Merendino,A., Pace,E., Rizzo,A., la Rocca,A.M., Bellia,V., Bonsignore,G., and Bousquet,J., Transforming growth factor-beta expression in mucosal biopsies in asthma and chronic bronchitis. *Am.J.Respir.Crit Care Med.* **156**, 591-599, 1997.

154. Vignola,A.M., Gagliardo,R., Guerrera,D., Chiappara,G., Chanez,P., Bousquet,J., and Bonsignore,G., New evidence of inflammation in asthma. *Thorax* **55 Suppl 2**, S59-S60, 2000.

155. Vural,K.M., Liao,H., Oz,M.C., and Pinsky,D.J., Effects of mast cell membrane stabilizing agents in a rat lung ischemia- reperfusion model. *Ann.Thorac.Surg.* **69**, 228-232, 2000.

156. Waters,C.M. and Savla,U., Keratinocyte growth factor accelerates wound closure in airway epithelium during cyclic mechanical strain. *J.Cell Physiol* **181**, 424-432, 1999.

157. Wayner,E.A. and Carter,W.G., Identification of multiple cell adhesion receptors for collagen and fibronectin in human fibrosarcoma cells possessing unique alpha and common beta subunits. *J.Cell Biol.* **105**, 1873-1884, 1987.

158. Wells,A., EGF receptor. *Int.J.Biochem.Cell Biol.* **31**, 637-643, 1999.

159. Wells,A., Gupta,K., Chang,P., Swindle,S., Glading,A., and Shiraha,H., Epidermal growth factor receptor-mediated motility in fibroblasts. *Microsc.Res.Tech.* **43**, 395-411, 1998.

160. Wells,E. and Mann,J., Phosphorylation of a mast cell protein in response to treatment with anti-allergic compounds. Implications for the mode of action of sodium cromoglycate. *Biochem.Pharmacol.* **32**, 837-842, 1983.

161. Werner,S., Keratinocyte growth factor: a unique player in epithelial repair processes. *Cytokine Growth Factor Rev.* **9**, 153-165, 1998.

162. Wilson,J.W., What causes airway remodelling in asthma? *Clin.Exp.Allergy* **28**, 534-536, 1998.

163. Yonemura,S., Hirao,M., Doi,Y., Takahashi,N., Kondo,T., and Tsukita,S., Ezrin/radixin/moesin (ERM) proteins bind to a positively charged amino acid cluster in the juxta-membrane cytoplasmic domain of CD44, CD43, and ICAM-2. *J.Cell Biol.* **140**, 885-895, 1998.

164. Zahm,J.M., Chevillard,M., and Puchelle,E., Wound repair of human surface respiratory epithelium. *Am.J.Respir.Cell Mol.Biol.* **5**, 242-248, 1991.

165. Zahm,J.M., Debordeaux,C., Raby,B., Klossek,J.M., Bonnet,N., and Puchelle,E., Motogenic effect of recombinant HGF on airway epithelial cells during the in vitro wound repair of the respiratory epithelium. *Journal of Cellular Physiology* **185**, 447-453, 2000.

166. Zhang,M., Wang,M.H., Singh,R.K., Wells,A., and Siegal,G.P., Epidermal growth factor induces CD44 gene expression through a novel regulatory element in mouse fibroblasts. *J.Biol.Chem.* **272**, 14139-14146, 1997.

167. Zhang,Y., Liou,G.I., Gulati,A.K., and Akhtar,R.A., Expression of phosphatidylinositol 3-kinase during EGF-stimulated wound repair in rabbit corneal epithelium. *Invest Ophthalmol.Vis.Sci.* **40**, 2819-2826, 1999.

168. Zhu,D. and Bourguignon,L., Overexpression of CD44 in pl85(neu)-transfected NIH3T3 cells promotes an up-regulation of hyaluronic acid-mediated membrane-cytoskeleton interaction and cell adhesion. *Oncogene* **12**, 2309-2314, 1996.

169. Zwick,E., Hackel,P.O., Prenzel,N., and Ullrich,A., The EGF receptor as central transducer of heterologous signalling systems. *Trends in Pharmacological Sciences* **20**, 408-412, 1999.